Development, Implementation and Normalization of SARS-CoV-2 Wastewater and Environmental Monitoring

Patrick Marcel D'Aoust

This doctoral thesis is submitted to the University of Ottawa
in partial fulfillment of the requirements for the degree of
Doctor of Philosophy in Environmental Engineering

Thesis Supervisors:

Dr. Robert Delatolla and Dr. Tyson E. Graber

Ottawa-Carleton Institute for Environmental Engineering
Department of Civil Engineering
Faculty of Engineering
University of Ottawa

© Patrick Marcel D'Aoust, Ottawa, Canada, 2025

Abstract

Wastewater and environmental monitoring (WEM) has for decades been a valuable resource for monitoring public health trends and providing insights into community-wide substance use, such as pharmaceuticals and illicit drugs, tracking infectious diseases like poliomyelitis and viral hepatitis. Despite its promise, WEM was historically underutilized, mainly limited to targeted studies or research efforts, and rarely integrated into real-time public health systems. The onset of the COVID-19 pandemic transformed WEM into a highly sought epidemiological tool, capable of complementing clinical testing and offering community-level data to better inform public health strategies. The COVID-19 pandemic exposed significant gaps in public health surveillance, emphasizing the need for tools that could monitor SARS-CoV-2 viral spread in real-time. WEM emerged as a promising approach, but early efforts faced several challenges: limited detection of the SARS-CoV-2 viral signal in wastewater during periods of low prevalence (low method sensitivity), pronounced variability in wastewater composition by location and season, the initial difficulty of scaling these methods to underserved, rural communities, and the lack of a universal biomarker or method of normalization to reduce the impact of flow and wastewater composition changes. The overarching hypothesis of this work was that WEM for SARS-CoV-2 could be established and refined through optimized sampling and sample processing methodologies, and that novel normalization strategies could improve the robustness of data interpretation and allow WEM to have predictive power as a public health tool. This dissertation addresses this hypothesis and bridges critical knowledge gaps by conducting six studies, establishing the methodologies, normalization strategies, and applications of normalization to WEM to improve its reliability and utility as a public health tool.

The first objective of the dissertation was to develop methodologies for SARS-CoV-2 detection and quantification in wastewater, and to develop the most effective wastewater sampling approach for quantifying SARS-CoV-2 RNA by comparing post-grit solids (PGS) and primary clarified sludge (PCS) and to evaluate the use various normalization biomarkers for reliable monitoring of infection trends, particularly during periods of low COVID-19 incidence. The results showed that primary clarified sludge (PCS) provided the most reliable and sensitive SARS-CoV-2 RNA measurements, with *pepper mild mottle virus* (PMMoV) serving as an effective normalization biomarker to track infection trends, particularly during periods of low incidence.

The second objective of the dissertation was to enhance the effectiveness of wastewater surveillance in detecting COVID-19 resurgences during periods of low clinical positivity and assess its predictive value as a complementary tool to traditional diagnostic methods. It aimed to determine whether wastewater measurements could provide early warnings of outbreaks, overcoming limitations such as testing biases and delayed hospitalization data. The results showed that SARS-CoV-2 RNA measurements in wastewater surged over 400% and were detected 48 hours before a 300% rise in positive cases and 96 hours before a 160% increase in hospitalizations, highlighting the predictive power of wastewater surveillance in tracking resurgences.

The third objective of the dissertation was to address the knowledge gap in wastewater surveillance by evaluating its effectiveness in small and rural communities, where reliable monitoring of COVID-19 and other pathogens remains challenging. Specifically, it aimed to compare SARS-CoV-2 RNA concentration from upstream pumping stations and downstream wastewater lagoons to determine the most effective sampling location for accurate community-level surveillance. The results showed that samples from the pumping station provided stronger, more stable RNA signals, while lagoon samples had lower concentrations and greater variability, suggesting that wastewater surveillance in rural or low-income regions should prioritize upstream locations like pumping stations for reliable monitoring.

The fourth objective of the dissertation was to investigate the relationship between SARS-CoV-2 wastewater signals and clinical case data through the wastewater-to-clinical-case (WC) ratio, aiming to address challenges in interpreting WEM data as clinical testing declines. It sought to determine whether the WC ratio could serve as a reliable indicator of underreported infections and the emergence of new variants in varying community immunity contexts. The results showed that increases in the WC ratio signaled periods of insufficient clinical testing, while changes in the ratio effectively tracked the spread of Alpha, Delta, and Omicron variants, demonstrating the WC ratio's potential to complement clinical metrics and enhance epidemiological monitoring.

The fifth objective of the dissertation was to assess the potential of tobamoviruses as fecal biomarkers for improving the accuracy and reliability of WEM, focusing on both their ability to indicate the presence of human fecal biomarkers and normalize viral signals in wastewater. This chapter presents a review aimed at addressing the limited research on tobamoviruses beyond PMMoV and *tomato brown rugose fruit virus*, as human-associated fecal biomarkers, despite their promising attributes for WEM applications. A critical review of over 240 studies, evaluating 43 *tobamoviruses*, was conducted. This review identified 15 with significant potential as biomarkers

across diverse global wastewater contexts, paving the way for future research to potentially improve future WEM normalization efforts.

Tying all of this work together, the sixth and final objective of the dissertation was to address an important gap in wastewater surveillance caused by the absence of a globally validated assay for PMMoV. It aimed to improve data comparability across WEM programs by identifying stable genomic regions of PMMoV that remain consistent despite variations in diets, wastewater composition, and environmental conditions. Testing 116 samples from 12 countries, the study identified the most stable region of the PMMoV genome between bases 2776-3023. Using this region, the research developed the P17 PMMoV assay, a highly sensitive and specific tool (ALOQ = 4.9 copies/reaction, ALOD = 3.4 copies/reaction) to ensure reliable normalization of WEM data worldwide, providing consistent performance across diverse environments.

This research transformed WEM early on in the pandemic by addressing critical challenges in sampling, normalization, and data interpretation, particularly during periods of low disease prevalence and in rural or underserved communities. By refining methodologies to improve signal reliability and predictive value, introducing the WC ratio for enhanced epidemiological insights, and exploring novel biomarkers to expand normalization strategies, this work significantly enhanced the utility of WEM as a public health tool, and contributed to shaping its adoption in Canada and abroad. Collectively, the findings provide a comprehensive framework for advancing wastewater surveillance, making it a more equitable, reliable, and globally applicable approach to monitoring infectious diseases and informing public health interventions.

Acknowledgements

The successful completion of this research project and subsequent dissertation owes much to the unwavering support from numerous individuals and organizations. I would like to shed light on some of the people and organizations who have contributed significantly. While this attempt to acknowledge help received isn't all-encompassing, and I may inadvertently omit some, I am grateful for every bit of support:

I would start by thanking my parents, Carole & Jérôme, for their continuous support throughout my decade-long post-secondary academic career. I would also like to thank my supervisors (Dr. Robert Delatolla & Dr. Tyson E. Graber for their support in and out of the lab, and for always having time to give me an ear and exchange ideas about what was happening with our experiments. I'd also like to thank our collaborators at the City of Ottawa, the University of Ottawa, and all the professors who helped me throughout my journey in this school. I would also take the time to thank my friends within the academic staff (Luc, Paula, Ali, Marie, Mark, Frantz, and all the staff on the third floor within the faculty). I'd also like to acknowledge and thank my friends at the University of Ottawa that accompanied me through this long, gruesome process that is graduate school (Brad, Ru, Liyu, Alex, Xin, Liz (M & R), Chandler, Joseph, Richard, Guillaume, Zach, Syeda, Howard, Nada, Lakshmi, Tram, Declan, Kieran, Antoine, Nathan, Peter and all others I will have forgotten in this list which have influenced my experience from close or from afar). I'd also like to thank Chris, Majid & Stéphanie, for their continued support, and give a special shout-out to my grandpa Marcel Savage for inspiring me to join the engineering profession, and the Department of Civil Engineering and the Faculty of Engineering at the University of Ottawa for allowing me to pursue a Ph.D. while employed at the University. There have been many sacrificed hours of sleep and many missed gatherings throughout my 20s and early 30s required to make this possible, and while I regret some of those missed memories, we carry on. Going back to my early 20s I wouldn't change anything in my academic career; however, I would be lying if I didn't sometimes dream of dropping everything and entering the trades :-). Most importantly, I am eternally grateful to my partner Hanna-Joy for supporting me through the most challenging periods of my life and sticking by my side through thick and thin.

Table of Contents

Abstract ii
Acknowledgements v
Preface xiii
List of abbreviations and acronyms xxi
List of figures xxii
List of tables xxv
Chapter 1 – Introduction 1
1.1. Background 1
1.2. Hypotheses and research objectives 5
1.3. Thesis organization 8
Chapter 2 – Quantitative Analysis of SARS-CoV-2 From Wastewater Solids in Communities With Low COVID-19 Incidence and Prevalence 11
2.1. Context 11
2.2. Abstract 11
2.3. Introduction 12
2.4. Materials and methods 14
2.4.1. Characteristics of the City of Ottawa and Gatineau WRRFs 14
2.4.2. Wastewater sampling and analysis 15
2.4.2.1. PGS samples 15
2.4.2.2. PCS samples 15
2.4.2.3. Wastewater quality characterization of samples 16
2.4.3. SARS-CoV-2 concentration 16
2.4.4. RNA extraction 17
2.4.5. Viral recovery efficiency 17
2.4.6. Variance of biomarkers for normalization 18
2.4.7. RT-qPCR 19
2.4.8. RT-ddPCR 20
2.4.9. Statistical analysis 20
2.5. Results & discussion 20
2.5.1. Viral RNA recovery efficiency 20
2.5.2. Comparison of RT-qPCR and RT-ddPCR for the detection and quantification of SARS-CoV-2 RNA 21
2.5.3. Detection and variance of SARS-CoV-2 viral RNA in PGS and PCS 23
2.5.4. Variability of normalization biomarkers 24
2.5.5. Quantification of SARS-CoV-2 viral RNA in PCS and correlation with COVID-19 case data 27
2.5.6. SARS-CoV-2 RNA in PCS and correlation with COVID-19 case data 28
2.5.7. Mass flux of primary clarified sludge copies SARS-CoV-2 RNA per day and correlation with COVID-19 case data 29
2.5.8. PMMoV-normalized SARS-CoV-2 RNA in PCS and correlation with COVID-19 case data 30
2.6. Conclusion 35
2.7. Limitations and 2025 field updates 35
2.8. Declaration of competing interests 36
2.9. Ethical considerations 36
2.10. Funding 36
2.11. Acknowledgements 36
2.12. References 38
Chapter 3 – Catching a Resurgence: Increase in SARS-CoV-2 Viral RNA Identified in Wastewater 48 Hours Before COVID-19 Clinical Tests and 96 Hours Before Hospitalizations 43
3.1. Context 43
3.2. Abstract 43
3.3. Introduction 44

3.4. Materials and methods 47
3.4.1. Characteristics of the City of Ottawa's water resource recovery facility 47
3.4.2. Sample collection, concentration, extraction and quantification 47
3.4.3. COVID-19 epidemiological data 48
3.4.4. Statistical analysis 49
3.5. Results, discussion and implications 50
3.5.1. Trend and peak of wastewater SARS-CoV-2 RNA viral level in wastewater compared to other clinical COVID-19 surveillance metrics 50
3.5.2. Correlation between wastewater and clinical surveillance metrics 53
3.5.3. Temporal association between surveillance metrics 54
3.6. Conclusions 56
3.7. Limitations and 2025 field updates 57
3.8. Declaration of competing interests 57
3.9. Ethical considerations 57
3.10. Funding 57
3.11. Acknowledgements 57
3.12. References 58
Chapter 4 – COVID-19 Wastewater-Based Epidemiology in Rural Communities: Comparison of Lagoon and Pumping Station Samples 61
4.1. Context 61
4.2. Abstract 62
4.3. Introduction 62
4.4. Experimental methods 65
4.4.1. Rural community sampling locations 65
4.4.2. Sample collection 67
4.4.3. Sample concentration, extraction, and PCR quantification 67
4.4.4. Assessment of RNA integrity 68
4.4.5. Collection of epidemiological data and correlation to wastewater viral signal 68
4.5. Results & discussion 68
4.6. Conclusions and recommendations 73
4.7. Limitations and 2025 field updates 74
4.8. Declaration of competing interests 75
4.9. Ethical considerations 75
4.10. Funding 75
4.11. Acknowledgements 75
4.12. References 76
Chapter 5 – Wastewater to Clinical Case (WC) Ratio of COVID-19 Identifies Insufficient Clinical Testing, Onset of New Variants of Concern and Population Immunity in Urban Communities 79
5.1. Context 79
5.2. Abstract 80
5.3. Introduction 80
5.4. Materials and methods 82
5.4.1. Sample collection, enrichment, concentration, and extraction 83
5.4.1.1. Ottawa 83
5.4.1.2. Toronto 83
5.4.1.3. Kitchener, Peel, and Waterloo 84
5.4.1.4. Edmonton and Calgary 85
5.4.2. RT-qPCR quantification of SARS-CoV-2, pepper mild mottle virus, Alpha, Delta, and Omicron VOCs in wastewater 85
5.4.3. Epidemiological data 86
5.4.4. Statistical analysis 88
5.4.5. Calculations of the WC ratio 88
5.4.6. Calculation of VOC allelic proportions 88
5.4.7. Standardization of SARS-CoV-2 measurements for comparison of curves 88

5.5. Results and discussion 89
5.5.1. Overview of SARS-CoV-2 surveillance at studied sites 89
5.5.2. The WC ratio as an indicator of key epidemiological occurrences in the cities 91
5.5.3. Event #1: WC ratio as an indicator of change in clinical testing strategy 92
5.5.4. Event #2: WC ratio as an indicator of the onset of the B.1.1.7 (Alpha) variant of concern 95
5.5.5. Event #3: WC ratio as an indicator of the onset of the B.1.617.2 (Delta) variant of concern 99
5.5.6. Event #4: WC ratio as an indicator of the onset of the B.1.1.529 (Omicron) variant of concern 103
5.6. Conclusions 106
5.7. Limitations and 2025 field updates 107
5.8. Declaration of competing interests 107
5.9. Ethical considerations 107
5.10. Funding 108
5.11. Acknowledgements 108
5.12. References 109
Chapter 6 – From Plant Pathogen to Public Health Tool: A Review Of Tobamoviruses and Their Role in Wastewater & Environmental Surveillance 124
6.1. Context 124
6.2. Abstract 124
6.3. Introduction 125
6.4. Methodologies 127
6.5. A brief overview of *tobamoviruses* 127
6.6. Tobacco mosaic virus (TMV) 128
6.6.1. Characteristics and features 128
6.6.2. Initial observations and discovery 128
6.6.3. Past, current and potential future uses 129
6.7. Pepper mild mottle virus (PMMoV) 129
6.7.1. Characteristics and features 129
6.7.2. Initial observations and discovery 129
6.7.3. Past, current and potential future uses 130
6.8. Tomato brown rugose fruit virus (ToBRFV) 131
6.8.1. Characteristics and features 131
6.8.2. Initial observations and discovery 131
6.8.3. Past, current and potential future uses 132
6.9. Cucumber green mottle mosaic virus (CGMMV) 132
6.9.1. Characteristics and features 132
6.9.2. Initial observations and discovery 132
6.9.3. Past, current and potential future uses 133
6.10. Cactus mild mottle virus (CMMoV) 133
6.10.1. Characteristics and features 133
6.10.2. Initial observations and discovery 133
6.10.3. Past, current and potential future uses 133
6.11. Paprika mild mottle virus (PaMMV) 134
6.11.1. Characteristics and features 134
6.11.2. Initial observations and discovery 134
6.11.3. Past, current and potential future uses 134
6.12. Streptocarpus flower break virus (SBFV) 135
6.12.1. Characteristics and features 135
6.12.2. Initial observations and discovery 135
6.12.3. Past, current and potential future uses 135
6.13. Tobacco mild green mosaic virus (TMGMV) 136
6.13.1. Characteristics and features 136
6.13.2. Initial observations and discovery 136
6.13.3. Past, current and potential future uses 136
6.14. Youcai mosaic virus (YMoV) 137
6.14.1. Characteristics and features 137

6.14.2. Initial observations and discovery 137
6.14.3. Past, current and potential future uses 137
6.15. Bell pepper mottle virus (BPeMV) 138
6.15.1. Characteristics and features 138
6.15.2. Initial observations and discovery 138
6.15.3. Past, current and potential future uses 138
6.16. Opuntia chlorotic ringspot virus (OCRV) 139
6.16.1. Characteristics and features 139
6.16.2. Initial observations and discovery 139
6.16.3. Past, current and potential future uses 139
6.17. Rattail cactus necrosis-associated virus (RCNaV) 139
6.17.1. Characteristics and features 140
6.17.2. Initial observations and discovery 140
6.17.3. Past, current and potential future uses 140
6.18. Clitoria yellow mottle virus (CYMV) 140
6.18.1. Characteristics and features 140
6.18.2. Initial observations and discovery 141
6.18.3. Past, current and potential future uses 141
6.19. Cucumber mottle virus (CMoV) 141
6.19.1. Characteristics and features 141
6.19.2. Initial observations and discovery 141
6.19.3. Past, current and potential future uses 142
6.20. Hibiscus latent Fort Pierce virus (HLFPV) 142
6.20.1. Characteristics and features 142
6.20.2. Initial observations and discovery 142
6.20.3. Past, current and potential future uses 143
6.21. Hibiscus latent Singapore virus (HLSV) 143
6.21.1. Characteristics and features 143
6.21.2. Initial observations and discovery 143
6.21.3. Past, current and potential future uses 144
6.22. Kyuri green mottle mosaic virus (KGMMV) 144
6.22.1. Characteristics and features 144
6.22.2. Initial observations and discovery 144
6.22.3. Past, current and potential future uses 145
6.23. Maracuja mosaic virus (MarMV) 145
6.23.1. Characteristics and features 145
6.23.2. Initial observations and discovery 145
6.23.3. Past, current and potential future uses 146
6.24. Obuda pepper virus (ObPV) 146
6.24.1. Characteristics and features 146
6.24.2. Initial observations and discovery 146
6.24.3. Past, current and potential future uses 147
6.25. Passion fruit mosaic virus (PafMV) 147
6.25.1. Characteristics and features 147
6.25.2. Initial observations and discovery 147
6.25.3. Past, current and potential future uses 147
6.26. Ribgrass mosaic virus (RiMV) 148
6.26.1. Characteristics and features 148
6.26.2. Initial observations and discovery 148
6.26.3. Past, current and potential future uses 148
6.27. Sunn-hemp mosaic virus (SHMV) 149
6.27.1. Characteristics and features 149
6.27.2. Initial observations and discovery 149
6.27.3. Past, current and potential future uses 149
6.28. Tomato mosaic virus (ToMV) 149
6.28.1. Characteristics and features 150

6.28.2. Initial observations and discovery 150
6.28.3. Past, current and potential future uses 150
6.29. Tomato mottle mosaic virus (ToMMV) 150
6.29.1. Characteristics and features 150
6.29.2. Initial observations and discovery 151
6.29.3. Past, current and potential future uses 151
6.30. Tropical soda apple mosaic virus (TSAMV) 151
6.30.1. Characteristics and features 151
6.30.2. Initial observations and discovery 152
6.30.3. Past, current and potential future uses 152
6.31. Turnip vein-clearing virus (TVCV) 152
6.31.1. Characteristics and features 152
6.31.2. Initial observations and discovery 152
6.31.3. Past, current and potential future uses 153
6.32. Ullucus mild mottle virus (UMMV) 153
6.32.1. Characteristics and features 153
6.32.2. Initial observations and discovery 153
6.32.3. Past, current and potential future uses 154
6.33. Wasabi mottle virus (WMoV) 154
6.33.1. Characteristics and features 154
6.33.2. Initial observations and discovery 155
6.33.3. Past, current and potential future uses 155
6.34. Brugmansia latent virus (BrLV) 155
6.34.1. Characteristics and features 155
6.34.2. Initial observations and discovery 155
6.34.3. Past, current and potential future uses 156
6.35. Brugmansia mild mottle virus (BMMV) 156
6.35.1. Characteristics and features 156
6.35.2. Initial observations and discovery 156
6.35.3. Past, current and potential future uses 157
6.36. Cucumber fruit mottle mosaic virus (CFMMV) 157
6.36.1. Characteristics and features 157
6.36.2. Initial observations and discovery 157
6.36.3. Past, current and potential future uses 158
6.37. Frangipani mosaic virus (FrMV) 158
6.37.1. Characteristics and features 158
6.37.2. Initial observations and discovery 158
6.37.3. Past, current and potential future uses 158
6.38. Hoya chlorotic spot virus (HoCSV) 159
6.38.1. Characteristics and features 159
6.38.2. Initial observations and discovery 159
6.38.3. Past, current and potential future uses 159
6.39. Odontoglossum ringspot virus (ORSV) 159
6.39.1. Characteristics and features 159
6.39.2. Initial observations and discovery 160
6.39.3. Past, current and potential future uses 160
6.40. Plumeria mosaic virus (PluMV) 160
6.40.1. Characteristics and features 160
6.40.2. Initial observations and discovery 161
6.40.3. Past, current and potential future uses 161
6.41. Rehmannia mosaic virus (ReMV) 161
6.41.1. Characteristics and features 161
6.41.2. Initial observations and discovery 162
6.41.3. Past, current and potential future uses 162
6.42. Tobacco latent virus (TLV) 162
6.42.1. Characteristics and features 162

6.42.2. Initial observations and discovery 163
6.42.3. Past, current and potential future uses 163
6.43. Yellow tailflower mild mottle virus (YTMMoV) 163
6.43.1. Characteristics and features 163
6.43.2. Initial observations and discovery 164
6.43.3. Past, current and potential future uses 164
6.44. Zucchini green mottle mosaic virus (ZGMMV) 164
6.44.1. Characteristics and features 164
6.44.2. Initial observations and discovery 164
6.44.3. Past, current and potential future uses 165
6.45. African eggplant-associated virus (AEaV) 166
6.46. Hibiscus latent Hawaii virus (HLHV) 166
6.47. Plantago tobamovirus 1 (PTV1) 167
6.48. Trichosanthes mottle mosaic virus (TrMMV) 167
6.49. Remarks and conclusions on the use of tobamoviruses as human fecal biomarkers 170
6.50. Limitations and 2025 field updates 171
6.51. Declaration of competing interests 172
6.52. Ethical considerations 172
6.53. Funding 172
6.54. Acknowledgments 172
6.55. References 173
Chapter 7 – Globally Validated PMMoV Assay for Wastewater & Environmental Surveillance Data Normalization 194
Context 194
Abstract 194
7.1. Introduction 195
7.2. Materials and methods 197
7.2.1. Wastewater sample collection and preservation 197
7.2.2. Nucleic acid extraction 198
7.2.3. Primer design for PCR panel overlapping the PMMoV genome 198
7.2.4. Primer and probe design for the universal PMMoV assay 200
7.2.5. PCR controls 200
7.2.6. Quantification of PMMoV RNA in wastewater by RT-qPCR 201
7.2.7. Assay limits of detection and quantification 201
7.2.8. Statistical analysis 202
7.3. Results and discussion 202
7.3.1. Concentrations and persistence of PMMoV locus in global wastewaters 202
7.3.2. Effects of geographical location on PMMoV RNA concentrations in wastewaters 203
7.3.3. Effects of sample type of PMMoV RNA concentrations in wastewaters 206
7.3.4. Effects of sewershed population size on PMMoV RNA concentrations in wastewaters 206
7.3.5. Description of the universal PMMoV RT-qPCR assay 207
7.3.6. Evaluating the P17 PMMoV assay 210
7.4. Conclusion 212
7.5. Limitations and 2025 field updates 213
7.6. Declaration of competing interest 213
7.7. Ethical considerations 213
7.8. Funding 214
7.9. Acknowledgments 214
7.10. References 215
Chapter 8 – Discussion and Conclusion 222
8.1. Optimization of sampling, detection and normalization of SARS-CoV-2 RNA in wastewater 223
8.2. Predictive value and correlation of wastewater surveillance metrics 224
8.3. Extending wastewater surveillance to rural and small communities 224
8.4. WC ratio as a public health metric 225

8.5. The role of tobamoviruses in wastewater and environmental surveillance 225
8.6. The development of a universal, globally validated PMMoV RT-qPCR assay 226
8.7. Novel contributions and practical implications 227
8.8. Future directions 228
8.9. References 228
Chapter 9 – Appendix & Supplementary Information 229

Preface

This dissertation is an original work prepared by Patrick M. D'Aoust under the supervision of Drs. Robert Delatolla and Tyson E. Graber. This dissertation contains six manuscripts, four of them which are published in peer-reviewed journals, and two which are in preparation for or "submitted" to peer-reviewed journals. Versions of these manuscripts are published in chapters 2 to 7 of this dissertation. Author contributions to each of the manuscripts are presented further below. Together, these studies contribute to the growing body of evidence supporting wastewater surveillance as a robust, timely, and cost-effective tool for managing COVID-19 and future pandemics in Canada and beyond. Furthermore, I acknowledge the University of Ottawa Academic Regulations (C-7) and confirm that I have obtained permission from each co-author, and publishers (as required) to include the aforementioned materials in my dissertation. The material presented reflects work completed during my full-time enrollment as a graduate student at the University of Ottawa. A percentage (%) value is added to the right of each author's contribution to provide an estimate of their contribution as a % of the total work.

I have also chosen to include the following two quotes as they encapsulate the guiding principles that shaped my research. These pieces offer clarity and perspective on why our collective efforts during the COVID-19 pandemic were so vital in turning innovative ideas into reality. They also serve as a reminder of the perseverance and collaboration required to bring such projects to life, allowing them to flourish and thrive.

"Of all the forms of inequality,
injustice in health is the most
shocking and inhumane."

-Martin Luther King Jr. (1966)

"Never doubt that a small group
of thoughtful, committed citizens
can change the world; indeed,
it's the only thing that ever has."

-Margaret Mead (2005)

Manuscript #1 – Thesis Chapter 2:

Quantitative Analysis of SARS-CoV-2 From Wastewater Solids in Communities With Low COVID-19 Incidence and Prevalence

A version of the following manuscript has been published in this chapter: D'Aoust, P.M., Mercier, É., Montpetit, D., Jia, J., Alexandrov, I., Neault, N., Baig, A.T., Mayne, J., Zhang, X., Alain, T., Langlois, M.-A., Servos, M.R., MacKenzie, M., Figeys, D., MacKenzie, A.E., Graber, T.E., Delatolla, R., 2021. *Quantitative analysis of SARS-CoV-2 RNA from wastewater solids in communities with low COVID-19 incidence and prevalence.* Water Res. 188, 116560. https://doi.org/10.1016/j.watres.2020.116560.

Patrick M. D'Aoust contributed to the experimental design, performed a large portion of the laboratory experiments, the sample collection and analysis of the data, prepared the figures, and prepared and revised the manuscript. (20%)

Élisabeth Mercier contributed to the experimental design, performed laboratory experiments, some sample collection, some analysis of the data and revised the manuscript. (12%)

Danika Montpetit performed a portion of the laboratory experiments, some of the analysis of the data and revised the manuscript. (5%)

Jian-Jun Jia performed a portion of the laboratory experiments and revised the manuscript. (10%)

Ilya Alexandrov performed complimentary analysis on some of the collected samples and revised the manuscript. (2%)

Nafisa Nault revised the manuscript. (1%)

Aiman T. Baig revised the manuscript. (1%)

Janice Mayne revised the manuscript. (1%)

Xu Zhang revised the manuscript. (1%)

Tommy Alain provided equipment support to the study and revised the manuscript. (2%)

Marc-André Langlois revised the manuscript. (1%)

Mark R. Servos revised the manuscript. (1%)

Malcolm MacKenzie provided complimentary analysis on some of the collected samples and revised the manuscript. (2%)

Daniel Figeys revised the manuscript. (1%)

Alex E. MacKenzie provided financial/equipment support to the study and revised the manuscript. (5%)

Tyson E. Graber (co-supervisor) performed complimentary analysis on some of the collected samples, provided help developing the research questions, contributed to the experimental design, and revised the manuscript. (15%)

Robert Delatolla (supervisor) designed and planned the study, developed the research question, directed the study and revised the manuscript. (20%)

Manuscript #2 – Thesis Chapter 3:
Catching a resurgence: Increase in SARS-CoV-2 viral RNA identified in wastewater 48 hours before COVID-19 clinical tests and 96 hours before hospitalizations

A version of the following manuscript has been published in this chapter: D'Aoust, P.M., Graber, T.E., Mercier, E., Montpetit, D., Alexandrov, I., Neault, N., Baig, A.T., Mayne, J., Zhang, X., Alain, T., Servos, M.R., Srikanthan, N., MacKenzie, M., Figeys, D., Manuel, D., Jüni, P., MacKenzie, A.E., Delatolla, R., 2021. *Catching a resurgence: Increase in SARS-CoV-2 viral RNA identified in wastewater 48 h before COVID-19 clinical tests and 96 h before hospitalizations.* Sci. Total Environ. 770, 145319. https://doi.org/10.1016/j.scitotenv.2021.145319.

Patrick M. D'Aoust performed a portion of the laboratory experiments, a portion of the sample collection and portion of the analysis of the data, prepared the figures, and prepared and revised the manuscript. (20%)

Tyson E. Graber (co-supervisor) provided help directing the study, prepared and revised the manuscript. (15%)

Élisabeth Mercier performed a large portion of the laboratory experiments, some of the sample collection, some of the analysis of the data and revised the manuscript. (15%)

Danika Montpetit performed a portion of the laboratory experiments, some of the analysis of the data and revised the manuscript. (10%)

Ilya Alexandrov revised the manuscript. (2%)

Nafisa Nault revised the manuscript. (1%)

Aiman T. Baig revised the manuscript. (1%)

Janice Mayne revised the manuscript. (1%)

Xu Zhang revised the manuscript. (1%)

Tommy Alain provided financial/equipment support to the study and revised the manuscript. (2%)

Mark R. Servos revised the manuscript. (1%)

Nivetha Srikanthan revised the manuscript. (1%)

Malcolm MacKenzie provided complimentary analysis on some of the collected samples and revised the manuscript. (2%)

Daniel Figeys revised the manuscript. (1%)

Douglas Manuel revised the manuscript. (1%)

Peter Jüni revised the manuscript. (1%)

Alex E. MacKenzie provided financial/equipment support to the study and revised the manuscript. (5%)

Robert Delatolla (supervisor) designed and planned the study, developed the research question, directed the study and revised the manuscript. (20%)

Manuscript #3 – Thesis Chapter 4:
COVID-19 wastewater-based epidemiology in rural communities: Comparison of lagoon and pumping station samples

A version of the following manuscript has been published in this chapter: D'Aoust, P.M., Towhid, S.T., Mercier, É., Hegazy, N., Tian, X., Bhatnagar, K., Zhang, Z., Naughton, C.C., MacKenzie, A.E., Graber, T.E., Delatolla, R., 2021. *COVID-19 wastewater surveillance in rural communities: Comparison of lagoon and pumping station samples.* Sci. Total Environ. 801, 149618. https://doi.org/10.1016/j.scitotenv.2021.149618.

Patrick M. D'Aoust contributed to the experimental design, performed a large portion of the laboratory experiments, sample collection and analysis of the data, prepared the figures, and prepared and revised the manuscript. (30%)

Syeda Tasneem Towhid performed a large portion of the laboratory experiments, helped prepare and revised the manuscript. (15%)

Élisabeth Mercier revised the manuscript. (13%)

Nada Hegazy revised the manuscript. (5%)

Xin Tian performed a portion of the laboratory experiments and revised the manuscript. (5%)

Kamya Bhatnagar revised the manuscript. (2%)

Zhihao Zhang revised the manuscript. (2%)

Colleen C. Naughton revised the manuscript. (1%)

Alex E. MacKenzie provided financial/equipment support to the study and revised the manuscript. (2%)

Tyson E. Graber (co-supervisor) provided help directing the study, and prepared and revised the manuscript. (10%)

Robert Delatolla (supervisor) designed and planned the study, developed the research question, directed the study and revised the manuscript. (15%)

Manuscript #4 – Thesis Chapter 5:
Wastewater to clinical case (WC) ratio of COVID-19 identifies insufficient clinical testing, onset of new variants of concern and population immunity in urban communities

A version of the following manuscript has been published in this chapter: D'Aoust, P.M., Tian, X., Towhid, S.T., Xiao, A., Mercier, E., Hegazy, N., Jia, J.J., Wan, S., Kabir, M.P., Fang, W., Fuzzen, M., Hasing, M., Yang, M.I., Sun, J., Plaza-Diaz, J., Zhang, Z., Cowan, A., Eid, W., Stephenson, S., Servos, M.R., Wade, M.J., MacKenzie, A.E., Peng, H., Edwards, E.A., Pang, X.L., Alm, E.J., Graber, T.E., Delatolla, R., 2022. *Wastewater to clinical case (WC) ratio of COVID-19 identifies insufficient clinical testing, onset of new variants of concern and population immunity in urban communities.* Sci. Total Environ. 853, 158547. https://doi.org/10.1016/j.scitotenv.2022.158547.

Patrick M. D'Aoust contributed to the experimental design, performed a portion of the laboratory experiments, the sample collection and analysis of the data, prepared the figures, and prepared and revised the manuscript. (17.5%)

Xin Tian performed a portion of the laboratory experiments, performed a portion of the analysis of the data and revised the manuscript. (10%)

Syeda Tasneem Towhid performed a portion of the laboratory experiments and revised the manuscript. (10%)

Amy Xiao revised the manuscript. (1%)

Élisabeth Mercier revised the manuscript. (4%)

Nada Hegazy revised the manuscript. (1%)

Jian-Jun Jia performed a portion of the laboratory experiments and revised the manuscript. (6%)

Shen Wan performed a portion of the laboratory experiments and revised the manuscript. (2%)

Md Pervez Kabir revised the manuscript. (1%)

Wanting Fang revised the manuscript. (1%)

Meghan Fuzzen revised the manuscript. (1%)

Maria Hasing performed a portion of the laboratory experiments and revised the manuscript. (2%)

Minqing Ivy Yang performed a portion of the laboratory experiments and revised the manuscript. (2%)

Jianxian Sun performed a portion of the laboratory experiments and revised the manuscript. (2%)

Julio Plaza-Diaz revised the manuscript. (1%)

Zhihao Zhang revised the manuscript. (1%)

Aaron Cowan revised the manuscript. (1%)

Walaa Eid revised the manuscript. (1%)

Sean E. Stephenson revised the manuscript. (1%)

Mark R. Servos provided financial/equipment support to the study and revised the manuscript. (1%)

Matthew J. Wade revised the manuscript. (1%)

Alex E. MacKenzie provided financial/equipment support to the study and revised the manuscript. (1%)

Hui Peng provided financial/equipment support to the study and revised the manuscript. (1%)

Elizabeth A. Edwards provided financial/equipment support to the study and revised the manuscript. (1%)

Xiao-Li Pang revised the manuscript. (1%)

Eric J. Alm provided help directing the statistical analyses and revised the manuscript. (1%)

Tyson E. Graber (co-supervisor) provided help directing the study, and prepared and revised the manuscript. (10%)

Robert Delatolla (supervisor) designed and planned the study, developed the research question, directed the study and revised the manuscript. (7.5%)

Manuscript #5 – Thesis Chapter 6:
From plant pathogen to public health tool: A review of tobamoviruses and their role in wastewater & environmental surveillance

A version of the following manuscript has been prepared for submittal to the journal *Reviews in Environmental Science and Bio/Technology*. D'Aoust, P.M., Nguyen, T.B., Wong, C.H., Hegazy, N., Stephenson, S., Renouf, E.M., Graber, T.E., Delatolla, R., *in preparation*. *From plant pathogen to public health tool: A review of tobamoviruses and their role in wastewater & environmental surveillance*.

Patrick M. D'Aoust defined the topic of review, designed and conducted the majority of the literature search, curated literature, performed formal analysis, prepared the original draft and revised the manuscript. (63%)

Tram B. Nguyen conducted some literature search, curated literature and contributed to the original draft. (10%)

Chandler H. Wong conducted some literature search and curated literature. (3%)

Nada Hegazy curated literature and reviewed the manuscript. (2%)

Sean Stephenson curated literature and reviewed the manuscript. (2%)

Elizabeth M. Renouf conducted some literature search, curated literature, reviewed and edited the manuscript. (7%)

Tyson E. Graber conducted some literature search, curated literature, provided critical review of the manuscript and edited the manuscript. (7%)

Robert Delatolla provided funding and critical review of the manuscript. (6%)

Manuscript #6 – Thesis Chapter 7:
Globally validated real-time PCR assay for the detection of pepper mild mottle virus in wastewater

A version of the following manuscript is being prepared for submittal to the Journal of Virological Methods. D'Aoust, P.M., Graber, T.E., Wong, C.H., Nguyen, T.B., Wan, S., Renouf, E.M., Gonzalez, R., Karaolia, P., Alpaslan Kocamemi, B., Maria, A., Mansfeldt, C., Fatta-Kassinos, D., Frigon, D., Celikkol, S., Murmane, K., Naughton, C.C., Kitajima, M., Székely, A.J., Towhid, S.T., Wyler, E., Ziels, R., Delatolla, R, *(in preparation)*. *Globally Validated PCR Assay for Pepper Mild Mottle Virus in Wastewater*.

Patrick M. D'Aoust contributed to the experimental design, performed a portion of the laboratory experiments, the sample collection and analysis of the data, prepared the figures, and prepared and revised the manuscript. (30%)

Tyson E. Graber conducted some literature search, curated literature, provided critical review, edited manuscript (co-supervisor). (10%)

Chandler H. Wong performed all nucleic acid extractions, some of the RT-qPCR work, and all RT-dPCR work. (17%)

Tram B. Nguyen conducted some literature search, helped with some of the data analysis techniques and contributed to the original draft. (5%)

Shen Wan reviewed and edited the manuscript. (3%)

Elizabeth M. Renouf conducted some literature search, curated literature, reviewed and edited the manuscript. (5%)

Raul Gonzalez revised the manuscript. (1%)

Parthenopi Karaolia revised the manuscript. (1%)

Bilge Alpaslan Kocamemi revised the manuscript. (1%)

Anna Maria revised the manuscript. (1%)

Cresten Mansfeldt revised the manuscript. (1%)

Despo Fatta-Kassinos revised the manuscript. (1%)

Dominic Frigon revised the manuscript. (1%)

Sukriye Celikkol revised the manuscript. (1%)

Kevin Murmane revised the manuscript. (1%)

Colleen C. Naughton revised the manuscript. (1%)

Masaaki Kitajima revised the manuscript. (1%)

Anna J. Székely revised the manuscript. (1%)

Syeda Tasneem Towhid revised the manuscript. (1%)

Emanuel Wyler revised the manuscript. (1%)

Ryan Ziels revised the manuscript. (1%)

Robert Delatolla provided critical review of the manuscript and edited the manuscript. (15%)

List of abbreviations and acronyms

AIDS: Acquired Immune Deficiency Syndrome
AEaV: African Eggplant-Associated Virus
ALOD: Assay Limit of Detection
ALOQ: Assay Limit of Quantification
APHA: American Public Health Association
BMMV: Brugmansia Mild Mottle Virus
BOD: Biochemical Oxygen Demand
BPeMV: Bell Pepper Mottle Virus
BPMM: Bell Pepper Mild Mottle Virus
BrLV: Brugmansia Latent Virus
CDC: Centers for Disease Control and Prevention
CDS: Coding Sequence
CFMMV: Cucumber Fruit Mottle Mosaic Virus
CGMMV: Cucumber Green Mottle Mosaic Virus
CIHR: Canadian Institutes of Health Research
CMoV: Cucumber Mottle Virus
COD: Chemical Oxygen Demand
COVID-19: Coronavirus Disease 2019
CYMV: Clitoria Yellow Mottle Virus
DNA: Deoxyribonucleic Acid
ELISA: Enzyme-Linked Immunosorbent Assay
EPA: Environmental Protection Agency
FrMV: Frangipani Mosaic Virus
GMP: Google Map Customizer
HLFPV: Hibiscus Latent Fort Pierce Virus
HLHV: Hibiscus Latent Hawaii Virus
HLSV: Hibiscus Latent Singapore Virus
HoCSV: Hoya Chlorotic Spot Virus
HPDE: High-Density Polyethylene
ICTV: International Committee on Taxonomy of Viruses
ICU: Intensive Care Unit
ISO: International Organization for Standardization
IUCN: International Union for Conservation of Nature
KGMMV: Kyuri Green Mottle Mosaic Virus
MarMV: Maracuja Mosaic Virus
MIQE: Minimum Information for Publication of Quantitative Real-Time PCR Experiments
MST: Microbial Source Tracking
NP: Nasopharyngeal
OCRV: Opuntia Chlorotic Ringspot Virus
ObPV: Obuda Pepper Virus
ORSV: Odontoglossum Ringspot Virus
PaMMV: Paprika Mild Mottle Virus
PafMV: Passion Fruit Mosaic Virus
PCS: Primary Clarified Sludge
PCR: Polymerase Chain Reaction
PluMV: Plumeria Mosaic Virus
PMMoV: Pepper Mild Mottle Virus
PTV1: Plantago Tobamovirus 1
RCNaV: Rattail Cactus Necrosis-Associated Virus
ReMV: Rehmannia Mosaic Virus
RiMV: Ribgrass Mosaic Virus
RNA: Ribonucleic Acid
RT-PCR: Reverse Transcription Polymerase Chain Reaction
RT-qPCR: Reverse Transcription Quantitative PCR
SARS: Severe Acute Respiratory Syndrome
SARS-CoV-2: SARS Coronavirus 2
SBFV: Streptocarpus Flower Break Virus
SHMV: Sunn-Hemp Mosaic Virus
SOP: Standard Operating Procedure
TLV: Tobacco Latent Virus
TMGMV: Tobacco Mild Green Mosaic Virus
TMV: Tobacco Mosaic Virus
ToBRFV: Tomato Brown Rugose Fruit Virus
ToMMV: Tomato Mottle Mosaic Virus
ToMV: Tomato Mosaic Virus
TrMMV: Trichosanthes Mottle Mosaic Virus
TSAMV: Tropical Soda Apple Mosaic Virus
TVCV: Turnip Vein-Clearing Virus
UMMV: Ullucus Mild Mottle Virus
USEPA: United States Environmental Protection Agency
USA: United States of America
VOC: Variant of Concern
VOI: Variant of Interest
VSS: Volatile Suspended Solids
WES: Wastewater and Environmental Surveillance
WHO: World Health Organization
WMoV: Wasabi Mottle Virus
WRRF: Water Resource Recovery Facility
WEM: Wastewater & Environmental Monitoring
YMoV: Youcai Mosaic Virus
YTMMoV: Yellow Tailflower Mild Mottle Virus
ZGMMV: Zucchini Green Mottle Mosaic Virus

List of figures

Figure 2-1: Location of the city of Ottawa and Gatineau WRRFs (GMP, 2020). 14

Figure 2-2: Flowchart showing sample work-up and processing for PGS and PCS, including RNA concentration, extraction and quantification. 17

Figure 2-3: Comparison of copies per 100 µL of extracted RNA in RT-qPCR and RT-ddPCR for PGS (n=6) and PCS (n=5). 22

Figure 2-4: Sensitivity of N1 and N2 RT-qPCR assays comparison between PCS and PGS samples. Significance between detections established using Chi-Squared test. Variance is shown with %CV (n=24). 24

Figure 2-5: Variance of PCS normalization biomarkers (and SARS-CoV-2 for reference), a) combined data set comprised of both cities samples, and b) data set separated by city. Analysis of variance and maximum change in C_t (ΔC_t) (n=8). 26

Figure 2-6: Ottawa WRRF trends of N1 and N2 SARS-CoV-2 viral copies with epidemiological metrics, a) copies/L of PCS, b) copies/d that was normalized by the mass flux through primary clarifier, c) copies/copies of PMMoV that was normalized by PMMoV reference gene and d) graph displaying the daily number of tests performed and the number of active COVID-19 cases/100K population. 32

Figure 2-7: Gatineau WRRF trends of N1 and N2 SARS-CoV-2 viral copies with epidemiological metrics, a) copies/L of PCS, b) copies/d that was normalized by the mass flux through primary clarifier, c) copies/copies of PMMoV that was normalized by PMMoV reference gene and d) graph displaying the daily number of tests performed and the number of active COVID-19 cases/100K population. 33

Figure 3-1: Bird's-eye view of the Ottawa WRRF, with the primary clarifiers identified. 47

Figure 3-2: Ct values of the SARS-CoV-2 N1 and N2 gene regions, and the PMMoV normalization gene (1:10 dilution shown), outlining the low variability of PMMoV, justifying its use as a normalization gene. The 10th and 90th percentile are displayed, along with the median (dotted line inside shapes). The variance of the different targets is also shown at the top. 50

Figure 3-3: Epidemiological metrics and SARS-CoV-2 viral concentrations over the study period; a) COVID-19-caused hospitalizations, b) percent test positivity (7-day mid-point floating average), c) percent test positivity and d) number of new daily cases, along with e) wastewater SARS-CoV-2 N1 and N2 gene copies/PMMoV gene copies. Open data points signify points which were below the limit of quantification. The dotted line in the background represents the number of daily clinical tests/100K pop. performed. 52

Figure 3-4: Figure of the new daily cases epidemiological metric (in red) with SARS-CoV-2 viral RNA signal in Ottawa's primary clarified sludge samples, with the precedence of SARS-COV-2 viral signal in wastewater clearly outlined. 55

Figure 4-1: Sampling locations and configurations: a) geographic locations of pumping station and lagoon, b) lagoon treatment system consisting of three cells, identification of sampling point, c) automatic sampler at pumping station, sampler dispenses samples into refrigerator, and d) automatic sampler under the solar panel at lagoon sampling point and sampling point. 66

Figure 4-2: Comparison of genomic copies/L of pumping station samples and waste stabilization pond samples over time for the N1 and N2 SARS-CoV-2 gene regions, and PMMoV. Bars with a star (*) indicate that the sample signal was below the ALOQ. 70

Figure 4-3: Electropherograms of samples from the a) pumping station and the b) lagoon, showing drastic differences in the RNA profiles. 71

Figure 4-4: Average SARS-CoV-2 signal in the pumping station wastewater samples expressed as a) PMMoV normalized SARS-CoV-2 viral genomic copies, b) SARS-CoV-2 viral copies/g and c) SARS-CoV-2 viral genomic copies/L, along with the weekly COVID-19 test percent positivity. 73

Figure 5-1: Comparison of a. scale-standardized PMMoV-normalized (Ottawa, Toronto, Kitchener, Peel and Waterloo) and non-PMMoV normalized (Edmonton and Calgary) SARS-CoV-2 viral signal measured in wastewater to reported new daily COVID-19 cases in the communities, with the onset of events of high epidemiological importance outlined with vertical dashed lines, coupled with b. summary of the immunization status of the populations living within the studied communities. 91

Figure 5-2: Comparison of the number of daily SARS-CoV-2 RT-PCR nucleic acid clinical tests performed and corresponding daily new COVID-19 positive cases, the daily viral signal measured through a SARS-CoV-2 wastewater surveillance program and the corresponding wastewater/clinical cases ratio (WC) during the same period in Ottawa..... 94

Figure 5-3: Comparison of a. the number of daily SARS-CoV-2 RT-PCR nucleic acid clinical tests performed and corresponding daily new COVID-19 positive cases in Ottawa, Canada, b. the daily viral signal measured through a SARS-CoV-2 wastewater surveillance program..... 96

Figure 5-4: Comparison of the WC ratio and B.1.1.7 allelic proportionality during the onset of the B.1.1.7 (Alpha) VOC in the additional 6 locations in Canada (Toronto, Kitchener, Peel, Waterloo, Edmonton, and Calgary). 97

Figure 5-5: Comparison of a. the number of daily SARS-CoV-2 RT-PCR nucleic acid clinical tests performed and corresponding daily new COVID-19 positive cases in Ottawa, Canada, b. the daily viral signal measured through a SARS-CoV-2 wastewater surveillance program..... 100

Figure 5-6: Comparison of the WC ratio and B.1.617.2 allelic proportionality during the onset of the B.1.617.2 (Delta) VOC in 6 additional locations in Canada (Toronto, Kitchener, Peel, Waterloo, Edmonton, and Calgary)..... 101

Figure 5-7: Comparison of a. the number of daily SARS-CoV-2 RT-PCR nucleic acid clinical tests performed and corresponding daily new COVID-19 positive cases in Ottawa, Canada, b. the daily viral signal measured through a SARS-CoV-2 wastewater surveillance program..... 104

Figure 5-8: Comparison of WC ratio amplitude during the 30-day periods of onset of the B.1.1.7 (Alpha), B.1.617.2 (Delta) and B.1.1.529 (Omicron) VOCs in Ottawa, Toronto, Kitchener, Peel and Waterloo.. 105

Figure 7-1: A map highlighting the countries (in blue) in which wastewater samples were harvested in this study..... 198

Figure 7-2: A summary graph of measured cycle threshold (Ct) values for all 35 targets within the PMMoV genome, highlighting in blue the benchmark PMMoV assay's location, and in red, two potential regions of interest for the development of a universal probe-based assay. The solid blue lines indicate the median values for the Ct values of each genomic region, and the dashed blue lines indicate the quartiles of the Ct values of each genomic region. A minimum of 116 samples were analyzed per genomic region. Including reruns, a total of 4,066 analyses were performed across all regions of the PMMoV genome. 203

Figure 7-3: A graph demonstrating the variance in measured cycle threshold (Ct) values for all 35 'genomic regions' within the PMMoV genome, organized per geographical region of the world (Americas, Europe, Oceania and Asia) of the analyzed samples. Regions 11 (blue), 17 and 31 (red) are highlighted. 204

Figure 7-4: A graph showing the distribution of PMMoV RNA concentration (inferred from Ct values) in wastewaters from the 12 sampled countries in this study. Solid lines indicate the average, and the dashed lines indicate the 1st and 3rd quartiles. Lower Ct values indicate a higher PMMoV RNA concentration. In this graph, measurements from all PMMoV genomic regions were consolidated on a per country basis. 205

Figure 7-5: A comparison of measured PMMoV RNA concentration (displayed as Ct values) comparing pre- and post-grit and primary sludge samples across the 35 genomic region within the PMMoV genome. Lower Ct values indicate a high measured concentration of PMMoV RNA in the sample. Data points and error bars represent the mean and standard deviation of the agglomorated Ct measurements across all tested samples in the study. Three regions are highlighted as genomic regions of interest: in blue the benchmark PMMoV's assay location (region 11), and in red, two potential regions of interest (regions 17 and 31). 206

Figure 7-6: Three panels illustrating the relationship between sewershed population size and measured PMMoV RNA concentrations across three genomic regions of interest (regions 11, 17, and 31). Linear regression analyses were performed independently for each region, comparing sewershed population size with measured Ct values. The results indicate that no strong linear relationships exist between sewershed population size and PMMoV RNA concentrations. 207

Figure 7-7: Alignment of the primers and probe of the P17 PMMoV assay proposed in this study. The primers and probe are aligned with 45 full-genome sequences of PMMoV to highlight any nucleotide mismatches. 208

Figure 7-8: Alignment of the primers and probe of the "benchmark" PMMoV assay proposed in this study. The primers and probe are aligned with 45 full-genome sequences of PMMoV to highlight any nucleotide mismatches. 209

Figure 7-9: Genomic map of the 6.4 kb genome of PMMoV, highlighting the four major ORFs, and the location of the benchmark and P17 PMMoV assays. 210

List of tables

Table 2-1: Correlation analyses between SARS-CoV-2 RNA signal in PCS in the Ottawa and Gatineau WRRFs with epidemiological metrics. RNA signal is expressed as copies/L of PCS, copies/d that was normalized by the mass flux through primary clarifier, and copies/copies of PMMoV that was normalized by PMMoV. Cells are color-coded from green to red based on the calculated Pearson's R correlation value, with green (1.000) representing the strongest correlation and red (0.000) representing no correlation at all. Significance values (p-value) are listed with red font used to identify non-significant correlations/relationships. 34

Table 3-1: Time-step analyses of correlations (Pearson's R) between normalized SARS-CoV-2 viral RNA signal (copies/copies PMMoV) and 7-day rolling average percent positivity, test percent positivity and daily new cases epidemiological metrics. 55

Table 4-1: Yearly average wastewater characteristics at the pumping station and lagoon effluent..... 66

Table 5-1: Testing periods and analyzed major epidemiological events identified per studied site, which were selected for consideration as part of this study. If no dates are shown for a particular event at a particular location, the data for that specific event was not available (testing had not commenced) or was measured to infrequently for sufficient analyses and interpretation. 83

Table 5-2: Summary of the RT-qPCR quantification of SARS-CoV-2 targets and PMMoV in all four laboratories which performed analyses for this study. 86

Table 5-3: Mean WC ratio and interquartile ranges (1st and 3rd quartiles) before and after the Alpha VOC onset along with the results of Mann-Whitney U tests performed on the WC ratio data sets to evaluate the significance of shifts before and after the Alpha VOC 98

Table 5-4: Mean WC ratio and interquartile ranges (1st and 3rd quartiles) before and after the Delta VOC onset along with the results of Mann-Whitney U tests performed on the WC ratio data sets to evaluate the significance of shifts before and after the Delta VOC. 102

Table 6-1:This table categorizes 43 t*obamoviruses* based on their likelihood (L = Likely, P = Possible, U = Unlikely) of use and current status (NIU = Not In Use, AIU = Already In Use) in WEM applications, with annotations on their suitability. This table also provides the GenBank accession numbers of *tobamoviruses* which were studied. 168

Table 7-1: List of forward and reverse primers developed for the panel of 35 overlapping SYBR Green PCR assays used to evaluate the relative persistence of the PMMoV genome..... 199

Table 7-2: Overlapping SYBR Green PCR amplicon characteristics (amplicon size, GC content, location, and genomic feature(s) intersecting the amplicon). 199

Table 7-3: Oligonucleotide sequences of the benchmark PMMoV and P17 qRT-PCR assays. 200

Table 7-4: Summary of the RT-qPCR testing conditions for the SYBR Green overlapping assays, and the PMMoV probe-based assays during this study. 201

Table 7-5: This table presents the descriptive statistics for the measured Ct values (representative of the concentration of PMMoV RNA in wastewater samples) in all tested wastewater samples (all PMMoV genomic locations combined), separated by geographical location. This table provides the number of measurements performed (n), the mean values, the standard deviation, the 1st and 3rd quartiles and the variance of the measured Ct values. In this table, measurements from all PMMoV genomic regions were consolidated on a per country basis. 205

Table 7-6: Validation of the benchmark and P17 PMMoV assays. This table provides shows a summary of PMMoV RNA measurements in 29 samples and one control, comparing both PMMoV assays. The RNA concentrations are expressed and compared as Ct values. 211

Chapter 1 – Introduction

1.1. Background

SARS-CoV-2, a pandemic virus that was first discovered in December 2019, has had profound and long-lasting impacts on the world. At the time of writing, over 776M individuals have contracted COVID-19 and more than 7.0M individuals have died as a result of complications caused by the disease (World Health Organization, 2024). The COVID-19 pandemic has had deep, lasting impacts on most nations during the early stages of the pandemic, and in the absence of effective immunization, the only tools available to public health units to mitigate negative effects on the health of the general population were public health messaging, encouraged hand hygiene, mandatory masking, distancing guidelines, curfews and lockdowns. As the pandemic progressed, widespread PCR clinical testing campaigns became the main tools available to public health units to assess the progress of the pandemic (Borkowska and Laurence, 2021; Miao et al., 2021; Razavi et al., 2020) in their respective communities. The first scientific communications related to COVID-19 came in the form of medical reports and medical studies describing symptoms, administered treatments and outcomes of COVID-19 patients, first in China, and later around the world (Bogoch et al., 2020; Leung, 2020; Zhu et al., 2020). Early "day-zero" medical studies and initial systemic reviews and meta-analyses of literature of SARS-CoV-2 symptoms revealed that approximately half of COVID-19 positive patients had positive identification of SARS-CoV-2 RNA in fecal/rectal swabs (Collivignarelli et al., 2020; Gupta et al., 2020; Lodder and de Roda Husman, 2020; Parasa et al., 2020; Park et al., 2020; Zhurakivska et al., 2020). These studies also revealed that there existed a higher incidence of SARS-CoV-2 RNA measurements in fecal material as compared to urine (Collivignarelli et al., 2020; Zhurakivska et al., 2020). Furthermore, it was also identified early on that among different types of COVID-19 patient specimens, rectal swabs or stool samples generally provided higher detection rates than nasopharyngeal (NP) swabs (Bwire et al., 2020), and that both children and adults were capable of shedding SARS-CoV-2 RNA via stool (Fontana and Villamagna, 2021; Gupta et al., 2020; Long et al., 2020; Xing et al., 2020), sometimes even when showing no symptoms of COVID-19.

In parallel, based on previous studies outlining possible fecal shedding and detection in wastewater of other pathogens, including some causing respiratory diseases, some researchers began investigating the detection of SARS-CoV-2 RNA in sewage in water resource recovery facilities (WRRFs). For decades, wastewater and environmental monitoring (WEM) had previously been successfully utilized by public health professionals to survey the emergence of new disease outbreaks such as poliomyelitis, measles and viral hepatitis, the use of pharmaceutical compounds or illicit drugs, or the onset of antimicrobial resistant

genes in communities (Ansari et al., 1992; Been et al., 2014; Benschop et al., 2017; Bucardo et al., 2011; Castiglioni et al., 2013; Choi, 2012; Daughton, 2018; Feng et al., 2018; Flannery et al., 2012; González-Mariño et al., 2020; Gushgari et al., 2018; Heijnen and Medema, 2011; Hellmér et al., 2014; Lorenzo and Picó, 2019; Metcalf et al., 1995; Pruden, 2014; Sinclair et al., 2008; Singer et al., 2013; Yang et al., 2017). At the onset of the COVID-19 pandemic, research out of the Netherlands (Medema et al., 2020) and Australia (Ahmed et al., 2020a) demonstrated that the measurement of SARS-CoV-2 RNA signal via quantitative reverse transcript polymerase chain reaction (RT-qPCR) in wastewater was possible and that measurements appeared to correlate with COVID-19 incidence in their respective communities. As a direct result of the initial successes in the Netherlands and Australia to measure SARS-CoV-2 RNA signal in wastewater and correlate decreases or increases in viral signal in wastewater to epidemiological events in the surveyed communities, attempts to replicate these findings subsequently occurred in many other locations throughout the world. A significant number of new surveillance initiatives soon followed, reporting similar observations globally (Alpaslan-Kocamemi et al., 2020; D'Aoust et al., 2021a; Gonzalez et al., 2020; Haramoto et al., 2020; Kumar et al., 2020; La Rosa et al., 2020; Nemudryi et al., 2020; Peccia et al., 2020b; Randazzo et al., 2020; Rimoldi et al., 2020; Sherchan et al., 2020; Westhaus et al., 2021; Wurtzer et al., 2020; Zhang et al., 2020). As the COVID-19 pandemic progressed, WEM saw unprecedented adoption and support, emerging as a tool allowing public health units, governments, and businesses to potentially obtain additional information on the burden of COVID-19 of individuals and their communities. As a result, five years into the COVID-19 pandemic, WEM of SARS-CoV-2 RNA load has now been conducted at over 4,600 sites in at least 72 countries (Naughton et al., 2021). Consequently, studies and research on the topic of WEM have been subject to increasing interest during, and after the pandemic.

The swift development of the field and application of SARS-CoV-2 WEM to track community health indicators such as the community-wide burden of COVID-19 has led to the rapid incremental development and improvement of methodologies and techniques. This has affected every portion of the surveillance process, from the sample collection and enrichment to the extraction of nucleic acids, quantification, and interpretation of results. Initial research into the improvement of surveillance of SARS-CoV-2 RNA load in wastewater focused primarily on analysis of SARS-CoV-2 RNA signal from wastewater solids, due to the established propensity for SARS-CoV-2 signal and RNA fragments to exist in fecal material and feces (Chen et al., 2020; Cheung et al., 2020; Santos et al., 2020; Xing et al., 2020). Due to the relatively rapid implementation of SARS-CoV-2 WEM worldwide, a significant gap in knowledge regarding the most effective sample processing and concentration techniques to optimize enrichment of SARS-CoV-2 RNA targets in wastewater-related solids was identified, especially in a context of low disease prevalence where the overall viral burden in a community could be relatively low

(Ahmed et al., 2020c, 2020b; Kitajima et al., 2020; Randazzo et al., 2020). In addition, as the pandemic progressed, the first major resurgences in SARS-CoV-2 infections in North America were observed while WEM programs were in operation, leading to significant interest but uncertainties regarding the ability of SARS-CoV-2 WEM to accurately track and potentially predict increases and decreases in other, more traditional epidemiological metrics such as reported daily new clinical cases of COVID-19, or reported daily new hospitalizations due to COVID-19. While several studies have begun investigating fundamental relationships existing between SARS-CoV-2 RNA signal in wastewater and related epidemiological metrics in the surveyed communities (Ai et al., 2021; Carrillo-Reyes et al., 2020; Galani et al., 2022; Melvin et al., 2021; Wang et al., 2021; Weidhaas et al., 2021; Wolfe et al., 2021; Wu et al., 2021), the results are not entirely conclusive due to some diverging results and until now few comprehensive large-scale studies have been conducted on the topic, with only one study investigating the intrinsic relationship of SARS-CoV-2 RNA signal in wastewater and reported daily new clinical cases of COVID-19 (WC ratio) (Xiao et al., 2022). Without a full understanding of the relationship existing between measured SARS-CoV-2 RNA signal in wastewater and reported daily new clinical cases of COVID-19 (WC ratio) in the community, the interpretation of WEM results and the possibilities regarding their application from a public health perspective may yet to be fully elucidated. Tackling these gaps of knowledge effectively will lead to a wider adoption of WEM, leading to improved health in urban and peri-urban communities by allowing public health units and governments to maintain broad disease surveillance programs, improving community health. Furthermore, effective WEM programs which generate well understood performance indices for public health units to monitor, allowing highly urbanized cities and regions to remain sustainable in the medium to long term, despite the threat of increasingly frequent, new and old re-emerging, pandemic-potential diseases (Chacón et al., 2021; Hassell et al., 2017; Naughton et al., 2021; Neiderud, 2015; Ram et al., 2022; Reyes et al., 2013).

Despite the fulgurant growth of WEM, certain inequalities and inconsistencies in terms of the application of SARS-CoV-2 surveillance have emerged. Specifically, the majority of surveillance programs have occurred in larger, more densely populated urban and peri-urban communities at the expense of smaller, less densely populated rural communities (Medina et al., 2022; Naughton et al., 2021), leading to a significant knowledge gap between the surveillance of larger urban and peri-urban sewersheds and smaller, rural sewersheds. While most of the SARS-CoV-2 surveillance in wastewater has predominantly been performed in larger, more affluent communities employing larger mechanical WWTPs, a significant proportion of communities in North America and Europe still treat their wastewater using lagoons and waste stabilization ponds, for which there has been very little SARS-CoV-2 surveillance research on. This has led to inequities in SARS-CoV-2 surveillance throughout the world due to a lack of knowledge for the

surveillance of communities employing these smaller systems, disproportionately leaving rural populations out of surveillance programs. Currently, at least 9,200 wastewater treatment lagoons are in operation in North America, and a further 5,500 are in operation in Europe (D'Aoust et al., 2021b; Mara, 2009; Statistics Canada, 2016; USEPA, 2011). Tackling the fundamental lack of knowledge regarding the methodologies, techniques, and interpretation of SARS-CoV-2 surveillance in wastewater in smaller rural sewersheds is crucial to ensure adequate and fair surveillance of SARS-CoV-2 and assessment of COVID-19 risks in these communities. These issues remain unresolved and require further research to help WEM mature into a mainstay of public health globally.

In addition to gaps in knowledge and uncertainties regarding sample processing and enrichment, several unknowns have remained regarding normalization, standardization, and correction of observed viral signal in sewersheds, particularly due to the lack of appropriate or fully understood human fecal biomarkers (Corpuz et al., 2020; Farkas et al., 2020; Michael-Kordatou et al., 2020).

As a result, significant efforts have been made to investigate the applicability and suitability of flow measurements, novel fecal biomarkers, or water quality characteristics as measures to standardize/normalize WEM viral signal and prevent deleterious sewershed-induced impacts on WEM measurements due to dilution of wastewater, changes in flow and changes in sewershed population or diet, a fundamental and critical aspect of WEM (Armanious et al., 2016). Very early on into the pandemic, it was acknowledged that there was an urgent need to normalize SARS-CoV-2 RNA load measurements in wastewater (Alpaslan-Kocamemi et al., 2020; Kaplan et al., 2020; Peccia et al., 2020a; Wu et al., 2020). Traditional normalizers such as flow, cross-assembly phage (crAssphage) (Bivins et al., 2020; Chen et al., 2021; Crank et al., 2020; Greenwald et al., 2021; Sala-Comorera et al., 2021; Wilder et al., 2021), a ubiquitous bacteria-infecting virus found in the human gut, or pepper mild mottle virus (PMMoV) (Gerrity et al., 2021; Graham et al., 2020; Kitamura et al., 2021; LaTurner et al., 2021; Loeb et al., 2020; Wolfe et al., 2021; Wu et al., 2020), an equally ubiquitous plant-virus found in many pepper-based foodstuffs (Mandal and Jain, 2010; Peng et al., 2015) have been used in the past, but no consensus has been reached regarding best practices regarding their use as a means to standardize/normalize WEM measurements. A recent survey (as of March 2022) of existing scientific literature searching for the combination of "SARS-CoV-2" and "PMMoV" keywords, compared to "SARS-CoV-2" and "crAssphage" keywords on Google Scholar using Harzing's Publish or Perish (version 8) revealed that PMMoV (209 publications/manuscripts, 2,981 citations) and crAssphage (203 publications/manuscripts, 3,132 citations) biomarkers appeared to have been studied in similar proportions for SARS-CoV-2 WEM since the beginning of the COVID-19 pandemic. While most of the detection and quantification of crAssphage has been performed with one single qPCR assay (Stachler et al., 2017). Meanwhile, for purposes of WEM, at least three RT-qPCR assays

have been used to detect and quantify PMMoV (Hamza et al., 2011; Haramoto et al., 2013; Zhang et al., 2006), which has led to uncertainties in the efficacy of the individual PMMoV assays to standardize/normalize WEM measurements for SARS-CoV-2 and other diseases where markers or fecally shed. Furthermore, while the three PMMoV RT-qPCR assays are situated in the same genomic region and appear to have been developed iteratively for surface water detection and quantification of PMMoV, it is currently unknown if the assay's selected genomic region is the most preserved and persistent in wastewater. Due to the global nature of the COVID-19 pandemic and SARS-CoV-2 WEM, the assays have not been globally validated as equivalent in performance, which makes direct comparisons of PMMoV-normalized data between surveyed sites more difficult. Inconsistencies between utilized PMMoV assays, and the lack of a globally validated assay could also be of particular importance due to the existence of region-specific strains of PMMoV, further hindering widespread adoption of PMMoV to normalize SARS-CoV-2 WEM measurements. As a result, a gap of knowledge regarding best practices for normalization using biomarkers still exists today.

1.2. Hypotheses and research objectives

Despite the rapid development of WEM, several questions and gaps in knowledge remain and the collection of publications and manuscripts in this thesis describe the efforts that were made to address some of these unknowns. As a result, three initial hypotheses were formulated and tested. As work progressed, a fourth and fifth hypotheses were also posited.

The first three hypotheses are as follow: 1) SARS-CoV-2 RNA can be measured in wastewater with sufficient sensitivity to perceive day-to-day variations in concentration, and support the establishment of a WEM program; 2) Trends of SARS-CoV-2 RNA concentrations in wastewater correlate with clinical disease metrics and can be used to offer early warning of increases or decreases in clinical case counts and hospitalizations; and 3) Incorporating measurement normalization strategies into WEM can enhance the robustness and interpretability of SARS-CoV-2 RNA concentration trends in wastewater. The fourth and fifth hypothesis were posited after initial findings demonstrated that PMMoV-normalization of SARS-CoV-2 RNA measurements in wastewater appeared to improve the interpretability of SARS-CoV-2 monitoring. The last hypotheses are as follow: 4) The concentration of PMMoV RNA fragments in wastewater is influenced by dietary intake and exhibits significant geographic variability; and 5) Additional tobamoviruses may be present in wastewater at concentrations sufficient for detection due to dietary intake, and could serve as alternative human fecal-associated biomarkers for wastewater-based epidemiology.

This research aims to address key methodological challenges in wastewater-based epidemiology (WBE) to enhance its reliability, interpretability, and utility as a public health tool. By doing so, it is hypothesized that WBE can provide early warning signals of infection dynamics, support public health decision-making, and improve community health outcomes. The specific objectives are as follow:

1) To improve laboratory methodologies for SARS-CoV-2 RNA detection in wastewater, with a focus on enhancing sensitivity and specificity during periods of low disease prevalence, to enable reliable day-to-day monitoring. This objective will be met by thoroughly investigating sampling locations at WRRFs.

2) To evaluate the effectiveness of WEM in detecting COVID-19 resurgences during periods of low clinical positivity and to develop WEM as an early warning tool complementary to traditional diagnostic methods. This objective will be met by performing extensive, time-lagged experiments to develop our understanding of the relationship between wastewater SARS-CoV-2 RNA concentrations, new clinical cases, and hospitalizations.

3) To assess and optimize sampling and testing strategies for small and rural sewersheds, including those served by non-mechanical wastewater treatment systems, to enable equitable implementation of WEM in smaller and rural communities. This objective will be met by comparing sampling locations in a small rural community and comparing the suitability of sampling locations, the correlation of measurements with clinical metrics and the integrity of RNA in the collected samples.

4) To investigate the utility of WC ratio in enhancing the interpretation of WEM data amid declining clinical testing and changing disease dynamics. This objective will be achieved through a meticulous, pan-Canadian study examining the intrinsic relationship between SARS-CoV-2 concentrations in wastewater and corresponding clinical case counts across seven major metropolitan areas.

5) To investigate the variability of PMMoV (concentrations in wastewater across geographic regions and populations, with a focus on understanding the influence of dietary intake on its reliability as a normalization biomarker, and to explore the presence and potential use of other tobamoviruses in wastewater as alternative human fecal-associated biomarkers, expanding the toolkit for normalization and improving the robustness of WEM data interpretation. This objective will be met by conducting a scoping review of all known tobamoviruses and comparing relative PMMoV RNA

concentrations in samples collected from numerous countries around the world to develop a better understanding of geographical and dietary effects on PMMoV concentrations in wastewater.

1.3. Thesis organization

The dissertation is structured as a manuscript-based thesis and comprises seven distinct chapters. Each chapter is designed to contribute a unique perspective and depth to the overall research, ensuring a comprehensive exploration of the subject matter. This organization allows for a detailed and systematic presentation of findings, methodologies, and discussions, providing a cohesive and thorough examination of the research topic.

Chapter 1 offers a comprehensive introduction to the study, outlining the overall and specific research objectives. It also provides a detailed description of the thesis structure, setting the stage for the subsequent chapters.

Chapter 2 (first manuscript) is a research article titled ***Quantitative analysis of SARS-CoV-2 RNA from wastewater solids in communities with low COVID-19 incidence and prevalence***. This article was published in *Water Research* in September 2020. This study investigates the feasibility of the detection and quantification of SARS-CoV-2 RNA in wastewater influent solids (post-grit solids; PGS) and primary clarified sludge (PCS) at two municipal water resource recovery facilities (WRRFs) serving Ottawa and Gatineau. Conducted during periods of decreasing (April to May 2020) and low (May to June 2020) COVID-19 incidence, the research aims to enhance viral detection sensitivity in low-prevalence communities. Utilizing RT-qPCR and RT-droplet digital (dd) PCR, the study compares the detection sensitivity of viral N1 and N2 RNA in PGS and PCS, addressing challenges of poor assay sensitivity and systematic variation. The research also examines human microbiome-specific HF183 Bacteroides 16S rRNA, human 18S rRNA, and pepper mild mottle virus (PMMoV) RNA as reliable fecal biomarkers to normalize SARS-CoV-2 signals. Findings suggest that PCS samples, especially when normalized to PMMoV, provide stable data correlating with regional public health metrics, positioning wastewater surveillance as a valuable tool for monitoring SARS-CoV-2 trends during low and declining COVID-19 incidence.

Chapter 3 (second manuscript) is a research article titled ***Catching a resurgence: Increase in SARS-CoV-2 viral RNA identified in wastewater 48 hours before COVID-19 clinical tests and 96 hours before hospitalizations***. This study was published in *Science of the Total Environment* in May 2021. This study investigates the effectiveness of wastewater-based COVID-19 surveillance in detecting resurgences of SARS-CoV-2 after periods of low prevalence. During the summer of 2020, SARS-CoV-2 RNA signals were measured in primary clarified sludge at Ottawa's water resource recovery facility every two days, when clinical testing showed daily percent positivity below 1%. The study detected a >400% increase in

normalized SARS-CoV-2 RNA in wastewater 48 hours before a >300% rise in reported positive cases and a >160% increase in hospitalizations by approximately 96 hours. This highlights the potential of WEM to complement, expand, and enhance traditional diagnostic testing. The research also compares the sensitivity of viral detection in primary clarified sludge versus influent and evaluates the use of fecal biomarkers like PMMoV and crAssphage to normalize SARS-CoV-2 signals. By correlating wastewater RNA signals with community infection rates and hospitalizations, the study aims to provide public health units with a predictive tool for early detection of COVID-19 resurgences.

Chapter 4 (third manuscript) is a research article titled ***COVID-19 wastewater-based epidemiology in rural communities: Comparison of lagoon and pumping station samples***. This study was published in *Science of the Total Environment* in December 2021. This study examines the implementation of WEM to monitor COVID-19 prevalence in small and rural communities, addressing a knowledge gap as most WEM efforts focus on urban areas. By comparing SARS-CoV-2 RNA signals from wastewater samples collected at an upstream pumping station and a downstream wastewater treatment lagoon in a rural Canadian community, the study evaluates the correlation with community COVID-19 incidence rates. Over a period of 5.5 weeks, real-time quantitative PCR (RT-qPCR) targeting the N1 and N2 genes showed strong viral signals in 24-hour composite samples from the pumping station, while samples from the lagoon were below the limit of quantification, indicating higher RNA stability upstream of the lagoon. Normalizing SARS-CoV-2 signals with PMMoV allowed for accurate detection of changes in community prevalence. The findings suggest that in small and rural communities with sewered systems, wastewater surveillance samples should be collected from pumping stations or the sewershed rather than lagoons, which present challenges due to RNA degradation and variable environmental conditions. This study supports the adaptation of WEM for effective monitoring of COVID-19 in smaller communities.

Chapter 5 (fourth manuscript) is a research article titled ***Wastewater to clinical case (WC) ratio of COVID-19 identifies insufficient clinical testing, onset of new variants of concern and population immunity in urban communities***. This study was published in *Science of the Total Environment* in December 2022. This study explores the use of the SARS-CoV-2 wastewater signal to clinical cases (WC) ratio as a diagnostic tool to complement clinical testing during the COVID-19 pandemic. By analyzing data from seven Canadian cities over periods ranging from 8 to 21 months, the study identifies significant epidemiological events. An increase in the WC ratio was observed when clinical testing eligibility shifted to appointment-only, indicating insufficient testing despite rising wastewater signals. The ratio also highlighted the emergence of the Alpha, Delta, and Omicron variants, with notable changes correlating to varying levels of community immunity. The study demonstrates that the WC ratio can provide valuable insights into testing efficacy and disease trends, enhancing the utility of WEM as a diagnostic technology,

especially as clinical testing declines in an endemic state. This research underscores the importance of integrating WEM data with clinical case counts to improve public health monitoring and response.

Chapter 6 (fifth manuscript) is a review article titled ***From plant pathogen to public health tool: A review of tobamoviruses and their role in wastewater & environmental surveillance***. This manuscript has been prepared and will be submitted to the journal *Reviews in Environmental Science and Bio/Technology*. This review article evaluates the potential of various tobamoviruses as biomarkers for WEM, with a focus on enhancing the accuracy and reliability of tracking respiratory diseases such as COVID-19. While PMMoV and ToBRFV have been widely used in WEM due to their high titers in wastewater, the suitability of other tobamoviruses remains underexplored. By reviewing over 240 studies and assessing 43 tobamoviruses, we identified 15 with significant promise as biomarkers. This comprehensive review addresses challenges in normalizing biomarker measurements and proposes the integration of these tobamoviruses to improve WEM applications. Our findings aim to pave the way for more robust environmental health monitoring strategies, contributing to the standardization of fecal biomarkers in global wastewater contexts and enhancing the efficacy of WEM as a diagnostic technology.

Chapter 7 (sixth manuscript) is a research article titled ***Globally validated real-time PCR assay for the detection of pepper mild mottle virus in wastewater***. This manuscript has been prepared and will soon be submitted to the journal *Journal of Virological Methods*. The study develops a globally validated RT-qPCR assay (P17 assay) for PMMoV quantification, a key biomarker in WEM. PMMoV normalization is crucial for accurately quantifying pathogen levels in wastewater, enabling public health officials to make better-informed decisions. However, existing assays lack global validation for sensitivity and consistency, leading to potential variability in data interpretation across geographical regions and changing diets.

To address this, 116 samples from 12 countries were analyzed, testing overlapping RT-qPCR assays across the PMMoV genome. A conserved region between bases 2776–3023 in the replication-associated protein-encoding sequence was identified. The P17 PMMOV assay targeting this region demonstrated superior sensitivity (ALOD: 3.4 copies/reaction; ALOQ: 4.9 copies/reaction) and similar real-world performance compared to existing assays. The primary goal of this work is to standardize PMMoV-based normalization globally, reducing variability and ensuring that wastewater surveillance data are reliable and actionable. By improving the accuracy of WEM, this assay supports global efforts to monitor and respond to public health threats more effectively.

Chapter 2 – Quantitative Analysis of SARS-CoV-2 From Wastewater Solids in Communities With Low COVID-19 Incidence and Prevalence

2.1. Context

The manuscript presented in this chapter of the doctoral dissertation is titled *Quantitative analysis of SARS-CoV-2 RNA from wastewater solids in communities with low COVID-19 incidence and prevalence*, by Patrick M. D'Aoust, Élisabeth Mercier, Danika Montpetit, Jian-Jun Jia, Ilya Alexandrov, Nafisa Neault, Aiman Tariq Baig, Janice Mayne, Xu Zhang, Tommy Alain, Marc-André Langlois, Mark R. Servos, Malcolm MacKenzie, Daniel Figeys, Alex E. MacKenzie, Tyson E. Graber, and Robert Delatolla, and was published in *Water Research* (January 2021). In this manuscript, different sampling locations and quantification technologies are investigated to determine the most sensitive and robust environmental monitoring strategy for measuring SARS-CoV-2 viral signal in wastewater. This manuscript was the first original research-based Canadian manuscript published on the topic, and is currently the 27th most cited manuscript in the journal *Water Research* over the last 5 years.

2.2. Abstract

In the absence of an effective vaccine to prevent COVID-19 it is important to be able to track community infections to inform public health interventions aimed at reducing the spread and therefore reduce pressures on healthcare, improve health outcomes and reduce economic uncertainty. Wastewater surveillance has rapidly emerged as a potential tool to effectively monitor community infections through the measurement of trends of RNA signal in wastewater systems. In this study SARS-CoV-2 viral RNA N1 and N2 genes are quantified in solids collected from influent post grit solids (PGS) and primary clarified sludge (PCS) in two water resource recovery facilities (WRRF) serving Canada's national capital region, i.e., the City of Ottawa, ON (pop. ≈ 1.1M) and the City of Gatineau, QC (pop. ≈ 280K). PCS samples show signal inhibition using RT-ddPCR compared to RT-qPCR, with PGS samples showing similar quantifiable concentrations of RNA using both assays. RT-qPCR shows higher frequency of detection of N1 and N2 genes in PCS (92.7, 90.6%, n = 6) as compared to PGS samples (79.2, 82.3%, n = 5). Sampling of PCS may therefore be an effective approach for SARS-CoV-2 viral quantification, especially during periods of declining and low COVID-19 incidence in the community. The pepper mild mottle virus (PMMoV) is determined to have a less variable RNA signal in PCS over a three-month period for two WRRFs, regardless of environmental conditions, compared to Bacteroides 16S rRNA or human 18S rRNA, making PMMoV a potentially useful biomarker for normalization of SARS-CoV-2 signal. PMMoV-normalized PCS RNA signal from WRRFs of two cities correlated with the regional public health epidemiological metrics,

identifying PCS normalized to a fecal indicator (PMMoV) as a potentially effective tool for monitoring trends during decreasing and low-incidence of infection of SARS-Cov-2 in communities.

2.3. Introduction

Since the onset of the novel coronavirus disease in 2019 (COVID-19), the rapid transmission and global spread of the disease has placed significant strain on public health agencies around the world. Detection of SARS-CoV-2 RNA in nasopharyngeal (NP) swab specimens by reverse transcription quantitative polymerase chain reaction (RT-qPCR) is the standard diagnostic test to confirm COVID-19. Accurately measuring the prevalence of COVID-19 in many countries has been complicated by limited and/or biased NP testing (targeting symptomatic groups) and an asymptomatic, or mildly symptomatic infectious period in a significant proportion of cases (Long et al., 2020; Pan et al., 2020). Additional detection tools are thus desirable to mitigate these challenges and provide public health agencies and governments new metrics to help guide their implementation of societal restrictions (Daughton, 2009; Hill et al., 2020; Thompson et al., 2020).

Recent systematic reviews and meta-analyses of the current peer-reviewed and preprint literature confirm fecal SARS-CoV-2 viral RNA detection in roughly half of COVID-19 patients (Gupta et al., 2020; Parasa et al., 2020). Moreover, a systematic review and meta-analysis of SARS-CoV-2 viral RNA detection profiles in several different types of COVID-19 patient specimens found that positive detection rates were higher in rectal and sputum swabs than in the commonly used NP swab (Bwire et al., 2020). These data provide a clear rationale to probe wastewater for SARS-CoV-2 RNA.

Medema et al. (2020) first reported the detection of SARS-CoV-2 viral RNA in wastewater from WRRFs located in seven different cities in the Netherlands. SARS-CoV-2 viral RNA has subsequently been identified and is being monitored at numerous WRRFs around the world (Ahmed et al., 2020; Alpaslan-Kocamemi et al., 2020; Bar Or et al., 2020; Gonzalez et al., 2020; Haramoto et al., 2020; La Rosa et al., 2020; Medema et al., 2020; Nemudryi et al., 2020; Peccia et al., 2020a; Randazzo et al., 2020; Rimoldi et al., 2020; Sherchan et al., 2020; Wu et al., 2020; Wurtzer et al., 2020; Zhang et al., 2020), with the first peer-reviewed study published by Ahmed et al. 2020a in Australia. The successful monitoring of the viral signal has led the Netherlands (National Institute for Public Health and the Environment, 2020), Australia (Dalzell, 2020), Germany (Pleitgen, 2020) and Finland (Yle, 2020) to plan and implement national wastewater surveillance programs for SARS-CoV-2 as a viral tracking tool to complement existing public health metrics. There are also early and promising indications from several research groups that wastewater

surveillance of SARS-CoV-2 might be predictive, providing earlier warning of community outbreak than current NP-based PCR diagnostics.

Although studies reported some success in the detection and even quantitation of SARS-CoV-2 RNA by RT-qPCR in wastewaters over the course of community COVID-19 outbreaks, poor assay sensitivity and systematic variation represent significant challenges, particularly in regions with low COVID-19 prevalence (Bar-On et al., 2020; Michael-Kordatou et al., 2020; Orive et al., 2020; Randazzo et al., 2020). Specifically, monitoring in communities with low incidence has demonstrated high PCR Ct values and hence variable or unquantifiable data being collected due to very low concentrations of the viral fragments in wastewaters. In this regard, at least two groups have identified improved sensitivity in solids-rich wastewater samples collected from WRRFs in communities with low incidence and prevalence (<25 active cases/100,000 population) (Balboa et al., 2020; Peccia et al., 2020b, 2020a). However, it has been observed that due to variations both in case numbers and influent wastewater sample data (Medema et al., 2020; Wu et al., 2020), studies have so far reported high day to day variance and noise (Balboa et al., 2020; Peccia et al., 2020a); which is a key challenge in establishing trends and extracting meaningful information from SARS-CoV-2 wastewater sentinel surveillance programs to date.

This study investigates and optimizes the detection of SARS-CoV-2 RNA in wastewater influent solids (post-grit solids; PGS) and primary clarified sludge (PCS) in two municipal WRRFs serving Ottawa and Gatineau beginning after the height of the epidemic with a period (April to May 2020) characterized by decreasing COVID-19 incidence and a subsequent period (May to June 2020) of low COVID-19 prevalence. Using both RT-qPCR and RT-droplet digital (dd) PCR, rigorous quality control metrics are applied to compare the detection sensitivity of viral N1 and N2 RNA in PGS compared to PCS using two different established primer/probe sets. Furthermore, the study tests the human microbiome-specific HF183 *Bacteroides* 16S ribosomal RNA (rRNA), human 18S rRNA and pepper mild mottle virus (PMMoV) RNA as reliable and robust nucleic acid normalization fecal biomarkers that can be used to control systematic noise associated with variances in WRRF daily operations, sampling, storage, processing and analysis of the samples. Finally, the study compares and correlates biomarker normalized longitudinal data sets of the two municipalities with epidemiological metrics to evaluate the usefulness of SARS-CoV-2 viral measurements in wastewater as a complimentary tool to clinical testing in a community during decreasing and low COVID-19 incidence.

2.4. Materials and methods

2.4.1. Characteristics of the City of Ottawa and Gatineau WRRFs

Post-grit chamber influent solids and primary clarified sludge samples were collected from the City of Ottawa's Robert O. Pickard Environmental Centre, Ontario and the City of Gatineau, Quebec water resource recovery facilities (WRRFs). The two facilities are located across the Ottawa River from each other in the national capital region of Canada (Figure 2-1). The two WRRFs service over 1.3 million people, or approximately 3.7% of Canada's total population. The sewershed of the City of Ottawa WRRF services approximately 1.1M people and the sewershed of the city of Gatineau WRRF services approximately 280K people.

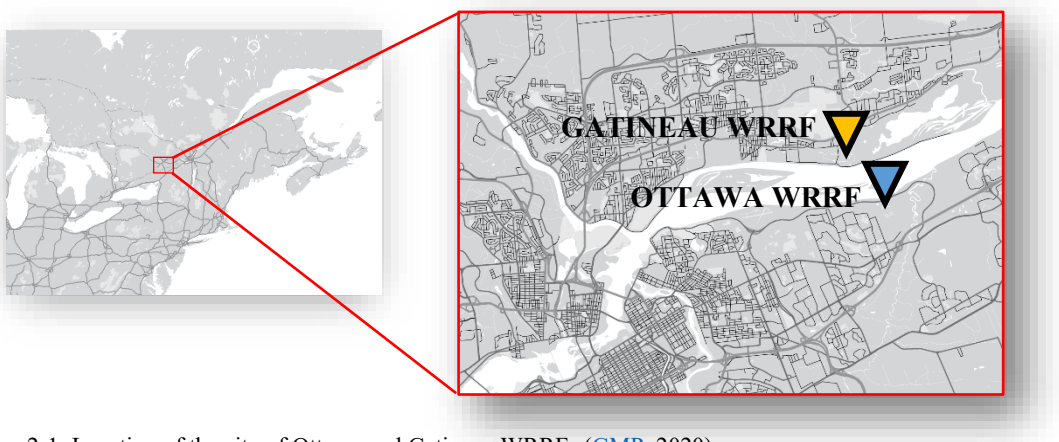


Figure 2-1: Location of the city of Ottawa and Gatineau WRRFs (GMP, 2020).

Ottawa and Gatineau WRRFs are designed and operated as conventional activated sludge treatment systems. The grit chambers of both facilities, where a portion of the samples are collected in this study, are located toward the front of both WRRF treatment trains and are fed by coarse and fine screened wastewaters. The grit chambers of both facilities subsequently feed the primary clarifiers, where remaining portion of the samples are collected in this study. The hydraulic residence time of the Ottawa sewershed ranges from 2 hours to 35 hours, with an average residence time of approximately 12 hours. In comparison, the hydraulic residence time of Gatineau's sewershed ranges from 2 hours to 7 hours, with an average of approximately 4 hours.

2.4.2. Wastewater sampling and analysis

2.4.2.1. PGS samples

Fourteen and nine 24-hour composite PGS samples were analyzed from the Ottawa and Gatineau WRRFs, respectively, between April 1st and June 30th, 2020. Clean 250 mL HDPE sampling bottles were sanitized with a 10% bleach solution and then washed with RNAse AWAY™ (ThermoFisher, Ottawa, Canada), rinsed with deionized water, and sealed. The PGS samples in this study are collected in the stream exiting the grit chambers. These samples have large debris removed via screens as was the dense grit via the grit chamber. A bio-banked wastewater influent sample from a nearby WRRF collected in August 2019 was utilized as a SARS-COV-2 negative control.

250 mL hourly composite samples were collected over a 24-hour period (for a total of 6 L) using an ISCO autosampler (Hoskin Scientific, Burlington, Canada) that collects directly from the exit stream of the grit chamber units at both facilities. The samples in the ISCO autosamplers were maintained at approximately 4°C during sampling with the frequent addition of ice (with a maximum recorded temperature of 7°C across the study). Starting in June, the ISCO autosamplers were linked to refrigerators, allowing the samples to be kept at temperatures of approximately 2°C immediately upon collection. The harvested samples were transported from the WRRFs to the laboratory in coolers packed on ice and were immediately refrigerated at 4°C for a maximum of 24 hours prior to analysis.

2.4.2.2. PCS samples

For the first 55 days of the study, between April 1st and June 30th, 2020, grab samples of PCS were collected every second week at the Ottawa and Gatineau WRRFs. These sludge samples were harvested from the primary sludge streams in the two facilities at the manifold where the primary clarified sludge that exits all primary clarifiers was mixed into a single stream. From day 56 onward, with the stronger RNA signal detected in PCS samples as compared to PGS samples, 24-hour composite PCS samples were collected by plant process technicians every other day at the Ottawa facility. The 24-hour composite samples collected at the Ottawa WRRF were comprised of four grab samples collected every 6 hours. Upon collection, samples were stored on-site at the Ottawa facility at 4°C in a refrigerator until mixed to form daily 24-hour composite samples and transported on ice to the laboratory the subsequent day. All samples were stored at 4°C at the laboratory and processed within 6 hours of arrival. Samples which could not immediately be analyzed were stored at 4°C for a maximum of 24 hours prior to analysis in the laboratory. Meanwhile, in Gatineau, an ISCO autosampler was linked to a refrigerator and was connected to a PCS

sampling port. The autosampler collected hourly grab samples of 250 mL, which were subsequently mixed to form a 24-hour composite sample. Due to the size differences of the two facilities in this study and the available resources at the two facilities during the COVID-19 pandemic in Canada, the Gatineau facility sampling frequency was limited to a maximum of once a week as opposed to every second day as was performed at the larger Ottawa facility. The 24-hour composite samples were collected and transported on ice to the laboratory as outlined for the Ottawa samples.

2.4.2.3. Wastewater quality characterization of samples

The following PGS and PCS sample wastewater quality constituents were analyzed upon collection: biological oxygen demand (BOD) (5210 B) (APHA, WEF, 2012), chemical oxygen demand (COD) (SM 5220 D) (APHA, WEF, 2012), total suspended solids, volatile suspended solids, total solids and total volatile solids (TSS, VSS, TS & VS) (SM 2540 D, E & B) (APHA, WEF, 2012), total ammonia nitrogen (TAN) (SM 4500-C) (APHA, 1989).

2.4.3. SARS-CoV-2 concentration

A preliminary study was first performed on partitioned 24-hour composite PGS samples to identify fractions with SARS-CoV-2 RNA positivity (Figure 2-2). The 6 L, 24-hour composite PGS samples were first settled at 4°C for an hour. The supernatant was subsequently decanted and serially filtered through a 1.5 µm glass fiber filter (GFF) followed by a 0.45 µm GF6 mixed cellulose ester (MCE) filter (filtrate fraction). An eluate fraction was then collected by passing 32 mL of elution buffer (0.05 M KH_2PO_4, 1.0 M NaCl, 0.1 % (v/v) Triton X-100, pH 9.2) through the spent filters. Each of the three fractions were subsequently PEG-concentrated and extracted and analyzed for SARS-CoV-2 RNA.

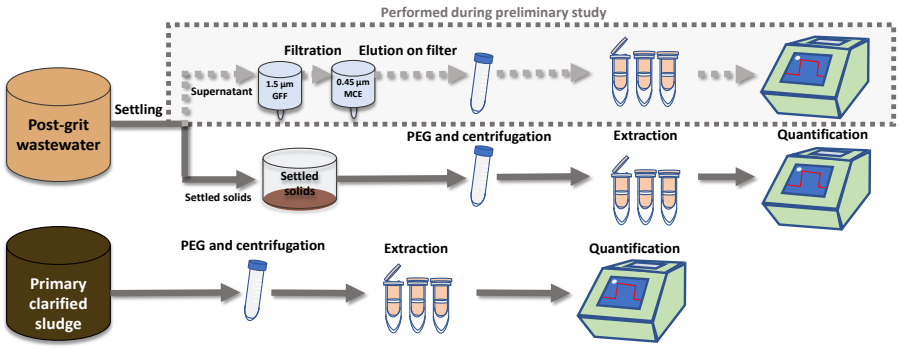


Figure 2-2: Flowchart showing sample work-up and processing for PGS and PCS, including RNA concentration, extraction and quantification.

To concentrate viral particles, nucleic acids, and proteins, 32 mL of PGS or PCS was precipitated with polyethylene glycol (PEG) 8000 at a final concentration of 80 g/L and 0.3M g/L NaCl, pH 7.3 and in a final volume of 40 mL (Comelli et al., 2008; Petterson et al., 2015). Samples were then agitated at 4°C on an orbital shaker set at 160 RPM for a period of 12 to 17 hours, then centrifuged at 10,000 x g for 45 minutes at 4°C. The supernatant was decanted, being careful to preserve any pellet. Samples were then centrifuged a second time at 10,000 x g for another 10 minutes and the remaining supernatant decanted. The resulting PCS and PGS pellets were transferred to a new RNase-free centrifuge tube and frozen at -80°C until RNA extraction.

2.4.4. RNA extraction

Viral RNA was extracted from PGS and PCS samples using the RNeasy PowerMicrobiome Kit (Qiagen, Germantown, MD), with the following deviations from the manufacturer's recommended protocol: i) 200 mg of sample pellet was added to the initial extraction step in place of 200 µL of liquid sample, and ii) the optional phenol-chloroform mixture addition to the lysis buffer was substituted with Trizol LS reagent (ThermoFisher, Ottawa, Canada) to maximize lysis of cells/virion encapsulated fragments and protect RNA prior to vortexing and centrifugation. The resulting aqueous phase of the lysis procedure was then retained and processed as per the recommended protocol including the on-column enzymatic DNA removal step. RNA was eluted in 100 µl of RNAse-free water.

2.4.5. Viral recovery efficiency

An important metric in the quantification of viral signal in wastewater is the process recovery efficiency for targets of interest, as it facilitates a comparison of results from study to study, even if different

sample processing or extraction methodologies/techniques are used. In this study, the efficiency of virus recovery following the fractionation, PEG concentration and RNA extraction process was determined by spiking vesicular stomatitis virus (VSV) (Hoang et al., 2019) into the sample and letting it mix at 4°C for one hour, before quantifying the recovered quantities of virus after sample processing. Spiking samples with a human coronavirus with low pathogenicity such as HCoV-229E as a recovery control (Gundy et al., 2009) was desirable but not practical due to the relative difficulty of its procurement in Canada at the time of this study and the difficulty of propagating coronaviruses in vitro. VSV is an enveloped, single stranded negative-sense RNA virus belonging to the *Rhabdoviridae* family, genus *Vesiculovirus* (Letchworth et al., 1999). The RNA genomes of both VSV and SARS-CoV-2 are encapsulated by a lipid envelope, and their particle sizes are similar; with VSV ranging from 70-200 nm (Cureton et al., 2010) and SARS-CoV-2 being approximately 100 nm (Bar-On et al., 2020). It was reasoned that these similar biophysical characteristics (lipid envelope and particle size) would lead both viruses to associate with wastewater matrices and to be precipitated with PEG with similar efficiencies. To maximize safety of the method, VSV was heat inactivated at 55°C for five minutes prior to use.

Recovery efficiency was quantified twice during this study, following procedures similar to those outlined in Annex G of ISO 15216-1:2017 (ISO, 2017; Lowther et al., 2019; Randazzo et al., 2020). VSV was quantified via RT-ddPCR for both PGS and PCS from triplicate, serial dilutions of $5.5x10^4$, $5.5x10^5$, $5.5x10^6$ and $5.5x10^7$ copies VSV/µL of inactivated stock VSV culture spiked into the collected PGS samples and the PCS samples. Throughout the study, quantified quantities were not corrected for process extraction efficiency or for PCR inhibition. Three PCS and PGS samples were each spiked with 10 µL aliquots of $5.5x10^4$, $5.5x10^5$, $5.5x10^6$ and $5.5x10^7$ copies/µL. These samples were directly concentrated, extracted and quantified using RT-qPCR. The VSV recovery efficiency (mean and standard deviation) was calculated based on the number of copies quantified using RT-qPCR. The equation for the calculations is as follows:

Eq. 2.1: $$Viral\ recovery\ efficiency\ (\%) = \frac{Total\ VSV\ gene\ copies\ recovered}{Total\ VSV\ gene\ copies\ spiked\ in\ grit/sludge} * 100\%$$

2.4.6. Variance of biomarkers for normalization

Analysis of variance was used to identify biomarkers with low variability and higher temporal consistency. The analysis of variance was conducted on 30 PGS and PCS samples over a period of 55 days (between April 8th 2020 and June 2nd 2020). The samples were analyzed for the following three internal normalization biomarkers: i) human microbiome-specific HF183 *Bacteroides* 16S ribosomal rRNA, ii) eukaryotic 18S rRNA and iii) PMMoV.

The three fecal content markers evaluated in this study for normalization of SARS-CoV-2 signal are all specific to humans and are detectable via probe-based qPCR. The 16S rRNA marker is expressed in gut-resident HF183 *Bacteroides* and has been previously detected in human feces and wastewater (Bernhard and Field, 2000; Green et al., 2014). 18S rRNA is expressed in human cells. PMMoV is a stable plant virus that is endemic in both sweet and hot pepper crops across the world and is shed in human feces following ingestion from pepper-containing foods (Rosario et al., 2009; Zhang et al., 2006). Importantly, unlike other enteric viruses that could be used as a fecal marker, PMMoV levels do not depend on active infection.

2.4.7. RT-qPCR

Preliminary testing of samples with the CDC N1, N2 and N3 primer-probe sets and the Sarbeco E-gene primer-probe set demonstrated best detection and least variance in technical replicates with the CDC N1 and N2 primer-probe sets. Singleplex, probe-based, one-step RT-qPCR (Reliance One-Step Multiplex RT-qPCR Supermix (Bio-Rad, Hercules, CA) was performed in this study using the 2019-nCoV Assay-RUO probe/primers mixes for CDC N1 and N2 gene regions (IDT, Kanata, Canada). Reactions were comprised of 1.5 µl of RNA template input, 500 nM each of forward and reverse primers along with 125 nM of the probes in a final reaction volume of 10 µl. Samples were run in triplicate. Using a CFX Connect qPCR thermocycler (Bio-Rad, Hercules, CA), RT was performed at 50ºC, 10 minutes, followed by polymerase activation at 95ºC for 10 minutes, and 45 cycles of denaturation, annealing/extension at 95ºC/10 s, then 60ºC/30 s, respectively. Serial dilutions of the viral RNA standard were run on every 96-well PCR plate to produce standard curves used to quantify the copies of SARS-CoV-2 genes. In addition, RT-ddPCR-quantified pooled samples of RNA template were serial diluted and utilized to construct standard curves for PMMoV normalization biomarker when RNA signal was normalized by the concentration of PMMoV. Additionally, RT-qPCR runs were validated with the use of non-template-controls (NTCs), positive controls, negative controls of pre-COVID 19 pandemic wastewater samples and dilutions.

The limit of detection of the RT-qPCR assay was determined for N1 and N2 gene regions, by determining the number of copies per reaction which corresponds to a detection rate of ≥ 95% (<5% false negatives), as recommended by the MIQE guidelines (Bustin et al., 2009). Furthermore, samples were discarded if they did not meet the following conditions: i) standard curves with $R^2 \geq 0.95$, ii) copies/reaction are in linear dynamic range of the curve and iii) primer efficiency between 90%-130%. Furthermore, sample replicates with values greater than 2 standard deviations from the mean of the triplicates were also identified as possible anomalies in this study and discarded.

2.4.8. RT-ddPCR

Singleplex, probe-based, one-step RT-ddPCR (1-Step RT-ddPCR Advanced Kit for Probes, Bio-Rad, Hercules, CA) was used for absolute quantification of SARS-CoV-2 N RNA in wastewaters using the CDC N1, N2 or N3 primer-probe sets, or E RNA expression, using the Sarbeco E-gene primer-probe set. Primers and probes used in this study were obtained from Integrated DNA Technologies, Inc (IDT, Kanata, Canada) and ThermoFisher. 5 µl of RNA template, 900 nM each of forward and reverse primers and 250 nM of the probe together with the supermix were assembled in a final reaction volume of 20ul. Samples were prepared and run in triplicate. Droplet generation was performed using a QX200 droplet generator (Bio-Rad, Hercules, CA). Droplets were transferred to a new microplate, and PCR was completed in a C1000 (Bio-Rad, Hercules, CA) thermocycler as follows: reverse transcriptase (RT) was performed at 50ºC, 60 minutes, followed by polymerase activation at 95ºC for 10 minutes, and 40 cycles of denaturation, annealing/extension at 94ºC/30 s, then 55ºC/60 s, respectively. The polymerase was deactivated at 98ºC for 10 minutes and droplets stabilized at 4ºC for 30 minutes. Droplets were then read using a QX200 droplet reader (Bio-Rad, Hercules, CA). Positive droplets were called manually, and absolute quantification was performed using Quantasoft Analysis Pro v.1.0 (Bio-Rad, Hercules, CA). The limit of detection of the RT-ddPCR assay was determined for N1 and N2 gene regions by determining the number of copies per reaction which corresponds to a detection rate of ≥ 95% (<5% false negatives), as recommended by the MIQE guidelines (Bustin et al., 2009).

2.4.9. Statistical analysis

In order to test for significant differences between data sets comparing the detection of SARS-CoV-2 in PGS and PCS samples, chi-square and Fisher's exact test statistical analyses were conducted using GraphPad's Prism 8.3 software (La Jolla, CA). A student's t-test was used to test for statistical differences between detection of RNA in RT-qPCR and RT-ddPCR assays for PGS and PCS. A student's t-test and Pearson's correlation analyses were performed to test for significance and the strength of the correlation between RNA signal and epidemiological data, with a *p*-value of 0.05 or lower signifying significance.

2.5. Results & discussion

2.5.1. Viral RNA recovery efficiency

The recovery through the concentration and extraction steps was quantified by spiking samples with serial dilutions of inactivated VSV. The percent recoveries for VSV spiked in PGS and PCS were 8.4 ± 3.6% and 9.3 ± 4.9%, respectively, determined by testing 30 samples. The recovery of the surrogate virus

through both PCS and PGS concentration and extraction was similar with all spiked-in quantities. Other recent studies investigating surrogate virus recoveries following similar PEG concentration reported variable results for various surrogates; <6% recovery of murine hepatitis virus (MHV) (Ye et al., 2016) along with reported recoveries of 33.3 ± 15.6% and 57% of *Escherichia virus* MS2 (MS2) by Balboa et al. (2020) (preprint) and Kumar et al. (2020). Other concentration methods have also been used, such as ultrafiltration and ultracentrifugation (~20% to 33.5% recovery efficiency of MHV) (Ahmed et al., 2020b; Ye et al., 2016) and aluminum hydroxide adsorption-precipitation (30.4 ± 11.0% recovery of *Mengovirus* (MGV)) (Medema et al., 2020). It is important to recognize that each study used slightly different methods and viral surrogates, making it difficult to make direct comparisons and generalizations (Lu et al., 2020; Michael-Kordatou et al., 2020). Each surrogate virus will differ in how it interacts with wastewater and this may also be dependent on the characteristics of the wastewater as well as the properties of the virus/fragment that may have very different partitioning/degradation characteristics. It is unclear yet how effective filtration-based concentration techniques perform with high-solid samples, especially with viruses that are highly associated with solids. When analyzing high solids containing samples, such as PGS and PCS, PEG precipitation or other flocculation approaches may be more effective due to an incompatibility of this matrix with ultrafiltration due to possible complication associated with membrane clogging (Fumian et al., 2010; Lu et al., 2020). The advantages of using PGS and PCS, which may have a greater and more consistent RNA signal, should be balanced against the apparent lower recovery of PEG precipitation. Additional studies are needed to develop and assess appropriate and effective methods and surrogates for analysis of SARS-Cov-2 in wastewaters.

2.5.2. Comparison of RT-qPCR and RT-ddPCR for the detection and quantification of SARS-CoV-2 RNA

This study tested the detection and quantification of RT-ddPCR and RT-qPCR for SARS-CoV-2 RNA signal in PGS and PCS samples. The in vitro transcribed RNA was observed to be reliably detected with primer-probe RT-ddPCR assays to a limit of detection of 5 copies/reaction in both N1 and N2 RT-ddPCR assays. This is consistent with the purported high sensitivity of the digital PCR technology. In vitro transcribed viral RNA was detected to a limit of detection of 2 copies/reaction in both the N1 and N2 RT-qPCR assays, (using the high sensitivity Bio-Rad One-Step Reliance Supermix (Bio-Rad, Hercules, CA)), which was unexpected when comparing to the RT-ddPCR limit of detection. Standard curves utilized for the quantification of different RNA targets for RT-qPCR are as follows: N1 (slope: -3.372, intercept: 38.184, R^2: 0.972, E: 97.96%), N2 (slope: -3.179, intercept: 37.870, R^2: 0.954, E: 106.32%), PMMoV (slope: -2.806, intercept: 39.142, R^2: 0.968, E: 127.17%) and VSV (slope: -3.518, intercept: 39.846, R^2: 0.995, E: 92.41%). The standard curves demonstrate good linearity for RT-qPCR in a range between 2 to 60

copies/reaction for N1 and N2, 1.4×10^2 to 3.6×10^4 copies/reaction for PMMoV and 1.6×10^0 to 1.6×10^4 copies/reaction for VSV. A comparison was performed between the one-step RT-qPCR and RT-ddPCR using the same singleplex N1 probe-primer set for the quantification of SARS-CoV-2 in solids-rich, low concentration SARS-CoV-2 RNA signal wastewaters (Figure 2-3). Six PGS samples and five PCS samples were analyzed using RT-qPCR and RT-ddPCR. All samples were collected from the two cities during the same low incidence periods (<60 active cases / 100,000 people) case number study period allowing the assessment of quantification and degree of variability in samples with low RNA concentrations. The mean and standard error of the PGS samples analyzed during the same period of low incidence cases are 133.4 ± 9.0 and 167.1 ± 25.6 N1 gene copies/100 µL of extracted RNA for RT-ddPCR and RT-qPCR, respectively. Meanwhile, the mean and standard error of the PCS samples are 33.5 ± 5.8 and 130.4 ± 20.8 gene copies/100 µL of extracted RNA for RT-ddPCR and RT-qPCR, respectively (Figure 2-3). Although a significant decrease in /detected copies for PCS samples with RT-ddPCR is observed, it is noted that the coefficient of variation (%CV) for the ddPCR assay (38.4%) compared to qPCR (35.7%). While the %CV for PGS samples for the ddPCR assay is lower (16.5%) compared to qPCR (37.5%).

The difference in quantification of the PCS samples between the N1 RT-qPCR and RT-ddPCR assays suggests inhibition of the reverse transcription and/or polymerase chain reaction of the PCS sample. Given that this assay partitions the sample volume into approximately 1 nL droplets, it's conceivable that the effective concentration of any RT and/or PCR inhibitors present in the PCS matrix are markedly increased. In contrast, RT-qPCR is performed in a non-partitioned assay volume and may thus be less sensitive to inhibition. The apparent inhibition in ddPCR may also be explained by differences in the reagents used for the RT-ddPCR and RT-qPCR assays. The inhibition resistance/inhibitor removal of the high sensitivity RT-qPCR reagent appears to provide better detection when utilized in pegged sludge

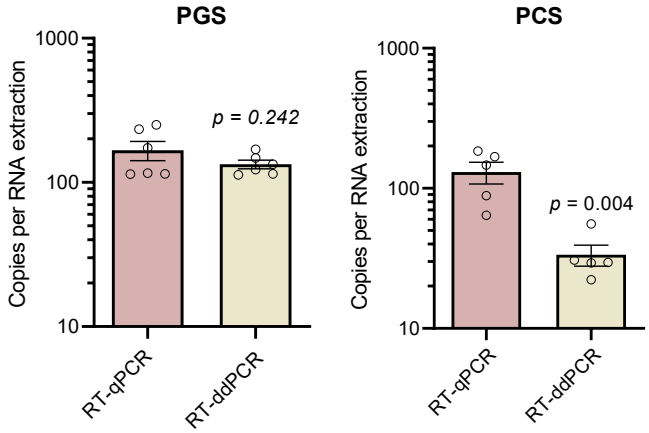


Figure 2-3: Comparison of copies per 100 µL of extracted RNA in RT-qPCR and RT-ddPCR for PGS (n=6) and PCS (n=5).

matrices. Quantification of two-fold and five-fold dilutions of PCS samples was performed and support the theory that RT-ddPCR was likely inhibited; RT-qPCR shows good quantification of diluted samples while RT-ddPCR suffered from inhibition. These findings contradict the theoretical assumption that RT-ddPCR is less prone to inhibition due to relative insensitivity to differences in amplification efficiencies (due to its binary "all-or-nothing" reporting of amplification) (Salipante and Jerome, 2020). However, at least one report found that undiluted raw wastewater inhibits one-step RT-ddPCR amplification of PMMoV RNA to the same degree as the RT-qPCR assay (Rački et al., 2014). Given that RNA in both PGS and PCS samples was at a very low concentration, approaching the limits of detection, it is highly likely that inhibitors in the PCS matrix are responsible for the decreased sensitivity observed in RT-qPCR vs. RT-ddPCR.

Of note, it was also attempted in this study to use a commercially available multiplex RT-ddPCR assay that employs primer-probe sets amplifying N1, N2 and N3 regions of the viral N RNA as well as a human transcript (SARS-CoV-2, Bio-Rad). However, it was determined that the discrimination between positive and negative droplets (fluorescence amplitude) was poor, making quantitative analysis impossible. RT-ddPCR has a myriad of theoretical advantages such as absolute quantification that is not dependent on calibration curves, insensitivity to common PCR inhibitors, and the ability to multiplex (Salipante and Jerome, 2020). There is a need to explore this further in future studies and to optimize these methods and quantification techniques for wastewater samples. However, based on the better detection using the current RT-qPCR approach, this method was utilized for the remainder of this study to quantify SARS-CoV-2 in both PGS and PCS solids from the Ottawa and Gatineau WRRFs.

2.5.3. Detection and variance of SARS-CoV-2 viral RNA in PGS and PCS

In this study, the sensitivity and variability of the RT-qPCR assay in PGS and PCS was compared by investigating the percentage of sample replicates; with replicates including repeated RNA extraction step and PCR quantification samples along with technical triplicates. The limit of detection used in the study for RT-qPCR assays is described above. Replicate runs (24 paired PGS and PCS samples, for a total of 72 technical replicates each) were collected on the same dates across 83 days. PCS samples collected and analyzed at the same time as PGS samples over a 3-month period exhibited stronger percent detection for N1 (92.7% for PCS compared to 79.2% for PGS, $p = 0.007$) and N2 (90.6% for PCS compared to 82.3% for PGS, $p = 0.092$) (Figure 2-4). Variance in percent detection of PCS was shown to be similar for all samples, with coefficients of variation ranging from 29.1% to 31.7%.

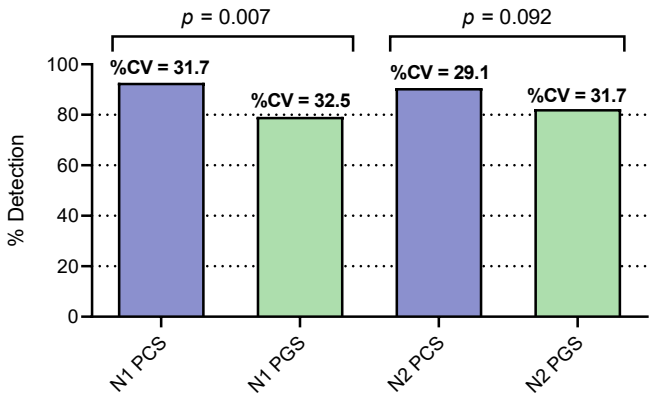


Figure 2-4: Sensitivity of N1 and N2 RT-qPCR assays comparison between PCS and PGS samples. Significance between detections established using Chi-Squared test. Variance is shown with %CV (n=24).

The decreased sensitivity of SARS-CoV-2 detection in PGS samples could be due to the increased susceptibility of solid particulate matter in this wastewater fraction to daily fluctuations in flowrate and wastewater biochemical characteristics at the WRRFs compared to the sludge samples collected in the primary clarifier stream. In addition, the PGS samples undergo a laboratory settling step in this study to isolate the settled solids from the liquid fraction of the sample. This additional step (which is not applied to the PCS samples) may also contributes to the lower percent detection of SARS-CoV-2 signal of these samples due to increased holding times and processing times. As such, the result of this study confirms PCS samples as the high-solids samples that demonstrate an elevated frequency of detection of SARS-CoV-2 N1 and N2 RNA in municipal wastewaters during decreasing and low incidence of community COVID-19 (Alpaslan-Kocamemi et al., 2020; Balboa et al., 2020; Peccia et al., 2020). In addition, it is noted that the viral RNA longitudinal trendline from the PGS samples did not show strong correlation with either the trendline from the PCS samples, or municipal epidemiological data, further supporting PCS sampling as the more robust basis for community COVID-19 monitoring in wastewater solids.

2.5.4. Variability of normalization biomarkers

A multitude of systematic variations exist in molecular wastewater surveillance that makes it challenging to accurately measure SARS-CoV-2 RNA across days, months and years. These include, but are not limited to: diurnal variation in plant flow, changes in gross proportions of solids, sample collection and storage, sample processing and sample analysis. Due to these factors, a critical aspect of wastewater epidemiology is sample normalization (Armanious et al., 2016). The necessity to normalize SARS-CoV-2 RNA data has also been identified in more recent studies (Alpaslan-Kocamemi et al., 2020; Kaplan et al.,

2020; Peccia et al., 2020; Wu et al., 2020). To compare the variability and temporal consistency of biomarkers in this study 8 PCS samples (24 including technical triplicates) were analyzed using RT-qPCR for all three biomarker gene regions: human-specific HF183 *Bacteroides* 16S rRNA, human eukaryotic 18S rRNA and PMMoV. All three tested biomarkers were detected in PCS samples with a relatively high level of expression (Ct values <30) compared to the incidence of SARS-CoV-2 N1 and N2 (Figure 2-5a). While all three biomarker targets were detected in PCS samples, it was observed that the distribution of their expression (i.e. quantified through an analysis of variance, VAR in Figure 2-5) of the fecal biomarker PMMoV was lower compared to the 16S and 18S biomarkers in PCS samples (Figure 2-5a). Date-correlated SARS-CoV-2 Ct values are also shown for reference (Figure 2-5). The lower variability of PMMoV (C_t variance = 1.18) compared to 16S (C_t variance = 5.32) and 18S (C_t variance = 5.12) may be due to the relative toughness and stability of the virus in difficult environments (Kitajima et al., 2018). The lower variability of PMMoV detection was also similar to the lower variability of the SARS-CoV-2 N1 and N2 data set. Furthermore, the viral fragments of the PMMoV biomarker may preferentially adhere to the solids fraction of wastewaters via electrostatic and/or hydrophobic effects (Armanious et al., 2016). Additionally, in order to quantify the variance of the normalization biomarkers in this study, the samples run this comparison were also verified across each surveyed WRRF independently (Figure 2-5b). The PMMoV internal normalization biomarker shows an improved consistency and lower variability (maximum change in C_t; ΔC_t = 0.01) between the WRRFs compared to 16S (ΔC_t = 1.47) and 18S (ΔC_t = 2.30); which demonstrates a relative steady signal between differing WRRFs. Due to the consistency of the PMMoV fecal biomarker in the PCS samples across 55 days of sampling, PMMoV was utilized in this study as a SARS-CoV-2 N1 and N2 RNA internal control for PCS samples. The low variance of PMMoV in PCS, coupled with the use of PMMoV as an internal normalization biomarker, was also recently reported by Wu et al. (2020). It is noted that for the purpose of using PMMoV as a normalization factor, it was always diluted 1:10 in pure water in order to ensure it remained in the quantifiable range of the PMMoV standard curve.

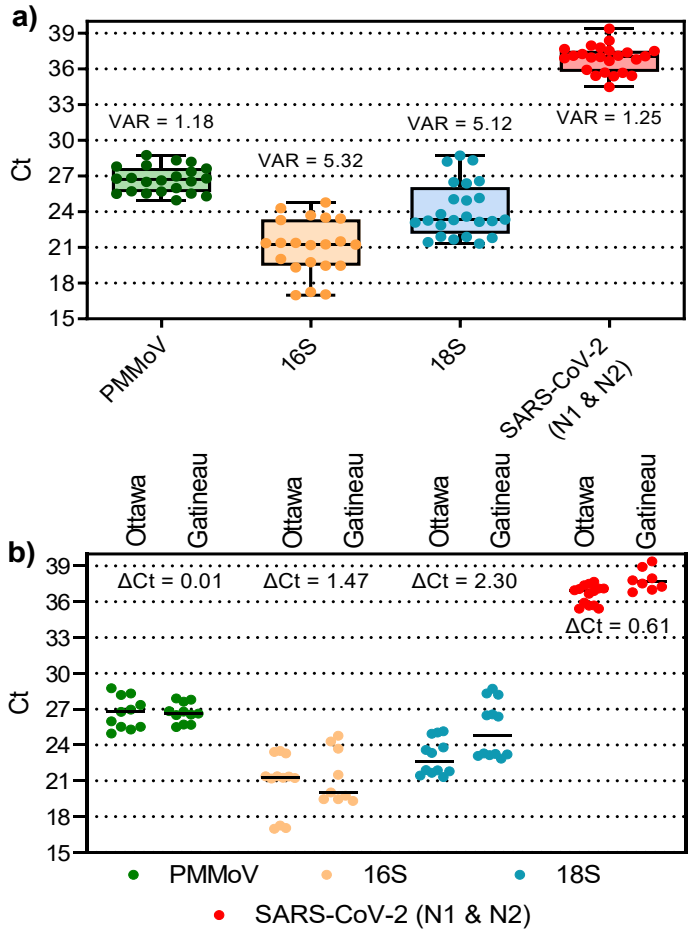


Figure 2-5: Variance of PCS normalization biomarkers (and SARS-CoV-2 for reference), a) combined data set comprised of both cities samples, and b) data set separated by city. Analysis of variance and maximum change in C_t (ΔC_t) (n=8).

2.5.5. Quantification of SARS-CoV-2 viral RNA in PCS and correlation with COVID-19 case data

As PCS was identified as the solids-rich sample showing the highest RNA detection rate, SARS-CoV-2 RNA was measured in PCS samples from Ottawa and Gatineau WRRFs between April 1st and June 30th, 2020. This sampling period encompasses a decreasing COVID-19 prevalence in two cities (peaks of 56.7 and 57.3 confirmed cases/100K inhabitants in Ottawa and Gatineau respectively) as well as an ensuing period of low prevalence characterized by many days with low new daily reported cases (56.7 → 4.8 and 57.3 → 10.2 confirmed cases/100K inhabitants in Ottawa and Gatineau, respectively). In addition to the technical triplicates of each sample, five of the 14 samples in Ottawa were re-extracted and re-quantified via RT-qPCR. In Gatineau, four of the 8 samples were re-extracted and re-quantified via RT-qPCR. Two distinct but complementary normalization approaches were applied to the observed SARS-CoV-2 RNA signal to account for variations in WRRF wastewater flow, composition and treatment along with temperature, time variations in travel and storage along with human errors in the processing of the samples. In particular, this study normalizes the RNA signal for i) the WRRF mass flux of solids in the sampled primary clarifier stream and ii) the PMMoV internal normalization biomarker expression. The SARS-CoV-2 viral RNA copies/L and the normalized viral data are benchmarked against and correlated to epidemiological metrics provided by the Ottawa public health agency and the regional public health agency of the city of Gatineau.

Three epidemiological data sets based on clinical testing were identified by the local public health agencies as best estimates of COVID-19 prevalence in the two cities: i) daily new cases of COVID-19, ii) active cases of COVID-19 based on an active period of fourteen days, and iii) percent positive of total daily reported clinical COVID-19 tests performed. Two key factors/limitations are noted with respect to these epidemiological data sets shown in this study. Firstly, the testing at the onset of the pandemic (March and April 2020) was variable and low in both cities due to limitations in human resources, laboratory reagents and testing equipment. Hence, the first four weeks of the twelve-week period for which wastewater samples were profiled were subject to variable and lower testing rates per day that likely under-reported both the number of new cases and active cases during this period. Secondly, early testing/screening was less available to the general population in both cities, with testing heavily biased towards hospitalized patients and health care workers. This potentially artificially inflates the percent positive data during the first four weeks of the study, with the effect on the percent positive being likely lesser than the effect of limited testing on the total case numbers.

2.5.6. SARS-CoV-2 RNA in PCS and correlation with COVID-19 case data

The average and standard deviation of technical triplicates and extraction replicates that repeated the concentration, extraction and RT-qPCR steps (shown as error bars in Figures 2-6 and 2-7) for the longitudinal viral RNA data sets in this study are plotted along with a percent positive and seven day floating average percent positive epidemiological data sets. Due to limited testing during the first four weeks of the longitudinal study, percent positive was identified as a potentially useful epidemiological metric of COVID-19 prevalence to compare to SARS-CoV-2 RNA measurements in wastewater. As such, this metric is included in Figures 2-6 and 2-7 to be benchmarked against the measured SARS-CoV-2 signal.

N1 and N2 RNA signal is first expressed in copies/L (of PCS) in this study (Figures 2-6a and 2-7a). Equivalent volumes of PCS were PEG concentrated and RNA extracted throughout the sampling period. As expected, and similar to other studies investigating primary sludge and wastewater solids, the raw copies/L data sets for the two cities (Figures 2-6a and 2-7a) are relatively noisy with no clear trend observed (Medema et al., 2020; Randazzo et al., 2020; Wu et al., 2020). The observed concentrations in this study (1.7×10^3 to 7.8×10^4 copies//L (Ottawa) and 6.6×10^4 to 3.8×10^5 copies/L (Gatineau)) are in agreement with other studies investigating SARS-CoV-2 RNA viral signal in PCS. Concentration ranges of 1.7×10^6 to 4.6×10^8 copies/L, 1×10^4 to 4×10^4 copies/L and 1.2×10^4 to 4.0×10^4 copies/L have been reported in PCS by (Alpaslan-Kocamemi et al., 2020; Balboa et al., 2020; Peccia et al., 2020) respectively. Note that these studies all used protocols with PEG concentration that are similar to this study.

Although the N1 and N2 RNA genes show similar longitudinal trends to each other in both the Ottawa and Gatineau WRRFs (Figures 2-6a and 2-7a), the inherent variations in signal results in noise, making it difficult to identify real changes in viral signal. In particular, this is seen in the large amplitudes of the standard deviations of many data points in the longitudinal data sets of Ottawa and Gatineau. The noise in the RNA data may be caused by inherent, weather-induced random variations in wastewater biochemical characteristics, solid composition and flowrate (e.g., due to weather, changes in daily household water consumption, etc.) as well as potentially significant effects associated with the collection and transport of the samples and RNA concentration, extraction and analysis. The copies/L longitudinal data in Ottawa and Gatineau clearly demonstrate that SARS-CoV-2 quantification in wastewater is inherently noisy and hence normalization of the data should be explored.

No significant correlation between N1 and N2 at either the Ottawa WRRF or the Gatineau WRRF is observed across the study time period (Table 2-1). Strong and significant correlation would have suggested that SARS-CoV-2 RNA might be intact in PCS prior to concentration and extraction, which is

not herein observed in this study. Critically, when comparing either N1 or N2 copies/L to each of the epidemiological metrics (daily cases, active cases and percent positive) it appears that in Ottawa no correlation exists between the N1 or N2 RNA copies/L signal and any of the three epidemiological metrics. Meanwhile, in Gatineau, significant correlations exist between the N1 and N2 copies/L signal and epidemiological data sets, with the strongest correlations being observed with the number of active cases (Table 2-1).

2.5.7. Mass flux of primary clarified sludge copies SARS-CoV-2 RNA per day and correlation with COVID-19 case data

To correct for systematic variability, the first normalization approach applied in this study is to normalize the N1 and N2 RNA signal to both the mass of the PEG-concentrated solids subject to nucleic acid extraction and also the daily mass flux (mass of volatile solids (VS) solids through the primary clarifier stream per day) at each WRRF (Figures 2-6b and 2-7b). This normalization approach results in units of N1 and N2 copies/day as a solids mass flux basis through the WRRF. This normalization approach is intended to compensate for variations in solids concentration and flowrate in the primary clarifier stream at the WRRF due to weather effects, precipitation and infiltration/inflow in the sewers. It is noted that no correlation was observed between N1 and N2 RNA signal and BOD mass flux, TSS mass flux or influent flow rate at the Ottawa and Gatineau WRRFs. Hence normalization of RNA signal with these parameters are not herein shown. The lack of correlation between RNA signal and these parameters in this study are likely due to the sampling location used in this study; as primary clarified sludge is less susceptible to influent mass flux and flow rate variations.

When comparing longitudinal plots in Ottawa of copies/L (Figure 2-6a) to copies/d (Figure 2-6b), the variance of the solids mass flux normalized data set of copies/d does not appear to have been significantly reduced the systemic noise of the copies/L data sets. Similar findings are observed for the Gatineau normalized data (Figures 2-7a and 2-7b). The substantial noise maintained in the solids mass flux normalized data sets of the two cities and the significantly large standard deviations of longitudinal data points indicates that the fluctuations associated with the solids concentration and flowrate in the primary clarifier stream was likely not a dominant source of the inherent variance in the copies/L data sets.

As observed for the copies/L data, the correlation between the N1 and N2 data sets were not significant for either Ottawa or Gatineau. Further, the normalization of the N1 and N2 data for solids mass flux at the WRRFs appear to worsen correlations, with anticorrelations increasing, for all three epidemiological metrics in Ottawa and Gatineau (Table 2-1). This lack of impact when normalizing

operational mass flux of solids at the two WRRFs in this study is likely due to the fact that both WRRFs directly control the flow of the primary clarifier stream at their respective facilities, hence reducing the variation in the flux of solids and in turn minimizing the impact of this variation in WRRF operation on the N1 and N2 signal. Thus, systematic variation in the data sets are likely associated with the sample collection and storage along with RNA concentration, extraction and analysis steps performed in the study.

2.5.8. PMMoV-normalized SARS-CoV-2 RNA in PCS and correlation with COVID-19 case data

PMMoV is the most abundant human fecal RNA virus (Kitajima et al., 2018) and has been previously proposed as a biomarker for fecal contamination in water (Hamza et al., 2011; Rosario et al., 2009). PMMoV has also more recently been used as an internal reference for SARS-CoV-2 in wastewater (Wu et al., 2020). The second normalization approach applied in this study is the division of the RNA N1 and N2 copies by PMMoV copies. Due to its low variability and high expression in PCS, PMMoV was identified as the preferred internal reference of the three tested biomarkers tested in this study.

PMMoV normalization appears to sufficiently reduce background noise associated with systematic variations in the Ottawa and Gatineau WRRF RNA signals that are possibly associated with the collection and transport of the samples along with the RNA concentration, extraction and analysis steps of PCS RNA signal during decreasing and low incidence periods of COVID-19 disease in this study (Figure 2-6c and 2-7c). In particular, the amplitude of the standard deviation associated with each data point in the longitudinal data sets of Ottawa and Gatineau decreased. This increase in precision ultimately allows for greater distinction between low-incidence data points, hence enabling improved identification of trends in the data sets.

Correlation between the PMMoV normalized N1 and N2 signals remained insignificant in Ottawa and Gatineau (Table 2-1). However, this normalization approach also outlines strong, significant and positive correlations between both the N1 gene and the N2 gene with all three epidemiological data sets in Ottawa. The strongest correlation between N1 and N2 PMMoV normalized RNA signal is observed with the 7-day rolling average percent positive epidemiological metric in Ottawa. Although the percent positive data during the first four weeks of the study may be biased towards hospitalized patients and health care worker testing, this clinical testing metric in Ottawa is identified as the preferred metric by the public health unit of the city (for the reasons described above). As such, decreasing the systematic variation in the data sets via PMMoV normalization establishes a modified trend of the RNA signal and this trend shows the strongest correlation of the RNA signal to city's identified preferred epidemiological metric.

Strong, significant and positive correlation is also shown between the N1 PMMoV normalized RNA signal with the active cases epidemiologic metric in Gatineau; while the N2 PMMoV normalized signal shows moderate, significant correlation to the active cases. Although the PMMoV normalized Gatineau RNA signal data shows agreement with the active cases epidemiological metric, results were varied when correlated to daily cases and 7-day rolling average percent positive. The strongest correlation observed in this study for the Gatineau RNA signal and the epidemiological metrics of the City exists between both the N1 and N2 copies/L RNA signal and the active cases. It is also noted that the longitudinal trends in N1 and N2 PMMoV signals in Gatineau are similar to those in Ottawa. This is expected as the two cities are geographically close with many inhabitants travelling across bridges between the cities. The observed differences in correlations between SARS-CoV-2 RNA signal in wastewater to clinical testing metrics in the two neighboring cities of this study is illustrative of the challenges associated with interpreting and correlating RNA signal acquired from distinct WRRFs to clinical testing metrics acquired from distinct health agencies.

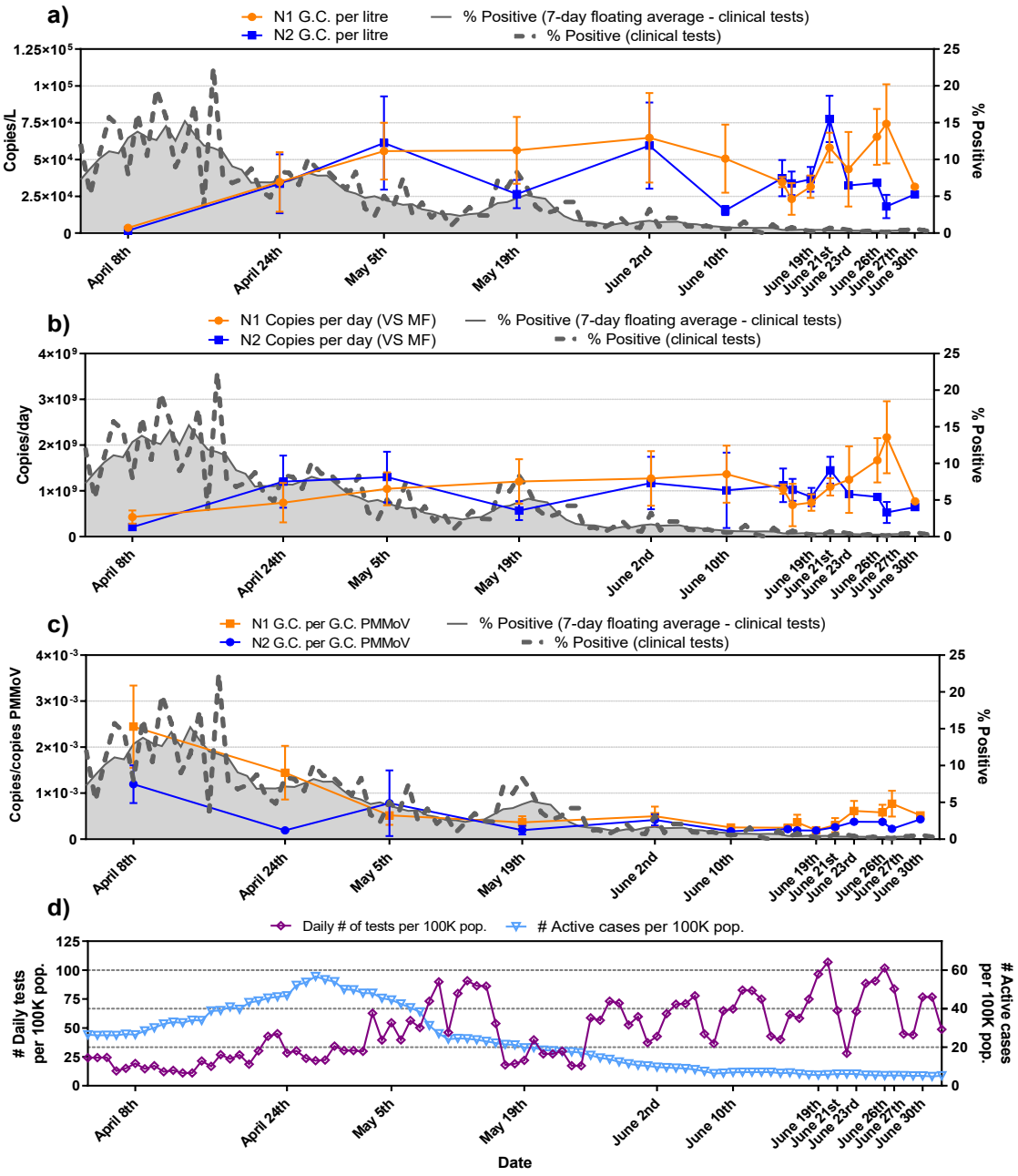


Figure 2-6: Ottawa WRRF trends of N1 and N2 SARS-CoV-2 viral copies with epidemiological metrics, a) copies/L of PCS, b) copies/d that was normalized by the mass flux through primary clarifier, c) copies/copies of PMMoV that was normalized by PMMoV reference gene and d) graph displaying the daily number of tests performed and the number of active COVID-19 cases/100K population.

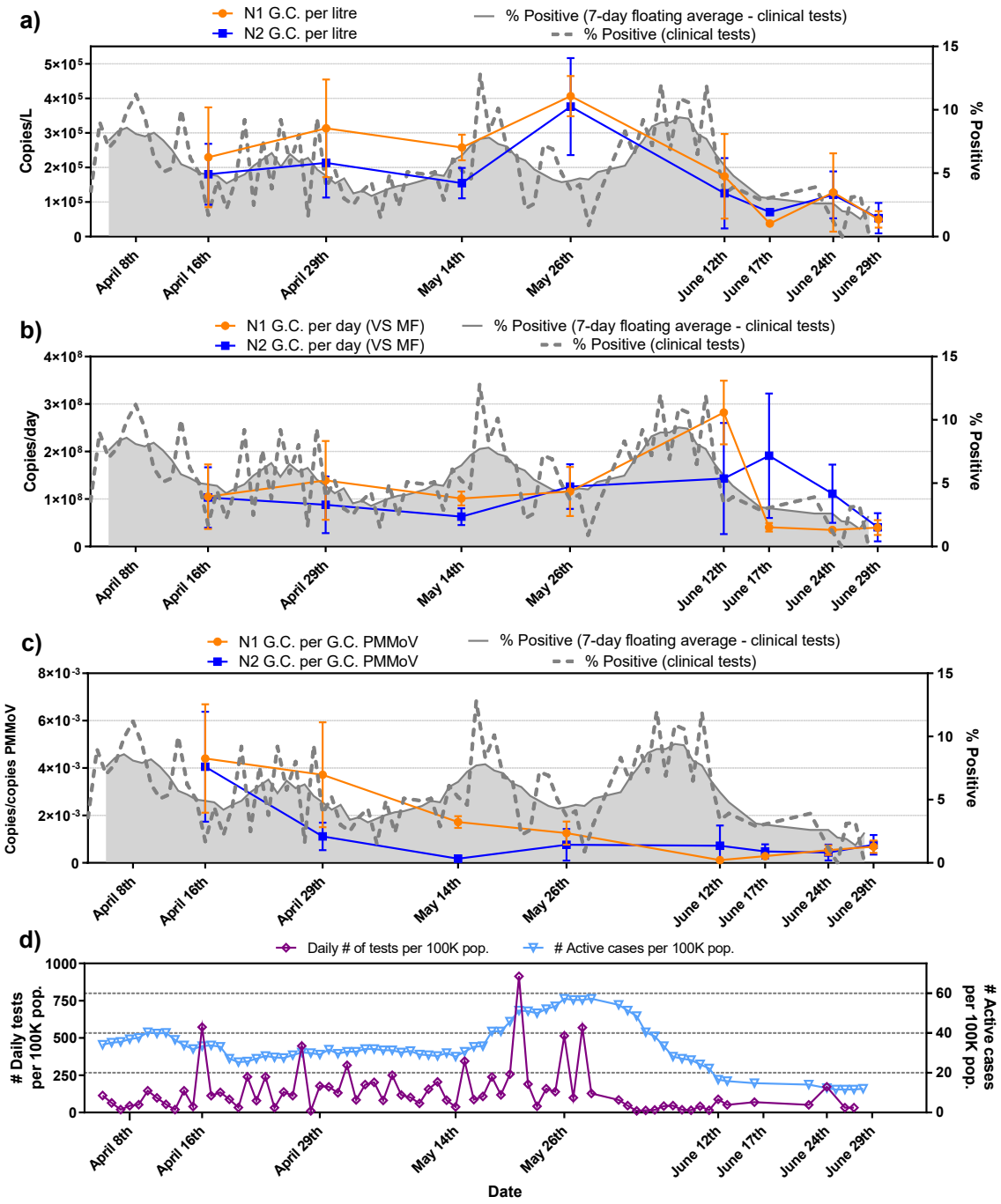


Figure 2-7: Gatineau WRRF trends of N1 and N2 SARS-CoV-2 viral copies with epidemiological metrics, a) copies/L of PCS, b) copies/d that was normalized by the mass flux through primary clarifier, c) copies/copies of PMMoV that was normalized by PMMoV reference gene and d) graph displaying the daily number of tests performed and the number of active COVID-19 cases/100K population.

Table 2-1: Correlation analyses between SARS-CoV-2 RNA signal in PCS in the Ottawa and Gatineau WRRFs with epidemiological metrics. RNA signal is expressed as copies/L of PCS, copies/d that was normalized by the mass flux through primary clarifier, and copies/copies of PMMoV that was normalized by PMMoV. Cells are color-coded from green to red based on the calculated Pearson's R correlation value, with green (1.000) representing the strongest correlation and red (0.000) representing no correlation at all. Significance values (p-value) are listed with red font used to identify non-significant correlations/relationships.

			Copies/L	Copies/d Normalized by mass flux through plant	Copies/copies PMMoV Normalized by copies of PMMoV
Ottawa	N1 vs. N2	*p-value*	*0.390*	*0.451*	*0.061*
		R	0.880	0.808	0.469
	N1 vs. daily cases	*p-value*	*<0.001*	*<0.001*	*0.049*
		R	-0.209	-0.328	0.143
	N2 vs. daily cases	*p-value*	*0.002*	*<0.001*	*0.003*
		R	-0.140	-0.213	0.372
	N1 vs. active cases	*p-value*	*<0.001*	*<0.001*	*0.003*
		R	-0.233	-0.289	0.243
	N2 vs. active cases	*p-value*	*0.002*	*<0.001*	*0.003*
		R	-0.163	-0.163	0.350
	N1 vs. 7-day rolling average % positive	*p-value*	*<0.001*	*<0.001*	*0.003*
		R	-0.378	-0.238	0.498
	N2 vs. 7-day rolling average % positive	*p-value*	*0.002*	*<0.001*	*0.049*
		R	-0.323	-0.274	0.639
Gatineau	N1 vs. N2	*p-value*	*0.063*	*0.983*	*0.201*
		R	0.938	0.178	0.761
	N1 vs. daily cases	*p-value*	*0.003*	*0.01*	*0.029*
		R	0.399	-0.050	0.383
	N2 vs. daily cases	*p-value*	*0.003*	*0.001*	*0.033*
		R	0.140	-0.480	-0.144
	N1 vs. active cases	*p-value*	*0.003*	*0.298*	*0.003*
		R	0.919	0.125	0.483
	N2 vs. active cases	*p-value*	*0.003*	*0.185*	*0.003*
		R	0.950	-0.108	0.256
	N1 vs. 7-day rolling average % positive	*p-value*	*0.003*	*0.008*	*0.123*
		R	0.55	0.178	0.322
	N2 vs. 7-day rolling average % positive	p-value	*0.003*	*<0.001*	*0.058*
		R	0.364	-0.129	-0.022

2.6. Conclusion

This study is the first investigation and detection of SARS-CoV-2 trends in wastewater in Canada. It identifies primary clarifiedsludge as a preferred solids-rich sample compared to post grit solids for the detection of SARS-CoV-2 signal during decreasing and low incidence of viral load in communities. Based on the reagents used in this study, RT-qPCR shows superior quantification of SARS-CoV-2 N1 and N2 gene signal in primary clarified sludge compared to RT-ddPCR. Finally, it is demonstrated that PMMoV is a potential effective normalization biomarker for RNA signal to reduce noise inherent to the WRRF operation along with the sampling, transport and processing of the samples. The normalization of N1 and N2 SARS-CoV-2 signal using PMMoV enables strong correlation to epidemiological metrics in two surveyed WRRFs across decreasing and low-incidence cases of COVID-19.

2.7. Limitations and 2025 field updates

This chapter presents the earliest Canadian demonstrations of SARS-CoV-2 detection in wastewater solids during a period of low incidence and prevalence. However, several relatively important limitations are noted: 1) The study was restricted to two WRRFs located in the same general geographical region of Canada, which may limit the generalizability of the findings; and 2) The findings were obtained with analytical methods focused on the analysis of fresh primary clarified sludge which is a considerably less common sample type (as opposed to untreated sewage collected from sewersheds or the headworks of a WRRF) (Shah et al., 2022; Bonanno Ferraro et al., 2022). Many regions, particularly in low- and medium-income countries do not have primary clarifiers allowing for sampling of representative samples of sludge, often relying on waste stabilization ponds instead (Mara, 2013). This, at the time of writing (2020-2021) may have made the findings and knowledge less transferable for widespread WEM applications.

Additionally, our evaluation of the ddPCR platform revealed lower-than-expected performance compared to qPCR. While ddPCR has been championed for its sensitivity and precision, our findings suggested that, in practice, performance may be influenced by specific factors such as the choice of supermix or underlying wastewater-matrix-specific interferences or chemistry. As it was later correctly identified by Ahmed et al., (2022), our study employed different template volumes in the qPCR (15% v/v) and ddPCR reactions (25% v/v), which may have led to an increase in the presence of PCR-reaction inhibitory substances. Although our initial findings in 2020-2021 seemed to support the opinion that RT-qPCR-based methods were more sensitive for SARS-CoV-2 detection in wastewater, there is now a growing consensus in the field of WEM that ddPCR may in fact offer higher sensitivity, particularly in low-

concentration, complex matrix wastewater samples (Ciesielski et al., 2021; Ding et al., 2024; Länsivaara et al., 2024; Ahmed et al., 2022).

Furthermore, since the time of writing, the field has rapidly evolved and the scope of WEM has expanded far beyond SARS-CoV-2 to include a diverse range of viral, bacterial, fungal and antimicrobial resistance targets (Parkins et al., 2024), positioning wastewater monitoring as a central pillar of One Health frameworks worldwide (O'Reilly et al., 2025). By 2025, WEM has begun to mature into a key public health preparedness tool in some locales (Adhikari and Halden, 2022; HERA, 2023), with global efforts underway to harmonize methodologies (Naughton et al., 2023; Servetas et al., 2022). Significant research interest still exists in optimizing RNA extraction and normalization strategies, and PMMoV remains a commonly used fecal strength marker, though its dietary dependency and regional variability continue to prompt discussion (Malla et al., 2024).

2.8. Declaration of competing interests

The authors declare that no known competing financial interests or personal relationships influenced the work reported in this manuscript.

2.9. Ethical considerations

This study involved the analysis of anonymized environmental wastewater samples and aggregated clinical data. All samples were collected from large municipal sewersheds, ensuring that no individual or household could be identified. As such, the research did not involve human subjects, personal identifiers, or interactions requiring ethical review.

2.10. Funding

This research was funded and supported by Ontario's Ministry of Environment, Conservation and Parks SARS-CoV-2 (awarded to Dr. Robert Delatolla) and by CHEO's (Children's Hospital of Eastern Ontario) CHAMO (Children's Hospital Academic Medical Organization) (awarded to Dr. Alex E. MacKenzie)

2.11. Acknowledgements

The authors wish to acknowledge the help and assistance of Ms. Tammy Rose, Mr. Pawel Szulc and Mr. Tyler Hicks of the City of Ottawa, Mr. Fabien Hollard of the City of Gatineau, Dr. Monir Taha of

Ottawa Public Health, Mr. François Tessier of le Centre intégré de santé et de services sociaux de l'Outaouais (CISSSO), Public Health Ontario and l'Institut national de santé publique [Québec] (INSPQ) and all their employees involved in the project during this study. Their time, facilities, resources and assistance provided throughout the study greatly contributed to this work.

2.12. References

Adhikari, S., Halden, R.U., 2022. Opportunities and limits of wastewater-based epidemiology for tracking global health and attainment of UN sustainable development goals. Environ. Int. 163, 107217. https://doi.org/10.1016/j.envint.2022.107217

Ahmed, W., Angel, N., Edson, J., Bibby, K., Bivins, A., O'Brien, J.W., Choi, P.M., Kitajima, M., Simpson, S.L., Li, J., Tscharke, B., Verhagen, R., Smith, W.J.M., Zaugg, J., Dierens, L., Hugenholtz, P., Thomas, K. V., Mueller, J.F., 2020. First confirmed detection of SARS-CoV-2 in untreated wastewater in Australia: A proof of concept for the wastewater surveillance of COVID-19 in the community. Sci. Total Environ. 728, 138764. https://doi.org/10.1016/j.scitotenv.2020.138764

Ahmed, W., Smith, W.J.M., Metcalfe, S., Jackson, G., Choi, P.M., Morrison, M., Field, D., Gyawali, P., Bivins, A., Bibby, K., Simpson, S.L., 2022. Comparison of RT-qPCR and RT-dPCR Platforms for the Trace Detection of SARS-CoV-2 RNA in Wastewater. ACS ES&T Water 2, 1871–1880. https://doi.org/10.1021/acsestwater.1c00387

Alpaslan-Kocamemi, B., Kurt, H., Sait, A., Sarac, F., Saatci, A.M., Pakdemirli, B., 2020. SARS-CoV-2 detection in Istanbul wastewater treatment plant sludges. medRxiv 2020.05.12.20099358. https://doi.org/10.1101/2020.05.12.20099358

Balboa, S., Mauricio-Iglesias, M., Rodríguez, S., Martínez-Lamas, L., Vasallo, F.J., Regueiro, B., Lema, J.M., 2020. The fate of SARS-CoV-2 in wastewater treatment plants points out the sludge line as a suitable spot for incidence monitoring. medRxiv 2020.05.25.20112706. https://doi.org/10.1101/2020.05.25.20112706

Bar-On, Y.M., Flamholz, A., Phillips, R., Milo, R., 2020. SARS-CoV-2 (COVID-19) by the numbers. Elife 9, 697–698. https://doi.org/10.7554/eLife.57309

Bar Or, I., Yaniv, K., Shagan, M., Ozer, E., Erster, O., Mendelson, E., Mannasse, B., Shirazi, R., Kramarsky-Winter, E., Nir, O., Abu-Ali, H., Ronen, Z., Rinott, E., Lewis, Y.E., Friedler, E.F., Paitan, Y., Bitkover, E., Berchenko, Y., Kushmaro, A., 2020. Regressing SARS-CoV-2 sewage measurements onto COVID-19 burden in the population: a proof-of-concept for quantitative environmental surveillance. medRxiv 2020.04.26.20073569. https://doi.org/10.1101/2020.04.26.20073569

Bonanno Ferraro, G., Veneri, C., Mancini, P., Iaconelli, M., Suffredini, E., Bonadonna, L., Lucentini, L., Bowo-Ngandji, A., Kengne-Nde, C., Mbaga, D.S., Mahamat, G., Tazokong, H.R., Ebogo-Belobo, J.T., Njouom, R., Kenmoe, S., La Rosa, G., 2022. A State-of-the-Art Scoping Review on SARS-CoV-2 in Sewage Focusing on the Potential of Wastewater Surveillance for the Monitoring of the COVID-19 Pandemic, Food and Environmental Virology. Springer US. https://doi.org/10.1007/s12560-021-09498-6

Bwire, G.M., Majigo, M. V., Njiro, B.J., Mawazo, A., 2020. Detection profile of SARS-CoV-2 using RT-PCR in different types of clinical specimens: a systematic review and meta-analysis. J. Med. Virol. https://doi.org/10.1002/jmv.26349

Ciesielski, M., Blackwood, D., Clerkin, T., Gonzalez, R., Thompson, H., Larson, A., Noble, R., 2021. Assessing sensitivity and reproducibility of RT-ddPCR and RT-qPCR for the quantification of SARS-CoV-2 in wastewater. J. Virol. Methods 297, 114230. https://doi.org/10.1016/j.jviromet.2021.114230

Dalzell, S., 2020. Australia to test sewage for coronavirus as testing net widens - ABC News [WWW Document]. ABC News Aust. URL https://www.abc.net.au/news/2020-04-17/australia-to-test-sewage-for-coronairus-as-testing-net-widens/12156858 (accessed 7.28.20).

Daughton, C.G., 2009. Chemicals from the practive of healthcare: challenges and unknowns posed by residues in the environment. Environ. Toxicol. Chem. 28, 2490–2494. https://doi.org/10.1897/09-138.1

Ding, J., Xu, X., Deng, Y., Zheng, X., Zhang, T., 2024. Comparison of RT-ddPCR and RT-qPCR platforms for SARS-CoV-2 detection: Implications for future outbreaks of infectious diseases. Environ. Int. 183, 108438. https://doi.org/10.1016/j.envint.2024.108438

Gonzalez, R., Curtis, K., Bivins, A., Bibby, K., Weir, M.H., Yetka, K., Thompson, H., Keeling, D., Mitchell, J., Gonzalez, D., 2020. COVID-19 surveillance in Southeastern Virginia using wastewater-based epidemiology. Water Res. 186, 116296. https://doi.org/10.1016/j.watres.2020.116296

Gupta, S., Parker, J., Smits, S., Underwood, J., Dolwani, S., 2020. Persistent viral shedding of SARS-CoV-2 in faeces – a rapid review. Color. Dis. 22, 611–620. https://doi.org/10.1111/codi.15138

Haramoto, E., Malla, B., Thakali, O., Kitajima, M., 2020. First environmental surveillance for the presence of SARS-CoV-2 RNA in wastewater and river water in Japan. Sci. Total Environ. 737, 140405. https://doi.org/10.1016/j.scitotenv.2020.140405

European Commission, 2023. Threat assessment and intelligence gathering [WWW Document]. URL https://health.ec.europa.eu/health-emergency-preparedness-and-response-hera/preparedness/threat-assessment-and-intelligence-gathering_en (accessed 4.10.25).

Hill, K., Zamyadi, A., Deere, D., Vanrolleghem, P.A., Crosbie, N.D., 2020. SARS-CoV-2 known and unknowns, implications for the water sector and wastewater-based epidemiology to support national responses worldwide: early review of global experiences with the COVID-19 pandemic. Water Qual. Res. J. 1–11. https://doi.org/10.2166/wqrj.2020.100

La Rosa, G., Bonadonna, L., Lucentini, L., Kenmoe, S., Suffredini, E., 2020. Coronavirus in water environments: Occurrence, persistence and concentration methods - A scoping review. Water Res. 179, 115899. https://doi.org/10.1016/j.watres.2020.115899

Länsivaara, A., Lehto, K.M., Hyder, R., Janhonen, E.S., Lipponen, A., Heikinheimo, A., Pitkänen, T., Oikarinen, S., 2024. Comparison of Different Reverse Transcriptase–Polymerase Chain Reaction–Based Methods for Wastewater Surveillance of SARS-CoV-2: Exploratory Study. JMIR Public Heal. Surveill. 10. https://doi.org/10.2196/53175

Long, Q.X., Tang, X.J., Shi, Q.L., Li, Q., Deng, H.J., Yuan, J., Hu, J.L., Xu, W., Zhang, Y., Lv, F.J., Su, K., Zhang, F., Gong, J., Wu, B., Liu, X.M., Li, J.J., Qiu, J.F., Chen, J., Huang, A.L., 2020. Clinical and immunological assessment of asymptomatic SARS-CoV-2 infections. Nat. Med. https://doi.org/10.1038/s41591-020-0965-6

Mara, D., 2013. Domestic Wastewater Treatment in Developing Countries, Sustainability (Switzerland). Routledge. https://doi.org/10.4324/9781849771023

Medema, G., Heijnen, L., Elsinga, G., Italiaander, R., Brouwer, A., 2020. Presence of SARS-Coronavirus-2 RNA in Sewage and Correlation with Reported COVID-19 Prevalence in the Early Stage of the Epidemic in The Netherlands. Environ. Sci. Technol. Lett. 7, 511–516. https://doi.org/10.1021/acs.estlett.0c00357

Michael-Kordatou, I., Karaolia, P., Fatta-Kassinos, D., 2020. Sewage analysis as a tool for the COVID-19 pandemic response and management: the urgent need for optimised protocols for SARS-CoV-2 detection and quantification. J. Environ. Chem. Eng. 8, 104306. https://doi.org/10.1016/j.jece.2020.104306

Naughton, C.C., Holm, R.H., Lin, N.J., James, B.P., Smith, T., 2023. Online dashboards for SARS-CoV-2 wastewater data need standard best practices: An environmental health communication agenda. J. Water Health 21, 615–624. https://doi.org/10.2166/wh.2023.312

National Institute for Public Health and the Environment, 2020. Sewage research: decline of novel coronavirus in the Netherlands | RIVM [WWW Document]. RIVM. URL https://www.rivm.nl/en/news/sewage-research-decline-of-novel-coronavirus-in-netherlands (accessed 7.28.20).

Nemudryi, A., Nemudraia, A., Surya, K., Wiegand, T., Buyukyoruk, M., Wilkinson, R., Wiedenheft, B., 2020. Temporal detection and phylogenetic assessment of SARS-CoV-2 in municipal wastewater. medRxiv 2020.04.15.20066746. https://doi.org/10.1101/2020.04.15.20066746

O'Reilly, K.M., Wade, M.J., Farkas, K., Amman, F., Lison, A., Munday, J.D., Bingham, J., Mthombothi, Z.E., Fang, Z., Brown, C.S., Kao, R.R., Danon, L., 2025. Analysis insights to support the use of wastewater and environmental surveillance data for infectious diseases and pandemic preparedness. Epidemics 51, 100825. https://doi.org/10.1016/j.epidem.2025.100825

Orive, G., Lertxundi, U., Barcelo, D., 2020. Early SARS-CoV-2 outbreak detection by sewage-based epidemiology. Sci. Total Environ. 732, 139298. https://doi.org/10.1016/j.scitotenv.2020.139298

Pan, X., Chen, D., Xia, Y., Wu, X., Li, T., Ou, X., Zhou, L., Liu, J., 2020. Asymptomatic cases in a family cluster with SARS-CoV-2 infection. Lancet Infect. Dis. 20, 410–411. https://doi.org/10.1016/S1473-3099(20)30114-6

Parasa, S., Desai, M., Thoguluva Chandrasekar, V., Patel, H.K., Kennedy, K.F., Roesch, T., Spadaccini, M., Colombo, M., Gabbiadini, R., Artifon, E.L.A., Repici, A., Sharma, P., 2020. Prevalence of gastrointestinal symptoms and fecal viral shedding in Patients with coronavirus disease 2019: A systematic review and meta-analysis. JAMA Netw. open 3, e2011335. https://doi.org/10.1001/jamanetworkopen.2020.11335

Parkins, M.D., Lee, B.E., Acosta, N., Bautista, M., Hubert, C.R.J., Hrudey, S.E., Frankowski, K., Pang, X.L., 2024. Wastewater-based surveillance as a tool for public health action: SARS-CoV-2 and beyond. Clin. Microbiol. Rev. https://doi.org/10.1128/cmr.00103-22

Peccia, J., Zulli, A., Brackney, D.E., Grubaugh, N.D., Edward, H., Casanovas-massana, A., Ko, A.I., Malik, A.A., Wang, D., 2020a. SARS-CoV-2 RNA concentrations in primary municipal sewage sludge as a leading indicator of COVID-19 outbreak dynamics 1.

Peccia, J., Zulli, A., Brackney, D.E., Grubaugh, N.D., Kaplan, E.H., Casanovas-Massana, A., Ko, A.I., Malik, A.A., Wang, D., Wang, M., Weinberger, D.M., Omer, S.B., 2020b. SARS-CoV-2 RNA concentrations in primary municipal sewage sludge as a leading indicator of COVID-19 outbreak dynamics. medRxiv 1, 2020.05.19.20105999. https://doi.org/10.1101/2020.05.19.20105999

Pleitgen, F., 2020. Covid-19: Sewage could hold the key to stopping new coronavirus outbreaks - CNN [WWW Document]. CNN. URL https://www.cnn.com/2020/06/01/europe/germany-sewage-coronavirus-detection-intl/index.html (accessed 7.28.20).

Randazzo, W., Truchado, P., Cuevas-Ferrando, E., Simón, P., Allende, A., Sánchez, G., 2020. SARS-CoV-2 RNA in wastewater anticipated COVID-19 occurrence in a low prevalence area. Water Res. 181. https://doi.org/10.1016/j.watres.2020.115942

Rimoldi, S.G., Stefani, F., Gigantiello, A., Polesello, S., Comandatore, F., Mileto, D., Maresca, M., Longobardi, C., Mancon, A., Romeri, F., Pagani, C., Moja, L., Gismondo, M.R., Salerno, F., 2020. Presence and vitality of SARS-CoV-2 virus in wastewaters and rivers. medRxiv 2020.05.01.20086009. https://doi.org/10.1101/2020.05.01.20086009

Servetas, S.L., Parratt, K.H., Brinkman, N.E., Shanks, O.C., Smith, T., Mattson, P.J., Lin, N.J., 2022. Standards to support an enduring capability in wastewater surveillance for public health: Where are we? Case Stud. Chem. Environ. Eng. 6, 100247. https://doi.org/10.1016/j.cscee.2022.100247

Shah, S., Gwee, S.X.W., Ng, J.Q.X., Lau, N., Koh, J., Pang, J., 2022. Wastewater surveillance to infer COVID-19 transmission: A systematic review. Sci. Total Environ. 804, 150060. https://doi.org/10.1016/j.scitotenv.2021.150060

Sherchan, S.P., Shahin, S., Ward, L.M., Tandukar, S., Aw, T.G., Schmitz, B., Ahmed, W., Kitajima, M., 2020. First detection of SARS-CoV-2 RNA in wastewater in North America: A study in Louisiana, USA. Sci. Total Environ. 743, 140621. https://doi.org/10.1016/j.scitotenv.2020.140621

Thompson, J.R., Nancharaiah, Y. V, Gu, X., Lin, W., Rajal, V.B., Haines, M.B., Girones, R., Ching, L., Alm, E.J., Wuertz, S., 2020. Making waves : Wastewater surveillance of SARS-CoV-2 for population-based health management 184. https://doi.org/10.1016/j.watres.2020.116181

Wu, F., Zhang, J., Xiao, A., Gu, X., Lee, W.L., Armas, F., Kauffman, K., Hanage, W., Matus, M., Ghaeli, N., Endo, N., Duvallet, C., Poyet, M., Moniz, K., Washburne, A.D., Erickson, T.B., Chai, P.R., Thompson, J., Alm, E.J., 2020. SARS-CoV-2 titers in wastewater are higher than expected from clinically confirmed cases. mSystems 5, 2020.04.05.20051540. https://doi.org/10.1128/mSystems.00614-20

Wurtzer, S., Marechal, V., Mouchel, J.-M., Maday, Y., Teyssou, R., Richard, E., Almayrac, J.L., Moulin, L., 2020. Evaluation of lockdown impact on SARS-CoV-2 dynamics through viral genome quantification in Paris wastewaters. medRxiv 2020.04.12.20062679. https://doi.org/10.1101/2020.04.12.20062679

Yle, 2020. THL to track coronavirus in waste water | Yle Uutiset | yle.fi [WWW Document]. Yle. URL https://yle.fi/uutiset/osasto/news/thl_to_track_coronavirus_in_waste_water/11315440 (accessed 7.28.20).

Zhang, T., Cui, X., Zhao, X., Wang, J., Zheng, J., Zheng, G., Guo, W., Cai, C., He, S., Xu, Y., 2020. Detectable SARS-CoV-2 viral RNA in feces of three children during recovery period of COVID-19 pneumonia. J. Med. Virol. 92, 909–914. https://doi.org/10.1002/jmv.25795

Chapter 3 – Catching a Resurgence: Increase in SARS-CoV-2 Viral RNA Identified in Wastewater 48 Hours Before COVID-19 Clinical Tests and 96 Hours Before Hospitalizations

3.1. Context

The manuscript presented in this chapter of the doctoral dissertation is titled *Catching a resurgence: Increase in SARS-CoV-2 viral RNA identified in wastewater 48 hours before COVID-19 clinical tests and 96 hours before hospitalizations*, by Patrick M. D'Aoust, Tyson E. Graber, Elisabeth Mercier, Danika Montpetit, Ilya Alexandrov, Nafisa Neault, Aiman Tariq Baig, Janice Mayne, Xu Zhang, Tommy Alain, Mark R. Servos, Nivetha Srikanthan, Malcolm MacKenzie, Daniel Figeys, Douglas Manuel, Peter Jüni, Alex E. MacKenzie and Robert Delatolla, and was published in *Science of the Total Environment* (May 2021). In this manuscript, the predictive ability of SARS-CoV-2 WEM is investigated in comparison to both reported clinical cases and hospitalizations. This manuscript was the second original research-based Canadian manuscript published on the topic.

3.2. Abstract

Curtailing the Spring 2020 COVID-19 surge required sweeping and stringent interventions by governments across the world. Wastewater-based COVID-19 epidemiology programs have been initiated in many countries to provide public health agencies with a complementary disease tracking metric and non-discriminating surveillance tool. However, their efficacy in prospectively capturing resurgences following a period of low prevalence is unclear. In this study, the SARS-CoV-2 viral signal was measured in primary clarified sludge harvested every two days at the City of Ottawa's water resource recovery facility during the summer of 2020, when clinical testing recorded daily percent positivity below 1%. In late July, increases of >400% in normalized SARS-CoV-2 RNA signal in wastewater were identified 48 hours prior to reported >300% increases in positive cases that were retrospectively attributed to community-acquired infections. During this resurgence period, SARS-CoV-2 RNA signal in wastewater preceded the reported >160% increase in community hospitalizations by approximately 96 hours. This study supports wastewater-based COVID-19 surveillance of populations in augmenting the efficacy of diagnostic testing, which can suffer from sampling biases or timely reporting as in the case of hospitalization census.

3.3. Introduction

Wastewater has been used as a window in the habits and health of populations. A relatively novel epidemiological technique called wastewater and environmental monitoring (WEM) has been successfully used by public health units and authorities for decades to track trends in the general population for numerous diverse substances: illicit and recreational drugs (Been et al., 2014; Feng et al., 2018; González-Mariño et al., 2016; Gushgari et al., 2018), toxic and harmful chemicals and pesticides (Du et al., 2018; Markosian and Mirzoyan, 2019; Rousis et al., 2017), as well as prevalence of disease and illness (Nordgren et al., 2009; Yang et al., 2017). An intense interest has developed in looking to sewage to seek out biomarkers, pathogens and viruses to further the understanding of the prevalence of diseases, diets and habits in the general population (Bowes and Halden, 2019; Lorenzo and Picó, 2019). The earliest occurrence of using sewage as a source of information was approximately 25 years ago, where scientists discovered that polio was in fact found and transmissible in sewage and human stool (Metcalf et al., 1995). One of the major advantages of WEM is that with well-designed sampling/testing regimes, it can be utilized to gain valuable, and sometimes otherwise unobtainable information for subsets of population, as small as a single building or neighborhood, or as large as a city or county (Choi et al., 2018; Tscharke et al., 2019).

Most recently, WEM has been applied to the quantification of COVID-19 disease signal. The COVID-19 global pandemic has had profound impacts on day-to-day life through sickness, death and the economic and social effects of lockdowns, closures and curfews put in place by local governments to control and limit the community spread of the disease. At the beginning of the pandemic, COVID-19 surveillance approaches invoked by nations around the world included case ascertainment of individual patients via nucleic acid-based tests, serological tests and contact tracing. As such, WEM has been investigated as a potential surveillance tool to obtain a rapid measure of the relative incidence rate of COVID-19 infections in the population at large, generating an entirely new epidemiological metric for public health units (PHU) to utilize. Fecal shedding of SARS-CoV-2 viral particles has been shown to occur before, during and after active COVID-19 infections, for periods ranging from a few days to several weeks (Chen et al., 2020; Cheung et al., 2020; Xing et al., 2020; Xu et al., 2020), with current literature suggesting that children may shed viral particles longer than adults (X. Li et al., 2020; Ma et al., 2020). Additionally, fecal shedding of SARS-CoV-2 viral particles in stool occurs in patients infected with COVID-19 and appears to be independent of the presence of SARS-CoV-2 viral particles in the upper respiratory tract.

WEM has been applied at wastewater resource recovery facilities (WRRFs), with early studies demonstrating that viral signal is detected from both influent and primary clarified sludge, with recent studies identifying that at WRRFs, primary clarified sludge may provide more sensitive measurements than

in influent (D'Aoust et al., 2021; Graham et al., 2020; Peccia et al., 2020). Additionally, recent studies outlined that viral particles of SARS-CoV-2 in wastewater could in fact be predominantly solid particle-bound (Canadian Water Network (CWN), 2020; Graham et al., 2020) due to the virus' lipid bilayer, which causes it to be lipophilic (Schoeman and Fielding, 2019). Furthermore, it was observed in several studies that SARS-CoV-2 viral signal in wastewater could be utilized as a tool to track epidemiological metric trends (Ahmed et al., 2020; Medema et al., 2020a; Nemudryi et al., 2020; Thompson et al., 2020). One of the recent developments to the field of WEM is the renewed interest in investigating biomarkers to normalize the SARS-CoV-2 viral signal. Previous WEM work identified several possible normalization biomarkers in wastewater such as 5-Hydroxyindoleacetic acid (Chen et al., 2014), caffeine and cotinine (Rico et al., 2017). However, due to the higher incidence of SARS-CoV-2 viral particles in feces as compared to urine (Collivignarelli et al., 2020; Jeong et al., 2020; Lodder and de Roda Husman, 2020; Zhurakivska et al., 2020), other biomarkers present in wastewater solids, such as pepper mild mottle virus (PMMoV) (Jafferali et al., 2020; Kitajima et al., 2018; Rosario et al., 2009; Symonds et al., 2014) and crAssphage (Crank et al., 2020; Polo et al., 2020) are being utilized for the normalization of SARS-CoV-2. Some recent studies have demonstrated that biomarker normalized SARS-CoV-2 viral signal may in fact be capable of tracking the incidence of COVID-19 infections in the community (Gerrity et al., 2021; Kitamura et al., 2021) more effectively than non-biomarker-normalized viral signal (Jafferali et al., 2020; Wu et al., 2020), even if accounting for corrections due to flow or solids mass flux (D'Aoust et al., 2021).

To appropriately utilize epidemiological data obtained by measuring SARS-CoV-2 viral signal in wastewater, PHUs require an understanding of the predictive ability of this epidemiological metric to appropriately action obtained data (Hart and Halden, 2020; Hill et al., 2020; Thompson et al., 2020). Recent studies appear to demonstrate that WEM was able to identify the onset of community infection prior to clinical testing during the first wave, (D'Aoust et al., 2021; Kaplan et al., 2020; La Rosa et al., 2020; Medema et al., 2020b; Nemudryi et al., 2020; Peccia et al., 2020; Sherchan et al., 2020; Vallejo et al., 2020; Wu et al., 2020) however, there isn't a clear consensus on how early WEM can detect resurgences of the disease. Due to reporting limitations or absence of widespread clinical PCR or serological testing at the onset of the first wave of the COVID-19 pandemic, the predictive qualities of SARS-CoV-2 viral signal tracking in wastewater may not have been fully assessed, creating a critical and fundamental lack of understanding of intrinsic predictive qualities of wastewater-based SARS-CoV-2 surveillance, particularly for subsequent resurgences of COVID-19 infections in the community. As such, it remains unclear whether WEM can have a role in identifying COVID-19 resurgences before other, more traditional epidemiological metrics, such as clinical and serological testing results. As a result, the objective of this study is to establish a relationship between SARS-CoV-2 RNA signal in wastewater during a resurgence in a community with

established clinical testing and (i) increases in SARS-CoV-2 RNA signal in wastewater, (ii) increases in the number of new COVID-19 positive patient cases in the community, and (iii) increases in the number of new hospitalizations of COVID-19 positive patients in the community.

3.4. Materials and methods

3.4.1. Characteristics of the City of Ottawa's water resource recovery facility

Primary clarified sludge samples were harvested from the City of Ottawa's Robert O. Pickard Environmental Centre, in Ottawa, ON, which services approximately 1M residents of the national capital region. The hydraulic residence time of the Ottawa sewershed ranges from 2 hours to 35 hours, with an average residence time of approximately 12 hours. The Ottawa water resource recovery facility (WRRF) has an average daily flow of 435,000 m3 per day. The facility is comprised of preliminary treatment consisting of coarse and fine screening and grit chambers for the removal of larger particles. The primary treatment units consist of rectangular primary clarifiers, where samples from this study are harvested (Figure 3-1), and the secondary treatment is a conventional activated sludge system operating without nitrification. Finally, chlorination is used as a disinfection method followed by dechlorination prior to discharge to receiving waters.



Figure 3-1: Bird's-eye view of the Ottawa WRRF, with the primary clarifiers identified.

3.4.2. Sample collection, concentration, extraction and quantification

24-hour composite samples of primary clarified sludge (PCS) were collected from the Ottawa WRRF at a frequency of every 2 days for a six-week period, from June 20th, 2020 until August 4th, 2020. Composite samples were collected at 6-hour increments and stored at 4°C with the four sample subsequently mixed and again stored at 4°C for a maximum of eight hours until collected for processing.

Processing of samples to concentrate, extract and quantify viral RNA was performed as per D'Aoust et al., (2021). To concentrate the samples, 32 mL of well homogenized PCS was first reacted with a sodium chloride (NaCl)/polyethylene glycol (PEG) solution with a final working concentration of 0.3M NaCl and 80 mg/L PEG (Comelli et al., 2008; Hovi et al., 2001; Petterson et al., 2015). Samples were then well mixed on an orbital agitator set to a speed of 160 RPM for 12-17 hours in a temperature-controlled chamber (4°C). Following this, samples were centrifuged twice at 10,000 x g in a refrigerated centrifuge set to 4°C, for 45 mins and 10 mins, respectively. After each centrifugation cycle, the supernatant was decanted, preserving the pellet. The pellet was homogenized, and viral RNA was extracted using the RNeasy PowerMicrobiome Kit (Qiagen, Germantown, MD). The extraction was performed as per the manufacturer's recommendation, with the exception of the substitution of a chloroform-phenol solution with Trizol LS reagent (ThermoFisher, Ottawa, Canada). Quantification of the SARS-CoV-2 and PMMoV viral signals in wastewater was performed via singleplex one-step RT-qPCR with the Reliance One-Step Multiplex RT-qPCR Supermix (Bio-Rad, Hercules, CA) on a CFX Connect qPCR thermocycler (Bio-Rad, Hercules, CA). It has been previously observed that normalization of SARS-CoV-2 viral copies with pepper mild mottle virus (copies SARS-CoV-2/copies PMMoV) is used to normalize viral SARS-CoV-2 signal for variations in wastewater physico-chemical characteristics, plant flows, wastewater solids organic/inorganic ratio and PCR amplification (D'Aoust et al., 2021). Evaluation of viral recovery efficiency was also performed as per D'Aoust et al. (2021); with the data in this study not being corrected for recovery efficiency. Dilution tests were periodically performed to determine if inhibition was present in the samples. The method's limit of detection for the N1 and N2 gene regions was accessed by determining the concentration at which a detection rate of $\geqslant$ 95% (<5% false negatives) was obtained, as per the MIQE recommendations (Bustin et al., 2009). Additionally, samples were discarded if they did not meet the following requirements: 1) standard curves are linear (R2 $\geqslant$ 0.95), 2) the copies/well are found in the linear range of the standard curve, and 3) the primer efficiency was between 90%-130%. Additionally, all samples were analyzed as technical triplicates and samples with values greater than 2 standard deviations away from the mean were discarded.

3.4.3. COVID-19 epidemiological data

During the study period, there were three main methods of COVID-19 surveillance used to compare to the wastewater RNA signal of SARS-CoV-2, with the three metrics being commonly communicated to the public. The first method was to observe the daily number of new confirmed COVID-19 infections, determined via laboratory-confirmed SARS-CoV-2 tests using reverse transcriptase-quantitative polymerase chain reaction (RT-qPCR) that targeted the RNA-Dependent RNA polymerase for multiple

genes. Tests were classified as positive for SARS-CoV-2 infection if at least one of any of the two gene "targets" were detected (Government of Ontario, 2020). There was a notable increase in COVID-19 testing in Ottawa during early June with an average daily testing increase from approximately 270 tests per day to approximately 800 tests per day. As a result of increased testing resources, additional testing was performed at dedicated community clinics, physician offices and in hospitals, retirement homes and long-term care facilities, ultimately improving the quality of clinical epidemiological data being generated daily.

A second method used for surveillance of COVID-19 infection is the test positivity rate of clinical testing within the health unit boundaries. COVID-19 test positivity is the proportion of positive COVID-19 cases of Ottawa residents reported as a percent of all individuals tested for COVID-19 on a specific date Test positivity is reported in this study on a daily basis and also as a seven-day mid-point average.

The third method used for COVID-19 surveillance was the daily hospital census counts, defined as the number of patients residing in Ottawa with confirmed COVID-19 infections as of midnight that day that were admitted to any of Ottawa's five acute care hospitals. The average length of stay during the study period was 19.5 days, interquartile range 22 days.

3.4.4. Statistical analysis

In order to test for significance and for strength of correlation between SARS-CoV-2 RNA signal and epidemiological metrics, a student's t-test and Pearson's correlation analyses were performed, with a p¬-value of 0.05 or lower signifying significance.

To evaluate if a lag existed between the appearance of increased SARS-CoV-2 RNA signal in wastewater and epidemiological metrics, time-step analyses were also performed where the correlations between viral RNA signal and epidemiological metrics were offset by a period of 1 to 7 days. The time-step analysis was performed across three discreet time-periods: i) pre-resurgence and resurgence, ending after the resurgence (June 21st to July 21st), ii) pre-resurgence and post-resurgence, extending to the end of the data set (June 21st to July 25th) and iii) full data period (June 21st to August 4th).

3.5. Results, discussion and implications

3.5.1. Trend and peak of wastewater SARS-CoV-2 RNA viral level in wastewater compared to other clinical COVID-19 surveillance metrics

This study compares PMMoV normalized SARS-CoV-2 viral copies, a metric outlined in previous SARS-CoV-2 WEM work (D'Aoust et al., 2021; Kitamura et al., 2021; Wu et al., 2020) with clinical epidemiological metrics. This WEM-based metric normalizes SARS-CoV-2 viral copies to the number of copies of PMMoV in wastewater to account for variations inherent to wastewater samples; in particular variations related to the wastewaters water quality, solids and fecal matter concentrations. In addition, PMMoV normalizes for variations associated with sampling, storage, and testing. PMMoV is ubiquitous in both the liquid and solid fraction of wastewater and is effective due to its low temporal variability in wastewater (Figure 3-2).

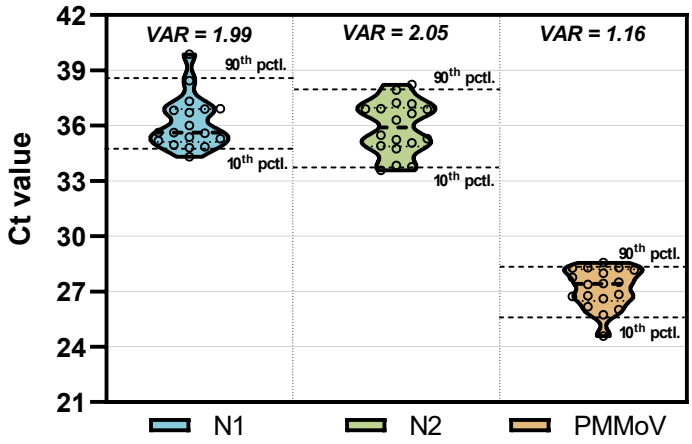


Figure 3-2: Ct values of the SARS-CoV-2 N1 and N2 gene regions, and the PMMoV normalization gene (1:10 dilution shown), outlining the low variability of PMMoV, justifying its use as a normalization gene. The 10th and 90th percentile are displayed, along with the median (dotted line inside shapes). The variance of the different targets is also shown at the top.

The lower temporal variability of PMMoV is likely to be linked to the stability and hardiness of its virions (Sassi et al., 2018). All conventional COVID-19 surveillance measures (# of hospitalized cases, 7-day mid-point floating average percent positivity, clinical test percent positivity and number of new daily cases; Figure 3-3 a-d) increase during the study period from a low level at the beginning of the study. The number of current hospitalized patient cases are at their highest on July 31-Aug 2 with a 168% increase compared to the week of July 13 (Figure 3-3 a-d). Meanwhile, percent positive cases and daily cases are at

their highest on July 19, with increases of 215% and 326% respectively, relative to the preceding 7-day period (Figure 3-3 b-d).

As observed with other epidemiological metrics, the PMMoV normalized viral signal in Ottawa's wastewater is also shown to be low at the beginning of the study period through to the week of July 13 with both N1 and N2 regions below 1.00x10-4 copies/copies PMMoV (Figure 3-3 e). There is a 450% relative increase ($p<0.05$) in N1 and 440% increase ($p<0.05$) in N2 viral signal on July 17 to 19 compared to July 13 to 15. An absolute increase of 2.03x10-4 and 3.01x10-4 copies/copies PMMoV is reported during this period of increase for N1 and N2 gene regions, respectively (Figure 3-3 e). The PMMoV normalized viral signal then decreases again following this peak, to levels higher than the previous baseline, but notably lower than the peak outlined between July 17 to 19.

Throughout the study, a good agreement is observed between N1 and N2 SARS-CoV-2 gene region targets ($R = 0.852$, $r2 = 0.726$), implying that some portions of the N1 and N2 gene regions may be preserved. This potentially indicates that RNA extracted from primary sludge and wastewater could be sequenced to track the transmission of new, and potentially more infectious mutations of the disease (Q. Li et al., 2020; Oude Munnink et al., 2020; Rockett et al., 2020; Volz et al., 2020).

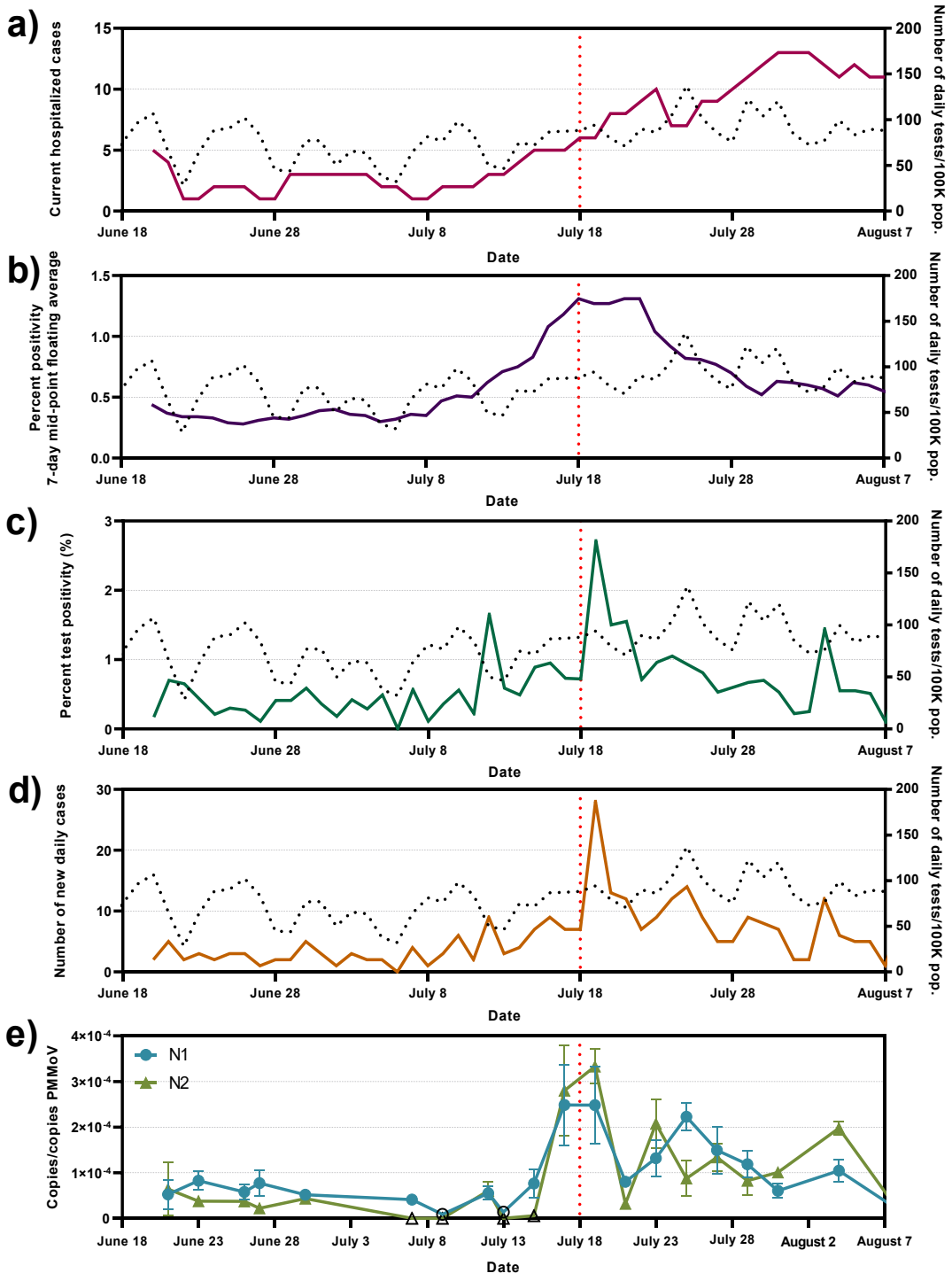


Figure 3-3: Epidemiological metrics and SARS-CoV-2 viral concentrations over the study period; a) COVID-19-caused hospitalizations, b) percent test positivity (7-day mid-point floating average), c) percent test positivity and d) number of new daily cases, along with e) wastewater SARS-CoV-2 N1 and N2 gene copies/PMMoV gene copies. Open data points signify points which were below the limit of quantification. The dotted line in the background represents the number of daily clinical tests/100K pop. performed.

This study also suggests that the PMMoV normalized viral signal peaks for a relatively short period of time before showing a subsequent rapid decrease in signal. This short peaking period may be an artifact of the inherent variation in wastewaters or associated with variations inherent to the assay. The short peak period may also be associated to fecal shedding patterns of the population contributing to the wastewater. It is noted that several current studies investigating fecal shedding timelines and intensity for SARS-CoV-2 may in fact be investigating the sickest of patients in a hospital setting (Chen et al., 2020; Fontana et al., 2020), and so patterns may not reflect occurrences in the general population, where a significant quantity of patients will likely suffer from milder symptoms, or no symptoms at all (Pan et al., 2020; Park et al., 2020). Furthermore, sicker or elderly patients may in fact "fall off" the wastewater monitoring efforts if bed pans or adult diapers are utilized as part of their treatment and convalescence in a hospital or retirement home (Coelho et al., 2015; Tsang et al., 2017).

Previous work on PMMoV identified that it is a useful environmental metric to track in surface waters and drinking waters as it correlated strongly with fecal contamination of said waters (Hamza et al., 2011; Haramoto et al., 2013; Rosiles-González et al., 2017). As a result, the use of PMMoV normalized data in SARS-CoV-2 is seeing increased utilization in several locales due to the metrics' ability to correct for the true quantity of fecal matter in wastewater (D'Aoust et al., 2021; Wu et al., 2020). It is hypothesized that due to the fact PMMoV signal in wastewater is likely diet based (due to consumption peppers, some tomatoes, or related foodstuff infected with PMMoV) (Jarret et al., 2008; Peng et al., 2015; Zhou et al., 2020), this approach will work best when performing a survey of a larger group of individuals or geographical area, where enough survey participants with varied enough diets will average out the signal.

3.5.2. Correlation between wastewater and clinical surveillance metrics

Positive correlations were observed (Figure 3-3 c, d and e) between the normalized viral RNA signal and both the number of new daily positive COVID-19 cases (N1: $R = 0.673$, $p<0.001$; N2: $R = 0.648$, $p<0.001$) and clinical testing percent positivity (N1: $R = 0.468$, $p<0.001$; N2: $R = 0.404$, $p<0.001$). These findings are in agreement with reported observations from previous studies (D'Aoust et al., 2021; Nemudryi et al., 2020; Peccia et al., 2020). This study, as opposed to an earlier study in the same region (D'Aoust et al., 2021), demonstrates that strong correlations do in fact exist between viral RNA signal and the epidemiological metric of clinical daily new COVID-19 cases, as supported by several other studies (Hart and Halden, 2020; Michael-Kordatou et al., 2020; Trottier et al., 2020; Wu et al., 2020). The moderate correlations between viral RNA signal and clinical daily new COVID-19 cases in previous work was largely attributed to inadequate resources to achieve a developed clinical testing framework early in the pandemic (lower daily # of tests). In this study, a strong testing regiment was deployed in Ottawa and hence produced

a more reliable daily new COVID-19 cases metric across this study period. A weak positive correlation exists between N1 and N2 SARS-CoV-2 PMMoV-normalized RNA signal and COVID-19-caused hospitalizations ($R = 0.347$, $p<0.001$ and $R = 0.464$, $p<0.001$ for N1 and N2, respectively; Figure 3-3 a and e). This supports previous findings that WEM efforts to track the rate of incidence of COVID-19 infections in the community provides useful and confirmatory information.

3.5.3. Temporal association between surveillance metrics

A visual comparison of clinical testing percent positivity and the number of new daily positive COVID-19 cases compared to the PMMoV-normalized RNA signal shows that the viral RNA signal predates both the clinical testing percent positivity and new daily positive COVID-19 cases epidemiological data.

A times-step correlation analysis suggests that increases in SARS-CoV-2 signal in wastewater precedes increases in new daily positive COVID-19 cases and clinical testing percent positivity by two days (N1: $R = 0.703$, $p<0.001$; N2: $R = 0.721$, $p<0.001$; N1: $R = 0.703$, $p<0.001$; N2: $R = 0.714$, $p<0.001$) (Table 3.1). Furthermore, the same time-step correlation analysis also suggests that increases in SARS-CoV-2 signal in wastewater precedes increases in the number of hospitalized cases by four days (N1: $R = 0.741$, $p<0.001$; N2: $R = 0.767$, $p<0.001$). This is further confirmed visually (Figure 3-4). The precedence of viral RNA signal vs. other epidemiological metrics has been reported elsewhere (Chavarria-Miró et al., 2020; Kumar et al., 2020; Peccia et al., 2020).

Table 3-1: Time-step analyses of correlations (Pearson's R) between normalized SARS-CoV-2 viral RNA signal (copies/copies PMMoV) and 7-day rolling average percent positivity, test percent positivity and daily new cases epidemiological metrics.

		Hospitalized cases		7-day rolling average test percent positivity		Test percent positivity		Daily new cases	
June 21 - July 21	Daily offset	N1	N2	N1	N2	N1	N2	N1	N2
	0	0.488	0.502	0.675	0.662	0.551	0.635	0.680	0.754
	1	0.599	0.578	0.662	0.647	0.634	0.723	0.642	0.692
	2	0.532	0.487	0.666	0.679	0.853	0.821	0.810	0.765
	3	0.747	0.754	0.556	0.593	0.191	0.208	0.354	0.310
	4	0.741	0.767	0.415	0.457	0.338	0.332	0.265	0.237
	5	0.512	0.487	0.301	0.341	0.144	0.140	0.375	0.405
	6	0.534	0.490	0.104	0.167	-0.031	0.023	0.107	0.190
	7	0.375	0.361	-0.012	0.077	-0.040	0.070	0.078	0.178
June 21 - July 25	Daily offset	N1	N2	N1	N2	N1	N2	N1	N2
	0	0.539	0.551	0.659	0.688	0.505	0.612	0.707	0.712
	1	0.689	0.562	0.631	0.653	0.637	0.747	0.662	0.709
	2	0.634	0.489	0.623	0.667	0.724	0.794	0.699	0.783
	3	0.786	0.695	0.488	0.576	0.128	0.203	0.277	0.346
	4	0.790	0.690	0.324	0.437	0.264	0.277	0.245	0.192
	5	0.632	0.483	0.188	0.303	0.114	0.108	0.378	0.354
	6	0.645	0.482	0.038	0.118	-0.073	0.008	0.102	0.202
	7	0.531	0.408	-0.074	0.015	-0.157	0.041	-0.032	0.163
Whole data set	Daily offset	N1	N2	N1	N2	N1	N2	N1	N2
	0	0.347	0.470	0.644	0.626	0.469	0.527	0.673	0.648
	1	0.453	0.484	0.606	0.602	0.634	0.668	0.654	0.634
	2	0.429	0.424	0.593	0.603	0.703	0.714	0.703	0.721
	3	0.556	0.565	0.448	0.491	0.027	0.081	0.182	0.375
	4	0.603	0.586	0.307	0.360	0.233	0.278	0.223	0.158
	5	0.497	0.477	0.165	0.234	0.079	-0.034	0.306	0.206
	6	0.546	0.500	0.020	0.064	-0.091	0.021	0.074	0.195
	7	0.468	0.443	-0.080	-0.119	-0.074	0.005	-0.025	0.178

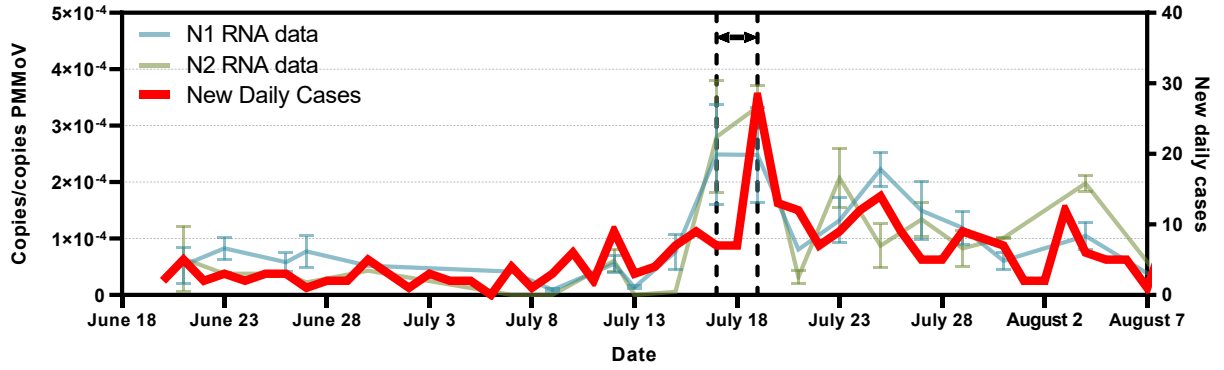


Figure 3-4: Figure of the new daily cases epidemiological metric (in red) with SARS-CoV-2 viral RNA signal in Ottawa's primary clarified sludge samples, with the precedence of SARS-COV-2 viral signal in wastewater clearly outlined.

Recent studies proposed that wastewater viral SARS-CoV-2 RNA signal may in fact precede hospital admissions by 1 to 5 days in primary sludge (Figure 3-4) (Kaplan et al., 2020; Peccia et al., 2020), and 6-14 days in raw wastewater (Kumar et al., 2020). This supports findings by Peccia et al. (2020), identifying that hospitalizations may begin peaking four days after an increased viral RNA signal, with the caveat that hospitalizations rates may be significantly higher when viral RNA signal is the result from shedding of an at-risk population group (young infants, elderly, immunocompromised, etc.). In addition,

the RNA signal post-resurgence indicates that the resurgence events in viral RNA signal serves to weaken the correlation of subsequent peaks with clinical testing metrics. It is hypothesized that early and later infections and overlapping shedding events of duration and intensity convolute peaks within a period of time following the initial new peaks/surges in COVID-19 infections. Nonetheless, the RNA epidemiological metric of copies/copies PMMoV may become extremely valuable to public health units in their preparation for the next COVID-19 resurgences.

Earlier studies investigating the predictive capabilities of SARS-CoV-2 WEM (Kumar et al., 2020; Peccia et al., 2020) may have been performed at times where clinical metrics were dampened due to limited clinical testing resources, which may in turn have impacted the conclusions regarding predictive ability. This present study was performed during a period of relatively higher testing intensity in the community (avg. 80.9 tests per/100K pop. performed) and confirms previous findings of early detection of SARS-CoV-2 WEM as compared to clinical metrics such as hospitalizations, new daily positives cases or percent positivity.

3.6. Conclusions

This study demonstrates that due to the general stability of SARS-CoV-2 RNA measurements in PCS, this fraction of wastewater can reliably be utilized to predict rapid increases or resurgences in COVID-19 cases in the community at large (Alpaslan-Kocamemi et al., 2020; D'Aoust et al., 2021; Peccia et al., 2020), and the results strongly suggest that PCS can be utilized as part of sentinel-type wastewater and environmental monitoring endeavors at WRRFs.

Advantages of this approach include: i) the analyses in water resource recovery facilities are high-enrollment surveys, which capture a majority of the urban population, regardless of individual's willingness to get tested clinically; ii) tests are anonymous and do not pose ethical challenges as opposed to mass clinical testing or targeted sewershed monitoring efforts; iii) data can be used as a confirmation to clinical tests, increases the effectiveness of local public health units and data remains independent of official testing strategies or media sentiment, and iv) provides an exit strategy/path forward for public health units as something to eventually transition to once immunization is available, to cut down on clinical testing costs, while maintaining broad surveillance capabilities. However, limitations to this WEM approach includes the following: i) data obtained only gives high-altitude view of the situation in the community, and it is currently not possible to correlate these data to an actual number of cases in the community; ii) testing protocols must be optimized and retain sensitivity at very-low levels of disease incidence to remain relevant; iii) widespread adoption of WEM requires scale-up of public health units' current capabilities and/or

partnership with private laboratories or research institutions, and iv) increases in resolution (more localized, upstream of water resource recovery facilities, for example) of tests in watersheds may lead to ethical questions for public health unit if it wishes to act upon the data, due to the potential risk for identifying or singling out small subgroups of a population. It is noted however that these issues are not dissimilar to other ethical issues currently existing with other COVID-19 public health endeavors, such as COVID-19 potential exposure notification smartphone applications.

3.7. Limitations and 2025 field updates

This chapter highlights the predictive value of SARS-CoV-2 measurements in PCS, detecting SARS-CoV-2 resurgences up to 48 hours before clinical test positivity and 96 hours before hospitalizations. However, a few limitations to this study exist: 1) PCS provides only a high-level view of community trends and may miss localized outbreaks without upstream sampling; and 2) It is now understood that the onset of new variants, immunization campaigns and public health restrictions and guidelines had profound impacts on the predictive ability of WEM for COVID-19 due to changes both in infection dynamics and the intrinsic relationship between wastewater signal and clinical metrics, limiting the generalizability of some of our findings of 2021 (Ghanbari et al., 2024).

3.8. Declaration of competing interests

The authors declare that no known competing financial interests or personal relationships influenced the work reported in this manuscript.

3.9. Ethical considerations

This study involved the analysis of anonymized environmental wastewater samples and aggregated clinical data. All samples were collected from municipal sewersheds, ensuring that no individual or household could be identified. As such, the research did not involve human subjects, personal identifiers, or interactions requiring ethical review.

3.10. Funding

This research was supported by a CHEO (Children's Hospital of Eastern Ontario) CHAMO (Children's Hospital Academic Medical Organization) grant, awarded to Dr. Alex E. MacKenzie.

3.11. Acknowledgements

The authors wish to acknowledge the help and assistance of the University of Ottawa, the Ottawa Hospital, the Children's Hospital of Eastern Ontario, the Children's Hospital of Eastern Ontario's Research Institute, the City of Ottawa, Ottawa Public Health, Public Health Ontario and all their employees involved in the project during this study. Their time, facilities, resources and thoughts provided throughout the study helped the authors greatly. The authors also wish to specifically outline the assistance of Dr. Monir Taha at Ottawa Public Health.

3.12. References

Ahmed, W., Angel, N., Edson, J., Bibby, K., Bivins, A., O'Brien, J.W., Choi, P.M., Kitajima, M., Simpson, S.L., Li, J., Tscharke, B., Verhagen, R., Smith, W.J.M., Zaugg, J., Dierens, L., Hugenholtz, P., Thomas, K. V., Mueller, J.F., 2020. First confirmed detection of SARS-CoV-2 in untreated wastewater in Australia: A proof of concept for the wastewater surveillance of COVID-19 in the community. Sci. Total Environ. 728, 138764. https://doi.org/10.1016/j.scitotenv.2020.138764

Alpaslan-Kocamemi, B., Kurt, H., Sait, A., Sarac, F., Saatci, A.M., Pakdemirli, B., 2020. SARS-CoV-2 detection in Istanbul wastewater treatment plant sludges. medRxiv 2020.05.12.20099358. https://doi.org/10.1101/2020.05.12.20099358

Balboa, S., Mauricio-Iglesias, M., Rodríguez, S., Martínez-Lamas, L., Vasallo, F.J., Regueiro, B., Lema, J.M., 2020. The fate of SARS-CoV-2 in wastewater treatment plants points out the sludge line as a suitable spot for incidence monitoring. medRxiv 2020.05.25.20112706. https://doi.org/10.1101/2020.05.25.20112706

Bar-On, Y.M., Flamholz, A., Phillips, R., Milo, R., 2020. SARS-CoV-2 (COVID-19) by the numbers. Elife 9, 697–698. https://doi.org/10.7554/eLife.57309

Bar Or, I., Yaniv, K., Shagan, M., Ozer, E., Erster, O., Mendelson, E., Mannasse, B., Shirazi, R., Kramarsky-Winter, E., Nir, O., Abu-Ali, H., Ronen, Z., Rinott, E., Lewis, Y.E., Friedler, E.F., Paitan, Y., Bitkover, E., Berchenko, Y., Kushmaro, A., 2020. Regressing SARS-CoV-2 sewage measurements onto COVID-19 burden in the population: a proof-of-concept for quantitative environmental surveillance. medRxiv 2020.04.26.20073569. https://doi.org/10.1101/2020.04.26.20073569

Bwire, G.M., Majigo, M. V., Njiro, B.J., Mawazo, A., 2020. Detection profile of SARS‐CoV‐2 using RT‐PCR in different types of clinical specimens: a systematic review and meta‐analysis. J. Med. Virol. https://doi.org/10.1002/jmv.26349

Dalzell, S., 2020. Australia to test sewage for coronavirus as testing net widens - ABC News [WWW Document]. ABC News Aust. URL https://www.abc.net.au/news/2020-04-17/australia-to-test-sewage-for-coronairus-as-testing-net-widens/12156858 (accessed 7.28.20).

Daughton, C.G., 2009. Chemicals from the practive of healthcare: challenges and unknowns posed by residues in the environment. Environ. Toxicol. Chem. 28, 2490–2494. https://doi.org/10.1897/09-138.1

Ghanbari, M., Huang, J., Luc, A., Arabi, M., Goldman, J.E., Byrne-Nash, R., Kane, S.J., Ferrell, R., Fielder, T., De Long, S.K., Wilusz, C.J., 2024. View of an Evolving Pandemic: Changes in the Relationship Between Clinical Cases and Levels of SARS-CoV-2 RNA in Colorado Wastewater. ACS ES&T Water 4, 2018–2030. https://doi.org/10.1021/acsestwater.3c00615

Gonzalez, R., Curtis, K., Bivins, A., Bibby, K., Weir, M.H., Yetka, K., Thompson, H., Keeling, D., Mitchell, J., Gonzalez, D., 2020. COVID-19 surveillance in Southeastern Virginia using wastewater-based epidemiology. Water Res. 186, 116296. https://doi.org/10.1016/j.watres.2020.116296

Gupta, S., Parker, J., Smits, S., Underwood, J., Dolwani, S., 2020. Persistent viral shedding of SARS-CoV-2 in faeces – a rapid review. Color. Dis. 22, 611–620. https://doi.org/10.1111/codi.15138

Haramoto, E., Malla, B., Thakali, O., Kitajima, M., 2020. First environmental surveillance for the presence of SARS-CoV-2 RNA in wastewater and river water in Japan. Sci. Total Environ. 737, 140405. https://doi.org/10.1016/j.scitotenv.2020.140405

Hill, K., Zamyadi, A., Deere, D., Vanrolleghem, P.A., Crosbie, N.D., 2020. SARS-CoV-2 known and unknowns, implications for the water sector and wastewater-based epidemiology to support national responses worldwide: early review of global experiences with the COVID-19 pandemic. Water Qual. Res. J. 1–11. https://doi.org/10.2166/wqrj.2020.100

La Rosa, G., Bonadonna, L., Lucentini, L., Kenmoe, S., Suffredini, E., 2020. Coronavirus in water environments: Occurrence, persistence and concentration methods - A scoping review. Water Res. 179, 115899. https://doi.org/10.1016/j.watres.2020.115899

Long, Q.X., Tang, X.J., Shi, Q.L., Li, Q., Deng, H.J., Yuan, J., Hu, J.L., Xu, W., Zhang, Y., Lv, F.J., Su, K., Zhang, F., Gong, J., Wu, B., Liu, X.M., Li, J.J., Qiu, J.F., Chen, J., Huang, A.L., 2020. Clinical and immunological assessment of asymptomatic SARS-CoV-2 infections. Nat. Med. https://doi.org/10.1038/s41591-020-0965-6

Medema, G., Heijnen, L., Elsinga, G., Italiaander, R., Brouwer, A., 2020. Presence of SARS-Coronavirus-2 RNA in Sewage and Correlation with Reported COVID-19 Prevalence in the Early Stage of the Epidemic in The Netherlands. Environ. Sci. Technol. Lett. 7, 511–516. https://doi.org/10.1021/acs.estlett.0c00357

Michael-Kordatou, I., Karaolia, P., Fatta-Kassinos, D., 2020. Sewage analysis as a tool for the COVID-19 pandemic response and management: the urgent need for optimised protocols for SARS-CoV-2 detection and quantification. J. Environ. Chem. Eng. 8, 104306. https://doi.org/10.1016/j.jece.2020.104306

National Institute for Public Health and the Environment, 2020. Sewage research: decline of novel coronavirus in the Netherlands | RIVM [WWW Document]. RIVM. URL

https://www.rivm.nl/en/news/sewage-research-decline-of-novel-coronavirus-in-netherlands (accessed 7.28.20).

Nemudryi, A., Nemudraia, A., Surya, K., Wiegand, T., Buyukyoruk, M., Wilkinson, R., Wiedenheft, B., 2020. Temporal detection and phylogenetic assessment of SARS-CoV-2 in municipal wastewater. medRxiv 2020.04.15.20066746. https://doi.org/10.1101/2020.04.15.20066746

Orive, G., Lertxundi, U., Barcelo, D., 2020. Early SARS-CoV-2 outbreak detection by sewage-based epidemiology. Sci. Total Environ. 732, 139298. https://doi.org/10.1016/j.scitotenv.2020.139298

Pan, X., Chen, D., Xia, Y., Wu, X., Li, T., Ou, X., Zhou, L., Liu, J., 2020. Asymptomatic cases in a family cluster with SARS-CoV-2 infection. Lancet Infect. Dis. 20, 410–411. https://doi.org/10.1016/S1473-3099(20)30114-6

Parasa, S., Desai, M., Thoguluva Chandrasekar, V., Patel, H.K., Kennedy, K.F., Roesch, T., Spadaccini, M., Colombo, M., Gabbiadini, R., Artifon, E.L.A., Repici, A., Sharma, P., 2020. Prevalence of gastrointestinal symptoms and fecal viral shedding in Patients ŵith coronavirus disease 2019: A systematic review and meta-analysis. JAMA Netw. open 3, e2011335. https://doi.org/10.1001/jamanetworkopen.2020.11335

Peccia, J., Zulli, A., Brackney, D.E., Grubaugh, N.D., Edward, H., Casanovas-massana, A., Ko, A.I., Malik, A.A., Wang, D., 2020a. SARS-CoV-2 RNA concentrations in primary municipal sewage sludge as a leading indicator of COVID-19 outbreak dynamics 1.

Peccia, J., Zulli, A., Brackney, D.E., Grubaugh, N.D., Kaplan, E.H., Casanovas-Massana, A., Ko, A.I., Malik, A.A., Wang, D., Wang, M., Weinberger, D.M., Omer, S.B., 2020b. SARS-CoV-2 RNA concentrations in primary municipal sewage sludge as a leading indicator of COVID-19 outbreak dynamics. medRxiv 1, 2020.05.19.20105999. https://doi.org/10.1101/2020.05.19.20105999

Pleitgen, F., 2020. Covid-19: Sewage could hold the key to stopping new coronavirus outbreaks - CNN [WWW Document]. CNN. URL https://www.cnn.com/2020/06/01/europe/germany-sewage-coronavirus-detection-intl/index.html (accessed 7.28.20).

Randazzo, W., Truchado, P., Cuevas-Ferrando, E., Simón, P., Allende, A., Sánchez, G., 2020. SARS-CoV-2 RNA in wastewater anticipated COVID-19 occurrence in a low prevalence area. Water Res. 181. https://doi.org/10.1016/j.watres.2020.115942

Rimoldi, S.G., Stefani, F., Gigantiello, A., Polesello, S., Comandatore, F., Mileto, D., Maresca, M., Longobardi, C., Mancon, A., Romeri, F., Pagani, C., Moja, L., Gismondo, M.R., Salerno, F., 2020. Presence and vitality of SARS-CoV-2 virus in wastewaters and rivers. medRxiv 2020.05.01.20086009. https://doi.org/10.1101/2020.05.01.20086009

Sherchan, S.P., Shahin, S., Ward, L.M., Tandukar, S., Aw, T.G., Schmitz, B., Ahmed, W., Kitajima, M., 2020. First detection of SARS-CoV-2 RNA in wastewater in North America: A study in Louisiana, USA. Sci. Total Environ. 743, 140621. https://doi.org/10.1016/j.scitotenv.2020.140621

Thompson, J.R., Nancharaiah, Y. V, Gu, X., Lin, W., Rajal, V.B., Haines, M.B., Girones, R., Ching, L., Alm, E.J., Wuertz, S., 2020. Making waves : Wastewater surveillance of SARS-CoV-2 for population-based health management 184. https://doi.org/10.1016/j.watres.2020.116181

Wu, F., Zhang, J., Xiao, A., Gu, X., Lee, W.L., Armas, F., Kauffman, K., Hanage, W., Matus, M., Ghaeli, N., Endo, N., Duvallet, C., Poyet, M., Moniz, K., Washburne, A.D., Erickson, T.B., Chai, P.R., Thompson, J., Alm, E.J., 2020. SARS-CoV-2 titers in wastewater are higher than expected from clinically confirmed cases. mSystems 5, 2020.04.05.20051540. https://doi.org/10.1128/mSystems.00614-20

Wurtzer, S., Marechal, V., Mouchel, J.-M., Maday, Y., Teyssou, R., Richard, E., Almayrac, J.L., Moulin, L., 2020. Evaluation of lockdown impact on SARS-CoV-2 dynamics through viral genome quantification in Paris wastewaters. medRxiv 2020.04.12.20062679. https://doi.org/10.1101/2020.04.12.20062679

Yle, 2020. THL to track coronavirus in waste water | Yle Uutiset | yle.fi [WWW Document]. Yle. URL https://yle.fi/uutiset/osasto/news/thl_to_track_coronavirus_in_waste_water/11315440 (accessed 7.28.20).

Zhang, T., Cui, X., Zhao, X., Wang, J., Zheng, J., Zheng, G., Guo, W., Cai, C., He, S., Xu, Y., 2020. Detectable SARS-CoV-2 viral RNA in feces of three children during recovery period of COVID-19 pneumonia. J. Med. Virol. 92, 909–914. https://doi.org/10.1002/jmv.25795

Chapter 4 – COVID-19 Wastewater-Based Epidemiology in Rural Communities: Comparison of Lagoon and Pumping Station Samples

4.1. Context

The manuscript presented in this chapter of the doctoral dissertation is titled *COVID-19 wastewater-based epidemiology in rural communities: Comparison of lagoon and pumping station samples,* by Patrick M. D'Aoust, Syeda Tasneem Towhid, Élisabeth Mercier, Nada Hegazy, Xin Tian, Kamya Bhatnagar, Zhihao Zhang, Colleen C. Naughton, Alex E. MacKenzie, Tyson E. Graber, Robert Delatolla, and was published in *Water Research* (December 2021). In this manuscript, SARS-CoV-2 WEM is investigated in a smaller rural community and two sampling locations were compared side-by-side to determine the most appropriate sampling location to obtain meaningful epidemiological information when tracking diseases such as SARS-CoV-2 through wastewater.

4.2. Abstract

WEM has been a topic of significant interest over the last year due to its application in SARS-CoV-2 surveillance to track prevalence of COVID-19 in communities. Although SARS-CoV-2 surveillance has been applied in more than 50 countries to date, the application of this surveillance has been largely focused on relatively affluent urban and peri-urban communities. As such, there is a knowledge gap regarding the implementation of reliable wastewater surveillance in small and rural communities for the purpose of tracking rates of incidence of COVID-19 and other pathogens or biomarkers. This study examines the relationships existing between SARS-CoV-2 viral signal from wastewater samples harvested from an upstream pumping station and from an access port at a downstream wastewater treatment lagoon with the community's COVID-19 rate of incidence (measured as percent test positivity) in a small, rural community in Canada. Real-time quantitative polymerase chain reaction (RT-qPCR) targeting the N1 and N2 genes of SARS-CoV-2 demonstrate that all 24-h composite samples harvested from the pumping station over a period of 5.5 weeks had strong viral signal, while all samples 24-h composite samples harvested from the lagoon over the same period were below the limit of quantification. RNA concentrations and integrity of samples harvested from the lagoon were both lower and more variable than from samples from the upstream pumping station collected on the same date, indicating a higher overall stability of SARS-CoV-2 RNA upstream of the lagoon. Additionally, measurements of PMMoV signal in wastewater allowed normalizing SARS-CoV-2 viral signal for fecal matter content, permitting the detection of actual changes in community prevalence with a high level of granularity. As a result, in sewered small and rural communities or low-income regions operating wastewater lagoons, samples for wastewater surveillance should be harvested from pumping stations or the sewershed as opposed to lagoons.

4.3. Introduction

In late 2019, cases of COVID-19 began to spread rapidly internationally (Li et al., 2020). It became clear to public health officials across the world that this new disease, caused by the severe acute respiratory syndrome coronavirus 2 (SARS-COV-2) (Eurosurveillance Editorial Team, 2020), was rapidly becoming a pandemic-potential pathogen due to its relatively low virulence but high degree of infectiousness (He et al., 2020). More than a year after the first cases of COVID-19, the world is still grappling with the disease and newer and more infectious variants of the virus are spreading (Duong, 2021; Galloway et al., 2021; Volz et al., 2020; Walensky et al., 2021), causing widespread disease and death (WHO COVID-19 Dashboard). At the time of writing (May 20th, 2021), more than 2.4% of the global population (191.1 M) has been infected by SARS-CoV-2, and 2.1% of those infected have died (4.1 M) (WHO COVID-19 Dashboard).

Now widely applied in over 1,000 sites in more than 50 countries worldwide (Ahmed et al., 2020; Arora et al., 2020; Bivins et al., 2020b; D'Aoust et al., 2021a; Gonzalez et al., 2020; Mao et al., 2020; Medema et al., 2020; Naughton et al., 2021; Polo et al., 2020; Randazzo et al., 2020; Sims and Kasprzyk-Hordern, 2020; Thompson et al., 2020), Wastewater and environmental monitoring (WEM) efforts conducted with RT-qPCR are underway around the world, focused primarily in larger metropolitan areas of higher income countries (Bivins et al., 2020b). By and large rural communities and low-income countries have not had the same services afforded to them as urban and peri-urban communities (WEF Network of Wastewater-Based Epidemiology, 2021) and higher income countries, which is based on numerous factors that include but are not limited to: i) discrepancies in financial and material resources, ii) distance to research, academic and governmental facilities capable of carrying out the analyses and iii) capacity of the local public health unit to take in the results and act upon them. Furthermore, smaller, rural communities and low-income countries without larger mechanical water resource recovery facilities may not have the staff, equipment or expertise to carry out sampling for SARS-CoV-2 viral detection in wastewater (Haider et al., 2016; Naughton et al., 2021; Switzer et al., 2016). Larger facilities are often equipped with automatic composite samplers throughout the plant, making the implementation of a WEM monitoring program in comparison relatively easy for routine purposes. Furthermore, there is a growing consensus that higher concentrations of SARS-CoV-2 viral particles are found in wastewater solids (Chik et al., 2021; D'Aoust et al., 2021b; Graham et al., 2020; Peccia et al., 2020; Pecson et al., 2021) and as such several WEM efforts are now focusing on measuring signal from solid fractions of samples (Chik et al., 2021; Wolfe et al., 2021). In small and rural communities, harvesting solids may be problematic as dedicated solid separation units present in larger facilities located in urban and peri-urban communities may not exist in smaller facilities, requiring different sampling approaches. Unfortunately, the limited resources available in small and rural communities or lower income countries often compromise the WEM efforts. The communities may in turn be at the mercy of funding or mandates due to the lack physical, material and/or financial resources. As an example of the precariousness of WEM in smaller communities, Finnish authorities recently announced in June 2021 that they would-be discontinuing SARS-CoV-2 WEM efforts in cities with populations smaller than 150,000 (Finnish institute for health and welfare, 2021). In contrast, remote communities in the Northwest Territories of Canada have implemented wastewater surveillance to monitor the communities for COVID-19 viral signal (Government of Northwest Territories, 2021), despite the low population of the geographic area (<45,000). Having clear guidelines, appropriate analytical methods and low-cost strategies for surveillance which are also applicable for smaller communities will therefore be critical to ensure that WEM efforts service the most residents in each region.

Most WEM efforts attempt to predict trends of epidemiological metrics of COVID-19 in the general population by quantifying increases and decreases in the rates of clinical cases of COVID-19 (Bivins et al., 2020a; D'Aoust et al., 2021a; Hill et al., 2020; Kumar et al., 2021; Polo et al., 2020). These environmental studies will often focus on collecting samples within the raw influent or primary sludge due to the relatively high concentration of solids in these wastewater streams (Hill et al., 2020). However, several municipalities operating smaller types of treatment systems such as waste stabilization ponds, also known as wastewater treatment lagoons, do not have direct access to raw influent or primary sludge. Smaller communities may however have direct access to the waste stabilization ponds and pumping/lift stations (MOE Ontario, 2008). Wastewater treatment lagoons are commonly used in the world, with over 1,200 in operation in Canada (Statistics Canada, 2016), over 5,500 in Europe (Mara, 2009), and over 8,000 in the United States alone (USEPA, 2011). Solids separation occurs in lagoons due to the slowing of flow velocities, leading to particle settling, particularly in the same area of the lagoon that oxidizes carbonaceous deleterious substances or in lagoon areas or isolated lagoon units designed specifically for solids sedimentation (Asano et al., 2007; D'Aoust et al., 2021c; Leblond et al., 2020). As such, harvesting of wastewater solids in lagoon treatment systems with the goal of performing WEM is very difficult due to potentially long retention times in lagoons, the degradation of RNA targets due to environmental temperature fluctuations and the difficulty of collecting "fresh" solids from a lagoon representing current incidence of COVID-19 in the community. Furthermore, as lagoon systems are located outdoors and exposed to ambient temperatures, in locales where air temperatures can dip below freezing these systems may become difficult to sample due to the presence of ice-cover. High temperatures during summer months and UV radiation from sunlight may also further degrade viral RNA (Verbyla et al., 2017). As a result, smaller communities may not have evident sampling locations to collect wastewater samples containing SARS-CoV-2 viral particles which can accurately represent changes in prevalence of the disease in the community. Another factor easing the implementation of WEM programs in small and rural communities is to see if the community is sewered or not. In communities that are not sewered and where centralized sampling points are not available, sewage brought to lagoons can be sampled from sewage and sludge trucks while they are being emptied at the facility (Telliard, 1989).

In preparation for applying SARS-CoV-2 wastewater surveillance initiatives in a small sewered community in Eastern Ontario (Canada), wastewater samples were collected from an access/sampling point situated between the first and second cells of a lagoon treatment system, and from the last pumping station on the sewer network located upstream of the lagoon treatment system. The specific objectives of this study were to: i) compare SARS-CoV-2 signal at both sampling locations for strength of the RNA viral signal and RNA integrity and ii) compare the higher integrity longitudinal SARS-CoV-2 signal to existing

community epidemiological data to ascertain the ability of WEM to track and predict and correlate with trends in rates of incidence of COVID-19 in small and rural communities.

4.4. Experimental methods

4.4.1. Rural community sampling locations

The wastewater of a rural community of less than 5,000 inhabitants in Eastern Ontario (Canada) were sampled in this study between October 2020 and May 2021 (Figure 4-1). The rural community is sewered, with the wastewater flowing into the main pumping station located 1.3 km upstream of a wastewater treatment lagoon. The lagoon system consists of 3 cells/ponds (total surface area of approximately 182,000 m^2) operated in-series that flow from cell #1 to #2 to #3. The lagoon receives continuous inflow with an average daily flow rate of 2,110 m^3/d. The lagoon system discharges to a nearby river twice annually, in Spring (Mar. 7th to May 15th) and Fall (Oct. 1st to Dec. 19th). The lagoon system does not include a wetland component. Cell #3 has bottom-mounted aerators that are engaged prior to and during discharge to strip hydrogen sulfide before the release of treated wastewater to the natural environment. To control phosphorus concentrations in the final effluent of the lagoon treatment facility, a polyaluminum sulphate solution is injected directly into the pressurized wastewater pipe following the pumping station (force main) immediately before being released to the first cell of the lagoon system. The yearly average treatment efficiency of $cBOD_5$, total suspended solids, total phosphorus, total ammonia nitrogen, total Kjeldahl nitrogen and alkalinity is of 96.0%, 94.9%, 98.0%, 96.9%, 94.1% and 64.6% removal efficiency, respectively.

Two locations were sampled for wastewater in the rural community: i) the upstream pumping station, which receives the same annual volumetric flow of wastewater as the wastewater treatment lagoon system itself, and ii) an access/sampling point situated between cells 1 and 2 of the lagoon treatment system (Figure 4-1). The wastewater travel time between the pumping station and the inlet of the lagoon is approximately 15 minutes, while the residence time of the wastewater at the sampling location between the two cells of the lagoon ranges significantly due to the annual discharge design of the system (approximated residence times ranging between 80 hours and 10 days during the period of the study). The typical wastewater characteristics at the pumping station and at the lagoon effluent are shown in Table 4-1.

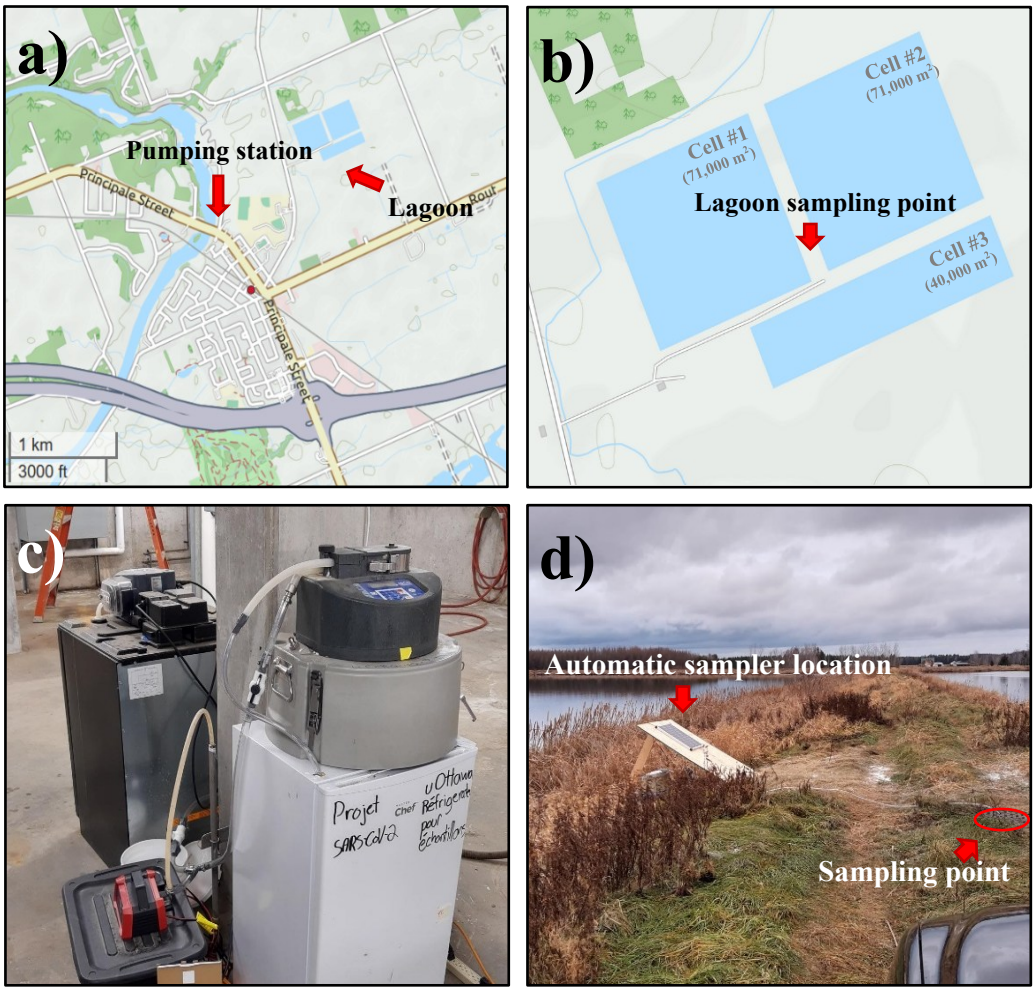


Figure 4-1: Sampling locations and configurations: a) geographic locations of pumping station and lagoon, b) lagoon treatment system consisting of three cells, identification of sampling point, c) automatic sampler at pumping station, sampler dispenses samples into refrigerator, and d) automatic sampler under the solar panel at lagoon sampling point and sampling point.

Table 4-1. Yearly average wastewater characteristics at the pumping station and lagoon effluent.

	Yearly average pumping station wastewater characteristics (avg. ± standard dev.)	Yearly average pumping lagoon wastewater characteristics (avg. ± standard dev.)
$cBOD_5$ (mg/L)	88.4 ± 80.3	3.5 ± 0.9
Total suspended solids (mg/L)	224.3 ± 154.1	11.4 ± 6.1
Total phosphorus (mg P/L)	8.0 ± 5.6	0.2 ± 0.1
Total ammonia nitrogen (mg N/L)	34.2 ± 10.5	1.1 ± 1.1
Total Kjeldahl nitrogen (mg N/L)	49.0 ± 20.9	2.9 ± 2.2
Alkalinity (mg/L as $CaCO_3$)	356.2 ± 60.4	126.2 ± 34.0

4.4.2. Sample collection

At the pumping station, 24-hr composite samples of wastewater were collected every 3 to 7 days from October 16th, 2020, to May 2nd, 2021, using an ISCO 6700 series automatic sampler (Teledyne ISCO, Lincoln, NE, USA). The autosampler located at the pumping station pumped the wastewater into a storage container located inside an adjacent refrigerator to maintain the samples at 4°C until collection (within 24 hours). At the lagoon sampling point, 24-hr composite samples of wastewater were also collected every 3 to 7 days from December 3rd, 2020, to January 11th, 2021. The autosampler located at the lagoon pumped the wastewater into a sealed bottle in an insulated foam container located adjacent to the autosampler. Outdoor temperatures at the lagoon during the study period (Dec. 3rd, 2020, to Jan. 11th, 2021) oscillated between -5.5°C and 1.3°C, hence allowing safe preservation of the samples between sampling and collection without additional refrigeration being required. Composite samples were comprised of twenty-four 50 mL aliquots. During the pairwise comparison of both locations from Dec. 3rd, 2020, to Jan. 11th, 2021), the automatic samplers were programmed to collect samples at the same time at both locations. After every sampling cycle ended, the composite samples were collected and were transported on ice to the laboratory for analysis. Once in the laboratory, samples were concentrated immediately, and the resulting pellets were frozen at -30°C and processed within 14 days. After January 11th, site access became difficult due to low outdoor temperatures, freezing of the lagoon, and snowing conditions, making access to the automatic sampler highly difficult, which led to the cessation of sampling at the lagoon.

4.4.3. Sample concentration, extraction, and PCR quantification

The composite samples were concentrated by allowing the samples to settle at 4°C for an hour, followed by the decantation of the supernatant to isolate the settled solids fraction. 40 mL of remaining solid fraction was then transferred to a 40 mL centrifuge tube and samples were then centrifuged for 45 mins at 10,000 x g at 4°C to isolate the centrifuged pellet. Sample pellets which could not be immediately processed were frozen at -30°C for a period of up to 14 days before being extracted. RNA was extracted and purified from the resulting pellet using the RNeasy PowerMicrobiome kit (Qiagen, Germantown, MD, USA) using a QIAcube Connect automated extraction platform, with the protocol modifications specified in an earlier study (D'Aoust et al., 2021b). The SARS-CoV-2 signal in the samples was assayed using a singleplex one-step RT-qPCR targeting the N1 and N2 gene regions of SARS-CoV-2 genome. The signal of pepper mild mottle virus (PMMoV) was also measured in each of the samples (samples were diluted 1/10 for measurements of PMMoV). In each PCR reaction, the reaction mix consisted of 1.5 µl of RNA template, 500 nM of each of forward and reverse primer (IDT, Kanata, Canada) in 4x TaqMan® Fast Virus 1-step Mastermix (Thermo-Fisher, USA) with 125 nM probe (IDT, Kanata, Canada) in final volume of 10

µl. The samples were run in triplicates with non-template controls and were quantified using a five-point gradient of the EDX SARS-CoV-2 COV-19 RNA standard (Exact Diagnostics, USA). Reverse transcription (RT) was performed at 50˚C for 5 minutes followed by RT inactivation and initial denaturation at 95˚C for 20 seconds. This was followed by 45 cycles of denaturation at 95˚C for 3 seconds and annealing/extension at 60˚C for 30 seconds with a CFX Connect qPCR thermocycler (Bio-Rad, USA). The assay limit of detection (ALOD, ≥95% detection) was assessed (D'Aoust et al., 2021b) and determined to be approximately 2 copies/reaction for both N1 and N2 SARS-CoV-2 gene targets. The assay limit of quantification (ALOQ, CV=35%) was determined to be approximately 3.2 copies/reaction for N1 and 8.1 copies/reaction for N2 SARS-CoV-2 gene targets. SARS-CoV-2 N1 and N2 gene region viral signals were normalized by dividing the N1 and N2 gene copies per reaction by the PMMoV gene copies per reaction, as a means of normalizing the N1 and N2 signal by the quantity of fecal matter in the sample (D'Aoust et al., 2021b, 2021a; Graham et al., 2020; Kitajima et al., 2018). Vesicular stomatitis virus (VSV) was used as an internal control to monitor the efficiency of the viral concentration and extraction processes and was spiked into the sample prior to extraction. The extraction efficiency quantified with the VSV spike-in was between 3-4.5%. All samples were checked for inhibition by diluting the samples by a factor of 4 and 10 and measuring the corresponding drop in signal of PMMoV.

4.4.4. Assessment of RNA integrity

Samples were analysed for RNA integrity using an Agilent 2100 Bioanalyzer. RNA (2 µL) of each sample was loaded on an RNA 6000 Pico Chip (#5067-1513). Data analysis and RNA concentration calculations were performed using Agilent's proprietary 2100 Expert software (version B.02.10.SI764).

4.4.5. Collection of epidemiological data and correlation to wastewater viral signal

Weekly epidemiological data was obtained from the ICES COVID-19 dashboard (https://www.ices.on.ca/DAS/AHRQ/COVID-19-Dashboard) and the Eastern Ontario Health Unit (EOHU) dashboard (https://eohu.ca/en/covid/covid-19-status-update-for-eohu-region). Correlation analyses were then performed between the PMMoV-normalized SARS-CoV-2 viral signal in wastewater and the available epidemiological data.

4.5. Results & discussion

During the pairwise comparison of samples collected from both locations at the same time-point, all samples (5/5) from the pumping station showed detectable signal for the N1 and N2 gene regions of SARS-CoV-2 (Figure 4-2), as well as for PMMoV. Measurements of viral signal for the N1 gene region of

the samples collected from the pumping station ranged from 5.5 x 10^3 - 4.6 x 10^4 genomic copies/L while measurements for the N2 gene region ranged from 4.3 x 10^3 – 3.2 x 10^4 genomic copies/L. Meanwhile, all composite samples collected at the lagoon sampling point between cells #1 and #2 of the lagoon were below the ALOQ and the ALOD for the N1 and N2 gene, and 4 out of 5 samples had no detectable SARS-CoV-2 viral signal altogether. During the same short span of side-by-side test period, PMMoV was only observed in three of the five lagoon samples.

In samples collected from the pumping station, measurements of PMMoV ranged from 1.4 x 10^5 – 4.8 x 10^6 genomic copies/L, and in lagoon samples with PMMoV measurements, the PMMoV concentration ranged from 6.9 x 10^2 – 9.9 x 10^5 genomic copies/L. The lack of PMMoV signal in some of the lagoon samples could potentially signify that near complete RNA degradation of PMMoV RNA occurred in the lagoon. When comparing viral signal measurements from the RT-qPCR analyses for the N1 and N2 SARS-CoV-2 gene regions and PMMoV between the pumping station and lagoon samples, pairwise comparisons clearly outline a stronger detection of both SARS-CoV-2 N gene regions and PMMoV viral signal in the samples collected from the pumping station (Figure 4-2). Furthermore, due to the ubiquity of PMMoV in wastewater, observing PMMoV measurements may allow to distinguish SARS-CoV-2 N1 and N2 gene region true non-detects from false-negatives caused by sample degradation or severe inhibition of the sample (Hong et al., 2021).

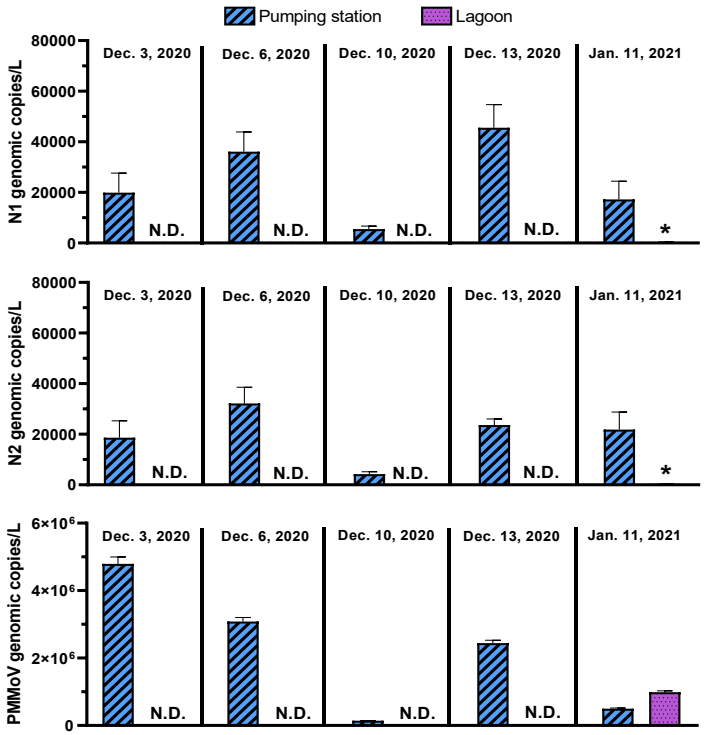


Figure 4-2: Comparison of genomic copies/L of pumping station samples and waste stabilization pond samples over time for the N1 and N2 SARS-CoV-2 gene regions, and PMMoV. Bars with a star (*) indicate that the sample signal was below the ALOQ.

RNA of the SARS-CoV-2 and PMMoV targets in samples collected from the sampling location in the lagoon may have experienced more degradation due to extended residence times within the lagoon. Although temperature and storage time have been shown to affect SARS-CoV-2 viral signal degradation in wastewater (Hart and Halden, 2020), the similar storage temperature of the pumping station and lagoon samples during the pairwise study along with the short storage time until analysis enable this study to isolate the difference in signals to the conditions of the two sampling locations. Furthermore, due to the low temperature of the wastewater in the pumping station and within the lagoon during the study, viral degradation due to elevated temperatures is not a likely pathway of degradation. It is also possible that the RNA of the samples in the lagoon may have been subject to UV degradation once within the lagoon itself (Fongaro et al., 2012; Verbyla et al., 2017). Furthermore, as SARS-CoV-2 viral particles are believed to likely partition preferentially to wastewater solids in typical wastewater conditions (Arora et al., 2020; Chakraborty et al., 2021; D'Aoust et al., 2021a; Graham et al., 2020; McLellan et al., 2021), a significant portion of the viral RNA may have settled throughout the first lagoon cell as the flow velocity of the wastewater immediately decreases upon entering the lagoon system's first cell. Additionally, this facility doses polyaluminum sulphate for phosphorus abatement, which likely contributes to a more rapid and pronounced settling of solids. It is believed that the polyaluminum may also help flocculate SARS-CoV-2

genetic material, as evidenced by several studies employing aluminum-driven flocculation concentration methods (Barril et al., 2021; Randazzo et al., 2020). It is noted that all mechanisms contributing to potential degradation of viral signal in the lagoon are symptomatic of treatment of wastewater in the lagoon. Further investigations with a control location which does not use polyaluminum sulphate could be conducted to verify this hypothesis.

Total RNA concentrations were measured in a series of samples collected from the pumping station and the lagoon sampling point. Results of the analyses are shown in Figure 4-3. RNA concentrations are distinctly lower in lagoon samples as compared to pumping station.

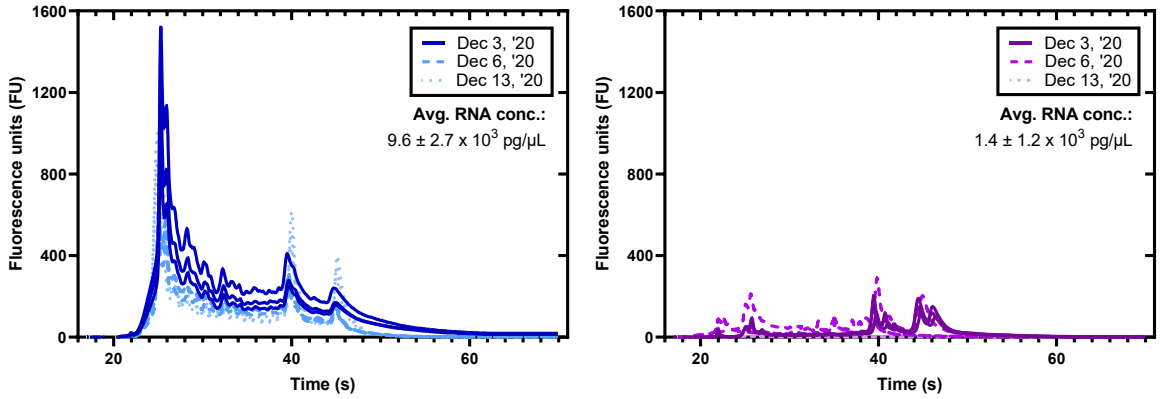


Figure 4-3: Electropherograms of samples from the a) pumping station and the b) lagoon, showing drastic differences in the RNA profiles.

The epidemiological data pertaining to this study were not available at the granulation of the studied community itself (pop.: ~4,000; ~5 km^2), but rather for a larger geographical region (pop.: ~200,000; ~5,300 km^2) that includes the community. The lack of available epidemiological data for the small community itself is indicative of the need for additional resources for small, rural communities and the potential for the application of WEM in these communities as an effective indicator of incidence of infections at the granulation of the community. Further, the clinical metric that was available at the geographic region level was percent positivity as opposed to daily clinical new cases. As such, this study compares the SARS-CoV-2 viral signal in wastewater to the percent positivity data acquired at the geographic region. The studied rural community (2,500-5,000 people) represents approximately 2% of the whole population within the health unit's geographical boundaries for which epidemiological data are available. Although travel between communities in this geographic area is common, it is noted that presentation of the community SARS-CoV-2 viral signal against the epidemiological data at the geographic region level assumes that this town and its citizens behave similar to the residents of the larger region, which may not necessarily be a

correct assumption. However, due to the limitations of available epidemiological information no other data were available to perform a comparison. As outlined by these results, it appears that samples harvested from the pumping station of the community could provide similar viral signal trends to the clinical data sets, making the pumping station a suitable sampling location for rural communities that are serviced by wastewater treatment lagoons. It is hypothesized that samples collected from the last pumping station of a smaller rural community will have similar usability for wastewater surveillance to samples collected from influent of a larger mechanical wastewater treatment plant.

When comparing the pumping station samples expressed as PMMoV-normalized viral genomic copies, viral genomic copies per gram of wastewater solids and viral genomic copies per L to available epidemiological data (clinical test percent positivity for the whole population) (Figure 4-4), a degree of visible agreement could be seen between the SARS-CoV-2 viral signal in wastewater and the reported percent positivity in the geographic region. However, this comparison may not be of significant relevance as the clinical data references a larger geographical zone than the sampled sewershed. It has been outlined in several studies that mass or volumetric normalization of SARS-CoV-2 viral signal alone may not truly capture sewershed dilution effects (Bivins et al., 2021; D'Aoust et al., 2021b; Wu et al., 2020). Furthermore, it is believed that while not observed or demonstrated with solid mass (copies/g) or volume (copies/L) normalized SARS-CoV-2 viral genomic copies, PMMoV-normalized viral genomic copies show a true change in community prevalence as the normalization with PMMoV helps account for the intrinsic quantity of fecal material in the wastewater (Graham et al., 2020; Kitamura et al., 2021; Wolfe et al., 2021; Wu et al., 2021). PMMoV normalization in WEM applications is believed to be particularly important in the context of surveillance of fecally shed pathogens as it allows to call true localized changes in prevalence which could otherwise be missed without normalizing for the quantity of fecal material in wastewater.

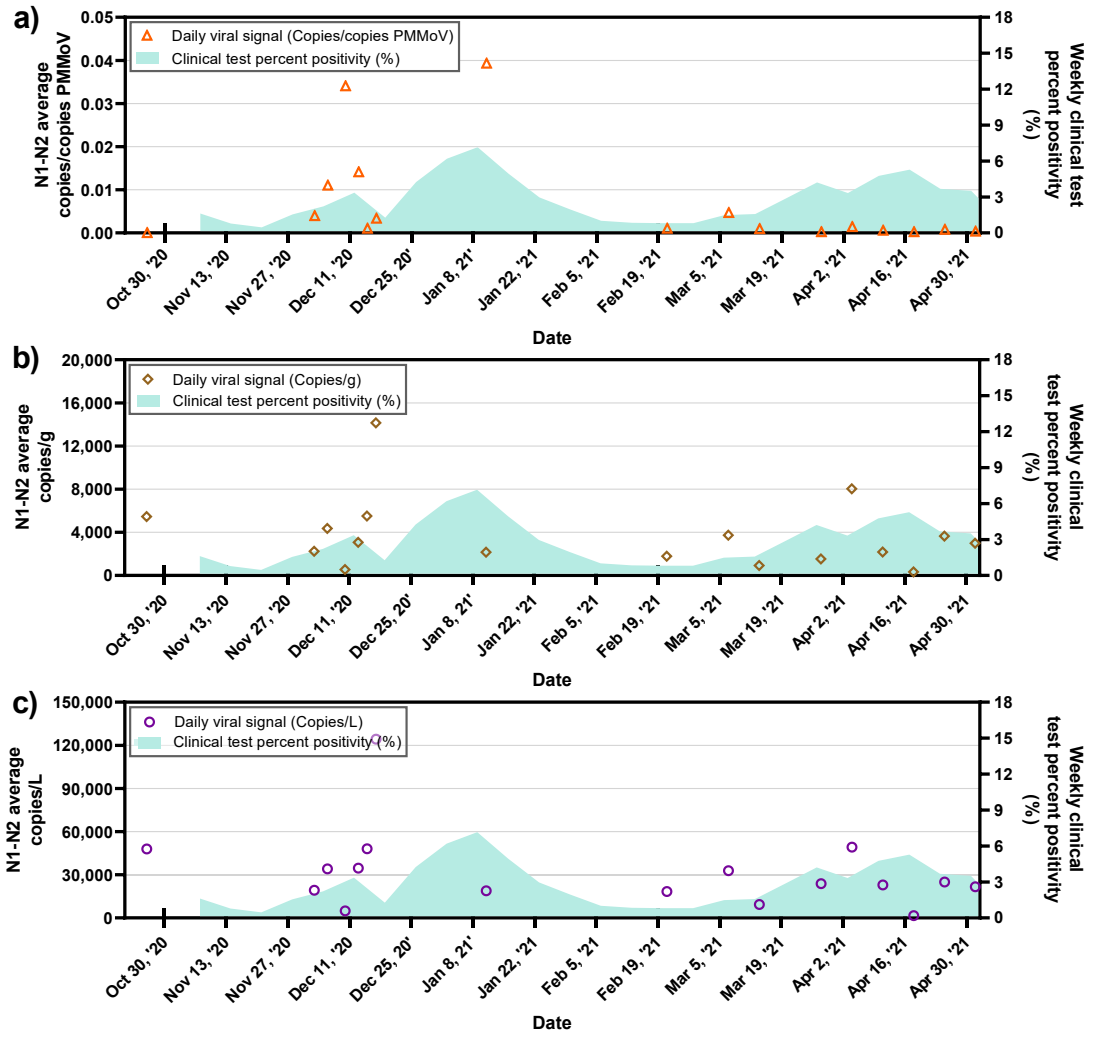


Figure 4-4: Average SARS-CoV-2 signal in the pumping station wastewater samples expressed as a) PMMoV normalized SARS-CoV-2 viral genomic copies, b) SARS-CoV-2 viral copies/g and c) SARS-CoV-2 viral genomic copies/L, along with the weekly COVID-19 test percent positivity.

4.6. Conclusions and recommendations

As many locations throughout the world have experienced new resurgence in COVID-19 cases due to the rapid spread of infectious variants of concern, it has become increasingly important for communities to implement effective COVID-19 wastewater monitoring programs that can rapidly detect and predict upcoming resurgences in COVID-19 cases. WEM programs may provide epidemiological information at a higher level of granularity to public health units than what is currently available in small, rural communities and low-income countries. Unfortunately, such programs are not frequently found in smaller, rural

communities or low-income countries, and these communities often rely on low-cost, more passive treatment systems, compounding the gap of knowledge between the application of WEM to high-income, peri-urban and urban communities compared to low-income and rural communities. These smaller communities are particularly vulnerable to changes in funding or mandates as they may not have the resources to take over or start WEM initiatives on their own.

In this study, it was observed that in municipalities with wastewater lagoons, surveillance of changes in incidence of COVID-19 in the general population is possible via sampling from an upstream pumping station within the sewershed. Measurements of N1 and N2 SARS-CoV-2 gene regions and PMMoV in wastewater demonstrate consistent strong detection in samples collected at the upstream pumping station, but not from samples collected in wastewater treatment lagoons. Preliminary results show that samples collected from the wastewater treatment lagoon dosing polyaluminum sulphate for phosphorus removal demonstrates significant weaker detection due to potential preferential partitioning of SARS-CoV-2 viral particles to solids which rapidly settle upon entering the lagoon inlet structure. Furthermore, degradation of SARS-CoV-2 and PMMoV genetic material in the lagoon may be associated with the long retention time of the system. Finally, UV light exposure and degradation of the genetic material may also be a potentially significant mechanism of genetic material degradation. Even though SARS-CoV-2 genetic material is largely attached/associated to solids, the long retention time of the lagoon system may enable UV degradation of the solids partitioned material across a significant period of time. Additionally, it is observed that PMMoV-normalized viral signal may allow for detection of true increases in prevalence by normalizing measurements for the quantity of fecal material in wastewater. By observing PMMoV viral signal in wastewater, it may also be possible to distinguish SARS-CoV-2 N1 and N2 non-detects from false-negatives caused by sample degradation or severe inhibition. Finally, it is observed that wastewater-acquired SARS-CoV-2 viral signal from the upstream pumping station can be measured without difficulty and as such, could be used effectively in tandem with local epidemiological data to help detect and track new and existing COVID-19 outbreaks, even where localized increases in COVID-19 prevalence would not be visible with low granularity publicly available weekly regional epidemiological information.

4.7. Limitations and 2025 field updates

This chapter underscores the development of sampling strategies for WEM in rural, sewered communities, showing that SARS-CoV-2 and PMMoV RNA can be reliably detected at upstream pumping stations. However, a few limitations to this study exist: 1) The selected experimental location had a relatively poor sampling location at the lagoon, which guaranteed a long wastewater retention time before sampling, which could have impacted results negatively (suppressing signal due to dilution, and UV-

irradiation of the molecular targets) for the lagoon samples; and 2) The correlations between the wastewater measurements of SARS-CoV-2 RNA and the clinical metrics relied on regional epidemiological data rather than community-level metrics, reducing the precision of correlations. As of 2025, expanding WEM into rural and low-income settings, particularly in locations that are unsewered or with decentralized sewage systems, remains a global challenge, with appropriate sampling locations, cold-chain constraints, and analytical capacity being major barriers (Hamilton et al., 2024; Cohen et al., 2024; Delgado Vela et al., 2024).

4.8. Declaration of competing interests

The authors declare that no known competing financial interests or personal relationships influenced the work reported in this manuscript.

4.9. Ethical considerations

This study involved the analysis of anonymized environmental wastewater samples and aggregated clinical data. All samples were collected from large municipal sewersheds, ensuring that no individual or household could be identified. As such, the research did not involve human subjects, personal identifiers, or interactions requiring ethical review.

4.10. Funding

This research was supported by the Province of Ontario's Wastewater Surveillance Initiative (WSI). This research was also supported by a CHEO (Children's Hospital of Eastern Ontario) CHAMO (Children's Hospital Academic Medical Organization) grant, awarded to Dr. Alex E. MacKenzie.

4.11. Acknowledgements

The authors wish to acknowledge the help and assistance of the University of Ottawa, the Ottawa Hospital, the Children's Hospital of Eastern Ontario, the Children's Hospital of Eastern Ontario's Research Institute, Public Health Ontario and all their employees involved in the project. Their time, facilities, resources, and feedback are greatly appreciated. The authors also wish to specifically outline the assistance of Mr. Alain Castonguay.

4.12. References

Ahmed, W., Angel, N., Edson, J., Bibby, K., Bivins, A., O'Brien, J.W., Choi, P.M., Kitajima, M., Simpson, S.L., Li, J., Tscharke, B., Verhagen, R., Smith, W.J.M., Zaugg, J., Dierens, L., Hugenholtz, P., Thomas, K. V., Mueller, J.F., 2020. First confirmed detection of SARS-CoV-2 in untreated wastewater in Australia: A proof of concept for the wastewater surveillance of COVID-19 in the community. Sci. Total Environ. 728, 138764. https://doi.org/10.1016/j.scitotenv.2020.138764

Alpaslan-Kocamemi, B., Kurt, H., Sait, A., Sarac, F., Saatci, A.M., Pakdemirli, B., 2020. SARS-CoV-2 detection in Istanbul wastewater treatment plant sludges. medRxiv 2020.05.12.20099358. https://doi.org/10.1101/2020.05.12.20099358

Balboa, S., Mauricio-Iglesias, M., Rodríguez, S., Martínez-Lamas, L., Vasallo, F.J., Regueiro, B., Lema, J.M., 2020. The fate of SARS-CoV-2 in wastewater treatment plants points out the sludge line as a suitable spot for incidence monitoring. medRxiv 2020.05.25.20112706. https://doi.org/10.1101/2020.05.25.20112706

Bar-On, Y.M., Flamholz, A., Phillips, R., Milo, R., 2020. SARS-CoV-2 (COVID-19) by the numbers. Elife 9, 697–698. https://doi.org/10.7554/eLife.57309

Bar Or, I., Yaniv, K., Shagan, M., Ozer, E., Erster, O., Mendelson, E., Mannasse, B., Shirazi, R., Kramarsky-Winter, E., Nir, O., Abu-Ali, H., Ronen, Z., Rinott, E., Lewis, Y.E., Friedler, E.F., Paitan, Y., Bitkover, E., Berchenko, Y., Kushmaro, A., 2020. Regressing SARS-CoV-2 sewage measurements onto COVID-19 burden in the population: a proof-of-concept for quantitative environmental surveillance. medRxiv 2020.04.26.20073569. https://doi.org/10.1101/2020.04.26.20073569

Bwire, G.M., Majigo, M. V., Njiro, B.J., Mawazo, A., 2020. Detection profile of SARS-CoV-2 using RT-PCR in different types of clinical specimens: a systematic review and meta-analysis. J. Med. Virol. https://doi.org/10.1002/jmv.26349

Cohen, A., Vikesland, P., Pruden, A., Krometis, L.A., Lee, L.M., Darling, A., Yancey, M., Helmick, M., Singh, R., Gonzalez, R., Meit, M., Degen, M., Taniuchi, M., 2024. Making waves: The benefits and challenges of responsibly implementing wastewater-based surveillance for rural communities. Water Res. 250, 121095. https://doi.org/10.1016/j.watres.2023.121095

Dalzell, S., 2020. Australia to test sewage for coronavirus as testing net widens - ABC News [WWW Document]. ABC News Aust. URL https://www.abc.net.au/news/2020-04-17/australia-to-test-sewage-for-coronairus-as-testing-net-widens/12156858 (accessed 7.28.20).

Daughton, C.G., 2009. Chemicals from the practive of healthcare: challenges and unknowns posed by residues in the environment. Environ. Toxicol. Chem. 28, 2490–2494. https://doi.org/10.1897/09-138.1

Delgado Vela, J., Philo, S.E., Brown, J., Taniuchi, M., Cantrell, M., Kossik, A., Ramaswamy, M., Ajjampur, S.S., Guerfali, F.Z., Holm, R.H., Meschke, J.S., Otero, M.C.B., Pickering, A.J., Rahman, M.,

Shaw, A.G., Shrestha, A., Sirikanchana, K., Tevuzula, V.M., Halden, R.U., Boehm, A.B., Bibby, K., 2024. Moving beyond Wastewater: Perspectives on Environmental Surveillance of Infectious Diseases for Public Health Action in Low-Resource Settings. Environ. Heal. 2–5. https://doi.org/10.1021/envhealth.4c00119

Gonzalez, R., Curtis, K., Bivins, A., Bibby, K., Weir, M.H., Yetka, K., Thompson, H., Keeling, D., Mitchell, J., Gonzalez, D., 2020. COVID-19 surveillance in Southeastern Virginia using wastewater-based epidemiology. Water Res. 186, 116296. https://doi.org/10.1016/j.watres.2020.116296

Gupta, S., Parker, J., Smits, S., Underwood, J., Dolwani, S., 2020. Persistent viral shedding of SARS-CoV-2 in faeces – a rapid review. Color. Dis. 22, 611–620. https://doi.org/10.1111/codi.15138

Hamilton, K.A., Wade, M.J., Barnes, K.G., Street, R.A., Paterson, S., 2024. Wastewater-based epidemiology as a public health resource in low- and middle-income settings. Environ. Pollut. 351, 124045. https://doi.org/10.1016/j.envpol.2024.124045

Haramoto, E., Malla, B., Thakali, O., Kitajima, M., 2020. First environmental surveillance for the presence of SARS-CoV-2 RNA in wastewater and river water in Japan. Sci. Total Environ. 737, 140405. https://doi.org/10.1016/j.scitotenv.2020.140405

Hill, K., Zamyadi, A., Deere, D., Vanrolleghem, P.A., Crosbie, N.D., 2020. SARS-CoV-2 known and unknowns, implications for the water sector and wastewater-based epidemiology to support national responses worldwide: early review of global experiences with the COVID-19 pandemic. Water Qual. Res. J. 1–11. https://doi.org/10.2166/wqrj.2020.100

La Rosa, G., Bonadonna, L., Lucentini, L., Kenmoe, S., Suffredini, E., 2020. Coronavirus in water environments: Occurrence, persistence and concentration methods - A scoping review. Water Res. 179, 115899. https://doi.org/10.1016/j.watres.2020.115899

Long, Q.X., Tang, X.J., Shi, Q.L., Li, Q., Deng, H.J., Yuan, J., Hu, J.L., Xu, W., Zhang, Y., Lv, F.J., Su, K., Zhang, F., Gong, J., Wu, B., Liu, X.M., Li, J.J., Qiu, J.F., Chen, J., Huang, A.L., 2020. Clinical and immunological assessment of asymptomatic SARS-CoV-2 infections. Nat. Med. https://doi.org/10.1038/s41591-020-0965-6

Medema, G., Heijnen, L., Elsinga, G., Italiaander, R., Brouwer, A., 2020. Presence of SARS-Coronavirus-2 RNA in Sewage and Correlation with Reported COVID-19 Prevalence in the Early Stage of the Epidemic in The Netherlands. Environ. Sci. Technol. Lett. 7, 511–516. https://doi.org/10.1021/acs.estlett.0c00357

Michael-Kordatou, I., Karaolia, P., Fatta-Kassinos, D., 2020. Sewage analysis as a tool for the COVID-19 pandemic response and management: the urgent need for optimised protocols for SARS-CoV-2 detection and quantification. J. Environ. Chem. Eng. 8, 104306. https://doi.org/10.1016/j.jece.2020.104306

National Institute for Public Health and the Environment, 2020. Sewage research: decline of novel coronavirus in the Netherlands | RIVM [WWW Document]. RIVM. URL

https://www.rivm.nl/en/news/sewage-research-decline-of-novel-coronavirus-in-netherlands (accessed 7.28.20).

Nemudryi, A., Nemudraia, A., Surya, K., Wiegand, T., Buyukyoruk, M., Wilkinson, R., Wiedenheft, B., 2020. Temporal detection and phylogenetic assessment of SARS-CoV-2 in municipal wastewater. medRxiv 2020.04.15.20066746. https://doi.org/10.1101/2020.04.15.20066746

Orive, G., Lertxundi, U., Barcelo, D., 2020. Early SARS-CoV-2 outbreak detection by sewage-based epidemiology. Sci. Total Environ. 732, 139298. https://doi.org/10.1016/j.scitotenv.2020.139298

Pan, X., Chen, D., Xia, Y., Wu, X., Li, T., Ou, X., Zhou, L., Liu, J., 2020. Asymptomatic cases in a family cluster with SARS-CoV-2 infection. Lancet Infect. Dis. 20, 410–411. https://doi.org/10.1016/S1473-3099(20)30114-6

Parasa, S., Desai, M., Thoguluva Chandrasekar, V., Patel, H.K., Kennedy, K.F., Roesch, T., Spadaccini, M., Colombo, M., Gabbiadini, R., Artifon, E.L.A., Repici, A., Sharma, P., 2020. Prevalence of gastrointestinal symptoms and fecal viral shedding in Patients ŵith coronavirus disease 2019: A systematic review and meta-analysis. JAMA Netw. open 3, e2011335. https://doi.org/10.1001/jamanetworkopen.2020.11335

Peccia, J., Zulli, A., Brackney, D.E., Grubaugh, N.D., Edward, H., Casanovas-massana, A., Ko, A.I., Malik, A.A., Wang, D., 2020a. SARS-CoV-2 RNA concentrations in primary municipal sewage sludge as a leading indicator of COVID-19 outbreak dynamics 1.

Peccia, J., Zulli, A., Brackney, D.E., Grubaugh, N.D., Kaplan, E.H., Casanovas-Massana, A., Ko, A.I., Malik, A.A., Wang, D., Wang, M., Weinberger, D.M., Omer, S.B., 2020b. SARS-CoV-2 RNA concentrations in primary municipal sewage sludge as a leading indicator of COVID-19 outbreak dynamics. medRxiv 1, 2020.05.19.20105999. https://doi.org/10.1101/2020.05.19.20105999

Pleitgen, F., 2020. Covid-19: Sewage could hold the key to stopping new coronavirus outbreaks - CNN [WWW Document]. CNN. URL https://www.cnn.com/2020/06/01/europe/germany-sewage-coronavirus-detection-intl/index.html (accessed 7.28.20).

Randazzo, W., Truchado, P., Cuevas-Ferrando, E., Simón, P., Allende, A., Sánchez, G., 2020. SARS-CoV-2 RNA in wastewater anticipated COVID-19 occurrence in a low prevalence area. Water Res. 181. https://doi.org/10.1016/j.watres.2020.115942

Rimoldi, S.G., Stefani, F., Gigantiello, A., Polesello, S., Comandatore, F., Mileto, D., Maresca, M., Longobardi, C., Mancon, A., Romeri, F., Pagani, C., Moja, L., Gismondo, M.R., Salerno, F., 2020. Presence and vitality of SARS-CoV-2 virus in wastewaters and rivers. medRxiv 2020.05.01.20086009. https://doi.org/10.1101/2020.05.01.20086009

Sherchan, S.P., Shahin, S., Ward, L.M., Tandukar, S., Aw, T.G., Schmitz, B., Ahmed, W., Kitajima, M., 2020. First detection of SARS-CoV-2 RNA in wastewater in North America: A study in Louisiana, USA. Sci. Total Environ. 743, 140621. https://doi.org/10.1016/j.scitotenv.2020.140621

Thompson, J.R., Nancharaiah, Y. V, Gu, X., Lin, W., Rajal, V.B., Haines, M.B., Girones, R., Ching, L., Alm, E.J., Wuertz, S., 2020. Making waves : Wastewater surveillance of SARS-CoV-2 for population-based health management 184. https://doi.org/10.1016/j.watres.2020.116181

Wu, F., Zhang, J., Xiao, A., Gu, X., Lee, W.L., Armas, F., Kauffman, K., Hanage, W., Matus, M., Ghaeli, N., Endo, N., Duvallet, C., Poyet, M., Moniz, K., Washburne, A.D., Erickson, T.B., Chai, P.R., Thompson, J., Alm, E.J., 2020. SARS-CoV-2 titers in wastewater are higher than expected from clinically confirmed cases. mSystems 5, 2020.04.05.20051540. https://doi.org/10.1128/mSystems.00614-20

Wurtzer, S., Marechal, V., Mouchel, J.-M., Maday, Y., Teyssou, R., Richard, E., Almayrac, J.L., Moulin, L., 2020. Evaluation of lockdown impact on SARS-CoV-2 dynamics through viral genome quantification in Paris wastewaters. medRxiv 2020.04.12.20062679. https://doi.org/10.1101/2020.04.12.20062679

Yle, 2020. THL to track coronavirus in waste water | Yle Uutiset | yle.fi [WWW Document]. Yle. URL https://yle.fi/uutiset/osasto/news/thl_to_track_coronavirus_in_waste_water/11315440 (accessed 7.28.20).

Zhang, T., Cui, X., Zhao, X., Wang, J., Zheng, J., Zheng, G., Guo, W., Cai, C., He, S., Xu, Y., 2020. Detectable SARS-CoV-2 viral RNA in feces of three children during recovery period of COVID-19 pneumonia. J. Med. Virol. 92, 909–914. https://doi.org/10.1002/jmv.25795

Chapter 5 – Wastewater to Clinical Case (WC) Ratio of COVID-19 Identifies Insufficient Clinical Testing, Onset of New Variants of Concern and Population Immunity in Urban Communities

5.1. Context

The manuscript presented in this chapter of the doctoral dissertation is titled *Wastewater to clinical case (WC) ratio of COVID-19 identifies insufficient clinical testing, onset of new variants of concern and population immunity in urban communities*, by Patrick M. D'Aoust, Xin Tian, Syeda Tasneem Towhid, Amy Xiao, Élisabeth Mercier, Nada Hegazy, Jian-Jun Jia, Shen Wan, Md Pervez Kabir, Wanting Fang, Meghan Fuzzen, Maria Hasing, Minqing Ivy Yang, Jianxian Sun, Julio Plaza-Diaz, Zhihao Zhang, Aaron Cowan, Walaa Eid, Sean E. Stephenson, Mark R. Servos, Matthew J. Wade, Alex E. MacKenzie, Hui Peng, Elizabeth A. Edwards, Xiao-Li Pang, Eric J. Alm, Tyson E. Graber, and Robert Delatolla, and was published in *Science of the Total Environment* (December 2022). In this manuscript, a novel parameter, the wastewater to clinical case (WC) ratio of COVID-19 is investigated as a potential bellwether parameter to infer changes in disease dynamics such as the arrival of a novel variant in a community, a drastic difference in how clinical tests are performed, or if sufficient tests are performed to accurately portray the disease burden in a given urban community.

5.2. Abstract

Clinical testing has been the cornerstone of public health monitoring and infection control efforts in communities throughout the COVID-19 pandemic. With the extent and anticipated reduction of clinical testing as the disease moves into an endemic state, SARS-CoV-2 wastewater and environmental monitoring (WEM) is likely to have greater value as an important diagnostic tool to inform public health. As the widespread adoption of WEM is relatively new at the scale employed for COVID-19, interpretation of data, including the relationship to clinical cases, has yet to be standardized. An in-depth analysis and understanding of the metrics derived from WEM is required for public health units/agencies to interpret and utilize WEM-acquired data effectively and efficiently, and of the most important challenges public health units/agencies are currently facing in regards to WEM are difficulties with interpretation of results (McClary-Gutierrez et al., 2021; O'Keeffe, 2021). In this study, the SARS-CoV-2 wastewater signal to clinical cases (WC) ratio was investigated across seven different cities in Canada over periods ranging from 8 to 21 months. This preliminary work demonstrated that significant increases in the WC ratio occurred when clinical testing eligibility was modified to appointment-only testing, identifying a period of insufficient clinical testing (resulting in a reduction to testing access and a reduction in the number of daily tests) in these communities, despite increases in the wastewater signal. Furthermore, the WC ratio decreased significantly in 6 of the 7 studied locations, serving as a potential signal of the emergence of the Alpha variant of concern (VOC) in a relatively non-immunized community's wastewater (40-60% allelic proportion), while a more muted decrease in the WC ratio signaled the emergence of the Delta VOC in a relatively well-immunized community's wastewater (40-60% allelic proportion). Finally, a rapid and significant decrease in the WC ratio signaled the emergence of the Omicron VOC, likely because of the variant's greater effectiveness at evading immunity, leading to a significant number of new reported clinical cases, even when vaccine-induced community immunity was high. The WC ratio, used as an additional monitoring metric, could complement clinical case counts and wastewater signals as individual metrics in its potential ability to identify important epidemiological occurrences, adding value to WEM as a diagnostic technology during the COVID-19 pandemic and likely for future pandemics.

5.3. Introduction

Severe acute respiratory syndrome coronavirus 2 (SARS-CoV-2) has had profound effects around the world, claiming millions of lives and significantly impacting public health since its initial identification in December 2019 (World Health Organization, 2021). The virus is an enveloped, positive-sense RNA virus and, like other coronaviruses, predominantly causes respiratory and intestinal tract infections (Chen et al., 2020; Xu et al., 2020; Zou et al., 2020). SARS-CoV-2 infections in humans can cause acute respiratory

illness leading to elevated mortality and morbidity rates (Challen et al., 2021; Fajnzylber et al., 2020; O'Driscoll et al., 2021). Early in the COVID-19 pandemic, molecular diagnostic assays based on the reverse transcription quantitative polymerase chain reaction (RT-qPCR) technology were rapidly developed (Zhu et al., 2020) and became the principal testing method used to determine if patients were infected with SARS-CoV-2. Other testing methodologies and technologies, such as rapid antigen testing and LAMP RT-PCR, were also used globally. However, RT-qPCR testing remains the gold standard due to its sensitivity and specificity, particularly at lower viral loads (Hirotsu et al., 2020; Uhteg et al., 2020). Clinical testing in most jurisdictions around the world, including Canada, has predominantly targeted symptomatic individuals (Long et al., 2020; Oran and Topol, 2020; Rivett et al., 2020). The incubation period of SARS-CoV-2, together with the inherent lag associated with the RT-qPCR clinical testing and reporting pipeline (typically measured in days) generates a significant delay between infection incidence and the reporting of results, potentially delaying life-saving public health actions. Wastewater and environmental monitoring (WEM) has emerged as an exemplary early indicator of the incidence and disease burden of SARS-CoV-2 in the community (Ahmed et al., 2020; Al Huraimel et al., 2020; Balboa et al., 2021; Cao and Francis, 2021; Cavany et al., 2022; D'Aoust et al., 2021a; Medema et al., 2020; Randazzo et al., 2020). In the first year of the pandemic, research on the pathogenicity of SARS-CoV-2 revealed that fecal shedding of viral RNA is frequent, where approximately 30-90% of cases feature fecal shedding (Cheung et al., 2020; Fontana et al., 2020; Hua et al., 2020; Huang et al., 2020; Jones et al., 2020; Ling et al., 2020; Parasa et al., 2020; Santos et al., 2020). Thus, community-level measurements of the viral signal in wastewater are thought to act as a proxy for community SARS-CoV-2 burden (Bibby et al., 2021a; D'Aoust et al., 2021a; Karthikeyan et al., 2021; La Rosa et al., 2020; Olesen et al., 2021; Quilliam et al., 2020). In addition, following wastewater-based viral signal over time provides near real-time information on the virus dynamics such as incidence, prevalence, and disease burden (Ahmed et al., 2020; Bivins et al., 2020; Chakraborty et al., 2021; D'Aoust et al., 2021c; Medema et al., 2020; Peccia et al., 2020; Randazzo et al., 2020; Sherchan et al., 2020; Wu et al., 2020). Furthermore, sequencing of wastewater or variant-specific RT-qPCR assays can also detect and track the emergence/re-emergence of variants of interest/variants under investigation/variants of concern (VOI/VUI/VOC) (Graber et al., 2021; Lee et al., 2021; Peterson et al., 2021; Yaniv et al., 2021).

With the growing amount of data available from multiple locations and COVID-19 resurgences, there now exists an opportunity to explore the relationships between clinical reporting and WEM results to better understand and interpret patterns of both. With this data, there is clear potential for hypothesis-driven approaches to identify mechanisms underlying relationships between clinical testing patterns and observed SARS-CoV-2 viral signal in wastewater within and between communities and facilities (Bibby et al., 2021b). It is hypothesized that analyzing the change in the intrinsic relationship existing between measured

SARS-CoV-2 viral signal in wastewater and reported daily new positive clinical tests may reveal additional information regarding testing strategy effectiveness in approximating true disease incidence in a community. This relationship, called the WC ratio, was first proposed by Xiao *et al*. (2022). As the ratio has the wastewater titers in the numerator and the reported new clinical cases in the denominator, Xiao et *al.* (2022) proposed that surveying the relative shifts in the WC ratio may yield information regarding clinical testing. They also reported that an increased WC ratio could be attributed to insufficient testing in the general population (i.e. testing not sufficient to capture the exponential growth of actual COVID-19 cases).

In this study, the WC ratio was analyzed over periods of 8 to 21 months in the seven Canadian cities/regions to help identify occurrences of major epidemiological importance during the COVID-19 pandemic. Four major epidemiological events were identified through retrospective analysis and were as follows: i) a period of insufficient clinical testing during a change in clinical testing strategy (i.e., walk-in testing changed to appointment-based testing); ii) the emergence of a more infectious VOC (Alpha) in the context of low vaccine- or naturally-acquired community immunity; iii) the emergence of a more transmissible and virulent VOC (Delta) in the context of high community immunity, and iv) the emergence of a more transmissible VOC (Omicron) in the context of immunity escape in a susceptible community. Furthermore, possible confounding factors such as the age, demographics, and vaccination/immunization rates of reported new clinical cases were also considered to assure that observed trends were not affected by these elements. The objective of this study was therefore to investigate and quantify the ability of the WC ratio to identify major epidemiological occurrences and further elucidate the relationship existing between WEM and reported clinical cases to complement and enhance the value of WEM and enhance its usefulness as an applied diagnostic technology.

5.4. Materials and methods

Analytical testing completed in this study occurred in four different laboratories throughout Canada, and as such specific methodologies, site-specific sampling schedules, sample processing, extraction, and quantification techniques differ slightly between the various cities/regions. Before starting, all employed methodologies were compared as part of a broader pan-Canadian interlaboratory study (Chik et al., 2021) and determined to be of similar performance under the tested conditions. A list of the testing periods included in this study and the major epidemiological events identified at each testing site is shown below in Table 5-1. The major epidemiological events selected for consideration as part of this study were selected on the basis of either: i) enactment or change in governmental policies impacting clinical testing, and ii) onset of a novel VOC in the community (as determined via an allelic proportionality in wastewater of 40-60%). Furthermore, a summary of the characteristics of each water resource recovery facility (WRRF) is

shown in Supplementary Material (Table S1). The studied data sets for most locations stopped in August 2021, however, the studied data set in Ottawa (most frequently sampled and tested) was chosen to be extended into the Omicron VOC onset.

Table 5-1: Testing periods and analyzed major epidemiological events identified per studied site, which were selected for consideration as part of this study. If no dates are shown for a particular event at a particular location, the data for that specific event was not available (testing had not commenced) or was measured to infrequently for sufficient analyses and interpretation.

Location	Studied period	Identified change in clinical testing strategy changed to appointment based only	Identified onset of allelic proportionality of B.1.1.7 (Alpha) VOC reaching 40-60%	Identified onset of allelic proportionality of B.1.617.2 (Delta) VOC reaching 40-60%	Identified onset of allelic proportionality of B.1.1.529 (Omicron) VOC reaching 40-60%
Ottawa	06-04-2020 to 09-01-2022	06-10-2020	23-03-2021	31-07-2021	20-12-2021
Toronto	11-02-2021 to 20-11-2021	-	02-03-2021	22-06-2021	-
Kitchener	01-12-2020 to 15-09-2021	-	10-03-2021	06-06-2021	-
Peel	20-09-2020 to 30-08-2021	-	22-02-2021	28-05-2021	-
Waterloo	07-12-2020 to 15-09-2021	-	27-03-2021	14-06-2021	-
Edmonton	12-07-2020 to 26-09-2021	-	23-02-2021	18-07-2021	-
Calgary	09-07-2020 to 21-09-2021	-	22-03-2021	18-07-2021	-

5.4.1. Sample collection, enrichment, concentration, and extraction

5.4.1.1. Ottawa

24-hour composite samples of primary clarified sludge were collected from the City of Ottawa's sole WRRF, the Robert O. Pickard Environmental Centre (ROPEC), starting on Apr. 8th, 2020, with daily sample collection beginning on Sep. 10th, 2020. The WRRF services approximately 91% of households and individuals in the City of Ottawa (pop.: 1.1M). Composites (500 mL) were collected every morning and kept on ice until transported to the University of Ottawa for analysis. In this study, samples were analyzed from Apr. 8th, 2020, until Jan. 5th, 2022. Primary sludge samples were first homogenized well by mixing and then 40 mL of each sludge sample was concentrated by centrifugation for 45 minutes at 10,000 x g. The supernatant was discarded, and the wet pellet was centrifuged a second time at 10,000 x g for an additional 5 minutes. The resulting pellet (5 to 7 g) was then homogenized, and 0.250 g ± 0.05 g of the resulting solids pellet was extracted as previously described using Qiagen's RNeasy PowerMicrobiome Kit (Qiagen, Germantown, MD) using a QIACube Connect automated extraction platform (D'Aoust et al., 2021a, 2021c). RNA was finally eluted in 100 µL of RNase-free water.

5.4.1.2. Toronto

24-hour composite samples (500 – 1,000 mL) of post-grit influent were collected from three water resource recovery facilities in the City of Toronto, including Ashbridge's Bay (TAB), Highland Creek (THC), and North Toronto (TNT) at frequencies of three to five times per week between Feb. 11th, 2021, and Nov. 22nd, 2021. After arriving at the laboratory at the University of Toronto, two pseudo-biological replicates (80 mL for TAB and THC samples, and 120 mL for TNT samples) of fully mixed post-grit influent wastewater were centrifuged. The wastewater samples were then transferred to 50 mL centrifuge tubes in 40 mL aliquots and centrifuged at 10,000 x g for 45 minutes at 4°C. After removal of the supernatant, the remaining wet pellet was transferred to a 2 mL screw-cap microcentrifuge tube and further centrifuged at 13,000 x g for 1 minute. After completely decanting the supernatant, the final pellet and microcentrifuge tube was weighed. For pellets not exceeding 250 mg, RNA extraction was performed as previously described using Qiagen's RNeasy PowerMicrobiome Kit (Qiagen, Germantown, MD) (D'Aoust et al., 2021a, 2021c)., with the following modifications to the protocol: 10 µL beta-mercaptoethanol and 100 µL phenol:chloroform:isoamyl alcohol (25:24:1 v/v) mixtures (Invitrogen, CAT# 15593031, USA) were added to the bead beating tube along with the lysis buffer in the kit. For pellets exceeding 250 mg, each pellet was split into two portions to proceed with cell lysis and inhibition removal (IRS), and only half of the combined supernatant from the IRS step was used in the remaining extraction steps. Whole process controls, which included extraction blanks, positive controls and negative controls were included for each extraction. RNA was finally eluted in 100 µL of RNase-free water.

5.4.1.3. Kitchener, Peel, and Waterloo

24-hour composite samples (500 – 1,000 mL) of post-grit influent were collected from the following locations: (Kitchener) Region of Waterloo's water resource recovery facility (Dec. 7th, 2020, to Sep. 15th, 2021), (Peel) Clarkson water resource recovery facility (Aug. 8th, 2020, to Sep. 15th, 2021) and G.E. Booth water resource recovery facility (Jul. 20th, 2020, to Aug. 30th, 2021), and (Waterloo) Waterloo water resource recovery facility (Dec. 7th, 2020, to Sep. 15th, 2021). Samples were collected at a frequency of three to five times per week. Samples were aliquoted into 250 mL HPDE bottles (Systems Plus, Baden, Canada) and transported on ice to the University of Waterloo. Upon arrival, the sample bottles were well mixed, and a 40 mL aliquot was poured into 50 mL centrifuge tubes containing 4 g PEG-8000 and 0.9 g NaCl and mixed on an orbital shaker at 4°C for 2 h before being stored at 4°C overnight. The samples were then centrifuged at 12,000 x g at 4°C for 90 minutes with no deceleration/brake applied. The majority of the supernatant was discarded, and the remaining sample was centrifuged again at 12,000 x g at 4°C for 5 minutes with no deceleration/brake applied. The remaining supernatant was decanted/pipetted out and the wet weight of the resulting pellet was recorded. Up to 250 mg of the pellet was used for RNA extraction using the RNeasy PowerMicrobiome Kit (Qiagen, Germantown, MD) with the addition of 100 µL of TRIzol

(Thermo Fisher, Ottawa, Canada) to the pellet before bead beating. RNA was finally eluted in 100 µL of RNase-free water.

5.4.1.4. Edmonton and Calgary

24-hour composite samples (500 mL) of post-grit wastewater influent were collected from the following locations: (Edmonton) EPCOR Gold Bar Wastewater Treatment (May 18th, 2020, to Sep. 26th, 2021) and the city of Calgary water resource recovery facility (May 17th, 2020, to Sep. 21st, 2021). Samples were collected at a frequency of three to five times per week. Wastewater concentration and RNA extraction were performed as previously described (Qiu et al., 2021). Briefly, 100 ml wastewater samples were spiked with 100 µl of a suspension of human coronavirus (HCoV) strain 229E (10^5 IU/ml titrated by TCID50) to monitor virus recovery. The spiked samples were adjusted to a pH of 9.6-10 using 5N NaOH, mixed vigorously for 30 seconds, and then centrifuged at 4,500 x g for 10 min to pellet solids. The liquid fraction was then transferred into a new container, adjusted to pH 7-7.5 using 1.2N HCl, and then concentrated by ultrafiltration using a Centricon Plus-70™ filter with a pore size or Nominal Molecular Weight Limit (NMWL) of 30 KDa (Merck Millipore, Carrigtwohill, Ireland) at 3000 x g for 10 minutes at 4°C. The concentrated sample was adjusted to a final volume of 1 ml by adding phosphate-buffered saline (PBS) and stored at −70°C until RNA extraction. Viral RNA was extracted from ultrafiltration wastewater concentrates using the MagMAX™-96 Viral RNA isolation kit (Thermo Fisher Scientific, Ottawa, Canada) and the King Fisher™ Flex Purification System (Thermo Fisher Scientific, Ottawa, Canada) using 400 µl of wastewater concentrate as input. RNA was finally eluted in 100 µL of elution buffer.

5.4.2. RT-qPCR quantification of SARS-CoV-2, pepper mild mottle virus, Alpha, Delta, and Omicron VOCs in wastewater

Singleplex RT-qPCR quantification of SARS-CoV-2 targets and Pepper Mild Mottle Virus (PMMoV) was performed in the four laboratories analyzing samples for this study. A summary of the targeted SARS-CoV-2 genes, RT-qPCR reaction characteristics, and QA/QC controls utilized in each laboratory during this study are shown below in Table 5-2. All probes and primers utilized in this study are included in the Supplementary Material (Table S2). For viral signal normalization, the copies of SARS-CoV-2 (N1/N2) detected per reaction were normalized against the quantified copies of PMMoV from corresponding samples. Observed slight differences between the ALOQ in this study between labs is likely caused by standard material used, preparation of standards and differences in primer and probe concentrations, an issue previously outlined in the literature (Bivins et al., 2021).

Table 5-2: Summary of the RT-qPCR quantification of SARS-CoV-2 targets and PMMoV in all four laboratories which performed analyses for this study.

	Ottawa	Toronto	Kitchener, Peel, and Waterloo	Edmonton and Calgary
Targeted SARS-CoV-2 regions	N1, N2, ND3L (Alpha), D63G (Delta), P13L (Omicron)	N1, N2, ND3L (Alpha), D63G/N200 (Delta)	N1, N2, ND3L (Alpha), D63G/N200 (Delta)	N1, N2, E, ND3L (Alpha), D63G (Delta)
Targeted biological normalizer	PMMoV	PMMoV	PMMoV	PMMoV
RNA template volume (µL)	3 (SARS-CoV-2 targets) / 1.5 (PMMoV)	4	5	5
Total RT-qPCR reaction volume (µL)	10	10	20	10
Supermix used	TaqMan™ 1-Step Fast Virus Master Mix (ABI)	TaqMan™ 1-Step Fast Virus Master Mix (ABI)	TaqPath™ 1-Step RT-qPCR Master Mix (ABI)	TaqMan™ 1-Step Fast Virus Master Mix (ABI)
Standard utilized	Exact Diagnostics SARS-CoV-2 RNA standard (COV019)	Custom concatenated plasmid containing N1, N2, and PMMoV gene regions	Exact Diagnostics SARS-CoV-2 RNA standard (COV019)	Custom in-vitro transcribed gblock
Standard curve points	5-6	5-6	5-6	5-6
Endogenous spike in	VSV	-	HCoV-229E, zebrafish dsDNA, MS2	-
Corrected for recovery efficiency?	No	No	No	No
Inhibition check?	Yes, via dilution	Yes, via dilution	Yes, via zebrafish dsDNA	Yes, via dilution
Assay limit of detection (ALOQ) for N1, N2, PMMoV targets (copies/reaction)	3.2 (N1), 8.1 (N2), 7.6 (PMMoV)	1.6 (N1), 1.6 (N2)	-	1.6 (N1), 1.6 (N2)
RT-qPCR conditions	(All targets) Reverse trans.: 5 min. @ 50°C, 1 cycle Initial denat.: 20 sec. @ 95°C, 1 cycle Denaturation: 3 sec. @ 95°C, 45 cycles Anneal/ext.: 30 sec. @ 60°C, 45 cycles	(All targets) Reverse trans.: 5 min. @ 50°C, 1 cycle Initial denat.: 20 sec. @ 95°C, 1 cycle Denaturation: 3 sec. @ 95°C, 45 cycles Anneal/ext.: 30 sec. @ 60°C, 45 cycles	(N2, HCoV-229E, MS2) Reverse trans.: 15 min. @ 50°C, 1 cycle Initial denat.: 2 min. @ 95°C, 1 cycle Denaturation: 3 sec. @ 95°C, 45 cycles Anneal/ext.: 60 sec. @ 60°C, 45 cycles (N1, PMMoV) Reverse trans.: 15 min. @ 50°C, 1 cycle Initial denat.: 2 min. @ 95°C, 1 cycle Denaturation: 3 sec. @ 95°C, 45 cycles Anneal/ext.: 60 sec. @ 60°C, 45 cycles	(N1, N2, E and ND3L) Reverse trans.: 5 min. @ 50°C, 1 cycle Initial denat.: 20 sec. @ 95°C, 1 cycle Denaturation: 3 sec. @ 95°C, 45 cycles Anneal/ext.: 30 sec. @ 60°C, 45 cycles (D63G) Reverse trans.: 5 min. @ 50°C, 1 cycle Initial denat.: 20 sec. @ 95°C, 1 cycle Denaturation: 3 sec. @ 95°C, 45 cycles Anneal/ext.: 30 sec. @ 55°C, 45 cycles
Primer and probe concentrations	500 µM (primers) 125 µM (probes)	500 µM (primers) 125 µM (probes)	500 µM (primers) 125 µM (probes)	800 nM (primers) and 200 nM (probes) (N1, N2, E) 900 nM (primers) and 250 nM (probe) (ND3L) 800 nM (primers) and 250 nM (probes) (D63G)
Replicate exclusion threshold	Ct ≥ 0.5	Ct ≥ 0.5	Ct ≥ 0.5	None
Standard curve acceptance characteristics	$R^2 \geq 0.95$, 90% ≤ Eff. ≤ 120%	$R^2 \geq 0.99$, 95% ≤ Eff. ≤ 105%	$R^2 \geq 0.95$, 95% ≤ Eff. ≤ 105%	External standard curve characteristics (data from 10 separate RT-qPCR runs): $R^2 \geq 0.99$ 95% ≤ Eff. ≤ 103% (N1 and N2) $R^2 \geq 0.99$ 92% ≤ Eff ≤ 113% (ND3L) $R^2 \geq 0.99$ 90% ≤ Eff ≤ 109% (D63G)
Other QA/QC performed	Extraction blank, no extrapolation of values, negative controls	Extraction blank, negative controls, positive controls	Extraction blank, no extrapolation of values, negative controls, positive controls, no RT controls	Extraction blank, negative controls. External standard curve was verified for each RT-qPCR run at two different standard dilutions; Ct values differences between standards in each run vs those from external standard curve should be within ± 1

5.4.3. Epidemiological data

Daily epidemiological data including new daily testing, reported positive COVID-19 cases, and demographics of new infections were obtained throughout the study via Ottawa Public Health's online portal (Ottawa Public Health, 2021), Public Health Ontario's COVID-19 online data tool (Public Health Ontario, 2021), and the COVID-19 surveillance database of the Government of Alberta (Government of Alberta, 2021). The epidemiological data were provided per geographical area by the various public health units (known in certain jurisdictions as public health agencies) to best match the sewershed of each studied location. stratified by geographic areas or sites having wastewater-based SARS-CoV-2 surveillance included in this study. Vaccination information was obtained via Public Health Ontario's COVID-19 online data tool (Public Health Ontario, 2021) for locations in Ontario, and from the Government of Canada's COVID-19 vaccination coverage information page (Government of Canada, 2021).

5.4.4. Statistical analysis

The Pearson's product-moment correlation coefficient (Pearson's r) was calculated to evaluate the strength of the relationship between PMMoV normalized SARS-CoV-2 viral signal measured in wastewater and reported clinical cases throughout the study. Furthermore, to establish if changes occurred in the WC ratio values during key epidemiological occurrences, the Mann-Whitney U test was performed on the 15-day periods preceding and following the key epidemiological occurrences. A non-parametric test (Mann-Whitney U test) was employed to establish significance in changes of the WC ratio during key epidemiological occurrences to remove distribution effects. In this study, due to the variance in distribution shape, the distribution means will carry more statistical significance than the p-value. A regression analysis and subsequent analysis of the residuals were also performed between the 7-day midpoint average daily new reported clinical cases and the 7-day midpoint average observed viral signal in wastewater to establish if any outliers existed.

5.4.5. Calculations of the WC ratio

The WC ratio in this study was calculated by using the PMMoV-normalized SARS-CoV-2 viral signal (arithmetic mean of the technical triplicates of the N1 and N2 gene region's measured viral signal in wastewater, in copies/copies PMMoV) and dividing this value by the reported number of new COVID-19 clinical cases on the same day (non-retrospective/corrected), similar to what was described previously in the literature (Xiao et al., 2022). No lead-lag correction was applied to the calculations of the WC ratio (Cavany et al., 2022; D'Aoust et al., 2021a; Galani et al., 2022; Olesen et al., 2021).

5.4.6. Calculation of VOC allelic proportions

The allelic proportions of different SARS-CoV-2 VOCs were calculated by dividing measured VOC-associated viral copies/g by the universal/non-mutated equivalent genomic region viral copies/g, to obtain a percentage/proportion, as previously described (Graber et al., 2021). This calculation allows to track what percentage of the viral signal observed in wastewater is attributable to the presence of circulating VOCs.

5.4.7. Standardization of SARS-CoV-2 measurements for comparison of curves

The viral signal was first standardized to be of a similar scale (on the same axis) by multiplying the PMMoV-normalized viral signal measurements in Ottawa and Toronto by 100,000, Kitchener by 300,000, Waterloo by 500,000, not modifying the measurement of Peel, and dividing the measurements of Edmonton

and Calgary by 1,000. This was performed to facilitate initial graphical comparison of results by community, and to aid with plotting/graphing.

5.5. Results and discussion

5.5.1. Overview of SARS-CoV-2 surveillance at studied sites

Surveillance of SARS-CoV-2 viral signal at the studied sites began on different dates due to the different laboratories employed to support WEM across the study cities. Ottawa samples consisted of primary sludge, whereas samples for all other tested locations were post-grit influent wastewater. This could potentially influence the PMMoV quantification and the corresponding calculated WC ratio because of a higher weight-normalized concentration of PMMoV found in primary sludge solids as compared to post-grit influent wastewater (D'Aoust et al., 2021b; LaTurner et al., 2021; Mercier et al., 2022; Nagarkar et al., 2022; Verily Life Sciences, 2021; Wolfe et al., 2021). Additionally, other factors such as the intra-day variations of laboratory measurements, the inherent variations present due to the technology employed (PCR), and the various normalization techniques (or lack thereof) may also impact reported results. Finally, for the purpose of the analyses performed in this study, shedding rate was also assumed to be relatively constant throughout the analyzed periods, due to each period analyzed in this study corresponding to a single SARS-CoV-2 dominant strain/variant (Bertels et al., 2022; Crank et al., 2022). The measured viral signals (normalized with PMMoV for all locations in Ontario, non-normalized for locations in Alberta) are shown to have a relatively good visual agreement with clinical data throughout the studied periods (Figure 5-1a.). The COVID-19 pandemic in Canada has so far has been characterized by a surge of COVID-19 cases in the early pre-vaccination stage of the pandemic (March 2020) followed by four subsequent resurgences (Figure 5-1a.) in September 2020, December 2020, March 2021, and December 2021. The scale-standardized viral signal observed in wastewater at all seven tested sites demonstrates a good general agreement with the observed 7-day midpoint average for new COVID-19 clinical cases reported by their respective public health units over the separate resurgence periods, as determined via correlation analysis. An alternative version of Figure 5-1, with all viral signals reported in copies/L, is also included in the Supplementary Material (Figure S1). A summary of the Pearson's r correlation analyses for the viral signal and clinical cases shown in Figure 5-1 is shown in the Supplementary Material (Table S3).

Mass immunization campaigns began in Canada in December 2020 for essential healthcare workers and the most vulnerable in the community (elderly and the immunocompromised). Vaccine rollout was relatively limited in early 2021, but vaccination rates increased rapidly throughout spring and summer. Facemask mandates were present throughout almost the entirety of the studied period, and intermittent

gathering restrictions were also imposed intermittently. All studied communities reached a full immunization rate of at least 60% by Sept. 1st, 2021, and a full immunization rate (two approved vaccine doses) of at least 70% by Nov. 1st, 2021 (Figure 5-1b.).

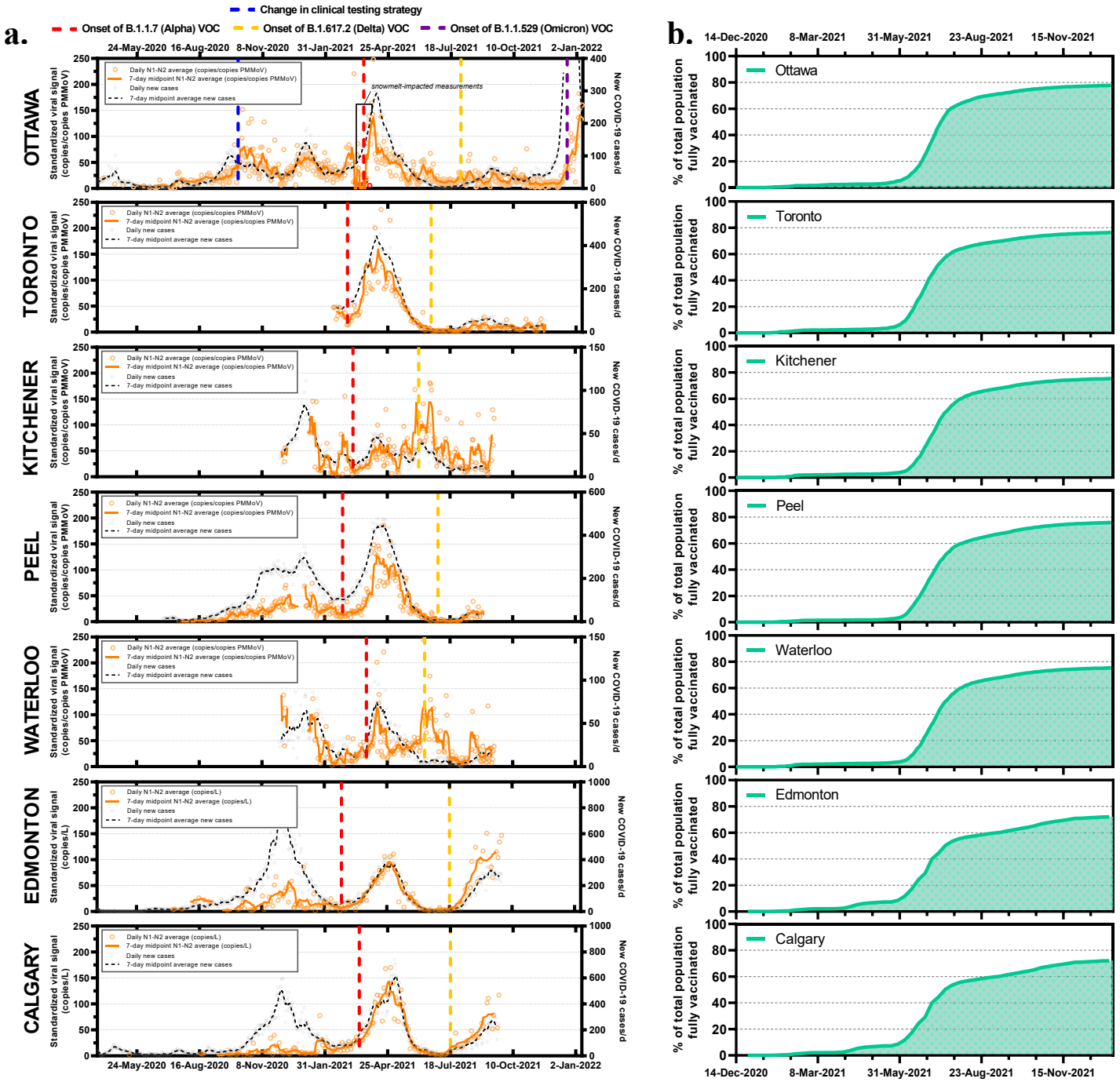


Figure 5-1: Comparison of a. scale-standardized PMMoV-normalized (Ottawa, Toronto, Kitchener, Peel and Waterloo) and non-PMMoV normalized (Edmonton and Calgary) SARS-CoV-2 viral signal measured in wastewater to reported new daily COVID-19 cases in the communities, with the onset of events of high epidemiological importance outlined with vertical dashed lines, coupled with b. summary of the immunization status of the populations living within the studied communities.

5.5.2. The WC ratio as an indicator of key epidemiological occurrences in the cities

When performing this particular analysis in all seven studied communities, significant changes in the WC ratio were hypothesized as being indicative of four major events: 1) a change in the clinical testing strategy that introduced the requirement to book a COVID-19 test appointment (5 out of 7 sites were in provinces that invoked this testing strategy); 2) the onset of the B.1.1.7 VOC during periods of low community immunity (all 7 sites were testing during this period), 3) the onset of the B.1.617.2 (Delta) VOC during periods of high community immunity (all 7 sites were testing during this period), and 4) the onset of the B.1.1.529 (Omicron) VOC during periods of high community immunization rates (75%+), with a VOC which has demonstrated immunity escape (a single site was testing during this period).

5.5.3. Event #1: WC ratio as an indicator of change in clinical testing strategy

Throughout the pandemic, public health units have adjusted their clinical testing strategies to better track the rate of incidence and prevalence of SARS-CoV-2 in their communities and help infer additional information, such as an approximate number of active disease cases and the pathogen's reproduction rate (China Center for Disease Control, 2020; Hoseinpour Dehkordi et al., 2020; Hyafil and Moriña, 2020; Khailaie et al., 2021; Kolifarhood et al., 2020; Pan et al., 2020). PCR-based clinical testing methods have been the primary metric of COVID-19 rates of incidence and prevalence in communities for public health professionals. However, RT-PCR nucleic acid clinical tests are not without limitations; first, individuals may decline clinical testing or refuse to seek medical treatment during a pandemic despite being symptomatic, complicating both tracking of cases and contact tracing (Novoa et al., 2021), and second, RT-PCR test results may suffer from a substantial false-negative rate, especially when considering the time of testing in relation to symptom onset and the type of sample collected (sputum, stool, nasopharyngeal, oropharyngeal, etc.) (da Rocha Araujo, 2020; Hatchette, 2009; Wikramaratna et al., 2020).

An epidemiologically important event occurred when changes in clinical testing strategies were effected in the province of Ontario (affecting Ottawa, Kitchener, Toronto, Peel and Waterloo), Canada on October 6th, 2020. In response to an increasing backlog of tests, and to ensure individuals could get tested at a specific time with minimal wait (Crawlley et al., 2020), provincial guidelines and the framework for the initiation of SARS-CoV-2 RT-PCR clinical testing were changed from an open-access, walk-in format to one in which individuals were required to book an appointment before testing. This change in testing strategy presented a significant, if brief, barrier for Ontario residents wanting to be tested for COVID-19 by necessitating online bookings, which made it more difficult for groups of the general population to access testing resources. Regular and consistent WEM had already been introduced in Ottawa during this period and, as such, a quantitative analysis of the effects of changes in testing strategies was performed. While the change occurred in 5 of the 7 locations, the effects of the change were only studied in Ottawa as other

locations either had not started their WEM, or were at the very beginning, and critical complementary data such as clinical testing information was missing.

When comparing the preceding 15-day period (Sept. 21st, 2020 – Oct. 5th, 2020) before the testing strategy change and the next 15-day period after enactment of the change (Oct. 6th, 2020 – Oct. 21st, 2020) in Ottawa the number of clinical tests performed on the general population decreased by an average of 23.2% (Figure 5-2). Concurrently, the local public health units reported a corresponding decrease of 16.8% in detected new clinical cases of COVID-19 in Ottawa (Figure 5-2). During the same period, Ottawa's normalized viral signal (average of N1-N2 viral copies/copies PMMoV) reported an increase of 55.9%, and the corresponding WC ratio increased by over 189% (Figure 5-2). The significant increase in the WC ratio in Ottawa occurred due to both increased wastewater signal and decreasing numbers of reported new clinical cases occurring simultaneously, thereby amplifying the increase in the WC ratio. During this period, variant testing in Ottawa's wastewater confirmed that no known major VOC was circulating in the general population, and an analysis of the age demographic of new cases (Figure S2) showed no statistically significant difference during the 30-day sample set. Furthermore, no vaccines were available to the general public during this first studied period. Based on the observed increase (>50%) in the WC ratio observed in Ottawa, it is hypothesized that the WC ratio may be an indicator of issues, such as flawed or difficult to access clinical testing resources, or overall insufficient clinical testing in relation to wastewater viral signal. This agrees with the findings and observations presented by Xiao et *al.* (2022). To determine the statistical significance of the change in WC ratio in Ottawa during the studied period, a non-parametric Mann-Whitney U test was performed, and the corresponding p-value was calculated. In Ottawa, the WC ratio before the change in strategy had a mean of 4.8×10^{-6} (IQR = 2.8×10^{-6} - 6.1×10^{-6}), while the mean after the change in testing strategy was 1.4×10^{-5} (IQR = 8.2×10^{-6} - 1.4×10^{-5}). As hypothesized, changes in the testing strategy correlated with an increase in WC ratio (p-value < 9×10^{-5}).

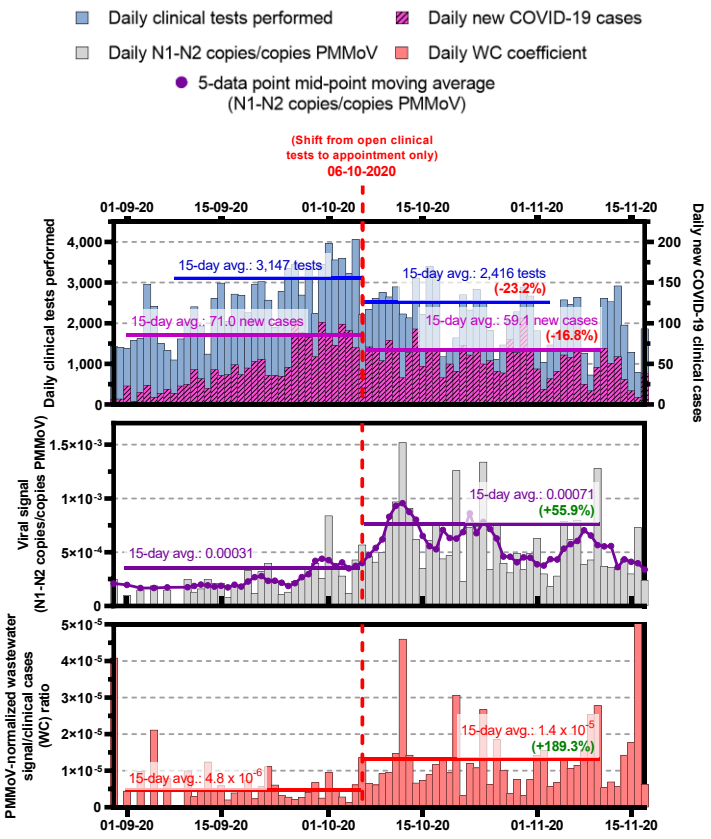


Figure 5-2: Comparison of the number of daily SARS-CoV-2 RT-PCR nucleic acid clinical tests performed and corresponding daily new COVID-19 positive cases, the daily viral signal measured through a SARS-CoV-2 wastewater surveillance program and the corresponding wastewater/clinical cases ratio (WC) during the same period in Ottawa.

While clinical testing currently remains the frontline measure of choice for the surveillance and tracking of COVID-19 incidence in the community, these findings strongly suggest that current and future disease surveillance efforts will benefit immensely from a multi-pronged surveillance approach incorporating more than the potentially biased case rates of clinically acquired diseases. COVID-19 and pandemic-potential diseases have been difficult to accurately track using traditional clinical testing methods as they are generally less effective at surveying disease burden due to many contributing factors, including testing capacity, the ability, and the desire of individuals to be tested (Gonsalves and Yamey, 2020; Jaiswal et al., 2020; Malinverni and Brigagão, 2020; Uscinski et al., 2020). It will continue to be difficult to conduct the widespread, mandatory disease surveillance of a population that is necessary to obtain information that could be interpreted as fully random and representative of the true rate of incidence of disease (McDermott and Newman, 2020; Pouwels et al., 2021; Rubin, 2020; Shao et al., 2020). In this context, it therefore appears highly useful to utilize WEM and the WC ratio to complement traditional clinical testing results. WEM and the resulting measured viral load can be used as a confirmatory measure of actual rates of disease burden in the community, while rapid changes in the WC ratio may help identify periods of inadequate or

altered clinical testing. Specifically, observing changes in the relative WC ratio may allow for the detection of changes in reported clinical cases that are not linked to actual changes in viral load in the community but are instead linked to shifts in testing rules and regulations, testing strategies, or fundamental changes in the disease vector. It is however important to also consider potential variations and uncertainties present in WEM (Ahmed et al., 2022; Li et al., 2021; Wade et al., 2022), as these will also have an impact on the WC ratio. It is hypothesized that in this study, due to trends observed during the change in testing strategies, is it likely that reported clinical cases may have been underreported in Ottawa following the modification to the testing strategies applied in these communities.

5.5.4. Event #2: WC ratio as an indicator of the onset of the B.1.1.7 (Alpha) variant of concern

SARS-CoV-2, being an RNA virus, is susceptible to mutations that can cause changes in its epidemiological characteristics, such as increased infectivity and/or virulence in comparison to its ancestral lineages (Burki, 2021; Drake and Holland, 1999; Duffy, 2018; Holmes and Rambaut, 2004). Throughout the COVID-19 pandemic, mutations of the SARS-CoV-2 spike (S) protein, referred to colloquially as D614G and N501Y, became hallmarks of the B.1.1.7 VOC, now referred to as the Alpha VOC. The onset of the Alpha VOC resulted in increased transmission of COVID-19 in the community (Frampton et al., 2021; Galloway et al., 2021; Graham et al., 2021), potentially affecting both observed viral load via WEM and new daily reported COVID-19 cases in the community by the public health unit. The period of onset of the Alpha VOC in the seven studied communities was confirmed via RT-qPCR allelic proportion determination (Figure 5-3) using a previously developed and validated assay (Graber et al., 2021). The onset of the Alpha VOC in a community was defined as such by determining when a consistent B.1.1.7 VOC allelic proportionality of between 40-60% of the SARS-CoV-2 viral signal in wastewater was reached and subsequently exceeded.

Using Ottawa as an initial test case, when comparing the average of the preceding 15-day period and the average of the next 15-day period after the period of onset of the B.1.1.7 VOC, the number of clinical tests performed on the general population increased by 19.6% (Figure 5-3a.) and the local public health team reported a corresponding increase of 188.3% in the detection of new daily clinical cases of COVID-19 (Figure 5-3b.). During the same period, normalized WEM reported a more modest increase of 70.8% in measured viral signal (average of N1-N2 viral copies/copies PMMoV). Furthermore, the WC ratio decreased by 56.3% (Figure 5-3c.). During the studied period, the onset of the Alpha VOC led to an observed change in the relationship between the number of reported COVID-19 cases and the observed WEM viral signal, and its hypothesized that the Alpha VOC may have altered viral fecal shedding dynamics in terms of viral load in fecal matter over time (Miura et al., 2021). An analysis of the age demographic of

new cases and changes in community immunization (Figure S3) showed no statistically significant difference during the studied 30-day period. The percentage of the total population fully immunized (2 doses +) increased from 2% to 2.3% during the studied 30-day period, but due to the time required for immuno-competence development and overall very low immunization rate, it is understood that vaccination was not likely to be an important factor in affecting reported clinical cases or viral fecal shedding dynamics during this period (Public Health Ontario, 2021).

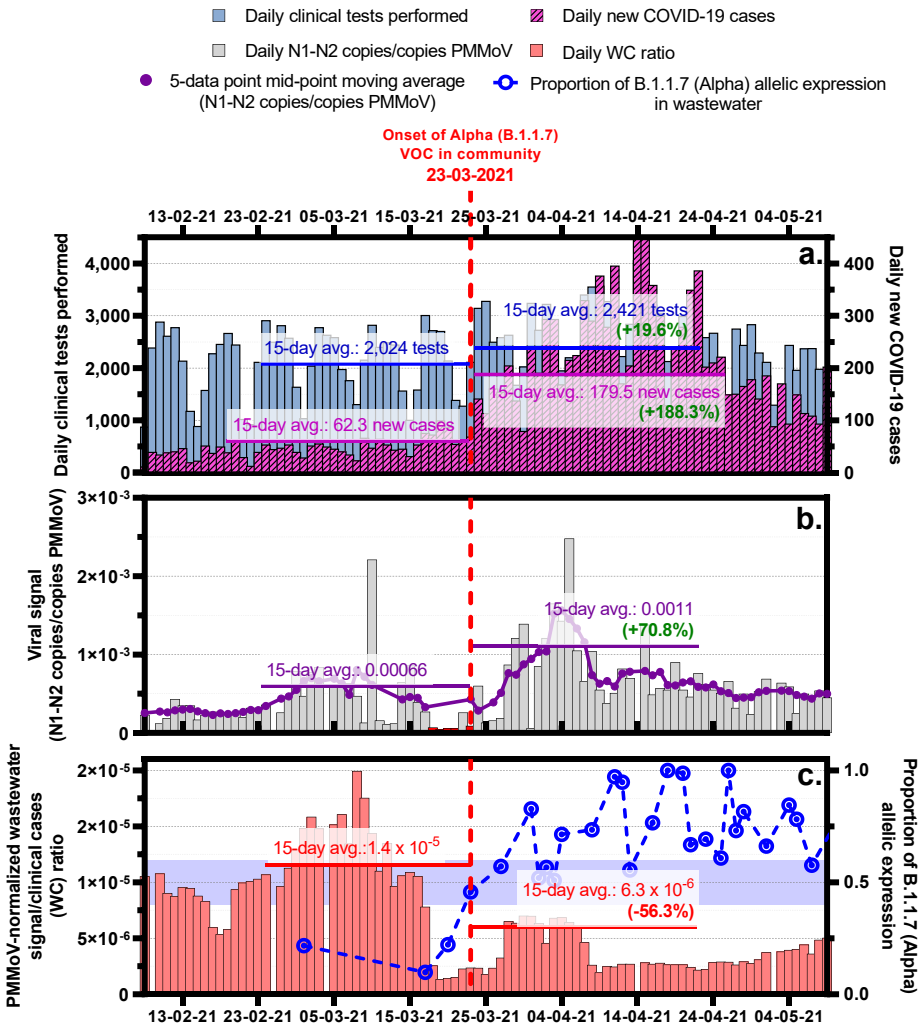


Figure 5-3: Comparison of a. the number of daily SARS-CoV-2 RT-PCR nucleic acid clinical tests performed and corresponding daily new COVID-19 positive cases in Ottawa, Canada, b. the daily viral signal measured through a SARS-CoV-2 wastewater surveillance program.

A summary of proportional observed changes in the preceding 15-day period and following 15-day period in reported clinical cases of COVID-19, measured viral signal in wastewater and WC ratio at all seven tested locations is shown in the Supplementary Material (Table S4). Individually, proportional

changes in reported clinical cases and measured SARS-CoV-2 viral signal in wastewater varied, however, in six of seven tested locations during this period, a marked decrease in the observed WC ratio (average decrease of 41.6%) was observed, which may signal the emergence of the B.1.1.7 VOC as the dominant

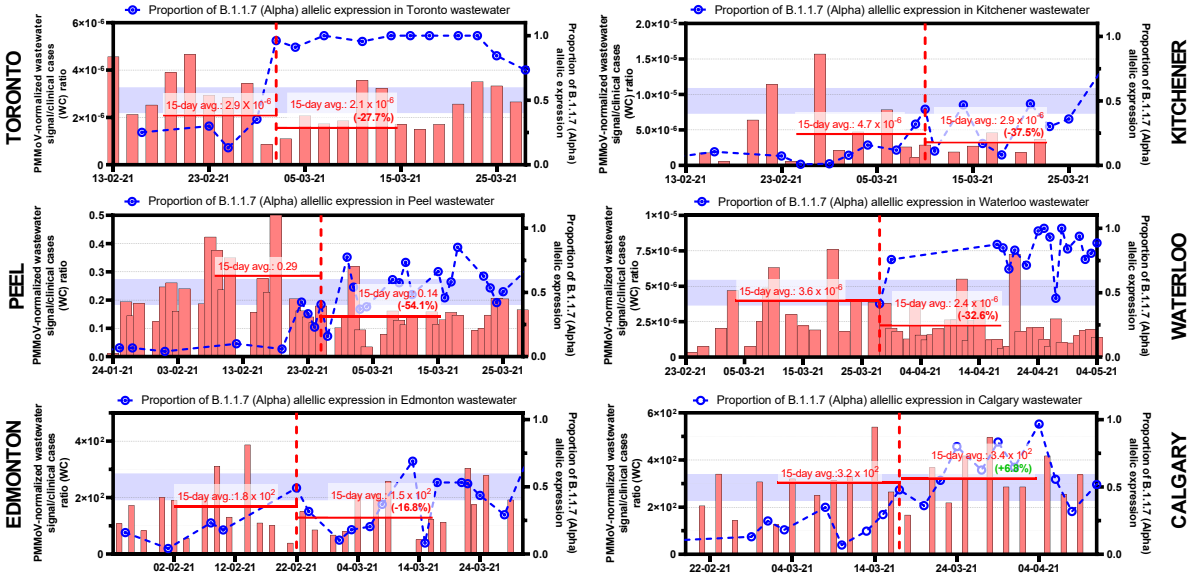


Figure 5-4: Comparison of the WC ratio and B.1.1.7 allelic proportionality during the onset of the B.1.1.7 (Alpha) VOC in the additional 6 locations in Canada (Toronto, Kitchener, Peel, Waterloo, Edmonton, and Calgary).

source of new infections (Figure 5-4). Only in Calgary did the WC ratio increase (6.4%) during the onset of the B.1.1.7 VOC. This trend in the decrease of the WC ratio potentially signaling important chances in disease dynamics is consistent with observations by Xiao et *al.* (2022) for the Boston area during the period where the Alpha VOC became dominant in wastewater (Lee et al., 2021). It has been suggested in the literature that there may be increased viral loading in symptomatic individuals caused by the Alpha variant as compared to the wild type of SARS-CoV-2 based on data obtained from nonhuman primates (Rosenke et al., 2021). However, there is not yet a consensus on this matter for human subjects (Badu et al., 2021; Zhu et al., 2021). The decrease in the WC ratio could also have been caused by a greater increase in transmissibility of the disease without a corresponding increase in fecal shedding (unequal variance in viral load in tissue and secretions), increased awareness in the general population, or increased severity of symptoms thereby leading more infected individuals to seek clinical testing, resulting in a lower WC ratio after the onset.

Mann-Whitney U tests were performed on each data set during the Alpha VOC onset to investigate the shifts in WC ratios in the studied locations. The results of the tests, along with accompanying interpretation, are shown below in Table 5-3. It is important to note that in this study, non-parametric Mann-Whitney U tests were chosen as the preferred analysis method over other parametric tests to establish if a

statistical change occurred before and after the studied major epidemiological events. This choice was made due to the non-normal distribution of WC ratio values. However, the Mann-Whitney U test and the interpretation of the p-value may be limited as the shape of the analyzed distributions are unlikely to be similar (as observed with the observable changes in WC ratio values over time). In this instance, more weight should be given to the comparison of the mean rank over the p-value.

Table 5-3: Mean WC ratio and interquartile ranges (1st and 3rd quartiles) before and after the Alpha VOC onset along with the results of Mann-Whitney U tests performed on the WC ratio data sets to evaluate the significance of shifts before and after the Alpha VOC

Location	**Mean WC ratio** (before)/(after)	**IQR** (1st / 3rd quartiles)	**Mann-Whitney U test p-value**	**Interpretation**
Ottawa	1.4×10^{-5} / 6.3×10^{-6}	$4.5 \times 10^{-6} – 2.4 \times 10^{-5}$ / $4.1 \times 10^{-6} – 8.5 \times 10^{-6}$	0.254	As hypothesized, decreases in the WC ratio occurred during the Alpha onset, however the Mann Whitney U test could not establish statistical significance ($p < 0.1$).
Toronto	2.9×10^{-6} / 2.1×10^{-6}	$2.4 \times 10^{-6} – 3.6 \times 10^{-6}$/ $1.7 \times 10^{-6} – 2.7 \times 10^{-6}$	0.165	As hypothesized, decreases in the WC ratio occurred during the Alpha onset however the Mann Whitney U test could not establish statistical significance ($p < 0.1$). Lower frequency of testing could have had an impact on the test results.
Kitchener	4.7×10^{-6} / 2.9×10^{-6}	$1.6 \times 10^{-6} – 6.3 \times 10^{-6}$/ $2.1 \times 10^{-6} – 3.5 \times 10^{-6}$	0.886	As hypothesized, decreases in the WC ratio occurred during the Alpha onset, however the Mann Whitney U test could not establish statistical significance ($p < 0.1$). Lower frequency of testing could have had an impact on the test results.
Peel	0.29 / 0.14	0.21 – 0.37 / 0.10 – 0.16	0.886	As hypothesized, decreases in the WC ratio occurred during the Alpha onset, however the Mann Whitney U test could not establish statistical significance ($p < 0.1$). Lower frequency of testing could have had an impact on the test results.
Waterloo	3.6×10^{-6} / 2.4×10^{-6}	$2.0 \times 10^{-6} – 3.7 \times 10^{-6}$ / $1.6 \times 10^{-6} – 2.9 \times 10^{-6}$	0.223	As hypothesized, decreases in the WC ratio occurred during the Alpha onset, however the Mann Whitney U test could not establish statistical significance ($p < 0.1$). Lower frequency of testing could have had an impact on the test results.
Edmonton	1.8×10^{2} / 1.5×10^{2}	$1.1 \times 10^{2} – 2.1 \times 10^{2}$ / $1.9 \times 10^{2} – 3.0 \times 10^{2}$	0.347	As hypothesized, decreases in the WC ratio occurred during the Alpha onset, however the Mann Whitney U test could not establish statistical significance ($p < 0.1$). Lower frequency of testing or lack of normalization for flow/dilution effects could have had an impact on the test results.
Calgary	3.2×10^{2} / 3.4×10^{2}	$1.1 \times 10^{2} – 2.1 \times 10^{2}$ / $1.9 \times 10^{2} – 3.0 \times 10^{2}$	0.391	Contrary to hypothesized, increases in the WC ratio occurred during the Alpha onset, however the Mann Whitney U test could not establish statistical significance ($p < 0.1$). Lower frequency of testing or lack of normalization for flow/dilution effects could have had an impact on the test results.

5.5.5. Event #3: WC ratio as an indicator of the onset of the B.1.617.2 (Delta) variant of concern

Mutations in the SARS-CoV-2 genome at the N-terminal domain (NTD) and receptor-binding domain (RBD) locations led to the rise of the B.1.617 lineage first identified in October 2020 in India (Cherian et al., 2021; Yadav et al., 2021), culminating in the dominance of the Delta variant (B.1.617.2) in new COVID-19 infections in most locations in North America, including Canada. The Delta variant is characterized by increased transmissibility and virulence compared to the Alpha variant (Kannan et al., 2021; Liu et al., 2021; Planas et al., 2021). The periods of onset of the Delta VOC in the four studied communities with available data (Ottawa, Kitchener, Peel, and Waterloo) were confirmed via RT-qPCR allelic proportion determination of the D63G portion of the genome using an assay developed and validated in-house. These periods of onset were defined as reaching a B.1.617.2 VOC allelic proportion of 40-60% of the SARS-CoV-2 viral signal in wastewater and subsequently exceeding this proportionality.

Using Ottawa as an initial test case, when comparing the average of the preceding 15-day period and the average of the next 15-day period after the onset of the B.1.617.2 VOC a modest increase (14.0%) in clinical tests that were performed was observed (Figure 5-5a.). Meanwhile, during the same period, the reported new clinical cases of COVID-19 more than doubled, increasing by 121.1% of the original value. This trend was similar to what was observed during the onset of the Alpha variant for both the number of clinical tests performed and new daily COVID-19 cases in Ottawa. However, the total numbers of new reported COVID-19 cases per day were substantially lower by approximately one order of magnitude during the onset of the Delta variant. Specifically, a 15-day average of 9.1 new cases per day was observed during the onset of the Delta variant, while the 15-day average was 117.3 new cases per day during Alpha variant onset. These differences in observed new COVID-19 cases in the community were likely driven by immunization effects; as of Mar. 23th, 2021 (onset of Alpha variant), only 2.2% of the population in Ottawa was fully immunized, compared to 63.1% in Jul. 31st, 2021 (onset of the Delta variant) (Public Health Ontario, 2021). During the same period, the normalized WEM signal increased by 45.8% (average of N1-N2 viral copies/copies PMMoV), which is similar to the trend observed during the onset of the Alpha variant (44.5% increase). These combined factors led to a slight decrease of only 18.7% in the WC ratio during the onset of the Delta variant, compared to a significantly larger decrease of 56.3% during the Alpha variant onset. An analysis of the age demographic of new cases and changes in community immunization (Figure S4) showed no statistically significant difference during the studied 30-day period. It is hypothesized that immunization impact dampened both increases in reported new COVID-19 cases and viral signal in wastewater, effectively dampening the expected effects of the onset of a new, more infectious variant of SARS-CoV-2 on the WC ratio. Accordingly, communities with lower rates of immunization could be expected to exhibit greater reductions of the WC ratio due to increased rates of infections resulting

in higher numbers of new daily COVID-19 cases. During the 30-day period where Delta emerged in Ottawa, full immunization in the total population (2 doses +) increased from 54.2% on Jul. 16th, 2021, to 66.9% on Aug. 14th, 2021), which likely limited the spread of the Delta variant within the community during this time, as attested by the observed viral load in wastewater and reported clinical cases (Figure 5-1a.).

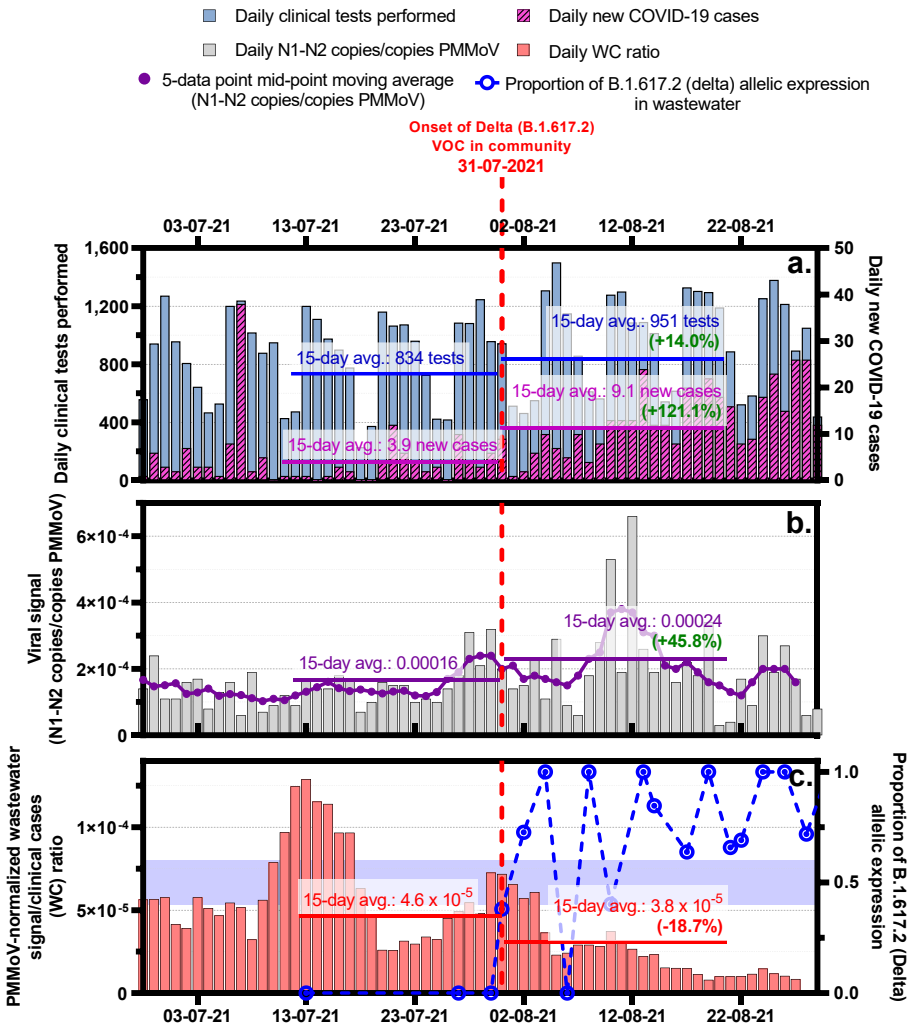


Figure 5-5: Comparison of a. the number of daily SARS-CoV-2 RT-PCR nucleic acid clinical tests performed and corresponding daily new COVID-19 positive cases in Ottawa, Canada, b. the daily viral signal measured through a SARS-CoV-2 wastewater surveillance program.

A summary of proportional observed changes in the preceding 15-day period and following 15-day period in reported clinical cases of COVID-19, measured viral signal in wastewater, and WC ratio at the tested locations is shown in the Supplementary Material (Table S5). Individually, proportional changes in reported clinical cases and measured SARS-CoV-2 viral signal in wastewater varied, however in three of the five tested locations (Ottawa, Toronto and Waterloo), the WC ratio decreased by an average of 27.0% during the emergence of the B.1.617.2 VOC as the dominant source of new infections. Meanwhile, in the four other tested locations with data during the emergence of the B.1.617.2 VOC (Peel, Kitchener, Edmonton and Calgary), the WC ratio instead increased by an average of 53.8%. A visual comparison of the WC ratio changes during the onset of the B.1.617.2 VOC is shown below in Figure 5-6. Contrary to trends observed during the B.1.1.7 VOC, the overwhelming trend in the WC ratio was not a decrease. It is believed that this increase in WC ratio in some of the locations (Peel, Kitchener, Edmonton and Calgary) may have been indicative of a disconnect between reported clinical cases in the communities and observed viral signal, caused partly by community immunization (hypothesized to lead to lower viral loads in feces) and local clinical testing capacity being reached or exceeded, leading to elevated WC ratio values caused by artificially low reported clinical cases. It is likely that in immunized communities without VOCs capable of immune escape, the change in the observed WC ratio will be lessened. Under such circumstances, the WC ratio is less indicative of the onset of new VOCs entering the community. Mann-Whitney U tests were

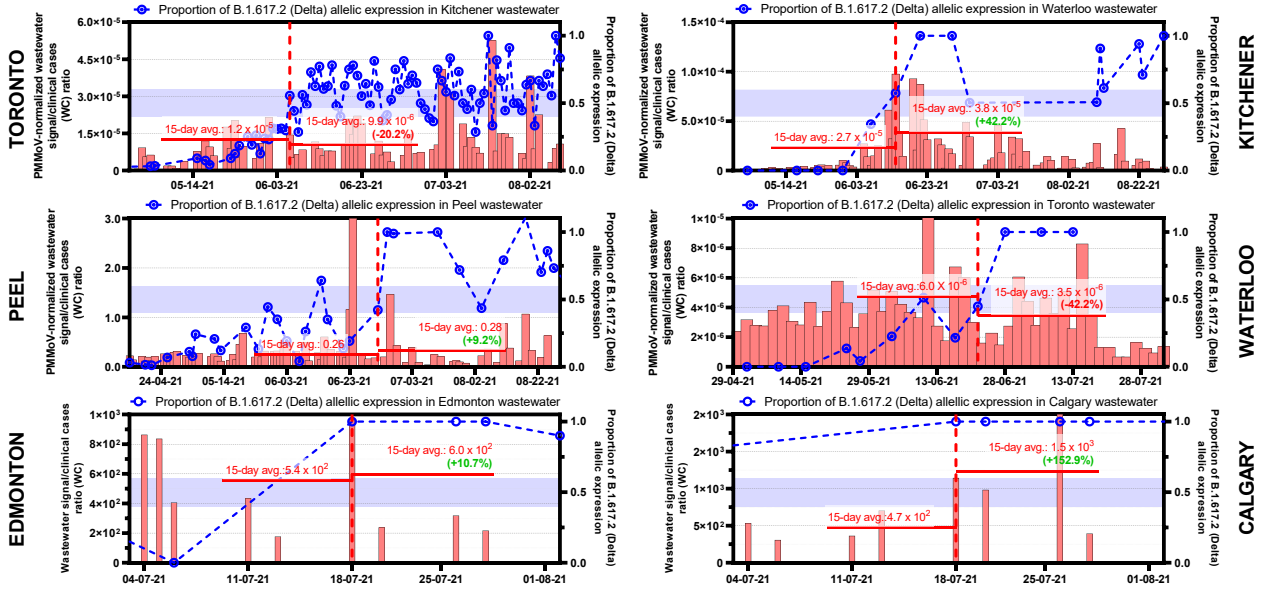


Figure 5-6: Comparison of the WC ratio and B.1.617.2 allelic proportionality during the onset of the B.1.617.2 (Delta) VOC in 6 additional locations in Canada (Toronto, Kitchener, Peel, Waterloo, Edmonton, and Calgary).

performed on each data set during the Delta VOC onset to investigate the shifts in WC ratios in the studied locations. The results of the tests, along with accompanying interpretation, are shown below in Table 5-4.

Table 5-4: Mean WC ratio and interquartile ranges (1st and 3rd quartiles) before and after the Delta VOC onset along with the results of Mann-Whitney U tests performed on the WC ratio data sets to evaluate the significance of shifts before and after the Delta VOC.

Location	**Mean WC ratio** (before)/(after)	**IQR** (1st / 3rd quartiles)	**Mann-Whitney U test p-value**	**Interpretation**
Ottawa	4.6×10^{-5} / 3.8×10^{-5}	$2.5 \times 10^{-5} – 6.4 \times 10^{-5}$ / $1.5 \times 10^{-5} – 4.3 \times 10^{-5}$	0.079	As hypothesized, decreases in the WC ratio occurred during the Delta onset, and the Mann Whitney U test could establish statistical significance ($p < 0.1$).
Toronto	6.0×10^{-6} / 3.5×10^{-6}	$3.0 \times 10^{-6} – 6.4 \times 10^{-6}$/ $2.1 \times 10^{-6} – 3.5 \times 10^{-6}$	0.132	As hypothesized, decreases in the WC ratio occurred during the Delta onset, however the Mann Whitney U test could not establish statistical significance ($p < 0.1$).
Kitchener	1.2×10^{-5} / 9.9×10^{-6}	$8.1 \times 10^{-6} – 1.8 \times 10^{-5}$/ $7.3 \times 10^{-6} – 1.1 \times 10^{-5}$	0.409	As hypothesized, decreases in the WC ratio occurred during the Delta onset, however the Mann Whitney U test could not establish statistical significance ($p < 0.1$). Lower frequency of testing could have had an impact on the test results.
Peel	0.26 / 0.28	0.16 – 0.32 / 0.24 – 0.45	0.257	Contrary to the emitted hypothesis, increases in the WC ratio occurred during the Delta onset, however the Mann Whitney U test could not establish statistical significance ($p < 0.1$). Lower frequency of testing could have had an impact on the test results.
Waterloo	2.7×10^{-5} / 3.8×10^{-5}	$6.1 \times 10^{-6} – 2.7 \times 10^{-5}$ / $2.2 \times 10^{-5} – 6.1 \times 10^{-5}$	0.065	Contrary to the emitted hypothesis, increases in the WC ratio occurred during the Delta onset, and the Mann Whitney U test established statistical significance ($p < 0.1$). Lower frequency of testing could have had an impact on the test results.
Edmonton	5.4×10^{2} / 6.0×10^{2}	$4.1 \times 10^{2} – 8.4 \times 10^{2}$ / $2.6 \times 10^{2} – 9.0 \times 10^{2}$	0.201	Contrary to hypothesized, increases in the WC ratio occurred during the Delta onset, however the Mann Whitney U test could not establish statistical significance ($p < 0.1$). Lower frequency of testing or lack of normalization for flow/dilution effects could have had an impact on the test results.
Calgary	4.7×10^{2} / 1.5×10^{3}	$3.5 \times 10^{2} – 5.8 \times 10^{2}$ / $7.5 \times 10^{2} – 1.1 \times 10^{3}$	0.624	Contrary to hypothesized, increases in the WC ratio occurred during the Delta onset, however the Mann Whitney U test could not establish statistical significance ($p < 0.1$). Lower frequency of testing or lack of normalization for flow/dilution effects could have had an impact on the test results.

5.5.6. Event #4: WC ratio as an indicator of the onset of the B.1.1.529 (Omicron) variant of concern

Later in the pandemic, further mutations on the S protein RBD locations resulted in a very genotypically different VOC, denoted B.1.1.529 (Omicron). The combination of several mutations observed previously in the C.37 (Lambda) variant and several new mutations on the S protein RBD resulted in a significantly more infectious yet symptomatically milder VOC (Halfmann et al., 2022; Shuai et al., 2022), which spread rapidly around the world and replacing Delta as the main VOC in the majority of the location where it established. One of the important characteristics of Omicron is its ability to potentially evade neutralization in sera, even in vaccine-immunized individuals (He et al., 2021; Zhang et al., 2021). Using Ottawa as an initial test case, when comparing the average of the preceding 15-day period and the average of the next 15-day period after the period of onset of the B.1.1.529 VOC (December 20th, 2021), the number of clinical tests performed on the general population increased by 29.6% and the local public health reported a corresponding increase of 497.3% in the detection new clinical cases of COVID-19 (Figure 5-7a.). During the same period, normalized WEM reported an important increase of 243.5% in measured viral signal (average of N1-N2 viral copies/copies PMMoV). At the same time, the WC ratio decreased by 41.9% (Figure 5-7c.). It is believed that significant decreases in the WC ratio are an indicator of the onset of new VOCs with immune escape abilities. An analysis of the age demographic of new cases and changes in community immunization (Figure S5) showed no statistically significant difference during the studied 30-day period. Daily vaccination rates during the studied 30-day period increased slightly over

time due to residents obtaining third-dose booster vaccinations, but due to the time required for immuno-competence development, it is understood that vaccination was not likely to be a major factor influencing changes of the WC ratio. To determine the statistical significance of the change in WC ratio in Ottawa during the Omicron VOC onset, a non-parametric Mann-Whitney U test was performed, and the corresponding p-value was calculated. The WC ratio before the Omicron VOC onset had a mean of 1.7 x 10-6 (IQR = 1.2 x 10-6 – 1.8 x 10-6), while the mean after the Omicron VOC onset was of 1.0 x 10-6 (IQR = 7.2 x 10-7 - 1.3 x 10-6). As hypothesized, the onset of a more infectious VOC (Omicron) corresponded with a decrease in WC ratio (p-value < 0.035).

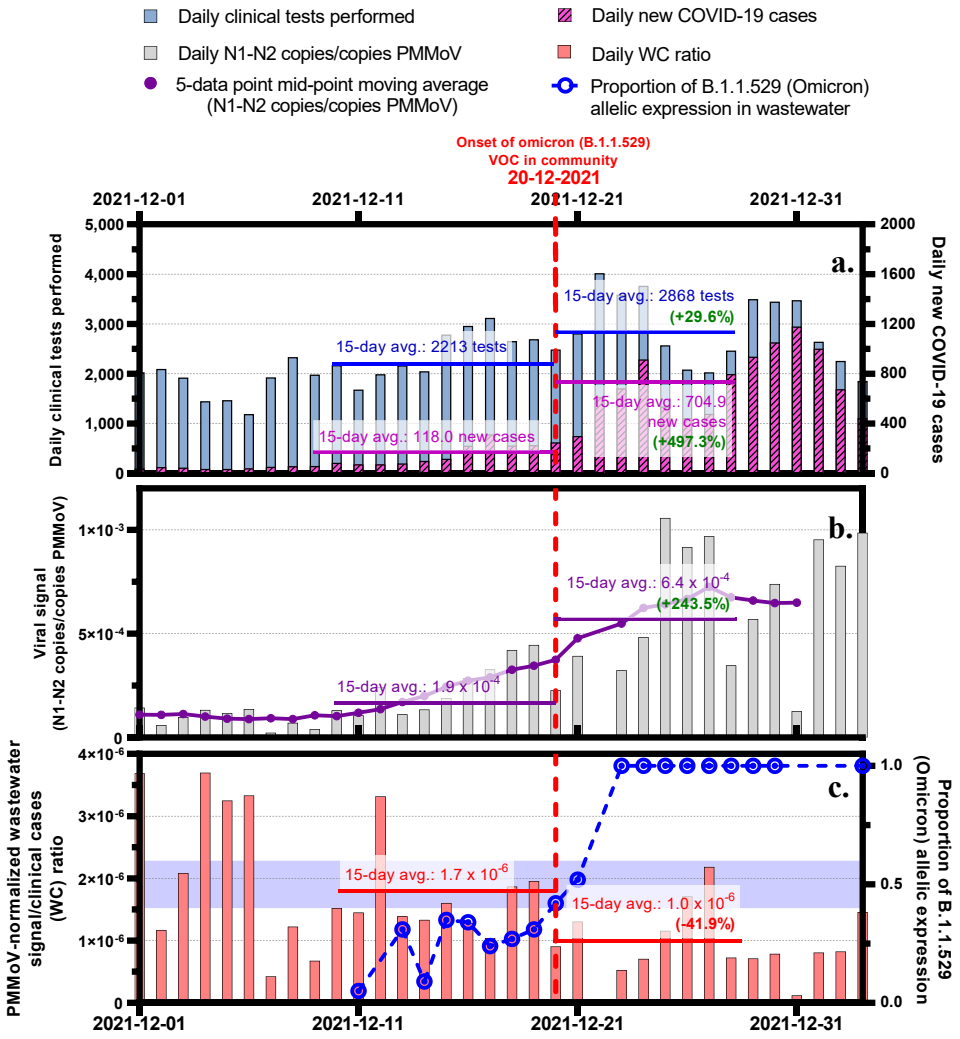


Figure 5-7: Comparison of a. the number of daily SARS-CoV-2 RT-PCR nucleic acid clinical tests performed and corresponding daily new COVID-19 positive cases in Ottawa, Canada, b. the daily viral signal measured through a SARS-CoV-2 wastewater surveillance program.

The data sets demonstrate that the magnitude of change in the WC ratio correlates with the overall disease burden in the community (Figure 5-8). The largest changes in WC ratios are observed during the Alpha variant and Omicron variant within the city of Ottawa, which are the two epidemiological events responsible for the highest disease burden within the city. In particular, the magnitude of the WC ratio during the Alpha and Omicron variants were similar and distinct from the period corresponding to the spread of the Delta variant in Ottawa. A distinction between the magnitudes of the WC ratio during the Alpha variant compared to the Delta variant also exists in the cities of Toronto, Kitchener, Peel and Waterloo. The in-depth analysis of the WC ratio during several major epidemiological events (as described in the above sections) revealed several major trends and findings: First, performed alone, both traditional clinical testing and WEM sometimes provide limited information for public health units that are monitoring a major pandemic disease like COVID-19. Clinical testing appears to sometimes suffer from underreporting due to the limited reach of the clinical tests, coupled with the limits in the ability and the desire of individuals to be tested, especially if they do not feel unhealthy. Furthermore, a strong relationship exists between the number of clinical tests performed and the number of detected new cases in the community, particularly during periods of disease resurgence, where a high degree of community transmission occurs, potentially

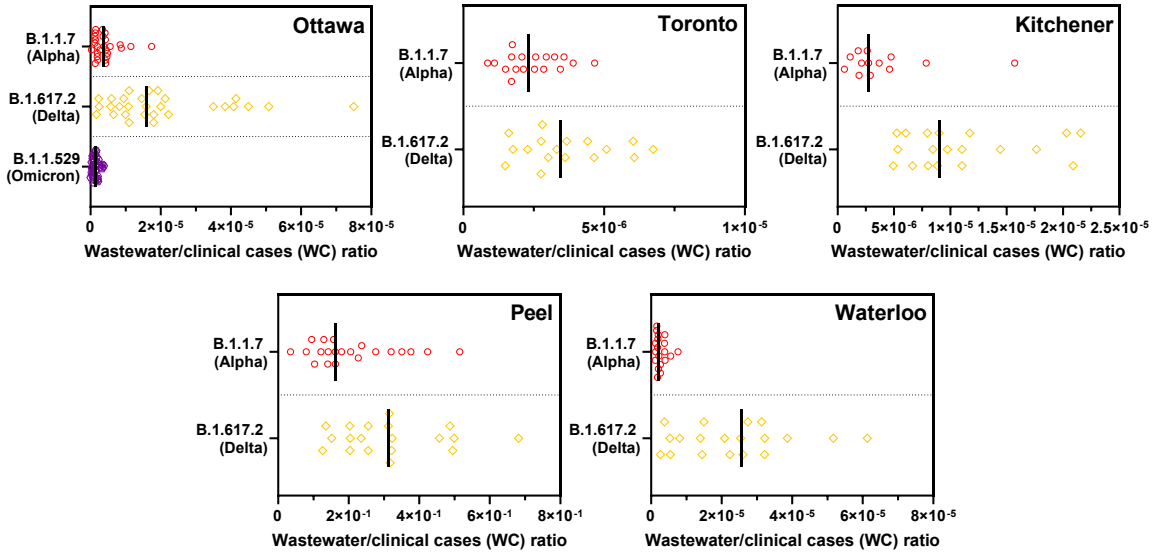


Figure 5-8: Comparison of WC ratio amplitude during the 30-day periods of onset of the B.1.1.7 (Alpha), B.1.617.2 (Delta) and B.1.1.529 (Omicron) VOCs in Ottawa, Toronto, Kitchener, Peel and Waterloo.

biasing interpretations of results. It is hypothesized that this weakness in traditional clinical testing is due to the difficulty in performing enough tests throughout the community to constitute testing rates that approximate a random distribution. In contrast, WEM effectively tests all individuals connected to the sewershed regardless of whether they are symptomatic or believe they have been exposed to the virus. Monitoring the WC ratio while performing RT-qPCR-based WEM can appears to provide accurate notice

of the time of arrival of new variants of concern in a community during a pandemic as quickly as traditional clinical testing and does not require infected individuals to seek clinical testing or enter the healthcare system. Throughout the study, it appears that a shift in the magnitude of change of the WC ratio and the relationship between reported clinical cases and observed WEM signal occurred for three reasons: (i) immunization may significantly reduce the number of individuals seeking COVID-19 testing due to a reduction of apparent symptoms caused by vaccination; (ii) as the pandemic progresses, disinterest may develop in the population, leading to a lower likelihood of symptomatic individuals seeking clinical testing, particularly if they have been immunized; and (iii) immunization may affect individual fecal shedding characteristics, impacting observed viral signal in wastewater. However, at present, it is still uncertain if this is the case, although preliminary results and unpublished data suggest this trend may exist (Bivins and Bibby, 2021). Furthermore, the effects of changes in tropism or to the ability of molecular tests to adequately detect SARS-CoV-2 or other surveyed pathogens would likely have impacts on the performance of the WC ratio as a tool.

5.6. Conclusions

This study strongly suggests that regular, daily monitoring of the WC ratio can reveal and detect the onset of changes in disease transmission patterns, and the arrival/onset and waning of more infectious variants or mutations of a pathogen or disease. When using traditional clinical case data and WEM, additional monitoring of the WC ratio may provide a greater understanding of the surveillance metrics during events of high epidemiological importance. The specific conclusions of this study are as follows: During periods of resurgence or increases in disease spread in a community, monitoring of reported clinical cases may provide a limited understanding of the true disease prevalence rates when community daily clinical testing is restricted or insufficient. The WC ratio will strongly increase when the disease burden increases in a community where an insufficient number of clinical tests are being performed to adequately approximate the disease burden in the community. Furthermore, if a community is not well immunized (less than 2.5% of individuals have received two doses of a COVID-19 vaccine), based on observed trends in this study, the onset of new, more infectious VOCs may lead to a decrease in the WC ratio. Meanwhile, if a community is well immunized (>60.0% of residents have received two doses of a COVID-19 vaccine), the onset of new, more infectious VOCs caused modest decreases in the WC ratio. Moreover, the onset of the Omicron VOC resulted in significant decreases in the WC ratio, as was observed during Alpha VOC dominance in early 2021, and this, irrespective of the immunization status of the community, is likely due to the immune escape capability of the Omicron VOC. It was observed that as a result, decreases in the WC can often be associated with the onset of a change in disease dynamics and the arrival of more infectious novel variants in the community and could be used as a tool to identify the emergence of new variants in

the future. Finally, it was determined that changes in the magnitude and inflection points in the WC ratio at a longitudinally surveyed location may be indicative of changes in disease burden and the ability of the pathogen to spread. These findings indicate that monitoring the WC ratio during the SARS-CoV-2 pandemic and other, future pandemics, will yield additional insight into the disease burden in a community and should be performed where possible.

5.7. Limitations and 2025 field updates

This chapter supports the use of the WC ratio as an add-on metric to identify mismatches between clinical case data and WEM signals during major epidemiological shifts caused by changing clinical testing strategies or the onset of new VOCs. While this approach provides valuable insight, a few limitations persist: 1) The usefulness and interpretability of the WC ratio relies on timely and geographically relevant clinical reporting (particularly important when sewersheds and health jurisdictions do not perfectly overlap). In cases where these two do not overlap well, the usefulness of the WC ratio may be diminished (Klaassen et al., 2023); and 2) If important differences in laboratory techniques (either methodological or sample type differences) between regions exist, the overall magnitude of the WC ratio may be significantly different and may complicate intra-region comparisons, requiring an across-the-board correction factor. As of 2025, the WC ratio isn't currently a topic of active investigation but could see a resurgence for targets other than SARS-CoV-2 as the interest in using WEM for the detection and monitoring of influenza, RSV, norovirus, tuberculosis, measles, mpox and other pathogens has reinforced the need for simple metrics which can contextualize wastewater signals in relation to changes in disease dynamics (the onset of new variants) or clinical testing strategies (Holcomb et al., 2024).

5.8. Declaration of competing interests

The authors declare that no known competing financial interests or personal relationships influenced the work reported in this manuscript.

5.9. Ethical considerations

This study involved the analysis of anonymized environmental wastewater samples and aggregated clinical data. All samples were collected from large municipal sewersheds, ensuring that no individual or household could be identified. As such, the research did not involve human subjects, personal identifiers, or interactions requiring ethical review.

5.10. Funding

This research was funded and supported by Ontario's Ministry of Environment, Conservation and Parks SARS-CoV-2 surveillance initiative (awarded to the University of Ottawa, the University of Toronto, and the University of Waterloo), by CHEO's (Children's Hospital of Eastern Ontario) CHAMO (Children's Hospital Academic Medical Organization) (awarded to Dr. Alex E. MacKenzie) and by CIHR/Alberta Health/Alberta Innovates (awarded to Dr. Xiao-Li Pang).

5.11. Acknowledgements

The authors wish to acknowledge the help and assistance of the University of Ottawa, the University of Toronto, the University of Waterloo, and the University of Alberta for their important contributions to the laboratories performing wastewater analysis. Furthermore, authors are very thankful of the support and continued cooperation of all wastewater treatment facility operators (City of Ottawa, the City of Toronto, the City of Waterloo, the Region of Peel, the City of Kitchener, EPCOR Utilities and the City of Calgary). Additional thanks go out to the Ottawa Hospital, the Children's Hospital of Eastern Ontario, the Children's Hospital of Eastern Ontario's Research Institute, Ottawa Public Health, Toronto Public Health, Peel Public Health, the Region of Waterloo Public Health and Emergency Services, Public Health Ontario and all their employees involved in the project during this study. Their time, facilities, resources, and thoughts provided throughout the study helped the authors greatly.

5.12. References

Ahmed, W., Angel, N., Edson, J., Bibby, K., Bivins, A., O'Brien, J.W., Choi, P.M., Kitajima, M., Simpson, S.L., Li, J., Tscharke, B., Verhagen, R., Smith, W.J.M., Zaugg, J., Dierens, L., Hugenholtz, P., Thomas, K. V., Mueller, J.F., 2020. First confirmed detection of SARS-CoV-2 in untreated wastewater in Australia: A proof of concept for the wastewater surveillance of COVID-19 in the community. Sci. Total Environ. 728, 138764. https://doi.org/10.1016/j.scitotenv.2020.138764

Ahmed, W., Simpson, S.L., Bertsch, P.M., Bibby, K., Bivins, A., Blackall, L.L., Bofill-Mas, S., Bosch, A., Brandão, J., Choi, P.M., Ciesielski, M., Donner, E., D'Souza, N., Farnleitner, A.H., Gerrity, D., Gonzalez, R., Griffith, J.F., Gyawali, P., Haas, C.N., Hamilton, K.A., Hapuarachchi, H.C., Harwood, V.J., Haque, R., Jackson, G., Khan, S.J., Khan, W., Kitajima, M., Korajkic, A., La Rosa, G., Layton, B.A., Lipp, E., McLellan, S.L., McMinn, B., Medema, G., Metcalfe, S., Meijer, W.G., Mueller, J.F., Murphy, H., Naughton, C.C., Noble, R.T., Payyappat, S., Petterson, S., Pitkänen, T., Rajal, V.B., Reyneke, B., Roman, F.A., Rose, J.B., Rusiñol, M., Sadowsky, M.J., Sala-Comorera, L., Setoh, Y.X., Sherchan, S.P., Sirikanchana, K., Smith, W., Steele, J.A., Subburg, R., Symonds, E.M., Thai, P., Thomas, K. V., Tynan, J., Toze, S., Thompson, J., Whiteley, A.S., Wong, J.C.C., Sano, D., Wuertz, S., Xagoraraki, I., Zhang, Q., Zimmer-Faust, A.G., Shanks, O.C., 2022. Minimizing errors in RT-PCR detection and quantification of SARS-CoV-2 RNA for wastewater surveillance. Sci. Total Environ. 805. https://doi.org/10.1016/j.scitotenv.2021.149877

Al Huraimel, K., Alhosani, M., Kunhabdulla, S., Stietiya, M.H., 2020. SARS-CoV-2 in the environment: Modes of transmission, early detection and potential role of pollutions. Sci. Total Environ. 744, 140946. https://doi.org/10.1016/j.scitotenv.2020.140946

Badu, K., Oyebola, K., Zahouli, J.Z.B., Fagbamigbe, A.F., de Souza, D.K., Dukhi, N., Amankwaa, E.F., Tolba, M.F., Sylverken, A.A., Mosi, L., Mante, P.K., Matoke-Muhia, D., Goonoo, N., 2021. SARS-CoV-2 Viral Shedding and Transmission Dynamics: Implications of WHO COVID-19 Discharge Guidelines. Front. Med. 8, 1–11. https://doi.org/10.3389/fmed.2021.648660

Balboa, S., Mauricio-Iglesias, M., Rodriguez, S., Martínez-Lamas, L., Vasallo, F.J., Regueiro, B., Lema, J.M., 2021. The fate of SARS-COV-2 in WWTPS points out the sludge line as a suitable spot for detection of COVID-19. Sci. Total Environ. 772, 145268. https://doi.org/10.1016/j.scitotenv.2021.145268

Bertels, X., Demeyer, P., Van den Bogaert, S., Boogaerts, T., van Nuijs, A.L.N., Delputte, P., Lahousse, L., 2022. Factors influencing SARS-CoV-2 RNA concentrations in wastewater up to the sampling stage: A systematic review. Sci. Total Environ. 820, 153290. https://doi.org/10.1016/j.scitotenv.2022.153290

Bibby, K., Bivins, A., Wu, Z., North, D., 2021a. Making waves : Plausible lead time for wastewater based epidemiology as an early warning system for COVID-19. Water Res. 202, 117438. https://doi.org/10.1016/j.watres.2021.117438

Bivins, A., Bibby, K., 2021. Wastewater Surveillance during Mass COVID-19 Vaccination on a College Campus. Environ. Sci. Technol. Lett. 8, 792–798. https://doi.org/10.1021/acs.estlett.1c00519

Bivins, A., Kaya, D., Bibby, K., Simpson, S.L., Bustin, S.A., Shanks, O.C., Ahmed, W., 2021. Variability in RT-qPCR assay parameters indicates unreliable SARS-CoV-2 RNA quantification for wastewater surveillance. Water Res. 203, 117516. https://doi.org/10.1016/j.watres.2021.117516

Bivins, A., North, D., Ahmad, A., Ahmed, W., Alm, E., Been, F., Bhattacharya, P., Bijlsma, L., Boehm, A.B., Brown, J., Buttiglieri, G., Calabro, V., Carducci, A., Castiglioni, S., Cetecioglu Gurol, Z., Chakraborty, S., Costa, F., Curcio, S., De Los Reyes, F.L., Delgado Vela, J., Farkas, K., Fernandez-Casi, X., Gerba, C., Gerrity, D., Girones, R., Gonzalez, R., Haramoto, E., Harris, A., Holden, P.A., Islam, M.T., Jones, D.L., Kasprzyk-Hordern, B., Kitajima, M., Kotlarz, N., Kumar, M., Kuroda, K., La Rosa, G., Malpei, F., Mautus, M., McLellan, S.L., Medema, G., Meschke, J.S., Mueller, J., Newton, R.J., Nilsson, D., Noble, R.T., Van Nuijs, A., Peccia, J., Perkins, T.A., Pickering, A.J., Rose, J., Sanchez, G., Smith, A., Stadler, L., Stauber, C., Thomas, K., Van Der Voorn, T., Wigginton, K., Zhu, K., Bibby, K., 2020. Wastewater-Based Epidemiology: Global Collaborative to Maximize Contributions in the Fight against COVID-19. Environ. Sci. Technol. 54, 7754–7757. https://doi.org/10.1021/acs.est.0c02388

Burki, T., 2021. Understanding variants of SARS-CoV-2. Lancet 397, 462. https://doi.org/10.1016/S0140-6736(21)00298-1

Cao, Y., Francis, R., 2021. On forecasting the community-level COVID-19 cases from the concentration of SARS-CoV-2 in wastewater. Sci. Total Environ. 786, 147451. https://doi.org/10.1016/j.scitotenv.2021.147451

Cavany, S., Bivins, A., Wu, Z., North, D., Bibby, K., Perkins, T.A., 2022. Inferring SARS-CoV-2 RNA shedding into wastewater relative to the time of infection. Epidemiol. Infect. 150, 2–9. https://doi.org/10.1017/S0950268821002752

Chakraborty, P., Pasupuleti, M., Jai Shankar, M.R., Bharat, G.K., Krishnasamy, S., Dasgupta, S.C., Sarkar, S.K., Jones, K.C., 2021. First surveillance of SARS-CoV-2 and organic tracers in community wastewater during post lockdown in Chennai, South India: Methods, occurrence and concurrence. Sci. Total Environ. 778, 146252. https://doi.org/10.1016/j.scitotenv.2021.146252

Challen, R., Brooks-Pollock, E., Read, J.M., Dyson, L., Tsaneva-Atanasova, K., Danon, L., 2021. Risk of mortality in patients infected with SARS-CoV-2 variant of concern 202012/1: Matched cohort study. BMJ 372, 1–10. https://doi.org/10.1136/bmj.n579

Chen, Y., Chen, L., Deng, Q., Zhang, G., Wu, K., Ni, L., Yang, Y., Liu, B., Wang, W., Wei, C., Yang, J., Ye, G., Cheng, Z., 2020. The presence of SARS-CoV-2 RNA in the feces of COVID-19 patients. J. Med. Virol. 92, 833–840. https://doi.org/10.1002/jmv.25825

Cherian, S., Potdar, V., Jadhav, Santosh, Yadav, P., Gupta, N., Das, M., Rakshit, P., Singh, S., Abraham, P., Panda, S., Patil, S., Jagtap, P., Kasabe, B., Shah, U., Sanjeev, T., Divekar, G., Korabu, K., Shelkande, S., Shinde, P., Zakiuddin, S., Vipat, V., Jadhav, Sheetal, Iyengar, K., Malik, V., Bhorekar, S.,

Kumar, A., Sahay, R., 2021. Convergent evolution of SARS-CoV-2 spike mutations, L452R, E484Q and P681R, in the second wave of COVID-19 in Maharashtra, India. bioRxiv 2021.04.22.440932.

Cheung, K.S., Hung, I.F.N., Chan, P.P.Y., Lung, K.C., Tso, E., Liu, R., Ng, Y.Y., Chu, M.Y., Chung, T.W.H., Tam, A.R., Yip, C.C.Y., Leung, K.-H., Fung, A.Y.-F., Zhang, R.R., Lin, Y., Cheng, H.M., Zhang, A.J.X., To, K.K.W., Chan, K.-H., Yuen, K.-Y., Leung, W.K., 2020. Gastrointestinal Manifestations of SARS-CoV-2 Infection and Virus Load in Fecal Samples From a Hong Kong Cohort: Systematic Review and Meta-analysis. Gastroenterology 81–95. https://doi.org/10.1053/j.gastro.2020.03.065

Chik, A.H.S., Glier, M.B., Servos, M., Mangat, C.S., Pang, X.L., Qiu, Y., D'Aoust, P.M., Burnet, J.B., Delatolla, R., Dorner, S., Geng, Q., Giesy, J.P., McKay, R.M., Mulvey, M.R., Prystajecky, N., Srikanthan, N., Xie, Y., Conant, B., Hrudey, S.E., 2021. Comparison of approaches to quantify SARS-CoV-2 in wastewater using RT-qPCR: Results and implications from a collaborative inter-laboratory study in Canada. J. Environ. Sci. 107, 218–229. https://doi.org/10.1016/j.jes.2021.01.029

China Center for Disease Control, 2020. The Epidemiological Characteristics of an Outbreak of 2019 Novel Coronavirus Diseases (COVID-19) - China, 2020. 中华流行病学杂志 41, 145–151.

Crank, K., Chen, W., Bivins, A., Lowry, S., Bibby, K., 2022. Contribution of SARS-CoV-2 RNA shedding routes to RNA loads in wastewater. Sci. Total Environ. 806, 150376. https://doi.org/10.1016/j.scitotenv.2021.150376

Crawlley, M., Powers, L., Nasser, S., Jabakhanji, S., The Canadian Press, 2020. Ontario implementing stricter public health measures as province sets COVID-19 case record | CBC News [WWW Document]. CBC News Toronto. URL https://www.cbc.ca/news/canada/toronto/covid-19-coronavirus-ontario-october-2-1.5747709 (accessed 9.10.21).

D'Aoust, P.M., Graber, T.E., Mercier, E., Montpetit, D., Alexandrov, I., Neault, N., Baig, A.T., Mayne, J., Zhang, X., Alain, T., Servos, M.R., Srikanthan, N., MacKenzie, M., Figeys, D., Manuel, D., Jüni, P., MacKenzie, A.E., Delatolla, R., 2021a. Catching a resurgence: Increase in SARS-CoV-2 viral RNA identified in wastewater 48 h before COVID-19 clinical tests and 96 h before hospitalizations. Sci. Total Environ. 770. https://doi.org/10.1016/j.scitotenv.2021.145319

D'Aoust, P.M., Mercier, É., Montpetit, D., Jia, J., Alexandrov, I., Neault, N., Baig, A.T., Mayne, J., Zhang, X., Alain, T., Langlois, M.-A., Servos, M.R., MacKenzie, M., Figeys, D., MacKenzie, A.E., Graber, T.E., Delatolla, R., 2021b. Quantitative analysis of SARS-CoV-2 RNA from wastewater solids in communities with low COVID-19 incidence and prevalence. Water Res. 188, 116560. https://doi.org/10.1016/j.watres.2020.116560

D'Aoust, P.M., Towhid, S.T., Mercier, É., Hegazy, N., Tian, X., Bhatnagar, K., Zhang, Z., Naughton, C.C., MacKenzie, A.E., Graber, T.E., Delatolla, R., 2021c. COVID-19 wastewater surveillance in rural communities: Comparison of lagoon and pumping station samples. Sci. Total Environ. 801, 149618. https://doi.org/10.1016/j.scitotenv.2021.149618

da Rocha Araujo, F.A.G., 2020. Uses and limits of the clinical laboratory in the COVID-19 pandemic: A didactic review. Rev. Assoc. Med. Bras. 66, 1718–1724. https://doi.org/10.1590/1806-9282.66.12.1718

Drake, J.W., Holland, J.J., 1999. Mutation rates among RNA viruses 1999, 18–21.

Duffy, S., 2018. Why are RNA virus mutation rates so damn high? PLoS Biol. 16, 1–6. https://doi.org/10.1371/journal.pbio.3000003

Fajnzylber, J., Regan, J., Coxen, K., Corry, H., Wong, C., Rosenthal, A., Worrall, D., Giguel, F., Piechocka-Trocha, A., Atyeo, C., Fischinger, S., Chan, A., Flaherty, K.T., Hall, K., Dougan, M., Ryan, E.T., Gillespie, E., Chishti, R., Li, Y., Jilg, N., Hanidziar, D., Baron, R.M., Baden, L., Tsibris, A.M., Armstrong, K.A., Kuritzkes, D.R., Alter, G., Walker, B.D., Yu, X., Li, J.Z., Abayneh, B.A. (Betty., Allen, P., Antille, D., Balazs, A., Bals, J., Barbash, M., Bartsch, Y., Boucau, J., Boyce, S., Braley, J., Branch, K., Broderick, K., Carney, J., Chevalier, J., Choudhary, M.C., Chowdhury, N., Cordwell, T., Daley, G., Davidson, S., Desjardins, M., Donahue, L., Drew, D., Einkauf, K., Elizabeth, S., Elliman, A., Etemad, B., Fallon, J., Fedirko, L., Finn, K., Flannery, J., Forde, P., Garcia-Broncano, P., Gettings, E., Golan, D., Goodman, K., Griffin, A., Grimmel, S., Grinke, K., Hartana, C.A., Healy, M., Heller, H., Henault, D., Holland, G., Jiang, C., Jordan, H., Kaplonek, P., Karlson, E.W., Karpell, M., Kayitesi, C., Lam, E.C., LaValle, V., Lefteri, K., Lian, X., Lichterfeld, M., Lingwood, D., Liu, H., Liu, J., Lopez, K., Lu, Y., Luthern, S., Ly, N.L., MacGowan, M., Magispoc, K., Marchewka, J., Martino, B., McNamara, R., Michell, A., Millstrom, I., Miranda, N., Nambu, C., Nelson, S., Noone, M., Novack, L., O'Callaghan, C., Ommerborn, C., Osborn, M., Pacheco, L.C., Phan, N., Pillai, S., Porto, F.A., Rassadkina, Y., Reissis, A., Ruzicka, F., Seiger, K., Selleck, K., Sessa, L., Sharpe, A., Sharr, C., Shin, S., Singh, N., Slaughenhaupt, S., Sheppard, K.S., Sun, W., Sun, X., Suschana, E. (Lizzie), Talabi, O., Ticheli, H., Weiss, S.T., Wilson, V., Zhu, A., 2020. SARS-CoV-2 viral load is associated with increased disease severity and mortality. Nat. Commun. 11, 1–9. https://doi.org/10.1038/s41467-020-19057-5

Fontana, L., Villamagna, A.H., Sikka, M.K., McGregor, J.C., 2020. Understanding Viral Shedding of SARS-CoV-2: Review of Current Literature. Infect. Control Hosp. Epidemiol. 2, 1–10. https://doi.org/10.1017/ice.2020.1273

Frampton, D., Rampling, T., Cross, A., Bailey, H., Heaney, J., Byott, M., Scott, R., Sconza, R., Price, J., Margaritis, M., Bergstrom, M., Spyer, M.J., Miralhes, P.B., Grant, P., Kirk, S., Valerio, C., Mangera, Z., Prabhahar, T., Moreno-Cuesta, J., Arulkumaran, N., Singer, M., Shin, G.Y., Sanchez, E., Paraskevopoulou, S.M., Pillay, D., McKendry, R.A., Mirfenderesky, M., Houlihan, C.F., Nastouli, E., 2021. Genomic characteristics and clinical effect of the emergent SARS-CoV-2 B.1.1.7 lineage in London, UK: a whole-genome sequencing and hospital-based cohort study. Lancet Infect. Dis. 21, 1246–1256. https://doi.org/10.1016/S1473-3099(21)00170-5

Galani, A., Aalizadeh, R., Kostakis, M., Markou, A., Alygizakis, N., Lytras, T., Adamopoulos, P.G., Peccia, J., Thompson, D.C., Kontou, A., Karagiannidis, A., Lianidou, E.S., Avgeris, M., Paraskevis, D., Tsiodras, S., Scorilas, A., Vasiliou, V., Dimopoulos, M.A., Thomaidis, N.S., 2022. SARS-CoV-2

wastewater surveillance data can predict hospitalizations and ICU admissions. Sci. Total Environ. 804, 150151. https://doi.org/10.1016/j.scitotenv.2021.150151

Galloway, S.E., Paul, P., MacCannell, D.R., Johansson, M.A., Brooks, J.T., MacNeil, A., Slayton, R.B., Tong, S., Silk, B.J., Armstrong, G.L., Biggerstaff, M., Dugan, V.G., 2021. Emergence of SARS-CoV-2 B.1.1.7 Lineage. Morb. Mortal. Wkly. Rep. 70, 95–99.

Gonsalves, G., Yamey, G., 2020. Political interference in public health science during covid-19. BMJ 371, 19–20. https://doi.org/10.1136/bmj.m3878

Government of Alberta, 2021. COVID-19 Alberta statistics | alberta.ca [WWW Document]. URL https://www.alberta.ca/stats/covid-19-alberta-statistics.htm (accessed 1.11.22).

Government of Canada, 2021. COVID-19 vaccination coverage in Canada - Canada.ca [WWW Document]. URL https://health-infobase.canada.ca/covid-19/vaccination-coverage/ (accessed 3.8.22).

Graber, T.E., Mercier, É., Bhatnagar, K., Fuzzen, M., D'Aoust, P.M., Hoang, H.-D., Tian, X., Towhid, S.T., Diaz, J.P., Eid, W., Alain, T., Butler, A., Goodridge, L., Servos, M., Delatolla, R., 2021. Near real-time determination of B.1.1.7 in proportion to total SARS-CoV-2 viral load in wastewater using an allele-specific primer extension PCR strategy. Water Res. 205, 117681. https://doi.org/10.1016/j.watres.2021.117681

Graham, M.S., Sudre, C.H., May, A., Antonelli, M., Murray, B., Varsavsky, T., Kläser, K., Canas, L.S., Molteni, E., Modat, M., Drew, D.A., Nguyen, L.H., Polidori, L., Selvachandran, S., Hu, C., Capdevila, J., Koshy, C., Ash, A., Wise, E., Moore, N., Mori, M., Cortes, N., Lynch, J., Kidd, S., Fairley, D.J., Curran, T., McKenna, J.P., Adams, H., Fraser, C., Golubchik, T., Bonsall, D., Hassan-Ibrahim, M.O., Malone, C.S., Cogger, B.J., Wantoch, M., Reynolds, N., Warne, B., Maksimovic, J., Spellman, K., McCluggage, K., John, M., Beer, R., Afifi, S., Morgan, S., Marchbank, A., Price, A., Kitchen, C., Gulliver, H., Merrick, I., Southgate, J., Guest, M., Munn, R., Workman, T., Connor, T.R., Fuller, W., Bresner, C., Snell, L.B., Patel, A., Charalampous, T., Nebbia, G., Batra, R., Edgeworth, J., Robson, S.C., Beckett, A.H., Aanensen, D.M., Underwood, A.P., Yeats, C.A., Abudahab, K., Taylor, B.E., Menegazzo, M., Clark, G., Smith, W., Khakh, M., Fleming, V.M., Lister, M.M., Howson-Wells, H.C., Berry, Louise, Boswell, T., Joseph, A., Willingham, I., Jones, C., Holmes, C., Bird, P., Helmer, T., Fallon, K., Tang, J., Raviprakash, V., Campbell, S., Sheriff, N., Blakey, V., Williams, L.A., Loose, M.W., Holmes, N., Moore, Christopher, Carlile, M., Wright, V., Sang, F., Debebe, J., Coll, F., Signell, A.W., Betancor, G., Wilson, H.D., Eldirdiri, S., Kenyon, A., Davis, T., Pybus, O.G., du Plessis, L., Zarebski, A.E., Raghwani, J., Kraemer, M.U., Francois, S., Attwood, S.W., Vasylyeva, T.I., Escalera Zamudio, M., Gutierrez, B., Torok, M.E., Hamilton, W.L., Goodfellow, I.G., Hall, G., Jahun, A.S., Chaudhry, Y., Hosmillo, M., Pinckert, M.L., Georgana, I., Moses, S., Lowe, H., Bedford, L., Moore, J., Stonehouse, S., Fisher, C.L., Awan, A.R., BoYes, J., Breuer, J., Harris, K.A., Brown, J.R., Shah, D., Atkinson, L., Lee, J.C., Storey, N., Flaviani, F., Alcolea-Medina, A., Williams, R., Vernet, G., Chapman, M.R., Levett, L.J., Heaney, J., Chatterton, W., Pusok, M., Xu-McCrae, L., Smith, D.L., Bashton, M., Young, G.R., Holmes, A., Randell, P.A., Cox, A., Madona, P., Bolt, F., Price, J., Mookerjee, S., Ragonnet-Cronin, M., Nascimento, F.F., Jorgensen, D., Siveroni, I., Johnson, R., Boyd, O., Geidelberg, L., Volz, E.M., Rowan, A., Taylor, G.P., Smollett, K.L., Loman, N.J., Quick, J., McMurray, C., Stockton, J.,

Nicholls, S., Rowe, W., Poplawski, R., McNally, A., Martinez Nunez, R.T., Mason, J., Robinson, T.I., O'Toole, E., Watts, J., Breen, C., Cowell, A., Sluga, G., Machin, N.W., Ahmad, S.S.Y., George, R.P., Halstead, F., Sivaprakasam, V., Hogsden, W., Illingworth, C.J., Jackson, C., Thomson, E.C., Shepherd, J.G., Asamaphan, P., Niebel, M.O., Li, K.K., Shah, R.N., Jesudason, N.G., Tong, L., Broos, A., Mair, D., Nichols, J., Carmichael, S.N., Nomikou, K., Aranday-Cortes, E., Johnson, N., Starinskij, I., da Silva Filipe, A., Robertson, D.L., Orton, R.J., Hughes, J., Vattipally, S., Singer, J.B., Nickbakhsh, S., Hale, A.D., Macfarlane-Smith, L.R., Harper, K.L., Carden, H., Taha, Y., Payne, B.A., Burton-Fanning, S., Waugh, S., Collins, J., Eltringham, G., Rushton, S., O'Brien, S., Bradley, A., Maclean, A., Mollett, G., Blacow, R., Templeton, K.E., McHugh, M.P., Dewar, R., Wastenge, E., Dervisevic, S., Stanley, R., Meader, E.J., Coupland, L., Smith, L., Graham, C., Barton, E., Padgett, D., Scott, G., Swindells, E., Greenaway, J., Nelson, A., McCann, C.M., Yew, W.C., Andersson, M., Peto, T., Justice, A., Eyre, D., Crook, D., Sloan, T.J., Duckworth, N., Walsh, S., Chauhan, A.J., Glaysher, S., Bicknell, K., Wyllie, S., Elliott, S., Lloyd, A., Impey, R., Levene, N., Monaghan, L., Bradley, D.T., Wyatt, T., Allara, E., Pearson, C., Osman, H., Bosworth, A., Robinson, E., Muir, P., Vipond, I.B., Hopes, R., Pymont, H.M., Hutchings, S., Curran, M.D., Parmar, S., Lackenby, A., Mbisa, T., Platt, S., Miah, S., Bibby, D., Manso, C., Hubb, J., Chand, M., Dabrera, G., Ramsay, M., Bradshaw, D., Thornton, A., Myers, R., Schaefer, U., Groves, N., Gallagher, E., Lee, D., Williams, D., Ellaby, N., Harrison, I., Hartman, H., Manesis, N., Patel, V., Bishop, C., Chalker, V., Ledesma, J., Twohig, K.A., Holden, M.T.G., Shaaban, S., Birchley, A., Adams, A., Davies, A., Gaskin, A., Plimmer, A., Gatica-Wilcox, B., McKerr, C., Moore, Catherine, Williams, C., Heyburn, D., De Lacy, E., Hilvers, E., Downing, F., Shankar, G., Jones, H., Asad, H., Coombes, J., Watkins, J., Evans, J.M., Fina, L., Gifford, L., Gilbert, L., Graham, L., Perry, M., Morgan, M., Bull, M., Cronin, M., Pacchiarini, N., Craine, N., Jones, R., Howe, R., Corden, S., Rey, S., Kumziene-SummerhaYes, S., Taylor, S., Cottrell, S., Jones, S., Edwards, S., O'Grady, J., Page, A.J., Mather, A.E., Baker, D.J., Rudder, S., Aydin, A., Kay, G.L., Trotter, A.J., Alikhan, N.F., de Oliveira Martins, L., Le-Viet, T., Meadows, L., Casey, A., Ratcliffe, L., Simpson, D.A., Molnar, Z., Thompson, T., Acheson, E., Masoli, J.A., Knight, B.A., Ellard, S., Auckland, C., Jones, C.R., Mahungu, T.W., Irish-Tavares, D., Haque, T., Hart, J., Witele, E., Fenton, M.L., Dadrah, A., Symmonds, A., Saluja, T., Bourgeois, Y., Scarlett, G.P., Loveson, K.F., Goudarzi, S., Fearn, C., Cook, K., Dent, H., Paul, H., Partridge, D.G., Raza, M., Evans, C., Johnson, K., Liggett, S., Baker, P., Bonner, S., Essex, S., Lyons, R.A., Saeed, K., Mahanama, A.I.K., Samaraweera, B., Silveira, S., Pelosi, E., Wilson-Davies, E., Williams, R.J., Kristiansen, M., Roy, S., Williams, C.A., Cotic, M., Bayzid, N., Westhorpe, A.P., Hartley, J.A., Jannoo, R., Lowe, H.L., Karamani, A., Ensell, L., Prieto, J.A., Jeremiah, S., Grammatopoulos, D., Pandey, S., Berry, Lisa, Jones, K., Richter, A., Beggs, A., Best, A., Percival, B., Mirza, J., Megram, O., Mayhew, M., Crawford, L., Ashcroft, F., Moles-Garcia, E., Cumley, N., Smith, C.P., Bucca, G., Hesketh, A.R., Blane, B., Girgis, S.T., Leek, D., Sridhar, S., Forrest, S., Cormie, C., Gill, H.K., Dias, J., Higginson, E.E., Maes, M., Young, J., Kermack, L.M., Gupta, R.K., Ludden, C., Peacock, S.J., Palmer, Sophie, Churcher, C.M., Hadjirin, N.F., Carabelli, A.M., Brooks, E., Smith, K.S., Galai, K., McManus, G.M., Ruis, C., Davidson, R.K., Rambaut, A., Williams, T., Balcazar, C.E., Gallagher, M.D., O'Toole, Á., Rooke, S., Hill, V., Williamson, K.A., Stanton, T.D., Michell, S.L., Bewshea, C.M., Temperton, B., Michelsen, M.L., Warwick-Dugdale, J., Manley, R., Farbos, A., Harrison, J.W., Sambles, C.M., Studholme, D.J., Jeffries, A.R., Darby, A.C., Hiscox, J.A., Paterson, S., Iturriza-Gomara, M., Jackson, K.A., Lucaci, A.O., Vamos, E.E., Hughes, M., Rainbow, L., Eccles, R., Nelson, C., Whitehead, M., Turtle, L., Haldenby, S.T., Gregory, R., Gemmell, M., Wierzbicki, C., Webster, H.J., de Silva, T.I., Smith, N., Angyal, A., Lindsey, B.B., Groves, D.C., Green, L.R., Wang, D., Freeman, T.M., Parker, M.D., Keeley, A.J., Parsons, P.J., Tucker, R.M., Brown, R., Wyles, M., Whiteley, M., Zhang, P., Gallis, M., Louka, S.F.,

Constantinidou, C., Unnikrishnan, M., Ott, S., Cheng, J.K.J., Bridgewater, H.E., Frost, L.R., Taylor-Joyce, G., Stark, R., Baxter, L., Alam, M.T., Brown, P.E., Aggarwal, D., Cerda, A.C., Merrill, T. V., Wilson, R.E., McClure, P.C., Chappell, J.G., Tsoleridis, T., Ball, J., Buck, D., Todd, J.A., Green, A., Trebes, A., MacIntyre-Cockett, G., de Cesare, M., Alderton, A., Amato, R., Ariani, C. V., Beale, M.A., Beaver, C., Bellis, K.L., Betteridge, E., Bonfield, J., Danesh, J., Dorman, M.J., Drury, E., Farr, B.W., Foulser, L., Goncalves, S., Goodwin, S., Gourtovaia, M., Harrison, E.M., Jackson, D.K., Jamrozy, D., Johnston, I., Kane, L., Kay, S., Keatley, J.P., Kwiatkowski, D., Langford, C.F., Lawniczak, M., Letchford, L., Livett, R., Lo, S., Martincorena, I., McGuigan, S., Nelson, R., Palmer, Steve, Park, N.R., Patel, M., Prestwood, L., Puethe, C., Quail, M.A., Rajatileka, S., Scott, C., Shirley, L., Sillitoe, J., Spencer Chapman, M.H., Thurston, S.A., Tonkin-Hill, G., Weldon, D., Rajan, D., Bronner, I.F., Aigrain, L., Redshaw, N.M., Lensing, S. V., Davies, R., Whitwham, A., Liddle, J., Lewis, K., Tovar-Corona, J.M., Leonard, S., Durham, J., Bassett, A.R., McCarthy, S., Moll, R.J., James, K., Oliver, K., Makunin, A., Barrett, J., Gunson, R.N., Hammers, A., Chan, A.T., Wolf, J., Spector, T.D., Steves, C.J., Ourselin, S., 2021. Changes in symptomatology, reinfection, and transmissibility associated with the SARS-CoV-2 variant B.1.1.7: an ecological study. Lancet Public Heal. 6, e335–e345. https://doi.org/10.1101/2021.03.28.21254404

Halfmann, P.J., Iida, S., Iwatsuki-Horimoto, K., Maemura, T., Kiso, M., Scheaffer, S.M., Darling, T.L., Joshi, A., Loeber, S., Singh, G., Foster, S.L., Ying, B., Case, J.B., Chong, Z., Whitener, B., Moliva, J., Floyd, K., Ujie, M., Nakajima, N., Ito, M., Wright, R., Uraki, R., Warang, P., Gagne, M., Li, R., Sakai-Tagawa, Y., Liu, Y., Larson, D., Osorio, J.E., Hernandez-Ortiz, J.P., Henry, A.R., Ciouderis, K., Florek, K.R., Patel, M., Odle, A., Wong, L.-Y.R., Bateman, A.C., Wang, Z., Edara, V.-V., Chong, Z., Franks, J., Jeevan, T., Fabrizio, T., DeBeauchamp, J., Kercher, L., Seiler, P., Gonzalez-Reiche, A.S., Sordillo, E.M., Chang, L.A., van Bakel, H., Simon, V., Alburquerque, B., Alshammary, H., Amoako, A.A., Aslam, S., Banu, R., Cognigni, C., Espinoza-Moraga, M., Farrugia, K., van de Guchte, A., Khalil, Z., Laporte, M., Mena, I., Paniz-Mondolfi, A.E., Polanco, J., Rooker, A., Sominsky, L.A., Douek, D.C., Sullivan, N.J., Thackray, L.B., Ueki, H., Yamayoshi, S., Imai, M., Perlman, S., Webby, R.J., Seder, R.A., Suthar, M.S., García-Sastre, A., Schotsaert, M., Suzuki, T., Boon, A.C.M., Diamond, M.S., Kawaoka, Y., 2022. SARS-CoV-2 Omicron virus causes attenuated disease in mice and hamsters. Nature 1–22. https://doi.org/10.1038/s41586-022-04441-6

Hatchette, T.F., 2009. The limitations of point of care testing for pandemic influenza: What Clinicians and Public Health professionals need to know. Can. J. Public Heal. 100, 204–207. https://doi.org/10.1007/bf03405541

He, X., Hong, W., Pan, X., Lu, G., Wei, X., 2021. SARS‐CoV‐2 Omicron variant: Characteristics and prevention. MedComm 2, 838‐845. https://doi.org/10.1002/mco2.110

Hirotsu, Y., Maejima, M., Shibusawa, M., Nagakubo, Y., Hosaka, K., Amemiya, K., Sueki, H., Hayakawa, M., Mochizuki, H., Tsutsui, T., Kakizaki, Y., Miyashita, Y., Yagi, S., Kojima, S., Omata, M., 2020. Comparison of automated SARS-CoV-2 antigen test for COVID-19 infection with quantitative RT-PCR using 313 nasopharyngeal swabs, including from seven serially followed patients. Int. J. Infect. Dis. 99, 397–402. https://doi.org/10.1016/j.ijid.2020.08.029

Holcomb, D.A., Christensen, A., Hoffman, K., Lee, A., Blackwood, A.D., Clerkin, T., Gallard-Góngora, J., Harris, A., Kotlarz, N., Mitasova, H., Reckling, S., de los Reyes, F.L., Stewart, J.R., Guidry, V.T., Noble, R.T., Serre, M.L., Garcia, T.P., Engel, L.S., 2024. Estimating rates of change to interpret quantitative wastewater surveillance of disease trends. Sci. Total Environ. 951. https://doi.org/10.1016/j.scitotenv.2024.175687

Holmes, E.G., Rambaut, A., 2004. Viral evolution and the emergence of SARS coronavirus. Philos. Trans. R. Soc. B Biol. Sci. 359, 1059–1065. https://doi.org/10.1098/rstb.2004.1478

Hoseinpour Dehkordi, A., Alizadeh, M., Derakhshan, P., Babazadeh, P., Jahandideh, A., 2020. Understanding epidemic data and statistics: A case study of COVID-19. J. Med. Virol. 92, 868–882. https://doi.org/10.1002/jmv.25885

Hua, C.Z., Miao, Z.P., Zheng, J.S., Huang, Q., Sun, Q.F., Lu, H.P., Su, F.F., Wang, W.H., Huang, L.P., Chen, D.Q., Xu, Z.W., Ji, L.D., Zhang, H.P., Yang, X.W., Li, M.H., Mao, Y.Y., Ying, M.Z., Ye, S., Shu, Q., Chen, E.F., Liang, J.F., Wang, W., Chen, Z.M., Li, W., Fu, J.F., 2020. Epidemiological features and viral shedding in children with SARS-CoV-2 infection. J. Med. Virol. 92, 2804–2812. https://doi.org/10.1002/jmv.26180

Huang, Y., Chen, S., Yang, Z., Guan, W., Liu, D., Lin, Z., Zhang, Y., Xu, Z., Liu, X., Li, Y., 2020. SARS-CoV-2 viral load in clinical samples from critically ill patients. Am. J. Respir. Crit. Care Med. 201, 1435–1438. https://doi.org/10.1164/rccm.202003-0572LE

Hyafil, A., Moriña, D., 2020. Analysis of the impact of lockdown on the reproduction number of the SARS-Cov-2 in Spain. Gac. Sanit. https://doi.org/10.1016/j.gaceta.2020.05.003

Jaiswal, J., LoSchiavo, C., Perlman, D.C., 2020. Disinformation, Misinformation and Inequality-Driven Mistrust in the Time of COVID-19: Lessons Unlearned from AIDS Denialism. AIDS Behav. 24, 2776–2780. https://doi.org/10.1007/s10461-020-02925-y

Jones, D.L., Baluja, M.Q., Graham, D.W., Corbishley, A., McDonald, J.E., Malham, S.K., Hillary, L.S., Connor, T.R., Gaze, W.H., Moura, I.B., Wilcox, M.H., Farkas, K., 2020. Shedding of SARS-CoV-2 in feces and urine and its potential role in person-to-person transmission and the environment-based spread of COVID-19. Sci. Total Environ. 749, 141364. https://doi.org/10.1016/j.scitotenv.2020.141364

Kannan, S.R., Spratt, A.N., Cohen, A.R., Naqvi, S.H., Chand, H.S., Quinn, T.P., Lorson, C.L., Byrareddy, S.N., Singh, K., 2021. Evolutionary analysis of the Delta and Delta Plus variants of the SARS-CoV-2 viruses. J. Autoimmun. 124, 102715. https://doi.org/10.1016/j.jaut.2021.102715

Karthikeyan, S., Ronquillo, N., Belda-ferre, P., Alvarado, D., Javidi, T., Longhurst, C.A., Knight, R., 2021. High-Throughput Wastewater SARS-CoV-2 Detection Enables. mSystems 6, 1–6.

Khailaie, S., Mitra, T., Bandyopadhyay, A., Schips, M., Mascheroni, P., Vanella, P., Lange, B., Binder, S.C., Meyer-Hermann, M., 2021. Development of the reproduction number from coronavirus

SARS-CoV-2 case data in Germany and implications for political measures. BMC Med. 19, 1–16. https://doi.org/10.1186/s12916-020-01884-4

Klaassen, F., Holm, R.H., Smith, T., Cohen, T., Bhatnagar, A., Menzies, N.A., 2024. Predictive power of wastewater for nowcasting infectious disease transmission: A retrospective case study of five sewershed areas in Louisville, Kentucky. Environ. Res. 240, 117395. https://doi.org/10.1016/j.envres.2023.117395

Kolifarhood, G., Aghaali, M., Saadati, H.M., Taherpour, N., Rahimi, S., Izadi, N., Nazari, S.S.H., 2020. Epidemiological and Clinical Aspects of COVID-19; a Narrative Review. Arch. Acad. Emerg. Med. 8, 1–9. https://doi.org/10.22037/aaem.v8i1.620

La Rosa, G., Bonadonna, L., Lucentini, L., Kenmoe, S., Suffredini, E., 2020. Coronavirus in water environments: Occurrence, persistence and concentration methods - A scoping review. Water Res. 179, 115899. https://doi.org/10.1016/j.watres.2020.115899

LaTurner, Z.W., Zong, D.M., Kalvapalle, P., Gamas, K.R., Terwilliger, A., Crosby, T., Ali, P., Avadhanula, V., Santos, H.H., Weesner, K., Hopkins, L., Piedra, P.A., Maresso, A.W., Stadler, L.B., 2021. Evaluating recovery, cost, and throughput of different concentration methods for SARS-CoV-2 wastewater-based epidemiology. Water Res. 197, 117043. https://doi.org/10.1016/j.watres.2021.117043

Lee, W.L., Imakaev, M., Armas, F., McElroy, K.A., Gu, X., Duvallet, C., Chandra, F., Chen, H., Leifels, M., Mendola, S., Floyd-O'Sullivan, R., Powell, M.M., Wilson, S.T., Berge, K.L.J., Lim, C.Y.J., Wu, F., Xiao, A., Moniz, K., Ghaeli, N., Matus, M., Thompson, J., Alm, E.J., 2021. Quantitative SARS-CoV-2 Alpha Variant B.1.1.7 Tracking in Wastewater by Allele-Specific RT-qPCR. Environ. Sci. Technol. Lett. 8, 675–682. https://doi.org/10.1021/acs.estlett.1c00375

Li, X., Zhang, S., Shi, J., Luby, S.P., Jiang, G., 2021. Uncertainties in estimating SARS-CoV-2 prevalence by wastewater-based epidemiology. Chem. Eng. J. 415, 129039. https://doi.org/10.1016/j.cej.2021.129039

Ling, Y., Xu, S.B., Lin, Y.X., Tian, D., Zhu, Z.Q., Dai, F.H., Wu, F., Song, Z.G., Huang, W., Chen, J., Hu, B.J., Wang, S., Mao, E.Q., Zhu, L., Zhang, W.H., Lu, H.Z., 2020. Persistence and clearance of viral RNA in 2019 novel coronavirus disease rehabilitation patients. Chin. Med. J. (Engl). 133, 1039–1043. https://doi.org/10.1097/CM9.0000000000000774

Liu, Y., Liu, J., Johnson, B.A., Xia, H., Ku, Z., Schindewolf, C., Widen, S.G., An, Z., Weaver, S., Menachery, V.D., Xie, X., Shi, P.-Y., 2021. Delta spike P681R mutation enhances SARS-CoV-2 fitness over Alpha variant. bioRxiv 1, 2021.08.12.456173.

Long, Q.X., Tang, X.J., Shi, Q.L., Li, Q., Deng, H.J., Yuan, J., Hu, J.L., Xu, W., Zhang, Y., Lv, F.J., Su, K., Zhang, F., Gong, J., Wu, B., Liu, X.M., Li, J.J., Qiu, J.F., Chen, J., Huang, A.L., 2020. Clinical and immunological assessment of asymptomatic SARS-CoV-2 infections. Nat. Med. https://doi.org/10.1038/s41591-020-0965-6

Malinverni, C., Brigagão, J.I.M., 2020. COVID-19: Scientific Arguments, Denialism, Eugenics, and the Construction of the Antisocial Distancing Discourse in Brazil. Front. Commun. 5. https://doi.org/10.3389/fcomm.2020.582963

McClary-Gutierrez, J.S., Mattioli, M.C., Marcenac, P., Silverman, A.I., Boehm, A.B., Bibby, K., Balliet, M., De Los Reyes, F.L., Gerrity, D., Griffith, J.F., Holden, P.A., Katehis, D., Kester, G., LaCross, N., Lipp, E.K., Meiman, J., Noble, R.T., Brossard, D., McLellan, S.L., 2021. SARS-CoV-2 wastewater surveillance for public health action. Emerg. Infect. Dis. 27, E1–E9. https://doi.org/10.3201/eid2709.210753

McDermott, J.H., Newman, W.G., 2020. Refusal of viral testing during the SARS-CoV-2 pandemic. Clin. Med. J. R. Coll. Physicians London 20, E163–E164. https://doi.org/10.7861/CLINMED.2020-0388

Medema, G., Heijnen, L., Elsinga, G., Italiaander, R., Brouwer, A., 2020. Presence of SARS-Coronavirus-2 RNA in Sewage and Correlation with Reported COVID-19 Prevalence in the Early Stage of the Epidemic in The Netherlands. Environ. Sci. Technol. Lett. 7, 511–516. https://doi.org/10.1021/acs.estlett.0c00357

Mercier, E., D'Aoust, P.M., Thakali, O., Hegazy, N., Jia, J., Zhang, Z., Eid, W., 2022. Wastewater surveillance of influenza activity : Early detection , surveillance , and subtyping in city and neighbourhood communities. medRx. https://doi.org/10.1101/2022.06.28.22276884

Miura, F., Kitajima, M., Omori, R., 2021. Duration of SARS-CoV-2 viral shedding in faeces as a parameter for wastewater-based epidemiology: Re-analysis of patient data using a shedding dynamics model. Sci. Total Environ. 769, 144549. https://doi.org/10.1016/j.scitotenv.2020.144549

Nagarkar, M., Keely, S.P., Jahne, M., Wheaton, E., Hart, C., Smith, B., Garland, J., Varughese, E.A., Braam, A., Wiechman, B., Morris, B., Brinkman, N.E., 2022. SARS-CoV-2 monitoring at three sewersheds of different scales and complexity demonstrates distinctive relationships between wastewater measurements and COVID-19 case data. Sci. Total Environ. 816, 151534. https://doi.org/10.1016/j.scitotenv.2021.151534

Novoa, K.C., Dunn, T., Curry, A., Froude, R., Simpson, S.A., 2021. Limitations of Traditional Models for Medical Decision-Making Capacity and Ethical Clinical Practice in Light of the SARS-CoV-2 Pandemic. Cureus 13, 2–5. https://doi.org/10.7759/cureus.14716

O'Driscoll, M., Ribeiro Dos Santos, G., Wang, L., Cummings, D.A.T., Azman, A.S., Paireau, J., Fontanet, A., Cauchemez, S., Salje, H., 2021. Age-specific mortality and immunity patterns of SARS-CoV-2. Nature 590, 140–145. https://doi.org/10.1038/s41586-020-2918-0

O'Keeffe, J., 2021. Wastewater-based epidemiology: current uses and future opportunities as a public health surveillance tool. Environ. Heal. Rev. 64, 44–52. https://doi.org/10.5864/d2021-015

Olesen, S.W., Imakaev, M., Duvallet, C., 2021. Making waves: Defining the lead time of wastewater-based epidemiology for COVID-19. Water Res. 202, 117433. https://doi.org/10.1016/j.watres.2021.117433

Oran, D.P., Topol, E.J., 2020. Prevalence of asymptomatic SARS-CoV-2 infection. A narrative review. Ann. Intern. Med. 173, 362–368. https://doi.org/10.7326/M20-3012

Ottawa Public Health, 2021. Daily COVID-19 Dashboard [WWW Document]. URL https://www.ottawapublichealth.ca/en/reports-research-and-statistics/daily-covid19-dashboard.aspx (accessed 9.29.21).

Pan, A., Liu, L., Wang, C., Guo, H., Hao, X., Wang, Q., Huang, J., He, N., Yu, H., Lin, X., Wei, S., Wu, T., 2020. Association of Public Health Interventions with the Epidemiology of the COVID-19 Outbreak in Wuhan, China. JAMA - J. Am. Med. Assoc. 323, 1915–1923. https://doi.org/10.1001/jama.2020.6130

Parasa, S., Desai, M., Thoguluva Chandrasekar, V., Patel, H.K., Kennedy, K.F., Roesch, T., Spadaccini, M., Colombo, M., Gabbiadini, R., Artifon, E.L.A., Repici, A., Sharma, P., 2020. Prevalence of gastrointestinal symptoms and fecal viral shedding in Patients ŵith coronavirus disease 2019: A systematic review and meta-analysis. JAMA Netw. open 3, e2011335. https://doi.org/10.1001/jamanetworkopen.2020.11335

Peccia, J., Zulli, A., Brackney, D.E., Grubaugh, N.D., Kaplan, E.H., Casanovas-Massana, A., Ko, A.I., Malik, A.A., Wang, D., Wang, M., Warren, J.L., Weinberger, D.M., Arnold, W., Omer, S.B., 2020. Measurement of SARS-CoV-2 RNA in wastewater tracks community infection dynamics. Nat. Biotechnol. 38, 1164–1167. https://doi.org/10.1038/s41587-020-0684-z

Peterson, S.W., Lidder, R., Daigle, J., Wonitowy, Q., Dueck, C., Nagasawa, A., Mulvey, M.R., Mangat, C.S., 2021. RT-qPCR detection of SARS-CoV-2 mutations S 69–70 del, S N501Y and N D3L associated with variants of concern in Canadian wastewater samples. Sci. Total Environ. 151283. https://doi.org/10.1016/j.scitotenv.2021.151283

Planas, D., Veyer, D., Baidaliuk, A., Staropoli, I., Guivel-Benhassine, F., Rajah, M.M., Planchais, C., Porrot, F., Robillard, N., Puech, J., Prot, M., Gallais, F., Gantner, P., Velay, A., Le Guen, J., Kassis-Chikhani, N., Edriss, D., Belec, L., Seve, A., Courtellemont, L., Péré, H., Hocqueloux, L., Fafi-Kremer, S., Prazuck, T., Mouquet, H., Bruel, T., Simon-Lorière, E., Rey, F.A., Schwartz, O., 2021. Reduced sensitivity of SARS-CoV-2 variant Delta to antibody neutralization. Nature 596, 276–280. https://doi.org/10.1038/s41586-021-03777-9

Pouwels, K.B., House, T., Pritchard, E., Robotham, J. V., Birrell, P.J., Gelman, A., Vihta, K.D., Bowers, N., Boreham, I., Thomas, H., Lewis, J., Bell, I., Bell, J.I., Newton, J.N., Farrar, J., Diamond, I., Benton, P., Walker, Ann Sarah, Pouwels, K.B., Walker, A. Sarah, Crook, D., Matthews, P.C., Peto, T., Stoesser, N., Howarth, A., Doherty, G., Kavanagh, J., Chau, K.K., Hatch, S.B., Ebner, D., Martins Ferreira, L., Christott, T., Marsden, B.D., Dejnirattisai, W., Mongkolsapaya, J., Hoosdally, S., Cornall, R., Stuart,

D.I., Screaton, G., Eyre, D., Bell, J., Cox, S., Paddon, K., James, T., Newton, J.N., Robotham, J. V., Birrell, P., Jordan, H., Sheppard, T., Athey, G., Moody, D., Curry, L., Brereton, P., Hay, J., Vansteenhouse, H., Lambert, A., Rourke, E., Hawkes, S., Henry, S., Scruton, J., Stokes, P., Thomas, T., Allen, J., Black, R., Bovill, H., Braunholtz, D., Brown, D., Collyer, S., Crees, M., Daglish, C., Davies, B., Donnarumma, H., Douglas-Mann, J., Felton, A., Finselbach, H., Fordham, E., Ipser, A., Jenkins, J., Jones, J., Kent, K., Kerai, G., Lloyd, L., Masding, V., Osborn, E., Patel, A., Pereira, E., Pett, T., Randall, M., Reeve, D., Shah, P., Snook, R., Studley, R., Sutherland, E., Swinn, E., Tudor, A., Weston, J., Leib, S., Tierney, J., Farkas, G., Cobb, R., Van Galen, F., Compton, L., Irving, J., Clarke, J., Mullis, R., Ireland, L., Airimitoaie, D., Nash, C., Cox, D., Fisher, S., Moore, Z., McLean, J., Kerby, M., 2021. Community prevalence of SARS-CoV-2 in England from April to November, 2020: results from the ONS Coronavirus Infection Survey. Lancet Public Heal. 6, e30–e38. https://doi.org/10.1016/S2468-2667(20)30282-6

Public Health Ontario, 2021. Ontario COVID-19 Data Tool | Public Health Ontario [WWW Document]. Public Heal. Ontario. URL https://www.publichealthontario.ca/en/data-and-analysis/infectious-disease/covid-19-data-surveillance/covid-19-data-tool?tab=vaccine (accessed 9.28.21).

Qiu, Y., Yu, J., Pabbaraju, K., Lee, B.E., Gao, T., Ashbolt, N.J., Hrudey, S.E., Diggle, M., Tipples, G., Maal-Bared, R., Pang, X., 2021. Validating and optimizing the method for molecular detection and quantification of SARS-CoV-2 in wastewater. Sci. Total Environ. 812, 151434. https://doi.org/10.1016/j.scitotenv.2021.151434

Quilliam, R.S., Weidmann, M., Moresco, V., Purshouse, H., O'Hara, Z., Oliver, D.M., 2020. COVID-19: The environmental implications of shedding SARS-CoV-2 in human faeces. Environ. Int. 140, 105790. https://doi.org/10.1016/j.envint.2020.105790

Randazzo, W., Truchado, P., Cuevas-Ferrando, E., Simón, P., Allende, A., Sánchez, G., 2020. SARS-CoV-2 RNA in wastewater anticipated COVID-19 occurrence in a low prevalence area. Water Res. 181. https://doi.org/10.1016/j.watres.2020.115942

Rivett, L., Sridhar, S., Sparkes, D., Routledge, M., Jones, N.K., Forrest, S., Young, J., Pereira-Dias, J., Hamilton, W.L., Ferris, M., Torok, M.E., Meredith, L., Curran, M.D., Fuller, S., Chaudhry, A., Shaw, A., Samworth, R.J., Bradley, J.R., Dougan, G., Smith, K.G.C., Lehner, P.J., Matheson, N.J., Wright, G., Goodfellow, I.G., Baker, S., Weekes, M.P., Lyons, P.A., Toshner, M., Warne, B., Scott, J.B., Cormie, C., Gill, H., Kean, I., Maes, M., Reynolds, N., Wantoch, M., Caddy, S., Caller, L., Feltwell, T., Hall, G., Hosmillo, M., Houldcroft, C., Jahun, A., Khokhar, F., Yakovleva, A., Butcher, H., Caputo, D., Clapham-Riley, D., Dolling, H., Furlong, A., Graves, B., Gresley, E. Le, Kingston, N., Papadia, S., Stark, H., Stirrups, K.E., Webster, J., Calder, J., Harris, J., Hewitt, S., Kennet, J., Meadows, A., Rastall, R., Brien, C.O., Price, J., Publico, C., Rowlands, J., Ruffolo, V., Tordesillas, H., Brookes, K., Canna, L., Cruz, I., Dempsey, K., Elmer, A., Escoffery, N., Jones, H., Ribeiro, C., Saunders, C., Wright, A., Nyagumbo, R., Roberts, A., Bucke, A., Hargreaves, S., Johnson, D., Narcorda, A., Read, D., Sparke, C., Warboys, L., Lagadu, K., Mactavous, L., Gould, T., Raine, T., Mather, C., Ramenatte, N., Vallier, A.L., Kasanicki, M., Eames, P.J., McNicholas, C., Thake, L., Bartholomew, N., Brown, N., Parmar, S., Zhang, H., Bowring, A., Martell, G., Quinnell, N., Wright, J., Murphy, H., Dunmore, B.J., Legchenko, E., Gräf, S., Huang, C., Hodgson, J., Hunter, K., Martin, J., Mescia, F., O'donnell, C., Pointon, L., Shih, J., Sutcliffe, R., Tilly, T., Tong, Z.,

Treacy, C., Wood, J., Bergamaschi, L., Betancourt, A., Bowyer, G., Sa, A. De, Epping, M., Hinch, A., Huhn, O., Jarvis, I., Lewis, D., Marsden, J., McCallum, S., Nice, F., 2020. Screening of healthcare workers for SARS-CoV-2 highlights the role of asymptomatic carriage in COVID-19 transmission. Elife 9, 1–20. https://doi.org/10.7554/eLife.58728

Rosenke, K., Feldmann, F., Okumura, A., Hansen, F., Tang-Huau, T., Meade-White, K., Kaza, B., Smith, B.J., Hanley, P.W., Lovaglio, J., Jarvis, M.A., Shaia, C., Feldmann, H., 2021. UK B.1.1.7 variant exhibits increased respiratory replication and shedding in nonhuman primates. bioRxiv 2021.06.11.448134.

Rubin, R., 2020. First It Was Masks; Now Some Refuse Testing for SARS-CoV-2. JAMA - J. Am. Med. Assoc. 324, 2015–2016. https://doi.org/10.1001/jama.2020.22003

Santos, V.S., Gurgel, R.Q., Cuevas, L.E., Martins-Filho, P.R., 2020. Prolonged Fecal Shedding of SARS-CoV-2 in Pediatric Patients: A Quantitative Evidence Synthesis. J. Pediatr. Gastroenterol. Nutr. 71, 150–152. https://doi.org/10.1097/MPG.0000000000002798

Shao, Ying, Shao, Yang, Fei, J.M., 2020. Psychiatry hospital management facing COVID-19: From medical staff to patients. Brain. Behav. Immun. 88, 947. https://doi.org/10.1016/j.bbi.2020.04.018

Sherchan, S.P., Shahin, S., Ward, L.M., Tandukar, S., Aw, T.G., Schmitz, B., Ahmed, W., Kitajima, M., 2020. First detection of SARS-CoV-2 RNA in wastewater in North America: A study in Louisiana, USA. Sci. Total Environ. 743, 140621. https://doi.org/10.1016/j.scitotenv.2020.140621

Shuai, H., Chan, J.F.-W., Hu, B., Chai, Y., Yuen, T.T.-T., Yin, F., Huang, X., Yoon, C., Hu, J.-C., Liu, H., Shi, J., Liu, Y., Zhu, T., Zhang, J., Hou, Y., Wang, Y., Lu, L., Cai, J.-P., Zhang, A.J., Zhou, J., Yuan, S., Brindley, M.A., Zhang, B.-Z., Huang, J.-D., To, K.K.-W., Yuen, K.-Y., Chu, H., 2022. Attenuated replication and pathogenicity of SARS-CoV-2 B.1.1.529 Omicron. Nature. https://doi.org/10.1038/s41586-022-04442-5

Uhteg, K., Jarrett, J., Richards, M., Howard, C., Morehead, E., Geahr, M., Gluck, L., Hanlon, A., Ellis, B., Kaur, H., Simner, P., Carroll, K.C., Mostafa, H.H., 2020. Comparing the analytical performance of three SARS-CoV-2 molecular diagnostic assays. J. Clin. Virol. 127, 104384. https://doi.org/10.1016/j.jcv.2020.104384

Uscinski, J.E., Enders, A.M., Klofstad, C., Seelig, M., Funchion, J., Everett, C., Murthi, M., 2020. Why do people believe COVID-19 conspiracy theories ? Research questions. Harvard Kennedy Sch. Misinformation Rev. 1, 1–12.

Verily Life Sciences, 2021. Detection of SARS-CoV-2 in wastewater is an efficient and scalable approach for community infection monitoring.

Wade, M.J., Lo Jacomo, A., Armenise, E., Brown, M.R., Bunce, J.T., Cameron, G.J., Fang, Z., Farkas, K., Gilpin, D.F., Graham, D.W., Grimsley, J.M.S., Hart, A., Hoffmann, T., Jackson, K.J., Jones, D.L., Lilley, C.J., McGrath, J.W., McKinley, J.M., McSparron, C., Nejad, B.F., Morvan, M., Quintela-Baluja, M., Roberts, A.M.I., Singer, A.C., Souque, C., Speight, V.L., Sweetapple, C., Walker, D., Watts,

G., Weightman, A., Kasprzyk-Hordern, B., 2022. Understanding and managing uncertainty and variability for wastewater monitoring beyond the pandemic: Lessons learned from the United Kingdom national COVID-19 surveillance programmes. J. Hazard. Mater. 424. https://doi.org/10.1016/j.jhazmat.2021.127456

Wikramaratna, P.S., Paton, R.S., Ghafari, M., Lourenço, J., 2020. Estimating the false-negative test probability of SARSCoV- 2 by RT-PCR. Eurosurveillance 25, 1–10. https://doi.org/10.2807/1560-7917.ES.2020.25.50.2000568

Wolfe, M.K., Archana, A., Catoe, D., Coffman, M.M., Dorevich, S., Graham, K.E., Kim, S., Grijalva, L.M., Roldan-Hernandez, L., Silverman, A.I., Sinnott-Armstrong, N., Vugia, D.J., Yu, A.T., Zambrana, W., Wigginton, K.R., Boehm, A.B., 2021. Scaling of SARS-CoV-2 RNA in Settled Solids from Multiple Wastewater Treatment Plants to Compare Incidence Rates of Laboratory-Confirmed COVID-19 in Their Sewersheds. Environ. Sci. Technol. Lett. https://doi.org/10.1021/acs.estlett.1c00184

World Health Organization, 2021. WHO Coronavirus Disease (COVID-19) Dashboard With Vaccination Data | WHO Coronavirus (COVID-19) Dashboard With Vaccination Data [WWW Document]. World Heal. Organ. URL https://covid19.who.int/%0Ahttps://covid19.who.int/region/searo/country/bd (accessed 3.22.22).

Wu, F., Zhang, J., Xiao, A., Gu, X., Lee, W.L., Armas, F., Kauffman, K., Hanage, W., Matus, M., Ghaeli, N., Endo, N., Duvallet, C., Poyet, M., Moniz, K., Washburne, A.D., Erickson, T.B., Chai, P.R., Thompson, J., Alm, E.J., 2020. SARS-CoV-2 titers in wastewater are higher than expected from clinically confirmed cases. mSystems 5, 2020.04.05.20051540. https://doi.org/10.1128/mSystems.00614-20

Xiao, A., Wu, F., Bushman, M., Zhang, J., Imakaev, M., Chai, P.R., Duvallet, C., Endo, N., Erickson, T.B., Armas, F., Arnold, B., Chen, H., Chandra, F., Ghaeli, N., Gu, X., Hanage, W.P., Lee, W.L., Matus, M., McElroy, K.A., Moniz, K., Rhode, S.F., Thompson, J., Alm, E.J., 2022. Metrics to relate COVID-19 wastewater data to clinical testing dynamics. Water Res. 212, 118070. https://doi.org/10.1016/j.watres.2022.118070

Xu, Y., Li, X., Zhu, B., Liang, H., Fang, C., Gong, Y., Guo, Q., Sun, X., Zhao, D., Shen, J., Zhang, H., Liu, H., Xia, H., Tang, J., Zhang, K., Gong, S., 2020. Characteristics of pediatric SARS-CoV-2 infection and potential evidence for persistent fecal viral shedding. Nat. Med. 26, 502–505. https://doi.org/10.1038/s41591-020-0817-4

Yadav, P.D., Sapkal, G.N., Abraham, P., Ella, R., Deshpande, G., Patil, D.Y., Nyayanit, D.A., Gupta, N., Sahay, R.R., Shete, A.M., Panda, S., Bhargava, B., Mohan, V.K., 2021. Neutralization of Variant Under Investigation B.1.617.1 With Sera of BBV152 Vaccinees. Clin. Infect. Dis. 20, 547–558. https://doi.org/10.1093/cid/ciab411

Yaniv, K., Ozer, E., Shagan, M., Lakkakula, S., Plotkin, N., Bhandarkar, N.S., Kushmaro, A., 2021. Direct RT-qPCR assay for SARS-CoV-2 variants of concern (Alpha, B.1.1.7 and Beta, B.1.351) detection and quantification in wastewater. Environ. Res. 201. https://doi.org/10.1016/j.envres.2021.111653

Zhang, X., Wu, S., Wu, B., Yang, Q., Chen, A., Li, Y., Zhang, Y., Pan, T., Zhang, H., He, X., 2021. SARS-CoV-2 Omicron strain exhibits potent capabilities for immune evasion and viral entrance. Signal Transduct. Target. Ther. 6, 10–12. https://doi.org/10.1038/s41392-021-00852-5

Zhu, N., Zhang, D., Wang, W., Li, X., Yang, B., Song, J., Zhao, X., Huang, B., Shi, W., Lu, R., Niu, P., Zhan, F., Ma, X., Wang, D., Xu, W., Wu, G., Gao, G.F., Tan, W., 2020. A Novel Coronavirus from Patients with Pneumonia in China, 2019. N. Engl. J. Med. 382, 727–733. https://doi.org/10.1056/nejmoa2001017

Zhu, Y., Oishi, W., Maruo, C., Saito, M., Chen, R., Kitajima, M., Sano, D., 2021. Early warning of COVID-19 via wastewater-based epidemiology: potential and bottlenecks. Sci. Total Environ. 767, 145124. https://doi.org/10.1016/j.scitotenv.2021.145124

Zou, L., Ruan, F., Huang, M., Liang, L., Huang, H., Hong, Z., Yu, J., Kang, M., Song, Y., Xia, J., Guo, Q., Song, T., He, J., Yen, H.-L., Peiris, M., Wu, J., 2020. SARS-CoV-2 Viral Load in Upper Respiratory Specimens of Infected Patients. N. Engl. J. Med. 382, 1177–1179. https://doi.org/10.1056/NEJMc2001737

Chapter 6 – From Plant Pathogen to Public Health Tool: A Review Of Tobamoviruses and Their Role in Wastewater & Environmental Surveillance

6.1. Context

The review manuscript presented in this chapter of the doctoral dissertation is titled *From plant pathogen to public health tool: A review of tobamoviruses and their role in wastewater & environmental surveillance*, by Patrick M. D'Aoust, Tram B. Nguyen, Chandler H. Wong, Nada Hegazy, Sean Stephenson, Elizabeth M. Renouf, Tyson E. Graber, and Robert Delatolla, and will be submitted to the journal *Reviews in Environmental Science and Bio/Technology* (January 2025). This review evaluates the potential of 43 tobamoviruses as biomarkers for the normalization of WEM data. While PMMoV and ToBRFV are commonly used, other tobamoviruses remain underexplored. Performing a systematics review of over 240 studies, we identify 15 promising tobamoviruses and discuss the challenges in normalizing biomarker measurements for accurate WEM. Our findings aim to enhance the standardization and effectiveness of global wastewater surveillance efforts.

6.2. Abstract

Wastewater and environmental monitoring (WEM) has been performed for decades to track diseases and population health. Since the COVID-19 pandemic, interest in tracking respiratory diseases has grown, driven by advancements in PCR techniques applied to wastewater, leading to several innovations to enhance WEM usability. Over time, it has been observed that normalization of WEM generally improved the interpretability, usability and reliability of WEM. One such method involves normalizing measured viral signals in wastewater using human-associated fecal biomarkers such as tobamoviruses. While Pepper mild mottle virus and Tomato brown rugose fruit virus have been extensively studied and utilized in hundreds of WEM studies, research on other members of the tobamovirus genus remains limited despite their promising attributes as biomarkers. We reviewed over 240 published studies, critically assessing the suitability of 43 tobamoviruses, for application as indicators of human fecal contamination or for normalization of population health signals in WEM applications. We also address challenges in normalizing biomarker measurements for accurate and reliable WEM. Our analysis identifies 15 tobamoviruses with significant potential as biomarkers across global wastewater contexts. This approach aims to pave the way for more robust environmental and fecal biomarker standardization and more efficient environmental health monitoring strategies.

6.3. Introduction

Wastewater and environmental monitoring (WEM) has been successfully utilized by public health professionals to survey the emergence of disease outbreaks such as polio, measles or hepatitis, the use of pharmaceutical compounds or illicit drugs, or the emergence and prevalence of genes conferring potential antimicrobial resistance in communities (Been et al., 2014; Benschop et al., 2017; Castiglioni et al., 2013; Choi, 2012; Daughton, 2018; Feng et al., 2018; González-Mariño et al., 2020; Gushgari et al., 2018; Hellmér et al., 2014; Lorenzo and Picó, 2019; Metcalf et al., 1995; Pruden, 2014; Singer et al., 2013; Yang et al., 2017). As a direct result of the COVID-19 pandemic, polymerase chain reaction (PCR)-based WEM has seen unprecedented adoption and support, growing into a tool which allows public health units, governments, and businesses to obtain complementary intelligence about the presence and in some cases, trends in prevalence of COVID-19, influenza, mpox, respiratory syncytial virus infection, tuberculosis, poliomyelitis, measles, viral hepatitis, and other respiratory or enteric infectious diseases. Mechanistically, this is feasible given the deposition patterns of the etiologic pathogens including fragments of their nucleic acids (which are detectable by PCR methods) from bodily excreta such as urine and/or feces into wastewaters. It has been almost universally accepted that to better understand and utilize the results of WEM initiatives, normalization of the observed wastewater-acquired signal using either physico-chemical parameters or biomarkers is highly desirable (Hsu et al., 2022; Hutchison et al., 2022; Maal-Bared et al., 2023; Mazumder et al., 2022). Normalization of wastewater-acquired nucleic acid signals using population metrics, physico-chemical parameters or biomarkers has been shown to often improve correlation between the measured nucleic acid signal and corresponding clinical health metrics (e.g. new daily clinical cases or new daily hospitalizations) (D'Aoust et al., 2021; Feng et al., 2021; Hsu et al., 2022; Maal-Bared et al., 2023; Wolfe et al., 2021; Zhan et al., 2022). However, there are significant challenges in identifying appropriate and effective (i.e. improving correlation between the measured nucleic acid signal and clinical health metrics) normalizing biomarkers for WEM applications. Biomarkers used for normalization should at a minimum be: stable in the environment, have low and consistent variability (and not be subject to major variations in concentration over time or subject to seasonality effects), readily and universally detectable, and sufficiently specific to human activity and diet (Gracia-Lor et al., 2017). Ideally, biomarkers used for normalization would also have similar persistence and stability in the environment to the targets they are normalizing. As a result of the propensity for much of the nucleic acid signal to, in wastewater, aggregate in feces and fecal-associated solids (D'Aoust et al., 2021; Graham et al., 2021; Isaksson et al., 2022; Mercier et al., 2022; Roldan-Hernandez et al., 2022; Wolfe et al., 2021), a significant portion of the literature on this topic has focused on normalizing the measured concentrations of pathogens of interest to human-associated fecal biomarkers. The following human-associated fecal biomarkers have historically been of

interest: bacteriophages of the order *Crassvirales* (also known as crAssphage), *Bacteriodes BacHuman* and HF183, wastewater physico-chemical parameters (ammonia, phosphorus, biological or chemical oxygen demand), caffeine, artificial sweeteners, several persistent chemical agents and tobamoviruses (Chettleburgh et al., 2023; Gracia-Lor et al., 2017; Polo et al., 2020; Vitale et al., 2021). As a direct result of the SARS-CoV-2 pandemic and ensuing growth in WEM initiatives, biomarkers that could easily be integrated (typically DNA or RNA targets) into the existing workflow of detecting SARS-CoV-2 in wastewater were highly attractive to researchers performing WEM. Due to their consistently high titers in wastewater, the following three human-associated fecal biomarkers have been the most popular in contemporary, respiratory virus-tracking WEM applications: Pepper mild mottle virus (PMMoV), Tomato brown rugose fruit virus (ToBRFV) and crAssphage. Of those three, the first two are tobamoviruses, a genus of plant-infecting viruses. Tobamoviruses are amongst the world's most persistent plant pathogens in the environment; virions (infectious viral particles) are often found in soil, surface waters and wastewater (Fillhart et al., 1998; Haňcinský et al., 2020; Lanter, 1982). PMMoV and ToBRFV are used as human-associated fecal biomarkers due to their almost universally high titers in wastewaters globally as the result of ingested virus via contaminated fresh and/or processed human foodstuffs, surviving the journey through the digestive tract (Aguado-García et al., 2020; Balique et al., 2015; Zhang et al., 2006). Despite the use of PMMoV and ToBRFV in WEM, little is known about other tobamoviruses and their suitability as environmental and fecal biomarkers or normalizers in WEM contexts. Faced with mounting evidence that normalizing biomarkers such as PMMoV and ToBRFV may have different prevalences in different sewersheds around the world (Brumfield et al., 2022; Rothman and Whiteson, 2022; Sherchan et al., 2023), it is critical to determine if other tobamoviruses, or a mixture of several tobamoviruses could be used as a universal normalizer to wastewater-acquired signals of pathogens of interest and improve their correlations to corresponding clinical health metrics. The present review article provides a critical review of the 43 currently identified tobamoviruses, describes their characteristics and initial observations in the environment, and discusses their past, current and potential future uses for WEM initiatives. It is organized as follows: First, we give a brief summary of tobamoviruses, and we highlight the tobamoviruses which have already been used and/or monitored in wastewater or surface water streams as a biomarkers or indicator organisms. This is followed by tobamoviruses that have been detected in the human gut and/or human feces, but that have not been used as biomarkers or indicator organisms. We then follow with tobamoviruses that have been identified as having the potential to be used as biomarkers due to their distribution, possible hosts and characteristics. We then end with tobamoviruses that are unlikely to be used as biomarkers due to their distribution, hosts and characteristics, provide a summary table of all evaluated tobamoviruses and provide closing remarks on the future direction of tobamoviruses-as-biomarkers research.

6.4. Methodologies

The systematic review involved querying the ICTV database (https://ictv.global/report/chapter/virgaviridae/virgaviridae/tobamovirus) to identify all recognized tobamoviruses, followed by an extensive literature review using Harzing's Publish or Perish (version 8) (Harzing, 2021) to trace their origins and ecological contexts. Additionally, a Google Scholar search was conducted to uncover novel or poorly characterized tobamoviruses not yet cataloged in the ICTV database, ensuring comprehensive coverage of both established and emerging tobamoviruses.

We then compared the sequence identity at the RNA level of tobamoviruses of interest to all other identified and sequenced tobamoviruses. The GenBank accession numbers of the studied tobamoviruses (if available) in this study are provided below in Table 6-1. A second table focusing on tobamoviruses likely to be effective fecal biomarkers (Table 6-2) and delves into the details of their potential application. In some instances, sequence identity comparisons were previously performed and are cited. In instances where the comparisons were not previously performed, we used the Benchling Align Sequences Tool (Benchling, 2024) to obtain the genetic similarity of tobamoviruses of interest to all other tobamoviruses.

6.5. A brief overview of *tobamoviruses*

Tobamoviruses are a significant group of (at the time of writing) 43 plant viruses characterized by a rod-shaped virions and positive-sensed, single-stranded RNA viruses belonging to the Virgaviridae family (Adams et al., 2017). Tobamoviruses are named after the type species, Tobacco mosaic virus (TMV), the first virus ever discovered and characterized in the late 19th century (Beijerinck, 1898; Ivanovsky, 1892). This discovery was pivotal in establishing virology as a scientific discipline (Okada, 2000; Scholthof, 2004). Infected plants often exhibit symptoms such as mosaic patterns, leaf distortion, and stunted growth, leading to substantial yield losses. The impact of tobamoviruses is significant, particularly in agriculture, as they infect a wide variety of crops, including tobacco, tomato, pepper, and cucumber, causing important damage to crops (Rao and Reddy, 2020; Scholthof et al., 2011). The genome organization of tobamoviruses is relatively simple, typically consisting of approximately 6,300-6,500 nucleotides with four open reading frames (ORFs) that encode four proteins.

These include two large proteins involved in viral RNA production (ORF1, with a typical mass of ~175-183 kDa, and ORF2, with a typical mass of ~123-128 kDa), a movement protein (ORF3, with a typical mass of ~28-30 kDa, often referred to simply as MP), and a capsid/coat protein (ORF4, with a typical mass of ~16-18 kDa, often referred to simply as CP) (Adams et al., 2017; Gibbs, 1999). The first two proteins

are involved in replication, while the movement protein facilitates the cell-to-cell movement of the virus within the host plant. Meanwhile the capsid protein encapsulates the viral RNA, providing protection and stability to the viral particle, and appears to control much of the susceptibility or resistance of plant hosts to tobamoviruses (Bendahmane and Beachy, 1999; Hilf and Dawson, 1993).

Tobamoviruses are known for their exceptional environmental stability, resilience and widespread distribution (Smith and Dombrovsky, 2020). This resilience is due to strong protein-protein interactions at the capsid level, giving inherent stability to the RNA genome. The capsids of tobamoviruses are arranged in a helical manner with numerous replicates of the capsid protein, giving the virus its distinctive rod-like shape. The helical arrangement of the capsid protein replicates allows for strong electrostatic interactions and hydrophobic girdles to form between the capsid proteins (Bloomer et al., 1978; Solovyev and Makarov, 2016). These structural factors allow tobamovirus particles to remain infectious in soil (Fillhart et al., 1998; Pares et al., 1996), water (Kitajima et al., 2018; Mehle and Ravnikar, 2012), and on surfaces for extended periods, often surviving adverse conditions that would inactivate other viruses (Smith and Dombrovsky, 2020).

6.6. Tobacco mosaic virus (TMV)

6.6.1. Characteristics and features

TMV is a rod-shaped, positive-sensed single-stranded RNA virus, measuring approximately 300 nm in length and 18 nm in width. It causes mosaic, mottling, necrosis, stunting, leaf curling, and yellowing of plant tissues in infected cultivars (Adams et al., 2017). TMV predominantly infects tobacco (Nicotiana spp.) cultivars (Scholthof, 2008). The full genome of TMV contains approximately 6,395 nucleotides encoding four proteins: ORF1: 183.3 kDa, ORF2: 126.1 kDa, ORF3: 30.0 kDa and ORF4: 17.6 kDa. Amongst tobamoviruses, TMV shows highest genetic similarity with Rehmannia mosaic virus, Tomato brown rugose fruit virus and Tomato mosaic virus (~83.9 %, 81.8 % and 79.2 % pairwise identity of nucleotides over the whole genome, respectively) (Adams et al., 2017).

6.6.2. Initial observations and discovery

TMV was the first virus discovered, initially studied by Russian microbiologist Dmitri Ivanovsky in 1892 (Bos, 1999; Ivanovsky, 1892). Interest in the disease began in 1877 when farmers in the Netherlands invited German plant biologist Adolf Mayer to investigate a mottling disease in local tobacco cultivars. Mayer and Ivanovsky both described the disease as a tobacco mottling disease transmitted by the sap of infected plants (Ivanovsky, 1892; Mayer, 1886). They initially thought the disease was caused by a microbe

or microbial toxin, which they were unable to isolate. In 1898, Dutch botanist Martinus Beijerinck published a study concluding that the infections and mottling in tobacco cultivars were caused by a non-cellular entity, which he termed 'virus' (Beijerinck, 1898; Bos, 1999). TMV is one of the most well-studied viruses, infecting a wide range of hosts, including members of at least nine plant families and over 125 identified species, such as tobacco, tomato, and pepper (Grant, 1934; Scholthof, 2023; Zamfir et al., 2023).

6.6.3. Past, current and potential future uses

There are several documented uses of TMV as an environmental and fecal biomarker. Due to TMV being the most well-understood tobamovirus and its exceptionally large host range, several studies have investigated its presence in wastewater (Shrestha et al., 2018; Tandukar et al., 2020). Despite routinely finding TMV in wastewater, it has received considerably less attention as a fecal biomarker, potentially due to lower observed concentrations in wastewater as compared to other tobamoviruses, or a higher plant pathogenicity, leading to less consumption. Nonetheless, TMV has sometimes been cited as being one of the most abundant viruses in wastewater (Shrestha et al., 2018; Tandukar et al., 2020). TMV's presence in wastewater and link to human consumption of infected cultivars is also supported by studies that detected TMV in the gastrointestinal tracts of infants (Aguado-García et al., 2020; Taboada et al., 2021).

6.7. Pepper mild mottle virus (PMMoV)

6.7.1. Characteristics and features

PMMoV is a rod-shaped, positive-sensed, single-stranded RNA virus, measuring approximately 300 nm in length and 18 nm in width. It causes mottling, necrosis, and chlorosis of leaves and fruits in infected cultivars (Martelli and Quacquarelli, 1983; Ojinaga et al., 2022). This virus predominantly infects pepper cultivars and can infect most pepper species (Capsicum spp.). There are also reports of PMMoV causing systemic or localized infections in other members of the Solanaceae family, such as tomatoes (Mizumoto et al., 2014; Zhou et al., 2020). The PMMoV genome, approximately 6,357 nucleotides long, encoding four proteins: ORF1: 183.0 kDa, ORF2: 126.0 kDa, ORF3: 30.0 kDa and ORF4: 17.3 kDa. (Alonso et al., 1991). PMMoV shows the highest sequence identity at the RNA level with the Tropical soda apple mosaic virus, with approximately 79.3% pairwise identity of nucleotides over the whole genome.

6.7.2. Initial observations and discovery

The origins of PMMoV are unclear, but a study documented occurrences of Tobacco Mosaic Virus (TMV) or Tomato Mosaic Virus (ToMV) infections in pepper cultivars as early as 1952 (McKinney, 1952).

This trend was confirmed by several studies where TMV proteins were identified via antibody cross-reactivity assays (Feldman and Oremianer, 1972; Rodríguez et al., 2004; Tóbiás et al., 1982; Wetter, 1984). However, mottling and necrosis-like symptoms in pepper cultivars, not attributable to TMV or ToMV infections, were formally reported in the United States in 1952. This TMV viral isolate, dubbed the 'Samsun [tobacco] latent strain,' was one of the first proto-PMMoV isolates collected in South Carolina, and possibly worldwide. This strain was of particular interest because it caused systemic mosaic-pattern mottling in pepper cultivars otherwise immune to TMV (McKinney, 1952). This same strain, or a close relative, this time isolated in pepper cultivars found in Alabama and Florida was further investigated in 1964 (Greenleaf et al., 1964). A similar strain isolated in Alabama and Florida in 1964 caused severe systemic disease in tabasco peppers (Capsicum frutescens) and sweet peppers (Capsicum annuum), while only causing local lesions in woodland tobacco (Nicotiana sylvestris) (Greenleaf et al., 1964). The name PMMoV was proposed by Wetter et al. in 1984 after the formal identification and isolation of the pepper-infecting tobamovirus (Wetter, 1984).

6.7.3. Past, current and potential future uses

PMMoV is the tobamovirus most documented for use as an environmental and fecal biomarker. Its mild symptoms have led to widespread integration of PMMoV-infected cultivars into human foodstuffs. A 2006 study showed that PMMoV was the most abundant virus in human feces (Colson et al., 2010; Zhang et al., 2006) tested in three stool samples collected from two individuals over 18 months. Early discussions of PMMoV as an environmental surveillance tool began around 2008-2009 (Rosario et al., 2009b; Symonds et al., 2008) focusing on detecting wastewater contamination in surface waters due to PMMoV's high presence and persistence in human fecal material (Rosario et al., 2009a; Zhang et al., 2006). Its use as a source-tracking tool for fecal pollution gained rapid interest following these studies. A study comparing PMMoV, human picobirnaviruses (hPBV), and Torque teno virus (TTV) concluded that PMMoV was a promising indicator of human fecal contamination in surface waters (Hamza et al., 2011). It was also demonstrated that tobamoviruses such as ToMV and PMMoV remained infectious for at least six months in aqueous plant nutrient solutions, supporting their use as persistent biomarkers in aquatic environments (Mehle and Ravnikar, 2012). Recent PCR-based environmental surveys have confirmed PMMoV's presence and persistence in various water sources, including surface waters, wastewaters, marine waters, and treated drinking water (Haramoto et al., 2013; Kitajima et al., 2018; Lopez-Roblero et al., 2024). Despite the fact that PMMoV viral signal has been detected in seagull, chicken, cow and goose feces (Hamza et al., 2011; Zhang et al., 2006), this signal is not expected to represent a significant portion of the PMMoV signal observed in domestic, municipal wastewater streams, due to the common practice of strictly separating sanitary and storm sewers during construction. Between 2013 and 2019, PMMoV became a

prominent marker in microbial source tracking (MST) studies, used in over a hundred studies to identify and trace sewage contamination in surface waters, coastal regions, and drinking water sources (Bofill-Mas et al., 2016; Hata et al., 2018; Malla et al., 2019; Shirasaki et al., 2018; Xiaoqiong, 2018). A survey revealed that 91.4% of environmental samples tested positive for PMMoV (Kitajima et al., 2018). Owing to its ubiquitous presence in human sewage, researchers began using PMMoV as a biomarker to normalize SARS-CoV-2 RNA concentrations in wastewater at the onset of the COVID-19 pandemic in late 2019. Since 2020, over 750 studies have employed PMMoV as an environmental and fecal biomarker.

6.8. Tomato brown rugose fruit virus (ToBRFV)

6.8.1. Characteristics and features

ToBRFV is a rod-shaped, positive-sensed single-stranded RNA virus, measuring approximately 300 nm in length and 18 nm in width. It causes mosaic, mottling, necrosis, stunting, leaf curling, and rugose (wrinkling) symptoms in infected cultivars (Adams et al., 2017). This virus predominantly infects tomato (Solanum lycopersicum) (Luria et al., 2017; Salem et al., 2016) and pepper (Capsicum annuum) cultivars. The full genome of ToBRFV contains approximately 6,393 nucleotides, encoding four proteins: ORF1: 183.3 kDa, ORF2: 126.2 kDa, ORF3: 29.8 kDa and ORF4: 17.5 kDa.. ToBRFV shows the highest genetic similarity with Tomato mottle mosaic virus, with about 86% pairwise identity of nucleotides over the whole genome (Adams et al., 2017; Salem et al., 2016). (Adams et al., 2017; Salem et al., 2016).

6.8.2. Initial observations and discovery

ToBRFV was first observed in several infected Solanum lycopersicum cultivars exhibiting mosaic and curling symptoms in Israel and Jordan in 2014 and 2015 (Luria et al., 2017; Salem et al., 2016). To identify the cause of the symptoms, isolates were observed under transmission electron microscopy, revealing rod-shaped particles, consistent with the presence of tobamoviruses. Genetic sequencing confirmed that the novel virus found in these infected cultivars was a new tobamovirus, which was named Tomato brown rugose fruit virus. Inoculation experiments in which numerous cultivars were exposed to isolated ToBRFV virions from cell lysates in an attempt to induce infection, revealed that ToBRFV has a wide host range, capable of causing symptomatic infections in the following cultivars: Chenopodium murale, Chenopodium amaranticolor, Chenopodium quinoa, Datura stramonium, and various cultivars of the Nicotiana family. ToBRFV did not cause significant symptomatic infection in the following cultivars: Petunia hybrida, Solanum tuberosum, Solanum nigrum and Solanum melongena. Further work revealed

that ToBRFV can infect at least 40 species of cultivars within 4 families of cultivars (Amaranthaceae, Apocynaceae, Asteraceae and Solanaceae) (Zhang et al., 2022).

6.8.3. Past, current and potential future uses

ToBRFV has been increasingly used as an environmental and fecal biomarker. First discovered in 2014, its presence in wastewater was reported in 2017 (Bačnik et al., 2020). Further studies confirmed its presence in river water (Lopez-Roblero et al., 2024), an indication that wastewater treatment may not completely eliminate ToBRFV viral signal from wastewater effluent. During the COVID-19 pandemic, the growth of wastewater-based surveillance for SARS-CoV-2 heightened interest in developing environmental and fecal biomarkers to normalize measured SARS-CoV-2 viral loads (Verma et al., 2023). Over the next four years, hundreds of studies investigated ToBRFV in wastewater. Due to its relatively mild symptoms in many cultivars and its wide host range of commonly consumed fruits and vegetables, ToBRFV is likely to continue being used as an environmental and fecal biomarker. Studies by Aguado-Garcia and Taboada highlighted the presence of ToBRFV in the gastrointestinal tracts of young infants (Aguado-García et al., 2020; Taboada et al., 2021).

6.9. Cucumber green mottle mosaic virus (CGMMV)

6.9.1. Characteristics and features

CGMMV is a rod-shaped, positive-sensed single-stranded RNA virus, measuring approximately 300 nm in length and 18 nm in width. It primarily infects cultivars of the Cucurbitaceae family, causing mild chlorosis and distortion of the leaves and fruits (Antignus et al., 2001). The full genome of CGMMV consists of approximately 6,421 nucleotides, encoding four proteins: ORF1: 186.0 kDa, ORF2: 129.0 kDa, ORF3: 29.0 kDa and ORF4: 17.2 kDa. (Ugaki et al., 1991). CGMMV shows high genetic similarity with related viruses such as Zucchini green mottle mosaic virus, Cucumber fruit mottle mosaic virus, Cucumber mottle virus and Kyuri green mottle mosaic virus (~83.4%, ~83.9%, ~84.0% and ~83.7% pairwise identity of nucleotides over the whole genome, respectively).

6.9.2. Initial observations and discovery

CGMMV was first identified in the United Kingdom in 1935, initially referred to as Cucumber virus 3 (CV3) and Cucumber virus 4 (CV4) (Ainsworth, 1935). Infected plants exhibited symptoms such as vein clearing, light mottling, and blistering of leaves, along with light stunting. These symptoms were

more pronounced in juvenile plants compared to mature ones. Typically, the fruit remained unmarked or only lightly mottled (Dombrovsky et al., 2017).

6.9.3. Past, current and potential future uses

CGMMV has been investigated as an environmental biomarker and a process indicator organism for assessing enteric virus removal through membrane treatment (Yasui et al., 2021). Studies have confirmed its presence in wastewater and river water, indicating that CGMMV could serve as a useful environmental and fecal biomarker for wastewater epidemiology (Bačnik et al., 2020; Lopez-Roblero et al., 2024; Rothman and Whiteson, 2022). This potential is further supported by findings that detected CGMMV in the gastrointestinal tracts of young infants (Aguado-García et al., 2020; Taboada et al., 2021).

6.10. Cactus mild mottle virus (CMMoV)

6.10.1. Characteristics and features

CMMoV is a rod-shaped, positive-sensed single-stranded RNA virus. It measures approximately 300 nm in length and 18 nm in width. This virus causes mild mottling and very mild mosaic symptoms in infected cactus cultivars. Despite predominantly affecting cacti, CMMoV is serologically distinct from other known viruses that infect cacti (Min et al., 2006). The full genome of CMMoV contains 6,449 nucleotides, encoding four proteins: ORF1: 186.0 kDa, ORF2: 120.0 kDa, ORF3: 33.0 kDa and ORF4: 17.6 kDa. (Min et al., 2009). From a genetic standpoint, CMMoV is distantly related to other tobamoviruses, sharing approximately 62% pairwise identity of nucleotides with the Rattail cactus necrosis-associated virus. (Min et al., 2009).

6.10.2. Initial observations and discovery

CMMoV was first observed in Suwon, South Korea, in 2001 as a distantly related tobamovirus primarily infecting cactus plants (Min et al., 2006). The virus was initially isolated from a diseased Gymnocalycium mihanovichii cactus cultivar. Originally believed to be caused by the Saguaro Virus (SOV), serological tests, often used in the detection of plant viruses by reacting virus-specific antibodies with antigens present in serum, revealed this diseased cultivar was not afflicted by SOV. Initial genetic sequencing analyses of the viral capsid revealed between 25.8 – 49.2% pairwise identity of nucleotides with the viral capsid of other tobamoviruses (Min et al., 2006).

6.10.3. Past, current and potential future uses

There are no documented uses of CMMoV as an environmental and fecal biomarker currently available. Uses of cacti as a primary food source for humans is limited but exists, primarily as food components and as ingredients in soups. However, the hardiness of cacti is leading to renewed interest in investigating edible cacti such as Prickly Pear Cactus (Opuntia spp.) as alternative food sources to combat food insecurity induced by climate change trends (Nefzaoui, 2009; Ranjan et al., 2016). As a result, it is plausible that CMMoV could become a target of interest as a fecal biomarker for WEM in the future due to its use in edible foodstuff in arid regions where cacti are commonly consumed. This hypothesis is also supported by the findings of Aguado-Garcia and Taboada, which described the presence of CMMoV in the gastrointestinal tract of young infants (Aguado-García et al., 2020; Taboada et al., 2021), proving that CMMoV-infected foodstuffs, be it cacti in origin or not, are periodically consumed by humans.

6.11. Paprika mild mottle virus (PaMMV)

6.11.1. Characteristics and features

PaMMV is a rod-shaped, positive-sensed single-stranded RNA virus, measuring approximately 300 nm in length and 18 nm in width (Hamada et al., 2003). It causes mild mosaic and mottling of the leaves, flowers, and fruits of infected cultivars. The full genome of PaMMV contains approximately 6,524 nucleotides, encoding four proteins: ORF1: 183.0 kDa, ORF2: 126.1 kDa, ORF3: 30.1 kDa and ORF4: 17.8 kDa. (Hamada et al., 2003). Amongst tobamoviruses, PaMMV shows highest genetic similarity with Obuda pepper virus (~78.2 % pairwise identity of nucleotides over the whole genome).

6.11.2. Initial observations and discovery

PaMMV is a rod-shaped, positive-sensed single-stranded RNA virus, measuring approximately 300 nm in length and 18 nm in width (Hamada et al., 2003). It causes mild mosaic and mottling of the leaves, flowers, and fruits of infected cultivars. The full genome of PaMMV contains approximately 6,524 nucleotides, encoding four proteins: ORF1: 183.0 kDa, ORF2: 126.1 kDa, ORF3: 30.1 kDa and ORF4: 17.8 kDa. (Hamada et al., 2003). Amongst tobamoviruses, PaMMV shows highest genetic similarity with Obuda pepper virus (~78.2 % pairwise identity of nucleotides over the whole genome).

6.11.3. Past, current and potential future uses

As a pathogen which only causes mild mottling in Capsicum spp. Cultivars (Luria et al., 2018), its likely that PaMMV will be found in some transformed products containing peppers. PaMMV may be present in transformed products containing peppers, as diseased fruits might be discarded or used in the

production of edible sauces or pastes. Consequently, PaMMV could be employed as an environmental and fecal biomarker for WEM. PaMMV's presence in wastewater was confirmed in Mexico (Wang et al., 2019). This is further supported by the findings of Aguado-Garcia and Taboada, which outlined the presence of PaMMV in the gastrointestinal tract of young infants (Aguado-García et al., 2020; Taboada et al., 2021).

6.12. Streptocarpus flower break virus (SBFV)

6.12.1. Characteristics and features

SBFV is a rod-shaped, positive-sensed single-stranded RNA virus, measuring approximately 300 nm in length and 18 nm in width. It causes flower color breakage and chlorotic spotting in infected cultivars (Adams et al., 2017; Tang et al., 2024; Verhoeven et al., 1995). SBFV primarily infects Streptocarpus spp. cultivars. The full genome of SBFV contains approximately 6,279 nucleotides, encoding four proteins: ORF1: 181.7 kDa, ORF2: 125.1 kDa, ORF3: 31.6 kDa and ORF4: 15.0 kDa. (Heinze et al., 2006). Amongst tobamoviruses, SBFV shows highest genetic similarity with Turnip vein-clearing virus and Youcai mosaic virus (~61.5 % and 62.0 % pairwise identity of nucleotides over the whole genome, respectively) (Adams et al., 2017).

6.12.2. Initial observations and discovery

SBFV was first observed in the Netherlands in 1995 in infected cultivars displaying color breaking symptoms (Verhoeven et al., 1995). SBFV does not typically cause significant symptoms in the leaves of Streptocarpus spp.. Symptoms are also not always present in the flowers of cultivars, despite the presence of a systemic infection. Inoculation experiments with SBFV revealed that SBFV caused localized, symptomatic infections in the following cultivars: Chenopodium quinoa, Cucumis sativus, Datura stramonium, Nicotiana glutinosa, Nicotiana rustica, Nicotiana tabacum and Petunia hybrida. SBFV also caused latent infections in Capsicum annuum, Lycopersicum esculentum and Nicotiana clevelandii, and systemic mottle in Nicotiana benthamiana, Nicotiana clevelandii and Nicotiana occidentalis (Pappu and Druffel, 2007; Tang et al., 2024; Verhoeven et al., 1995)

6.12.3. Past, current and potential future uses

There are no documented uses of SBFV as an environmental and fecal biomarker. However, due to its multiple possible hosts and relatively mild symptoms in cultivars, it is possible that infected cultivars and fruits could be processed for human consumption. Consequently, SBFV might be considered as a

potential environmental and fecal biomarker for WEM. This potential is supported by findings that detected SBFV in the gastrointestinal tracts of young infants (Aguado-García et al., 2020; Taboada et al., 2021).

6.13. Tobacco mild green mosaic virus (TMGMV)

6.13.1. Characteristics and features

TMGMV is a rod-shaped, positive-sensed single-stranded RNA virus, measuring approximately 300 nm in length and 18 nm in width. It causes yellowing, mosaic, mottling, and lesions on the leaves of infected cultivars (Adams et al., 2017). This virus predominantly infects tobacco (Nicotiana spp.) cultivars. The full genome of TMGMV contains approximately 6,355 nucleotides, encoding four proteins: ORF1: 182.7 kDa, ORF2: 125.8kDa, ORF3: 28.4 kDa and ORF4: 17.6 kDa. (García-Arenal, 1988; Solis and Garcia-Arenal, 1990). Amongst tobamoviruses, TMGMV shows highest genetic similarity with Tobacco mosaic virus and Tomato mosaic virus (~64.4 % and 66.0 % pairwise identity of nucleotides over the whole genome, respectively) (Adams et al., 2017).

6.13.2. Initial observations and discovery

TMGMV was first observed in several infected cultivars exhibiting mosaic symptoms during the 1926-1927 expedition of A.V. Armour in the Canary Islands, West Africa, and Gibraltar (McKinney, 1929). Over the years, TMGMV was known by several different names due to repeated encounters worldwide: Mild dark-green tobacco mosaic virus (Knight, 1942; Svobodová, 1959), Para-tobacco mosaic virus (Köhler and Hauschild, 1947), Mild strain of tobacco mosaic virus (Johnson, 1947), South Carolina mild mottling strain of tobacco mosaic (H. H. McKinney, 1952) virus , Strains U2 and U5 of tobacco mosaic virus (Bald and Solberg, 1961) and Green-tomato atypical mosaic virus (Magne et al., 1977). The virus was eventually named Tobacco mild green mosaic virus to encompass all previous names. TMGMV typically causes mild symptoms, including dark green mosaic patterns in infected cultivars. It is often found in transformed tobacco products like cigarettes (Wetter, 1975), but it has also been identified in other cultivars worldwide, such as Solanum lycopersicum (Ong et al., 2020), Solanum melongena (Chai et al., 2018) and Capsicum annuum (Choi et al., 2002; Herrera‐Vásquez et al., 2009; Salem et al., 2020).

6.13.3. Past, current and potential future uses

There are no documented uses of TMGMV as an environmental and fecal biomarker. However, due to the mild symptoms caused by the virus in cultivars and its global dissemination and wide host range in common food staples, it is plausible that TMGMV could be encountered in processed food products.

This is supported by findings that detected TMGMV in the gastrointestinal tracts of young infants (Aguado-García et al., 2020; Taboada et al., 2021). Of particular interest for wastewater surveillance is the use of the TMGMV U2 strain as a bioherbicide for controlling certain weeds, such as the tropical soda apple (Solanum viarum) (Charudattan et al., 2024). This could lead to high viral loads of TMGMV in wastewater that are unrelated to human consumption of infected cultivars, making its use as a fecal biomarker challenging in areas where it is employed to control noxious weeds.

6.14. Youcai mosaic virus (YMoV)

6.14.1. Characteristics and features

YMoV is a rod-shaped, positive-sensed single-stranded RNA virus, measuring approximately 300 nm in length and 18 nm in width. It causes rugose and mottling symptoms on the leaves and fruits of infected cultivars (Aguilar et al., 1996). YMoV can exhibit a wide range of symptoms in its hosts, from mild to severe, potentially leading to plant death. This virus predominantly infects Brassica napus cultivars but has a broad host range. The full genome of YMoV contains approximately 6,303 nucleotides, encoding four proteins: ORF1: 181.4 kDa, ORF2: 124.8 kDa, ORF3: 29.9 kDa and ORF4: 17.7 kDa. (Aguilar et al., 1996). YMoV shows highest genetic similarity Ribgrass mosaic virus (RiMV) and Turnip vein clearing virus (TVCV) (~84% and ~82% pairwise identity of nucleotides over the whole genome, respectively) (Adams et al., 2017; Aguilar et al., 1996).

6.14.2. Initial observations and discovery

YMoV was first observed and isolated in infected Brassica napus cultivars by Aguilar et al. in 1996 in China (Aguilar et al., 1996). Initially referred to as Chinese rape mosaic virus or Oilseed rape mosaic virus, the name was later changed to Youcai mosaic virus following virological naming conventions. YMoV has been reported to cause a range of effects on its hosts, from mild symptoms to severe cases resulting in plant death. It has been observed to infect a variety of hosts, including several Nicotiana spp. Cultivars, Brassica pekinensis, Brassica chinensis, Brassica juncea (Aguilar et al., 1996), and has more recently been observed causing infections in Capsicum annuum (Zhang et al., 2015), Solanum nigrum (Gu et al., 2024), Digitalis lanata (Dong et al., 2017) and Rehmannia glutinosa (Kwon et al., 2017).

6.14.3. Past, current and potential future uses

There are no documented uses of YMoV as an environmental and fecal biomarker. However, given the widespread use of Brassica napus as a source for rapeseed oil (also known as Canola oil), it is plausible

that YMoV could potentially be used as an environmental and fecal biomarker due to rapeseed oil being the third most consumed culinary oil globally (Shen et al., 2023). As a result, it is likely that YMoV could be used as an environmental and fecal biomarker for WEM. This is supported by the findings of Aguado-Garcia and Taboada, which outlined the presence of YMoV in the gastrointestinal tract of young infants (Aguado-García et al., 2020; Taboada et al., 2021).

6.15. Bell pepper mottle virus (BPeMV)

6.15.1. Characteristics and features

BPeMV is a rod-shaped, positive-sensed single-stranded RNA virus, measuring approximately 300 nm in length and 18 nm in width. It causes mottling, necrosis, chlorosis, and can lead to plant death in infected cultivars. BPeMV exclusively infects pepper cultivars (Capsicum spp.). The full genome of BPeMV contains 6,357 nucleotides, encoding four proteins: ORF1: 181.0 kDa, ORF2: 126.0 kDa, ORF3: 30.0 kDa and ORF4: 18.0 kDa. (Rhie et al., 2007). BPeMV shows high genetic similarity to Tomato Mosaic Virus (ToMV) with ~76% pairwise identity of nucleotides over the whole genome (Adams et al., 2017).

6.15.2. Initial observations and discovery

BPeMV was first observed in 1987 after serological tests on isolates originating from samples collected in Argentina in 1968 (Gracia et al., 1968; Wetter et al., 1987). Wetter distinguished BPeMV from related tobamoviruses such as Tobacco mosaic virus, Tomato mosaic virus, Opuntia chlorotic ringspot virus and PMMoV via serological and inoculation experiments. Specifically, serological tests revealed that BPeMV reacted strongly with PMMoV antibodies, but inversely PMMoV showed little reactivity with BPeMV antibodies (Adams et al., 2017). Since BPeMV primarily infects bell peppers (Capsicum annuum), the name Bell pepper mottle virus was proposed to differentiate it from other tobamoviruses.

6.15.3. Past, current and potential future uses

No documented uses of BPeMV as an environmental and fecal biomarker could be identified. Wetter noted in 1987 that BPeMV appeared to have a higher degree of lethality in infected cultivars than some other tobamoviruses (Wetter et al., 1987). BPeMV has been detected in wastewater at low concentrations (Rothman and Whiteson, 2022), but its low abundance in wastewater may limit its use as an environmental and fecal biomarker. The higher lethality of BPeMV likely reduces its presence in the human food chain, as infected plants are less likely to reach maturity and be harvested, thus limiting its signature in wastewater. Despite this, BPeMV might still be considered as an environmental and fecal biomarker for

WEM. Support for the theory that BPeMV observed in wastewater is caused by the ingestion of infected cultivars is found in the findings of Aguado-Garcia and Taboada, which outlined the presence of BPeMV in the gastrointestinal tract of young infants (Aguado-García et al., 2020; Taboada et al., 2021).

6.16. Opuntia chlorotic ringspot virus (OCRV)

6.16.1. Characteristics and features

OCRV is a rod-shaped, positive-sensed single-stranded RNA virus, measuring approximately 300 nm in length and 18 nm in width (Wetter and Paul, 1967). It causes mottling, yellowing, mosaic patterns, and necrotic lesions on the trunk and flowers of infected cultivars. This virus predominantly infects cultivars of the Opuntia genus. The full genome of OCRV has not yet been sequenced but is expected to contain approximately ~6,400 nucleotides and have 4 ORFs, in typical tobamovirus organization (ORF1: ~182 kDa, ORF2: ~126 kDa, ORF3: ~30 kDa and ORF4: ~18 kDa).

6.16.2. Initial observations and discovery

OCRV was first observed in Arizona, United States, in 1961 (Sammons and Chessin, 1961). It was initially described as causing 'cigar-shaped spindles' within cells of Opuntia spp. pads (Sammons and Chessin, 1961). Inoculation experiments demonstrated that OCRV caused local lesions in Chenopodium quinoa, but would not cause apparent infections in Nicotiana tabacum and Nicotiana glutinosa (Milbrath, 1971). Originally named Sammons's Opuntia virus, it was renamed Opuntia chlorotic ringspot virus in 2017.

6.16.3. Past, current and potential future uses

There are no documented uses of OCRV as an environmental and fecal biomarker that could be identified. While the typical hosts (cultivars of the Opuntia genus) of OCRV are considered edible, it's unclear how much infected foodstuff is encountered in human foodstuffs. Despite this, due to the relatively large host range of the OCRV, it is likely that OCRV could be used as an environmental and fecal biomarker for WEM. Despite these doubts, the theory of consumption of OCRV-infected cultivars is supported by the findings of Aguado-Garcia and Taboada, which outlined the presence of OCRV in the gastrointestinal tract of young infants (Aguado-García et al., 2020; Taboada et al., 2021).

6.17. Rattail cactus necrosis-associated virus (RCNaV)

6.17.1. Characteristics and features

RCNaV is a rod-shaped, positive-sensed single-stranded RNA virus, measuring approximately 300 nm in length and 18 nm in width. It causes necrotic lesions on infected cultivars (Adams et al., 2017; Kim et al., 2012; Murcia Bermudez et al., 2024). This virus predominantly infects Opuntia (O. albicarpa) cultivars. The full genome of RCNaV contains approximately 6,506 nucleotides, encoding four proteins: ORF1: 185.0 kDa, ORF2: 128.0 kDa, ORF3: 36.0 kDa and ORF4: 19.0 kDa. (Kim et al., 2012). Amongst tobamoviruses, RCNaV shows highest genetic similarity with Cactus mild mottle virus (~62.0 % pairwise identity of nucleotides over the whole genome) (Adams et al., 2017; Kim et al., 2012).

6.17.2. Initial observations and discovery

RCNaV was first observed in Korea in 2012 in infected Aporocactus flagelliformis cultivars which were showing symptoms of disease (necrotic lesions) (Kim et al., 2012). Inoculation experiments conducted by Min et al. showed that RCNaV caused symptomatic infections in Nicotiana benthamiana (systemic leaf crinkling and mosaic), Nicotiana tabacum (localized necrotic lesions), and asymptomatic infections in Nicotiana glutinosa, Nicotiana rustica, Cucumis sativus, Vigna unguiculata and Chenopodium amaranticolor (Kim et al., 2012; Min et al., 2006).

6.17.3. Past, current and potential future uses

There are no documented uses of RCNaV as an environmental and fecal biomarker that could be identified. However, the asymptomatic host range of the virus is significant, suggesting that RCNaV could potentially be used as an environmental and fecal biomarker for WEM due to the human consumption of RCNaV-infected foodstuffs. This theory is supported by the findings of Aguado-Garcia and Taboada, which outlined the presence of RCNaV in the gastrointestinal tract of young infants (Aguado-García et al., 2020; Taboada et al., 2021).

6.18. Clitoria yellow mottle virus (CYMV)

6.18.1. Characteristics and features

CYMV is a rod-shaped, positive-sensed single-stranded RNA virus, measuring approximately 300 nm in length and 18 nm in width. It causes localized chlorosis, pale necrotic lesions, and dark spreading halos on the leaves of infected cultivars. This virus predominantly infects legumes and leafy cultivars such as Chenopodium quinoa, Pisum sativum and various strains of tobacco, but does not appear to infect

Brasicca chinensis, Lactuca sativa, Lycopersicon esculentum, Ocimum basilicum or Zinnia elegans (Wei et al., 2012). The full genome of CYMV contains 6,514 nucleotides, encoding four proteins: ORF1: 186.0 kDa, ORF2: 128.0 kDa, ORF3: 32.7 kDa and ORF4: 18.0 kDa.. CYMV shows high genetic similarity with Sunn-hemp mosaic virus (~64% pairwise identity of nucleotides over the whole genome) (Wei et al., 2012).

6.18.2. Initial observations and discovery

In 1995, a disease afflicting an African forage legume (Clitoria ternatea) in Australia was causing chlorosis and visible lesions to leaves of the cultivar. Samples of the affected cultivar, which showed chlorosis and vein clearing, were harvested and a sample was extracted from the cultivar to perform inoculation experiments, which identified several cultivars that could be infected by the novel virion (Chenopodium quinoa, Pisum sativum and various strains of tobacco). Due to the symptoms caused by the novel virus in Clitoria ternatea, the virus was named Clitoria yellow mottle virus (Wei et al., 2012).

6.18.3. Past, current and potential future uses

There are no documented uses of CYMV as an environmental and fecal biomarker. However, given the types of cultivars CYMV can infect and the significant role of legumes such as quinoa and beans in human nutrition, it is possible that CYMV could enter human foodstuffs. If infected cultivars are not culled and are transformed into food products, CYMV could potentially serve as a biomarker in communities and regions where legumes are consumed in large quantities. This potential use should be investigated further.

6.19. Cucumber mottle virus (CMoV)

6.19.1. Characteristics and features

CMoV is a rod-shaped, positive-sensed single-stranded RNA virus, measuring approximately 300 nm in length and 18 nm in width. It causes mottling on the leaves and fruits of infected cultivars (Orita et al., 2007). This virus predominantly infects cucurbits of the Cucumis genus. The full genome of CMoV contains 6,485 nucleotides, encoding four proteins: ORF1: 188.0 kDa, ORF2: 130.0 kDa, ORF3: 28.0 kDa and ORF4: 18.0 kDa. (Orita et al., 2007). CMoV, unsurprisingly, shows high genetic similarity with other cucurbit infecting tobamoviruses such as Cucumber green mottle mosaic virus (~63.5% pairwise identity of nucleotides over the whole genome) (Adams et al., 2017; Orita et al., 2007).

6.19.2. Initial observations and discovery

CMoV was first observed in Southern Japan in 2006 after the discovery of a novel tobamovirus-like virus causing systemic infection and mottling in greenhouse-grown cucumbers. Initial identification attempts included serological experiments, which revealed poor reactivity between extracts from infected cultivars and existing assays for Cucumber Green Mottle Mosaic Virus and Kyuri Green Mottle Mosaic Virus, hinting at the presence of a new virus. Inoculation experiments revealed that this novel virus could lead to lesions when infecting Chenopodium amaranticolor, but not when infecting Datura stramonum, a behavior also observed with Cucumber Green Mottle Mosaic Virus (Orita et al., 2007).

6.19.3. Past, current and potential future uses

There are no documented uses of CMoV as an environmental and fecal biomarker that could be identified. However, given the significant role of cucurbits, particularly cultivars of the Cucumis genus, in human nutrition (McCreight, 2017; Vänninen, 2019), CMoV could have significant uses as a fecal biomarker. This potential relies on the assumption that infected cultivars are not immediately culled and could enter the human food chain through transformed food products containing infected cucumbers. Therefore, the use of CMoV as a fecal biomarker is plausible and should be investigated further.

6.20. Hibiscus latent Fort Pierce virus (HLFPV)

6.20.1. Characteristics and features

HLFPV is a rod-shaped, positive-sensed single-stranded RNA virus, measuring approximately 300 nm in length and 18 nm in width. It causes diffuse chlorosis and mottling on the leaves, fruits, and flowers of infected cultivars (Adkins et al., 2003). This virus predominantly infects Hisbiscus spp. cultivars. The full genome of HLFPV contains approximately 6,431 nucleotides, encoding four proteins: ORF1: 187.0 kDa, ORF2: 128.0 kDa, ORF3: 31.0 kDa and ORF4: 18.0 kDa. (Yoshida et al., 2014). Amongst tobamoviruses, HLFPV shows highest genetic similarity with Hibiscus Latent Singapore Virus (~70.3% pairwise identity of nucleotides over the whole genome) (Adams et al., 2017).

6.20.2. Initial observations and discovery

HLFPV was first observed in 2003 in Fort Pierce, United States, described as an unusual strain of tobacco mosaic virus causing virus-like symptoms in Hibiscus cultivars (Adkins et al., 2003). It was observed in hibiscus across the southeastern portion of the state of Florida, USA. This novel tobamovirus, discovered shortly after reports of the discovery of another hibiscus-infecting tobamovirus, Hibiscus latent Singapore virus (HLSV), differed from HLSV due to different symptomology in infected cultivars, and

differing coat protein sequence, clearly establishing HLFPV as a separate and distinct tobamovirus (Adkins et al., 2003). Sap extracts from infected cultivars were used to inoculate Chenopodium quinoa cultivars to increase viral load before performing widespread inoculation experiments across 51 individual species of cultivars. Out of the 51 inoculated cultivars, 11 were successfully infected (but showed no symptoms), 35 were not successfully infected and only 5 developed symptomatic infection (Adkins et al., 2003). Cultivars that developed symptomatic infection are as follow: Chenopodium amaranticolor, Chenopodium quinoa, Nicotiana glutinosa, Nicotiana rustica and Petunia x hybrida (Adkins et al., 2003). Asymptomatic infections were observed in the following cultivars: Gomphrena globosa, Abelmoshus esculentus (cv. Clemon Spineless + North and South hybrid), Gossypium hirsutum cv. DES 607, Hibiscus cannabinus, Hibiscus rosa-sinensis, Malvaviscus arboreus, Nicotiana benthamiana, Nicotiana debneyi, Nicotiana excelsior and Nicotiana occidentalis (Adkins et al., 2003).

6.20.3. Past, current and potential future uses

There are no documented uses of HLFPV as an environmental and fecal biomarker. However, due to the wide range of hosts HLFPV can infect without producing symptoms, it is plausible that HLFPV may be observed in some wastewater samples and could have relevance in WEM, particularly due to its ability to infect okra (Abelmoshus esculentus).

6.21. Hibiscus latent Singapore virus (HLSV)

6.21.1. Characteristics and features

HLSV s a rod-shaped, positive-sensed single-stranded RNA virus, measuring approximately 300 nm in length and 18 nm in width. It causes diffuse chlorosis and mottling on the leaves, fruits, and flowers of infected cultivars. This virus predominantly infects. This virus predominantly infects Hibiscus spp. cultivars. The full genome of HLSV contains approximately 6,486 nucleotides, encoding four proteins: ORF1: 186.0 kDa, ORF2: 128.0 kDa, ORF3: 30.9 kDa and ORF4: 18.2 kDa. (Srinivasan et al., 2005). Amongst tobamoviruses, HLSV shows highest genetic similarity with Hibiscus Latent Singapore Virus (~70.3% pairwise identity of nucleotides over the whole genome).

6.21.2. Initial observations and discovery

HLSV was first observed in 1982 in Japan and was described as a disease infecting Hibiscus rosa-sinensis, causing yellowing of the veins and mosaic mottling (Kashiwazaki et al., 1982). Phylogenetic analyses of the coat and movement proteins revealed it belonged to a subgroup of tobamoviruses, leading

to the novel virus being tentatively named Hibiscus yellow mosaic tobamovirus. Sequencing of the coat and movement protein genes revealed that this virus was novel and sufficiently distinct from other existing tobamoviruses to be considered a novel tobamovirus. As a result, the novel virus was tentatively renamed Hibiscus virus S (HVS) by Srinivasan et al. in 2002. Inoculation experiments revealed mild or no symptoms in many cultivars, and similarly to HLFPV, a wide host range. The name Hibiscus virus S did not meet the current naming convention and in an attempt to differentiate it from another tobamovirus infecting hibiscus in Florida (HLFPV), naming conventions typically attempt to incorporate the city or country where a virus is first discovered, leading to the renaming of HVS to Hibiscus latent Singapore virus, to highlight the origin of this particular species where it was first observed (Singapore) (Adams et al., 2017).

6.21.3. Past, current and potential future uses

There are no documented uses of HLSV as an environmental and fecal biomarker. However, due to the wide range of hosts HLSV can infect without producing symptoms, it is plausible that HLSV may be observed in some wastewater samples and could have relevance in WEM.

6.22. Kyuri green mottle mosaic virus (KGMMV)

6.22.1. Characteristics and features

KGMMV is a rod-shaped, positive-sensed single-stranded RNA virus, measuring approximately 300 nm in length and 18 nm in width. It causes round, ring-patterned chlorosis and mottling on the leaves and flowers of infected cultivars. This virus predominantly infects cultivars of the family Cucurbitacea. The full genome of KGMMV contains approximately 6,514 nucleotides, encoding four proteins: ORF1: 189.0 kDa, ORF2: 131.5 kDa, ORF3: 28.3 kDa and ORF4: 17.2 kDa. (Yoon et al., 2001). Amongst tobamoviruses, KGMMV shows highest genetic similarity with Zucchini green mottle mosaic virus (~83.8% pairwise identity of nucleotides over the whole genome).

6.22.2. Initial observations and discovery

KGMMV was first observed in the Kansai region of Japan in 1966 and was described as a disease infecting greenhouse cucumbers (Inouye et al., 1967). Infections caused green vein banding and a dark mosaic in the leaves of infected cucurbit cultivars, and the authors described the symptoms as significantly different from symptoms caused by Cucumber mosaic virus and Watermelon mosaic virus. The virus was also reported to cause severe chlorosis, warping and distortions of the fruits of infected cultivars (Inouye et al., 1967). This virus was at the time designated as the ‘cucumber strain’ of the cucumber green mottle

mosaic virus, to distinguish it from the 'watermelon strain' of the same virus (Inouye et al., 1967), due to differences in host tropism and symptoms on infected cultivars. Further work by Francki et al. in 1986 demonstrated via a series of serological and hybridization analyses that the cucumber green mottle mosaic virus was in fact closely related or the same as the CV3 virus Ainsworth described 50 years earlier (Ainsworth, 1935; Francki et al., 1986). Francki et al.'s findings led to the retention of the name cucumber green mottle mosaic virus to encompass CV3, CV4 and the 'watermelon strain' of cucumber green mottle mosaic virus, and proposal of a new name, kyuri green mottle mosaic virus as the name for the virus formally known as the 'cucumber strain' of cucumber green mottle mosaic virus (Francki et al., 1986). Further studies on KGMMV revealed that the virus had an extensive host range, as inoculation experiments in 30 different hosts in the Amaranthaceae, Chenopodiaceae, Cucurbitaceae, Leguminosae and Solanaceae families demonstrated that KGMMV caused symptoms in 26, and infections in 28 of the 30 host cultivars. Only cultivars in the Leguminosae family were not susceptible to infection (Daryono et al., 2005; Yoon et al., 2001).

6.22.3. Past, current and potential future uses

There are no documented uses of KGMMV as an environmental and fecal biomarker that could be identified. However, due to the wide range of hosts KGMMV is capable of infecting, despite intense and severe symptoms in some of the hosts, it is plausible to expect that KGMMV could one day be observed in some wastewater and therefore have some relevance in WEM.

6.23. Maracuja mosaic virus (MarMV)

6.23.1. Characteristics and features

The Maracuja mosaic virus (MarMV) is a rod-shaped, positive-sensed single-stranded RNA virus, measuring approximately 300 nm in length and 18 nm in width. It causes localized necrotic lesions on the leaves and flowers of infected cultivars. This virus predominantly infects cultivars of the family Passifloraceae. The full genome of MarMV contains approximately 6,794 nucleotides, encoding four proteins: ORF1: 180.8 kDa, ORF2: 126.0 kDa, ORF3: 34.0 kDa and ORF4: 18.2 kDa. (Song et al., 2006). Amongst tobamoviruses, MarMV shows highest genetic similarity with Passionfruit mosaic virus (~73.7% pairwise identity of nucleotides over the whole genome) (Adams et al., 2017).

6.23.2. Initial observations and discovery

MarMV was first observed in northern Peru in 1982. Passiflora edulis Sims cultivars displayed symptoms of disease in the form of leaf mosaic and mottling of the leaves and fruits of the infected cultivars (Fribourg et al., 1987). Inoculation experiments revealed that MarMV was also capable of infecting Chenopodium amaranticolor, Chenopodium quinoa and Nicotiana benthamiana (Adams et al., 2017; Song et al., 2006). Inoculation experiments in 27 different species of cultivars revealed that mechanical inoculation led to systemic infections in only 2 of the species: Passiflora edulis and Nicotiana benthamiana. In the other 25 tested species, mechanical inoculation only led to localized MarMV infection (Fribourg et al., 1987).

6.23.3. Past, current and potential future uses

There are no documented uses of MarMV as an environmental and fecal biomarker that could be identified. It is however important to note that MarMV, despite a large host range, tends to cause only localized infections and not systemic infections, therefore potentially limiting its use as an environmental and fecal biomarker. Despite this, it is plausible to expect that MarMV could one day be observed in some wastewater and therefore have some relevance in WEM.

6.24. Obuda pepper virus (ObPV)

6.24.1. Characteristics and features

ObPV is a rod-shaped, positive-sensed single-stranded RNA virus, measuring approximately 300 nm in length and 18 nm in width. It causes yellowing and spotting on the leaves, fruits and flowers of infected cultivars. This virus predominantly infects cultivars of the genus Capsicum. The full genome of ObPV contains approximately 6,507 nucleotides, encoding four proteins: ORF1: 182.9 kDa, ORF2: 126.0 kDa, ORF3: 30.6 kDa and ORF4: 18.0 kDa. (Csilléry et al., 1983; Ikeda et al., 1993). Amongst tobamoviruses, ObPV shows highest genetic similarity with Paprika mild mottle virus (~78.2% pairwise identity of nucleotides over the whole genome).

6.24.2. Initial observations and discovery

ObPV was first observed in Óbuda, Hungary in 1978. The virus was described as a novel disease showing typical tobamovirus symptoms in Capsicum annuum, causing yellowing and yellow spotting in the upper leaves of infected cultivars (Csilléry et al., 1983; Csilléry and Ruskó, 1980). As a result of the symptoms and early inoculation experiments, the virus was initially called “new strain of tomato mosaic virus (ToMV-Ob)”. Inoculation experiments made with crude leaf extracts revealed that ObPV was also

capable of infecting several other cultivars: Chenopodium quinoa, Datura stramonium, Plantago major, Nicotiana sylvestris, Nicotiana glutinosa, Nicotiana tabacum, Nicotiana rustica, Petunia hybrida, Lycopersicon esculentem, and Capsicum spp.. Systemic infections were observed only in cultivars of genus Nicotiana and Capsicum (Csilléry et al., 1983).

6.24.3. Past, current and potential future uses

There are no documented uses of ObPV as an environmental and fecal biomarker that could be identified. It is however important to note that ObPV, despite a large host range, tends to cause only localized infections and not systemic infections, therefore potentially limiting its use as an environmental and fecal biomarker. Despite this, it is plausible to expect that ObPV could one day be observed in some wastewater and therefore have some relevance in WEM.

6.25. Passion fruit mosaic virus (PafMV)

6.25.1. Characteristics and features

PafMV is a rod-shaped plant virus, approximately 300 nm in length and 18 nm in width. It causes mottling and virus-like symptoms on the leaves and fruits of infected plants (Lewandowski and Dawson, 2000; Song et al., 2006). This virus predominately infects Passiflora spp. and was first identified in this specific host. The full genome of PafMV contains 6,791 nucleotides, encoding four proteins: ORF1: 184.0 kDa, ORF2: 125.0 kDa, ORF3: 40.0 kDa and ORF4: 18.0 kDa.(Song and Ryu, 2011). Amongst tobamoviruses, PafMV shows the highest genetic similarity with the Peru isolate of maracuja mosaic virus (68.1% to 77.9% at the nucleotide level of the ORFs) (Song and Ryu, 2011).

6.25.2. Initial observations and discovery

PafMV was first observed in Florida in 2000 and was initially misidentified as an isolate of maracuja mosaic virus (MarMV-FL) in Passiflora incarnate L. cultivars (Song and Ryu, 2011). Following genomic sequencing analysis, it was discovered that the isolate should be a new species due to its significant phylogenic differences and thus was named PafMV. Inoculation experiments revealed that PafMV could cause systemic mosaic on Nicotiana benthamiana and local lesions on N. tabacum, N. glutinosa and Gomphrena globosa (Song and Ryu, 2011).

6.25.3. Past, current and potential future uses

There are no documented uses of PafMV as an environmental and fecal biomarker that could be identified. Hosts of PafMV include Passiflora edulis, also known as yellow passion fruit (Song and Ryu, 2011). P. edulis is native to South America and the fruit is usually eaten fresh (Lim, 2012) and is also known to be used as traditional folk medicine in many countries for the treatment of coughing and constipation. Like many other imported fruits, the importation of fresh passion fruit is commonly limited in certain countries due to quarantine restrictions preventing the spread of insects (Canada Food Inspection Agency, 2020; USDA, 2022). It is therefore unlikely that PafMV-infected cultivars will be commonly consumed by humans, limiting PafMV's potential for use as a fecal biomarker.

6.26. Ribgrass mosaic virus (RiMV)

6.26.1. Characteristics and features

RiMV is a rod-shaped, positive-sensed single-stranded RNA virus, measuring approximately 300 nm in length and 18 nm in width. It causes vein banding, mosaic, and mottling in infected cultivars (Adams et al., 2017; Chavan et al., 2012; Chessin et al., 1980; Wetter, 1986). This virus predominantly infects Plantago spp. cultivars. The full genome of RiMV contains approximately 6,311 nucleotides, encoding four proteins: ORF1: 182.1 kDa, ORF2: 125.4 kDa, ORF3: 30.1 kDa and ORF4: 19.0 kDa. (Chavan et al., 2012). Amongst tobamoviruses, RiMV shows highest genetic similarity with Turnip vein-clearing virus, Youcai mosaic virus and Wasabi mottle virus (~86.7 %, 80.8 % and 81.9 % pairwise identity of nucleotides over the whole genome, respectively) (Adams et al., 2017).

6.26.2. Initial observations and discovery

RiMV was first observed in the United States in 1941 as a novel virus infecting Plantago lanceolata and Plantago major cultivars (Holmes, 1941). Initially named TMV-ribgrass strain, RiMV was also known as Holmes' ribgrass, Crucifer TMV, Turnip vein clearing virus (incorrectly), and TMV-wasabi (Chavan et al., 2012; Gibbs, 1999). The virus was for almost three decades thought to simply be a specific strain of Tobacco mosaic virus before being recognized as its own unique virus (Chessin et al., 1980; Harrison et al., 1971; Oshima and Harrison, 1975). RiMV has a notably large host range (50+ host species), which likely contributed to its misidentification in the wild for over 30 years.

6.26.3. Past, current and potential future uses

There are no documented uses of RiMV as an environmental and fecal biomarker that could be identified. RiMV has a very large host range, and as a result it is plausible that infected cultivars could be consumed in transformed products, but no evidence of this yet exists.

6.27. Sunn-hemp mosaic virus (SHMV)

6.27.1. Characteristics and features

SHMV is a rod-shaped, positive-sensed single-stranded RNA virus, measuring approximately 300 nm in length and 18 nm in width. It causes mosaic, necrotic spots, and banding on the leaves, fruits, and flowers of infected cultivars (Crotalaria juncea spp.) cultivars. The full genome of SHMV contains approximately 6,483 nucleotides, encoding four proteins: ORF1: 186.3 kDa, ORF2: 128.6 kDa, ORF3: 31.0 kDa and ORF4: 18.4 kDa. (Mise et al., 1996; Silver et al., 1996). Amongst tobamoviruses, SHMV shows highest genetic similarity with Clitoria yellow mottle virus (~64.4 % pairwise identity of nucleotides over the whole genome) (Adams et al., 2017).

6.27.2. Initial observations and discovery

SHMV was first observed by Capoor et al. in 1942 in India in infected Vigna unguiculata cultivars showing dwarfed leaves, mosaic and chlorosis symptoms (Capoor et al., 1947). Over the years, SHMV has also been referred to as the Cowpea mosaic virus (Lister and Thresh, 1955), Catjang mosaic virus (Capoor et al., 1947), Dolichos enation mosaic virus (Capoor and Varma, 1948), Southern sunn-hemp mosaic virus (Capoor, 1962, 1950) and Crotalaria mucronata mosaic virus (Raychaudhuri and Pathanian, 1950). The name Sunn-hemp mosaic virus became the generally accepted name due to sunn-hemp being the mainly infected cultivar of this particular tobamovirus (Van Regenmortel and Fraenkel-Conrat, 1996). Inoculation experiments demonstrated that SHMV has a wide host range: over 40 individual species, including Nicotiana tabacum, Pisum sativum, Lycopersicon esculentum, Datura strumonium and Cyamopsis tetragonoloba (Deb et al., 2023).

6.27.3. Past, current and potential future uses

There are no documented uses of SHMV as an environmental and fecal biomarker that could be identified. Despite this, SHMV has a very large host range and as a result it is possible that it could consumed in transformed foodstuffs.

6.28. Tomato mosaic virus (ToMV)

6.28.1. Characteristics and features

ToMV is a rod-shaped, positive-sensed single-stranded RNA virus. It measures approximately 300 nm in length and 18 nm in width. This virus causes mosaic, mottling, chlorosis, and discoloration of leaves and fruits in infected tomato (Adams et al., 2017). This virus predominantly infects tomato (Solanum lycopersicum) cultivars (Allard, 1916; Clinton, 1909). The full genome of ToMV contains approximately 6,383 nucleotides, encoding four proteins: ORF1: 183.5 kDa, ORF2: 126.4 kDa, ORF3: 29.3 kDa and ORF4: 17.8 kDa.. Amongst tobamoviruses, ToMV shows highest genetic similarity with the Tomato mottle mosaic virus and the Tomato brown rugose fruit virus (~84.2 and ~81.0% pairwise identity of nucleotides over the whole genome, respectively) (Adams et al., 2017).

6.28.2. Initial observations and discovery

ToMV was first observed in infected Solanum lycopersicum cultivars exhibiting mosaic and chlorosis in the United States in 1909 (Allard, 1916; Clinton, 1909). Serological tests show strong cross-reactivity between ToMV and TMV, and ToMV was largely considered only a strain of TMV until the 1980s by many eminent scientists in the field. However, with the advent of modern molecular tools such as high throughput sequencing and a distinct host range, ToMV was accepted as a tobamovirus species of its own (Gibbs et al., 1970; Martelli and Quacquarelli, 1983). ToMV has a wide host range and inoculation tests revealed that ToMV also causes infection in the following cultivars: Capsicum spp., Solanum tuberosum, Prunus avium, Pyrus communis, Malus sylvestris, Vitis vinifera, Chenopodium murale and even Picea rubens (Fillhart et al., 1997; Gibbs, 1986).

6.28.3. Past, current and potential future uses

There are no recent documented uses of ToMV as an environmental and fecal biomarker that could be identified. However, it is important to note that infectious ToMV has been detected in greenhouse wastewater (Liu et al., 1999), clouds (Castello et al., 1995), surface water bodies (Koenig, 1986) and trees (Fillhart et al., 1998, 1997). Due to the exceptionally large host range of ToMV, it's likely that it could be encountered in wastewater. As a result, it is likely that ToMV could be used as an environmental and fecal biomarker.

6.29. Tomato mottle mosaic virus (ToMMV)

6.29.1. Characteristics and features

ToMMV is a rod-shaped, positive-sensed single-stranded RNA virus. It measures approximately 300 nm in length and 18 nm in width. This virus causes severe leaf distortion, discoloration, and necrosis in infected cultivars (Adams et al., 2017). ToMMV predominantly infects tomato (Solanum lycopersicum) and Capsicum annuum cultivars (Li et al., 2013). The full genome of ToMMV contains approximately 6,398 nucleotides, encoding four proteins: ORF1: 183.3 kDa, ORF2: 126.3 kDa, ORF3: 29.9 kDa and ORF4: 17.7 kDa.. Amongst tobamoviruses, ToMMV shows highest genetic similarity with Tomato mosaic virus and Tomato brown rugose fruit virus (~84.2 and ~80.8% pairwise identity of nucleotides over the whole genome, respectively) (Adams et al., 2017).

6.29.2. Initial observations and discovery

ToMMV was first observed in diseased greenhouse tomatoes in Mexico and Jordan in 2009 and 2015, respectively (Li et al., 2013; Salem et al., 2016). Initial efforts to diagnose the source of the disease in cultivars via antibody assays revealed that the symptoms were caused by a tobamovirus. Subsequent genomic sequencing revealed that the virus infecting the cultivars was a novel tobamovirus, and not simply a strain of ToMV nor TMV. This led to the coining of the name Tomato mottle mosaic virus. Inoculation experiments revealed that ToMMV was capable of infecting at least 16 different cultivars including common food staples including Solanum lycopersicum, Capsicum annuum, various cultivars of the Nicotiana genus, Brassica pekinensis, Brassica chinensis, and Raphanus sativus (Li et al., 2017).

6.29.3. Past, current and potential future uses

There are no documented uses of ToMMV as an environmental and fecal biomarker that could be identified. Despite ToMMV having a wide host range, ToMMV infections typically cause severe symptoms and as a result it is less likely that ToMMV-infected cultivars would be consumed in transformed products.

6.30. Tropical soda apple mosaic virus (TSAMV)

6.30.1. Characteristics and features

TSAMV is a rod-shaped, positive-sensed single-stranded RNA virus, measuring approximately 300 nm in length and 18 nm in width. It causes leaf mosaic, mottling, and yellowing of plant tissues and fruits in infected cultivars (Adams et al., 2017; Fillmer et al., 2016). This virus predominantly infects tomato (Solanum lycopersicum) cultivars (Fillmer et al., 2016). The full genome of TSAMV contains approximately 6,350 nucleotides, encoding four proteins: ORF1: 182.8 kDa, ORF2: 126.1 kDa, ORF3: 28.3

kDa and ORF4: 17.7 kDa. Amongst tobamoviruses, TSAMV shows highest genetic similarity with Pepper mild mottle virus (~79.3 % pairwise identity of nucleotides over the whole genome).

6.30.2. Initial observations and discovery

TSAMV was first observed in infected in infected Solanum viarum weeds in Florida in 2007. Nicotiana benthamiana cultivars were mechanically inoculated with sap from the weeds showing symptoms and it was observed by microscopy that rod-shaped virions, typical of tobamoviruses, were present. Genetic sequencing revealed that this tobamovirus was novel, and as a result of its discovery in Solanum viarum weeds (Tropical soda apple), the name Tropical soda apple mosaic virus was coined (Adkins et al., 2007). Inoculation experiments with TSAMV revealed a large host range, capable of infecting 16 different species within the Solanaceae family (Fillmer et al., 2016).

6.30.3. Past, current and potential future uses

There are no documented uses of TSAMV as an environmental and fecal biomarker that could be identified. However, TSAMV has a large host range, and as a result it is plausible that infected cultivars could be consumed in transformed products. Evidence of this exists as a recent study has determined that TSAMV was found in river water, wastewater and primary sludge in several sites in Mexico (Lopez-Roblero et al., 2024).

6.31. Turnip vein-clearing virus (TVCV)

6.31.1. Characteristics and features

TVCV is a rod-shaped, positive-sensed single stranded RNA virus, measuring approximately 300 nm in length and 18 nm in width, which causes mosaic, mottling, and vein clearing of plant tissues in infected cultivars (Adams et al., 2017). This virus predominantly infects turnips (Brassica spp.) cultivars (Lartey et al., 1995, 1994). The full genome of TVCV contains approximately 6,311 nucleotides, encoding four proteins: ORF1: 182.0 kDa, ORF2: 125.2 kDa, ORF3: 30.1 kDa and ORF4: 17.6 kDa.. Amongst tobamoviruses, TVCV shows highest genetic similarity with Ribgrass mosaic virus, Plantago tobamovirus 1, Wasabi mottle virus and Youcai mosaic virus (~86.7, ~85.6, ~82.7 and ~82.4% pairwise identity of nucleotides over the whole genome).

6.31.2. Initial observations and discovery

TVCV was first observed in Brasicca rapa cultivars showing in the United States in 1993 (Lartey et al., 1993). The virus was discovered when unexpected nucleic acid bands were observed during routine gel electrophoresis experiments were performed to investigate a lower-than-expected total nucleic acid concentration in a plant DNA preparation. Initial inoculation experiments revealed that in tobacco cultivars, the etiologic agent caused TMV-like symptoms, however in Brassica rapa cultivars the main (and often only) symptom was vein clearing (Lartey et al., 1993). Further inoculation experiments revealed that TVCV caused symptomatic infections in several cultivars: Nicotiana clevelandii, Nicotiana tabacum, Capsicum annuum, Capsicum frutenscens, Datura stramonium, Plantago major, Pixum sativum and Chenopodium amaranticolor. TVCV also cause asymptomatic infections in several cultivars including Brassica oleracea, Mamium maculatum and Abutilon theophrastii (Lockhart et al., 2008).

6.31.3. Past, current and potential future uses

There are no documented uses of TVCV as an environmental and fecal biomarker that could be identified. Due to the small number of cultivars TVCV infects asymptomatically, and the rather apparent symptoms it causes in many other commonly consumed cultivars, it is unlikely that TVCV will be consumed or transformed into foodstuffs.

6.32. Ullucus mild mottle virus (UMMV)

6.32.1. Characteristics and features

UMMV is a rod-shaped, positive-sensed single stranded RNA virus, measuring approximately 300 nm in length and 18 nm in width. UMMV induces mild mottle, distortion of leaves, and symptomless or near-symptomless infections of the roots in Ullucus tuberosus (Brunt et al., 1982a). This virus predominantly infects Ullucus tuberosus, a cultivar endogenous to the Andean region, consumed predominantly as a root vegetable. The genome of UMMV has not been fully sequenced but in typical tobamovirus organization, it is expected to have 4 ORFs, and be approximately 6,350-6,500 nucleotides long. The 4 ORFs are expected to be as follows: ORF1: ~184-186 kDa, ORF2: ~126-128 kDa, ORF3: ~30 kDa and ORF4: ~18 kDa (Gibbs, 1999, 1986; Offei et al., 1995). As UMMV's full genome is not yet available in literature, it is impossible to affirm with full certainty which other tobamovirus UMMV shows highest genetic similarity, however serological experiments performed by Brunt et al. in 1982 revealed a distant relationship between UMMV, Ribgrass mosaic virus, Tobacco mosaic virus and Tomato mosaic virus (Brunt et al., 1982b).

6.32.2. Initial observations and discovery

UMMV was first proposed by Brunt et al. in 1982 and was described as a virus found co-infecting Ullucus tuberosus in Peru, which caused mild mottle and distortion of leaves, while causing mostly asymptomatic infections in the potato-like roots of the cultivars. UMMV was not reported to be found in cultivars not also co-infected with at least another virus, and cultivar inoculation experiments showed that UMMV was capable of infecting at least 21 different species of cultivars (out of 30 total tested) (Brunt et al., 1982b). Infections in the 21 different species ranged from very apparent to almost asymptomatic, causing chlorotic and necrotic lesions in some Nicotiana cultivars and mild but systemic mosaic in Nicotiana clevelandii, Nicotiana benthamiana and Datura metel. UMMV caused asymptomatic infections in Nicotiana debneyi, Petunia hybrida and Lycopersicon esculentem. Importantly, UMMV was unable to infect Capsicum frutenscens and Solanum tuberosum (Brunt et al., 1982b). A novel tobamovirus infecting Ullucus tuberosus was also reported in 2018 and referred to as Ullucus tobamovirus 1 (UTobV1) but because UMMV has not been sequenced previously, it's currently impossible to assert if these two viruses are the same entity.

6.32.3. Past, current and potential future uses

There are no documented uses of UMMV as an environmental and fecal biomarker that could be identified. The relatively constrained native geographical cultivation zones for Ullucus tuberosus (Andean highlands of Peru and Bolivia) limit the reach of UMMV, however due to the wide range of hosts UMMV is capable of infecting while producing no symptoms (particularly Lycopersicon esculentem (tomato)), it is plausible to expect that UMMV may be observed in some wastewaters and therefore have some relevance in WEM.

6.33. Wasabi mottle virus (WMoV)

6.33.1. Characteristics and features

WMoV is a rod-shaped, positive-sensed single stranded RNA virus, measuring approximately 300 nm in length and 18 nm in width, which causes rugose and mottle of the leaves and fruits of infected cultivars (Kashiwazaki et al., 1990). This virus predominantly infects Eutrema japonicum (wasabi/Japanese horseradish) cultivars. The full genome of WMoV contains approximately 6,298 nucleotides, encoding four proteins: ORF1: 181.2 kDa, ORF2: 124.6 kDa, ORF3: 30.0 kDa and ORF4: 17.6 kDa.. WMoV shows highest genetic similarity Youcai mosaic virus (YoMV) and Turnip vein clearing virus (TVCV) (~84% and ~82% pairwise identity of nucleotides over the whole genome, respectively) (Adams et al., 2017; Orita et al., 2007).

6.33.2. Initial observations and discovery

WMoV was first observed by Kashiwazaki et al. in 1985 and was initially referred to the Wasabi strain of tobacco mosaic virus (Kashiwazaki et al., 1990), as it was first isolated from Eutrema japonicum cultivars. An analysis of the host range and amino acids in the coat protein of virus led to researschers then believing that WMoV should instead be considered as a strain of Ribgrass mosaic virus (Kashiwazaki et al., 1990; Oshima and Harrison, 1975). As a result of further serological studies on the virus performed by Kashiwazaki in 1990, a new name for WMoV was proposed: Wasabi strain of crucifer tobamovirus. This new name was chosen due to host tropism, whereas the virus was observed to not only being able to infect Eutrema japonicum cultivars, but also various tobacco plants, and some species of Cruciferae such as Arabidopsis thaliana (Kashiwazaki et al., 1990). The name of the virus would change once more to Wasabi mottle virus to conform with viral nomenclature rules.

6.33.3. Past, current and potential future uses

There are no documented uses of WMoV as an environmental and fecal biomarker that could be identified. Due to the relative limited reach of Eutrema japonicum as an everyday food source, it is unlikely that WMoV will be used as an environmental and fecal biomarker. However, it is to be noted that WMoV in theory could be used as such.

6.34. Brugmansia latent virus (BrLV)

6.34.1. Characteristics and features

BrLV is a rod-shaped, positive-sensed stranded RNA virus, measuring approximately 300 nm in length and 18 nm in width, and does not appear to cause obvious disease on Brugmansia cultivars (Brugmansia spp.). The full genome of BrLV contains 6,397 nucleotides, encoding four proteins: ORF1: 183.0 kDa, ORF2: 126.0 kDa, ORF3: 31.0 kDa and ORF4: 18.0 kDa. (Scott-Brown et al., 2020a). BrLV shows high genetic similary with BMMV (69.7% pairwise identity of nucleotides over the whole genome) (Scott-Brown et al., 2020b).

6.34.2. Initial observations and discovery

BrLV was first observed in the United Kingdom in 2020 (Scott-Brown et al., 2020b). While screening several ornamental Brugmansia spp. cultivars held in the Royal Botanic Gardens, Kew (United Kingdom) for suspected infections caused by Colombian datura virus (CDV), general screening for

tobamoviruses using a degenerate primer assay for the detection of tobamoviruses (Adkins et al., 2018) was also performed. Despite cultivars not showing any obvious signs of disease, two specific cultivars tested positive for both CDV and a tobamovirus. High-throughput genetic sequencing revealed that this tobamovirus, previously unidentified, had traditional tobamovirus genomic organization, but only had 69.7% pairwise identity of nucleotides with BMMV, meeting the definition of >10% deviation in pairwise identity of nucleotides from other known tobamoviruses to be considered a novel specie. Due to the lack of obvious symptoms caused by the novel virus identified in the Brugmansia spp. held at the Royal Botanical Gardens, Kew, the name Brugmansia latent virus (BrLV) was proposed.

6.34.3. Past, current and potential future uses

There are no documented uses of BrLV as an environmental and fecal biomarker that could be identified. As with other viruses capable of infecting Brugmansia spp., due to the toxic nature of cultivars belong to the Brugmansia genus, it is unlikely that they will willingly be consumed or ingested (Algradi et al., 2021; Kerchner and Farkas, 2020a).

6.35. Brugmansia mild mottle virus (BMMV)

6.35.1. Characteristics and features

BMMV is a rod-shaped, positive-sensed single stranded RNA virus, measuring approximately 300 nm in length and 18 nm in width, which causes mottling and necrosis in infected cultivars. This virus predominantly infects ornamental cultivars within Brugmansia spp.. The full genome of BMMV contains 6,381 nucleotides, encoding four proteins: ORF1: 182.0 kDa, ORF2: 125.0 kDa, ORF3: 30.0 kDa and ORF4: 17.6 kDa. (Ilmberger et al., 2007). BMMV shows high genetic similarity with ToMV (~74% pairwise identity of nucleotides over the whole genome) (Adams et al., 2017; Ilmberger et al., 2007).

6.35.2. Initial observations and discovery

BMMV was first observed in 2006 (Ilmberger et al., 2007) from Brugmansia sp. cultivars. While performing inoculation experiments with TMV, TVCV and a novel tobamovirus, isolated from Brugmansia sp. (Pride of Hannover), it was observed that when inoculating Nicotiana rustica the two former viruses induced chlorosis and the novel virus induced vein necrosis, hinting at fundamental differences in the etiologic agent. This led to further characterization of the genome, finding that the novel virus had >10% deviation in pairwise identity of nucleotides from other known tobamoviruses. Due to the symptoms caused by the novel virus in Brugmansia sp., the name Brugmansia mild mottle virus was proposed.

6.35.3. Past, current and potential future uses

There are no documented uses of BMMV as an environmental and fecal biomarker that could be identified. BMMV is known to be capable of infecting all seven species within the Brugmansia genus. Due to the production of natural toxic tropane alkaloid compounds in many of these species belonging to the Brugmansia genus, it is unlikely that they will willingly be consumed or transformed as foodstuff due to the health risks associated with their ingestion or use (Algradi et al., 2021; Kerchner and Farkas, 2020b; Preissel and Preissel, 2002). Furthermore, all seven Brugmansia species no longer exist outside of human cultivation activities or only exist in the wild as the odd escapee and are listed as Extinct in the Wild (EW) according to the International Union for Conservation of Nature (IUCN) (Preissel and Preissel, 2002). As a result, the use of BMMV as an environmental and/or fecal biomarker is unlikely to occur due to the aforementioned health risks associated with the consumption of cultivars belonging to the Brugmansia genus.

6.36. Cucumber fruit mottle mosaic virus (CFMMV)

6.36.1. Characteristics and features

CFMMV is a rod-shaped, positive-sensed single stranded RNA virus, measuring approximately 300 nm in length and 18 nm in width, which causes severe chlorosis, distortion and necrotic lesions in the leaves and fruits of infected cultivars. This virus predominantly infects cultivars of the family Cucurbitacea (Antignus et al., 2001; Rhee et al., 2014). The full genome of CFMMV contains approximately 6,562 nucleotides, encoding four proteins: ORF1: 188.6 kDa, ORF2: 131.0 kDa, ORF3: 27.8 kDa and ORF4: 17.4 kDa.. CFMMV shows high genetic similarity with Zucchini green mottle mosaic virus (~87.3% pairwise identity of nucleotides over the whole genome).

6.36.2. Initial observations and discovery

CFMMV was first observed in Israel in 1992 following the discovery of diseased Cucumis sativus cv. Hassan cultivars in a greenhouse. The infected cultivars showed bright mottling and mosaic on the fruits, and severe mottling and mosaic on the leaves. Some of the cultivars also showed wilting and plant collapse (Antignus et al., 2001). Inoculation experiments performed with CFMMV revealed a wide range of hosts, causing symptoms in Chenopodium amaranticolor, Citrullus vulgaris, Cucumis sativus, Cucumis melo, Curcubita pepo, Datura stramonium, and Nicotiana bethamiana, and also caused symptomless infection in Chenopodium quinoa. These tests also revealed that Capsicum annuum and Lycopersicon esculentum were not hosts for CFMMV (Antignus et al., 2001).

6.36.3. Past, current and potential future uses

There are no documented uses of CFMMV as an environmental and fecal biomarker that could be identified. Low recovery of the virus in wastewater is expected, as the higher lethality of the virus to cultivars likely reduces its ability to enter the human food-chain (cultivars and fruits not making it to maturity, hence not being harvested), greatly limiting its signature in wastewaters.

6.37. Frangipani mosaic virus (FrMV)

6.37.1. Characteristics and features

FrMV is a rod-shaped, positive-sensed single stranded RNA virus, measuring approximately 300 nm in length and 18 nm in width, which causes mottling, vein banding, bronzing and ringspots and virus-like symptoms on the leaves and fruits of infected cultivars (Francki et al., 1971a; Gibbs et al., 1970). This virus predominantly infects Plumeria acutifolia and was the first virus identified to infect this specific host. The full genome of FrMV contains 6,643 nucleotides, encoding four proteins: ORF1: 186.0 kDa, ORF2: 128.0 kDa, ORF3: 30.0 kDa and ORF4: 18.0 kDa. (Lim et al., 2010). Amongst tobamoviruses, FrMV shows highest genetic similarity with Cactus Mild Mottle Virus (~47.7% pairwise identity of nucleotides over the whole genome) (Adams et al., 2017).

6.37.2. Initial observations and discovery

FrMV was first observed in Australia in 1971 and describes an unusual strain of tobacco mosaic virus causing virus-like symptoms on leaves of frangipani (Plumeria acutifolia Poir) cultivars (Francki et al., 1971a). Inoculation experiments with extracts from leaves of the infected frangipani specimens caused systemic infection and chlorosis and sometimes necrotic lesions in Datura stramonium and wet, blotchy lesions in Nicotiana glutinosa. However, Nicotiana tabacum appeared immune to the virus, showing no symptoms post inoculation. Further observations led Francki to determine that the novel virus showed all hallmark signs of Tobacco mosaic virus infections but had an unusual host range and significantly varied symptomology in infected cultivars (Francki et al., 1971b).

6.37.3. Past, current and potential future uses

There are no documented uses of FrMV as an environmental and fecal biomarker that could be identified. Most hosts of FrMV are not readily edible and rarely encountered in human foodstuffs. Some cultivars within the plumeria genus are considered to have edible leaves, but other (Plumeria Rubra, for

example) are known to contain toxic, naturally occurring alkaloid compounds. It is therefore unlikely that FrMV-infected cultivars will be consumed by humans, limiting its potential for use as a fecal biomarker.

6.38. Hoya chlorotic spot virus (HoCSV)

6.38.1. Characteristics and features

HoCSV is a rod-shaped, positive-sensed single stranded RNA virus, measuring approximately 300 nm in length and 18 nm in width, which causes round, ring-patterned chlorosis and mottle on the leaves and flowers of infected cultivars. This virus predominantly infects Hoya spp. cultivars. The full genome of HoCSV contains approximately 6,386 nucleotides, encoding four proteins: ORF1: 184.4 kDa, ORF2: 126.4 kDa, ORF3: 30.4 kDa and ORF4: 17.9 kDa. (Adkins et al., 2018). Amongst tobamoviruses, HoCSV shows highest genetic similarity with Ribgrass mosaic virus (~81.8% pairwise identity of nucleotides over the whole genome).

6.38.2. Initial observations and discovery

HoCSV was first observed in infected Hoya spp. Cultivars in a plant nursery located in Florida, USA (Adkins et al., 2018). Propagation of the virus revealed that HoCSV was also capable of infecting C quinoa and Nicotiana benthamiana. Further inoculation experiments in 18 different species of cultivars revealed that mechanical inoculation led to systemic infections in only 4 of the species: Adenium obesum, Hoya spp. Krimson Queen, Hoya spp. Indian Rope, and Nicotiana benthamiana. In addition to these species, mechanical inoculation also led to localized HoCSV infection in Datura stramonium and Petunia x hybrida ‘Red Supercascade’ (Adkins et al., 2018).

6.38.3. Past, current and potential future uses

There are no documented uses of HoCSV as an environmental and fecal biomarker that could be identified. Due to the limited range of hosts HoCSV is capable of infecting while producing no symptoms, it is unlikely that HoCSV will be observed in wastewater and environmental surveillance.

6.39. Odontoglossum ringspot virus (ORSV)

6.39.1. Characteristics and features

ORSV is a rod-shaped, positive-sensed single stranded RNA virus, measuring approximately 300 nm in length and 18 nm in width, which causes mottling, ringspot and necrotic lesions on the leaves and

flowers of infected cultivars (Jensen and Gold, 1951). This virus predominantly infects monocotyledonous cultivars of the Orchidaceae family. The full genome of OSRV contains approximately 6,618 nucleotides, encoding four proteins: ORF1: 181.6 kDa, ORF2: 126.5 kDa, ORF3: 33.6 kDa and ORF4: 17.8 kDa. (Ryu and Park, 1995). Amongst tobamoviruses, ORSV shows highest genetic similarity with Youcai mosaic virus and Tropical soda apple mosaic virus (~60.0% and ~59.9% pairwise identity of nucleotides over the whole genome, respectively).

6.39.2. Initial observations and discovery

ORSV was first observed in California, United States, in 1951 in Odontoglossum grande cultivars. This occurrence of Tobacco mosaic virus-like infections in cultivars of the Orchidaceae family was again reported in 1954 (Zaitlin et al., 1954). This virus has also been referred to as various other diseases in literature (Edwardson and Zettler, 1986): “orchid strain” of Tobacco mosaic virus, Cymbidium diamond mottle (Jensen, 1951), Cattleya infectious blossom necrosis (Izadpanah et al., 1968), Cattleya mild flow break (Jensen, 1949) and Cattleya color break (Murakishi, 1958). The name Odontoglossum ringspot virus would be first employed by Murakishi in 1958 and would be ratified in 1971 by the International Committee on Taxonomy of Viruses (ICTV). ORSV is one of the most destructive pathogens of orchids in Korea (Kado et al., 1968), Taiwan (Inouye and Leu, 1983; Ko, 1982), China (Liu et al., 2013), Japan (Zheng et al., 2010) and the United States (Hu, J.S., Ferreira, S., Wang, M., Xu, 1993; Hu et al., 1994; Ishii and Martinez, 1973; Zaitlin et al., 1954). Inoculations tests revealed that in addition to causing systemic infections in cultivars of the Orchidaceae family, ORSV also caused localized lesions in Gomphrena spp., Chenopodium spp., Nicotiana tabacum and Tetragonia spp. (Jensen, 1970).

6.39.3. Past, current and potential future uses

There are no documented uses of ORSV as an environmental and fecal biomarker that could be identified. While the typical hosts (cultivars of the Orchidaceae family) of ORSV are edible, the lethality of ORSV to cultivars likely limits the rate at which ORSV is encountered in human foodstuffs. It is therefore unlikely that ORSV-infected cultivars will be consumed by humans, limiting its potential for use as a fecal biomarker.

6.40. Plumeria mosaic virus (PluMV)

6.40.1. Characteristics and features

PluMV is a rod-shaped, positive-sensed single stranded RNA virus, measuring approximately 300 nm in length and 18 nm in width, which causes mosaic, necrotic lesions, bronzing and banding on the leaves, flowers and stems of infected cultivars (Adams et al., 2017; Kumar et al., 2013; Lutgen et al., 2023). This virus predominantly infects frangipani (Plumeria spp.) cultivars. The full genome of PluMV contains approximately 6,688 nucleotides , encoding four proteins: ORF1: 188.3 kDa, ORF2: 130.5 kDa, ORF3: 28.6 kDa and ORF4: 19.0 kDa. (Kumar and Mandal, 2014). Amongst tobamoviruses, PluMV shows highest genetic similarity with Frangipani mosaic virus (~71.3% pairwise identity of nucleotides over the whole genome) (Adams et al., 2017).

6.40.2. Initial observations and discovery

PluMV was first observed in India in 2010 in diseased Plumeria spp. cultivars (Kumar et al., 2017). Inoculation experiments determined that this virus had a significantly different host range and symptomatology as compared to Frangipani mosaic virus, and was therefore named Plumeria mosaic virus (Kumar et al., 2017). Further inoculation experiments revealed that PluMV, in addition to infecting cultivars of the Plumeria genus, could infect and cause symptomatic infections in Nicotiana tabacum (localized white necrotic lesions), Nicotiana benthamiana (systemic white ringspots and blistering), Datura stramonium (systemic chlorosis), Gomphrena globose (localized red spotting), and could cause asymptomatic infections in Solanum melongena and Capsicum annuum cultivars (Kumar et al., 2022).

6.40.3. Past, current and potential future uses

There are no documented uses of PluMV as an environmental and fecal biomarker that could be identified. The typical hosts of PluMV are non-edible plants (flowers/trees) and as a result it is unlikely that PluMV-infected cultivars will be consumed by humans. However, the virus is also capable of causing localized, asymptomatic infections in Capsicum annuum cultivars, which could be consumed by humans. Overall, it is unlikely that PluMV could be used as a fecal biomarker.

6.41. Rehmannia mosaic virus (ReMV)

6.41.1. Characteristics and features

ReMV is a rod-shaped, positive-sensed single stranded RNA virus, measuring approximately 300 nm in length and 18 nm in width, which causes flowering of the leaves, rolling of the leaves, and wilting of infected cultivars (Adams et al., 2017; J. Chen et al., 2022). This virus predominantly infects rehmannia (Rhemannia glutinosa) cultivars, but is also found in several other hosts. The full genome of ReMV contains

approximately 6,395 nucleotides, encoding four proteins: ORF1: 183.5 kDa, ORF2: 126.2 kDa, ORF3: 29.9 kDa and ORF4: 17.6 kDa. (Zhang et al., 2008). Amongst tobamoviruses, ReMV shows highest genetic similarity with Tomato mosaic virus, Tobacco mosaic virus and Tomato brown rugose fruit virus (~78.1 %, 83.9 % and 80.7 % pairwise identity of nucleotides over the whole genome, respectively) (Adams et al., 2017).

6.41.2. Initial observations and discovery

ReMV was first observed in China in 2004 (Zhenchen et al., 2004) as a novel virus infecting Rehmannia glutinosa cultivars. Originally identified as a potential strain of Tobacco mosaic virus, genomic sequencing revealed that the novel virus shared less than 90% pairwise identity of nucleotides with Tobacco mosaic virus, indicating that the novel virus was in fact a new species which predominantly infected Rehmannia spp. cultivars. As a result, Zhenchen et al. proposed the name Rehmannia mosaic virus as a name for the novel virus (Zhenchen et al., 2004). Inoculation experiments revealed that ReMV was capable of symptomatically infecting at least 10 individual plant species. It caused necrotic/chlorotic lesions in the following cultivars: Nicotiana glutinosa, Nicotiana rustica, Datura stramonium, Chenopodium quinoa, Capsicum annuum (Kubota et al., 2012), Chenopodium amaranticolor and Tetragonia expensa (Zhenchen et al., 2004). It also caused systemic mosaic Nicotiana benthamiana, Nicotiana tabacum, Lycopersicon esculentum and Brassica pekinensis (Adams et al., 2017; Zhenchen et al., 2004).

6.41.3. Past, current and potential future uses

There are no documented uses of ReMV as an environmental and fecal biomarker that could be identified. The typical host of ReMV is not edible and despite ReMV having a wide host range, ReMV infections typically cause severe symptoms and as a result it is unlikely that ReMV-infected cultivars would be consumed in transformed products.

6.42. Tobacco latent virus (TLV)

6.42.1. Characteristics and features

TLV is a rod-shaped, positive-sensed single stranded RNA virus, measuring approximately 300 nm in length and 18 nm in width, which causes chlorotic mottling and vein banding (Adams et al., 2017; Ladipo et al., 2003) in infected cultivars. This virus predominantly infects tobacco (Nicotiana spp.) cultivars. The genome of TLV has not been fully sequenced but in typical tobamovirus organization, it is expected to have 4 ORFs, and be approximately 6,350-6,500 nucleotides long. The 4 ORFs are expected to be as follow:

ORF1: ~184-186 kDa, ORF2: ~126-128 kDa, ORF3: ~30 kDa and ORF4: ~18 kDa (Gibbs, 1999, 1986; Offei et al., 1995). As TLV's full genome is not yet available in literature, it is impossible to affirm with full certainty which other tobamovirus TLV shows highest genetic similarity, however it is expected that TLV will share some genomic similarities with Tobacco mosaic virus.

6.42.2. Initial observations and discovery

TLV was first observed in infected Nicotiana spp. cultivars in Nigeria in 2003 (Ladipo et al., 2003). At the time of discovery, few known viruses were infecting Nicotiana spp. cultivars in Nigeria, and inoculation experiments revealed that a potentially novel tobamovirus was present in cultivars showing chlorotic mottling and veinbanding in certain cultivars (Ladipo et al., 2003). The novel virus was initially coined Nigerian tobacco latent virus, which eventually became simply Tobacco latent virus. Inoculation experiments revealed that this tobamovirus could cause symptomless infections in Antirrhinum majus, Gomphrena globose, and symptomatic infections in most species of Nicotiana spp. cultivars (Ladipo et al., 2003).

6.42.3. Past, current and potential future uses

There are no documented uses of TLV as an environmental and fecal biomarker that could be identified. Because the full genome has not yet been fully elucidated (only part of ORF4 (capsid protein) has been sequenced), no diagnostic RT-qPCR assays specific to TLV have so far been developed. As a result, it's currently unlikely that TLV will be used as an environmental/fecal biomarker for WEM applications in the near future.

6.43. Yellow tailflower mild mottle virus (YTMMoV)

6.43.1. Characteristics and features

YTMMoV is a rod-shaped, positive-sensed single stranded RNA virus, measuring approximately 300 nm in lenght and 18 nm in width, which causes mild mottling and chlorosis of plant tissues in infected cultivars (Adams et al., 2017). This virus predominantly infects turnips (Brassica spp.) cultivars (Wylie et al., 2014). The full genome of YTMMoV contains approximately 6,379 nucleotides, encoding four proteins: ORF1: 183.2 kDa, ORF2: 126.5 kDa, ORF3: 30.1 kDa and ORF4: 17.8 kDa.. Amongst tobamoviruses, YTMMoV shows highest genetic similarity with Obuda pepper virus and Brugmansia mild mottle virus (~66.73 and 64.46% pairwise identity of nucleotides over the whole genome).

6.43.2. Initial observations and discovery

YTMMoV was first observed and isolated in Anthocercis littorea cultivars in Australia in 2014 (Wylie et al., 2014). Inoculation experiments demonstrated that while YTMMoV only causes mild symptoms in Anthocercis littorea cultivars, YTMMoV causes necrotic lesions in Chenopodium amaranticolor and Chenopodium quinoa, and severe symptoms in Solanum lycopersicum, Solanum betaceum, Solanum melongena, Solanum nigrum, Capsicum annuum and 19 different cultivars of the Nicotiana genus (Koh et al., 2018; Li et al., 2016; Wylie et al., 2015, 2014).

6.43.3. Past, current and potential future uses

There are no documented uses of YTMMoV as an environmental and fecal biomarker that could be identified. Because of the severity of symptoms in infected cultivars, it is unlikely that YTMMoV will be consumed in human foodstuffs.

6.44. Zucchini green mottle mosaic virus (ZGMMV)

6.44.1. Characteristics and features

ZGMMV is a rod-shaped, positive-sensed single stranded RNA virus, measuring approximately 300 nm in length and 18 nm in width, which causes mosaic, mottling, necrosis, stunting, leaf curling, and yellowing of plant tissues in infected cultivars (Adams et al., 2017). This virus predominantly infects cultivars of the cucurbits family (Ju et al., 2002). The full genome of ZGMMV contains approximately 6,513 nucleotides, encoding four proteins: ORF1: 188.6 kDa, ORF2: 131.2 kDa, ORF3: 28.2 kDa and ORF4: 17.2 kDa.. Amongst tobamoviruses, ZGMMV shows highest genetic similarity with Turnip vein-clearing virus and Kyuri green mottle mosaic virus (~85.3 and 83.8% pairwise identity of nucleotides over the whole genome, respectively).

6.44.2. Initial observations and discovery

ZGMMV was first observed and identified in infected Cucurbita pepo cultivars in Korea in 1999 (Ryu et al., 2000). Originally thought to simply be a novel strain of the Cucumber green mottle mosaic virus or the Kyuri green mottle mosaic virus, serological analyses and sequencing revealed that this novel virus was instead a novel tobamovirus (Francki et al., 1986; Ryu et al., 2000). Inoculation experiments revealed that ZGMMV could cause local necrotic lesions in Chenopodium amaranticolor and Datura

stramonium cultivars, and systemic infections in Nicotiana benthamiana, Cucumis stativus, Cucurbita moschata, Cucurbita pepo and Lagenaria siceraria cultivars (Li et al., 2018; Ryu et al., 2000).

6.44.3. Past, current and potential future uses

There are no documented uses of ZGMMV as an environmental and fecal biomarker that could be identified. ZGMMV in cultivars appear to almost always be symptomatic and quite severe, and as a result it is less likely that ZGMMV will be used as an environmental/fecal biomarker for WEM applications in the future.

Recently described tobamovirus

The increasing accessibility of advanced next-generation sequencing technologies, primarily driven by decreasing costs, will likely accelerate the discovery of viruses in the environment. This review primarily discusses tobamoviruses officially recognized by the International Committee on Taxonomy of Viruses (Adams et al., 2017). However, it also considers several recently discovered tobamoviruses that could potentially serve as environmental and fecal biomarkers in WEM. Below is an overview of these emerging tobamoviruses, along with a brief description of their possible future applications.

6.45. African eggplant-associated virus (AEaV)

AEaV was first observed in Solanum macrocarpon cultivars imported from Mexico into the Netherlands in 2018 (Giesbers et al., 2023). Genomic sequencing revealed that the new virus had highest genetic similarity with Pepper mild mottle virus (~75% pairwise identity of nucleotides over the whole genome). Because this virus shares less than 90% of its genomic identity with other tobamoviruses, the name African eggplant-associated virus was proposed. AEaV was shown to infect several cultivars of the Solanaceae family, including Solanum lycopersicum, Capsicum annuum, Solanum macrocarpon and Petunia integrifolia. AEaV sometimes caused local chlorotic lesions, growth inhibition, rugose, and/or vein banding in infected cultivars, and occasionally caused latent or asymptomatic infections. Therefore, AEaV-infected cultivars or their fruits may be inadvertently introduced or consumed in foodstuffs. As a result, AEaV could potentially be used as an environmental and fecal biomarker in WEM initiatives in the future (Giesbers et al., 2023).

6.46. Hibiscus latent Hawaii virus (HLHV)

HLHV was first observed in Hibiscus spp. cultivars in Hawaii, United States, in 2020 (Wang et al., 2023). Genetic sequencing revealed highest genetic similarity with Hibiscus latent Fort Pierce virus – Japan isolate (~68.1% pairwise identity of nucleotides over the whole genome). Because this virus shares less than 90% of its genomic identity with other tobamoviruses, the name Hibiscus latent Hawaii virus was proposed. Inoculation experiments, where hosts were exposed to numerous different viruses to evaluate infection potential revealed that HLHV could also infect Nicotiana benthamiana (Wang et al., 2023). HLHV is believed to cause mild mosaic, ringspot, and chlorosis, although this is unverified, as HLHV typically appears alongside other viruses infecting Hibiscus spp. cultivars. Insufficient information on this virus is currently available and it is therefore impossible to accurately determine if it could be used as an

environmental/fecal biomarker in WEM initiatives. Further environmental surveillance in wastewaters and foodstuffs would be required to determine the distribution of the virus.

6.47. Plantago tobamovirus 1 (PTV1)

PTV1 was first observed in Plantago major cultivars in Slovenia in 2019 (Rivarez et al., 2023). This novel tobamovirus was discovered during a high-throughput-sequencing (HTS) survey study of cultivars in Slovenia. PTV1 has the highest genetic similarity with Ribgrass mosaic virus and Turnip vein-clearing virus (~85.7 and 85.3% pairwise identity of nucleotides over the whole genome, respectively). Because this novel virus shares less than 90% of its genomic identity with other existing tobamoviruses, the name Plantago tobamovirus 1 was proposed. Inoculation experiments demonstrated that PTV1 could cause symptomatic infections in Nicotiana benthamiana and Nicotiana clevelandii, and asymptomatic infections in Lycopersicon esculentum cultivars (Rivarez et al., 2023). Due to PTV1's ability to asymptomatically infect Lycopersicon esculentum cultivars, it is plausible that PTV1 could be relevant as an environmental/fecal biomarker in WEM initiatives.

6.48. Trichosanthes mottle mosaic virus (TrMMV)

TrMMV was first observed in Trichosanthes kirilowii cultivars in China in 2021 (C. Chen et al., 2022). Genomic sequencing of the new virus revealed highest genetic similarity with Zucchini green mottle mosaic virus (~87.8% pairwise identity of nucleotides over the whole genome). Because this novel virus shares less than 90% of its genomic identity with other existing tobamoviruses, the name Trichosanthes mottle mosaic virus was proposed. It was demonstrated that in addition to infecting Trichosanthes kirilowii cultivars, TrMMV was also capable of infecting Nicotiana benthamiana and the following cucurbis: Cucumis sativus, Cucumis melo, Cucumis pepo, Citrulus lanatus and Luffa aegyptiaca. TrMMV was observed to cause mottling and mosaic symptoms in infected cultivars (C. Chen et al., 2022). Due to the relatively wide host range of readily consumable cultivars, it is possible that TrMMV could have relevance as an environmental/fecal biomarker in WEM initiatives.

Table 6-1:This table categorizes 43 t*obamoviruses* based on their likelihood (L = Likely, P = Possible, U = Unlikely) of use and current status (NIU = Not In Use, AIU = Already In Use) in WEM applications, with annotations on their suitability. This table also provides the GenBank accession numbers of *tobamoviruses* which were studied.

Virus		**Usability as a WEM fecal biomarker**		**Usage notes**
	NCBI GenBank accession number	Possible to use? **L** – likely **P** – possible **U** – unlikely	Has it been used? **Y** – Yes **N** – No	
Tobacco mosaic virus*	NC_001367	L	Y	Virus has exceptionally wide host range and infected cultivars likely to be consumed.
Pepper mild mottle virus*	NC_003630	L	Y	Infected fruit products are common. Most common *tobamovirus* in WES.
Tomato brown rugose fruit virus*	NC_028478	L	Y	Virus has very common host range and infected cultivars likely to be consumed.
Cucumber green mottle mosaic virus*	NC_001801	L	Y	Virus causes very few symptoms to fruits, likely to be consumed.
Cactus mild mottle virus*	NC_011803	L	N	Limited reach as cacti as a food item is limited.
Paprika mild mottle virus*	NC_004106	L	N	Virus causes few symptoms and fruits are likely to be consumed.
Streptocarpus flower break virus*	NC_008365	L	N	Virus causes latent infections and could be consumed unknowingly.
Tobacco mild green mosaic virus*	NC_001556	L	N	Virus has wide host range and infected cultivars likely to be consumed.
Youcai mosaic virus*	NC_004422	L	N	Virus' host is one of the most common sources of cooking oil.
Bell pepper mottle virus*	NC_009642	P	N	Infections cause high mortality in cultivars.
Opuntia chlorotic ringspot virus*	NC_040685	P	N	Virus has few hosts and is unclear how it is consumed.
Rattail cactus necrosis-associated virus*	NC_016442	P	N	Virus can cause some asymptomatic infections in consumed cultivars.
Clitoria yellow mottle virus	NC_016519	P	N	Virus mostly constrained to ornamental plants
Cucumber mottle virus	NC_008614	P	N	Virus causes very few symptoms to fruits, likely to be consumed.
Hibiscus latent Fort Pierce virus	NC_025381	P	N	Virus has multiple potential hosts and produces few symptoms. Likely to be consumed.
Hibiscus latent Singapore virus	NC_008310	P	N	Virus has multiple potential hosts and produces few symptoms. Likely to be consumed.
Kyuri green mottle mosaic virus	NC_003610	P	N	Virus causes severe symptoms – likely to only be found in products with transformed fruits.
Maracuja mosaic virus	NC_008716	P	N	Virus causes few systemic infections, but has wide host range, Possible to be consumed.
Obuda pepper virus	NC_003852	P	N	Virus causes few systemic infections, but has wide host range. Possible to be consumed.
Passion fruit mosaic virus	NC_015552	P	N	Virus' hosts are regularly consumed, however symptoms of infection visible may limit ingestion.
Ribgrass mosaic virus	NC_002792	P	N	Virus has a very large host range. It is plausible that infected cultivars could be consumed.
Sunn-hemp mosaic virus	D84000	P	N	Virus has a very large host range and could possible be consumed unknowingly.
Tomato mosaic virus	NC_002692	P	N	Virus has exceptionally wide host range and infected cultivars likely to be consumed.
Tomato mottle mosaic virus	NC_022230	P	N	Virus has very large host range but infected cultivars are severely affected. Unlikely to be consumed.
Tropical soda apple mosaic virus	NC_030229	P	N	Virus has a very large host range. It is plausible that infected cultivars could be consumed.
Turnip vein-clearing virus	NC_001873	P	N	Virus has a large host range. It is plausible that infected cultivars could be consumed.
Ullucus mild mottle virus	*MH645158*†	P	N	Virus causes few symptoms and fruits are likely to be consumed.
Wasabi mottle virus	NC_003355	P	N	Virus has limited host range but affected cultivars may still be transformed and consumed.
Brugmansia latent virus	MK012556	U	N	Most susceptible cultivars are moderately-to-acutely toxic to humans.
Brugmansia mild mottle virus	NC_010944	U	N	Most susceptible cultivars are moderately-to-acutely toxic to humans.
Cucumber fruit mottle mosaic virus	NC_002633	U	N	Virus causes high crop damage and may be avoided in human foodstuffs by culling.
Frangipani mosaic virus	NC_014546	U	N	Most susceptible cultivars are not readily edible, and some are toxic to humans.
Hoya chlorotic spot virus	NC_034509	U	N	Virus mostly constrained to ornamental plants.
Odontoglossum ringspot virus	NC_001728	U	N	Very limited human consumption of cultivars of the *Orchidaceae* family.
Plumeria mosaic virus	NC_026816	U	N	Virus mostly constrained to ornamental plants but can asymptomatically infect *Capsicum annuum*.
Rehmannia mosaic virus	NC_009041	U	N	Virus has several possible hosts but infections cause severe symptoms. Unlikely to be consumed.
Tobacco latent virus	NC_038703	U	N	Causes some asymptomatic infections, but genome not fully sequenced and no RT-qPCR assays currently exist.
Yellow tailflower mild mottle virus	NC_022801	U	N	Infected cultivars are severely affected, and may be avoided in human foodstuffs.
Zucchini green mottle mosaic virus	NC_003878	U	N	Virus causes high crop damage and may be avoided in human foodstuffs by culling.
African eggplant-associated virus	OP729508.1	P	N	Recently described virus. Virus causes mild or asymptomatic infections. Closest genomically to PMMoV. Infected fruits may be consumed.
Hibiscus latent Hawaii virus	ON614664.1	U	N	Recently described virus. Limited information on the virus' host range is available. Causes mild symptoms. Infected fruits may be consumed.
Plantago *tobamovirus* 1	PRJNA772045	P	N	Recently described virus. Virus appears able to asymptomatically infect tomatoes, which may lead to human consumption.
Trichosanthes mottle mosaic virus	OL404963	P	N	Recently described virus. Virus appears to symptomatically infect cultivars of the *Cucurbit*

***** indicates that the virus has previously been identified in the human gut. / † the NCBI Genbank accession number is tentative because identification is not confirmed.

Table 6-2: Tobamoviruses proposed as fecal biomarkers for WEM, with feasibility, food system relevance, and key limitations for each.

Virus	Feasibility as Fecal Biomarker (Strengths & Weaknesses)	Geographic/Food System Relevance	Key Unknowns or Limitations
Tobacco mosaic virus	• TMV is highly stable in the environment, capable of surviving harsh conditions. • However, it is infrequently ingested by humans since it is not part of the regular diet. • As a result, detection in feces is rare and considered incidental, limiting its reliability as a biomarker.	• TMV is cultivated globally for tobacco production. • It is not a part of human diet but may contaminate crops. • Human exposure likely comes from indirect contact or tobacco use.	• Sparse data on TMV fecal detection. • May reflect incidental contamination rather than dietary intake. • Not reliable or consistent across populations.
Pepper mild mottle virus	• PMMoV is exceptionally stable and abundant in fecal samples, making it a strong candidate for monitoring. • It is consistently shed in high quantities following the consumption of pepper products. • While diet-dependent, its widespread presence in global cuisine minimizes variability.	• PMMoV is present in diverse global cuisines that use peppers. • Found in fresh, dried, and processed pepper products. • It is nearly universally ingested due to widespread use of Capsicum.	• PMMoV is well-studied with minimal limitations. • Some variability may occur with reduced pepper intake in specific diets. • Otherwise consistent across cultures and seasons.
Tomato brown rugose fruit virus	• ToBRFV has a robust structure and is increasingly detected in wastewater and fecal samples. • It has shown high concentrations in some regions, indicating strong potential as a biomarker. • However, as a recently discovered virus, more studies are needed to confirm its long-term reliability.	• ToBRFV is linked to tomato and pepper trade across many countries. • Exposure is more likely in regions that consume raw or lightly processed tomatoes and peppers. • Its prevalence is increasing globally due to agricultural spread.	• ToBRFV's reliability as a biomarker is still being validated. • Prevalence depends on agricultural outbreaks and contamination. • Long-term fecal shedding trends remain unclear.
Cucumber green mottle mosaic virus	• CGMMV is a highly stable virus capable of withstanding food processing and digestion. • It is detectable in human stool following raw consumption of cucurbit crops like cucumbers and melons. • Its utility may vary seasonally and with cultural dietary habits.	• CGMMV is found in cucurbit crops like cucumbers and melons worldwide. • Frequently consumed raw in salads and fresh dishes. • Its relevance depends on regional and seasonal dietary patterns.	• CGMMV may not be present outside cucurbit growing or consuming seasons. • Underrepresented in current wastewater studies. • Dietary influence can lead to inconsistent detection.
Cactus mild mottle virus	• CaMMV has been confirmed in the feces of individuals from cactus-consuming regions. • Its stable viral structure suggests potential as a niche biomarker. • However, its global relevance is limited due to restricted dietary exposure.	• CaMMV has dietary relevance primarily in cactus-consuming regions. • Found in cultures that eat prickly pear or cactus pads. • Limited to arid and semi-arid regions where such foods are consumed.	• CaMMV has limited detection studies and is mostly niche. • Relevance is constrained to specific populations and food habits. • Generalizability is limited outside cactus-consuming regions.
Paprika mild mottle virus	• PaMMV is structurally similar to PMMoV and is likely present in foods containing paprika or chili peppers. • Its presence in human feces is supported by emerging evidence. • Despite this, it remains less prevalent and less studied, warranting further investigation.	• PaMMV is most relevant in cuisines that use paprika and chili peppers. • Detected in spice-heavy diets particularly in Asia and parts of Europe. • May be found in sauces, powders, and processed pepper products.	• PaMMV is often overshadowed by PMMoV in detection efforts. • Difficult to distinguish without targeted assays. • Requires more prevalence and stability studies.
Streptocarpus flower break virus	• SFBV is a tobamovirus with a stable capsid, allowing it to survive digestion in theory. • However, it is not linked to human food systems and likely enters the gut incidentally. • As such, it has low feasibility as a consistent fecal biomarker.	• SFBV infects ornamental plants and is not associated with any food source. • Human exposure is likely environmental or incidental. • It is globally distributed in home gardening contexts	• SFBV's fecal presence is likely incidental or environmental. • No known dietary exposure route. • Lacks the consistency required for reliable monitoring.
Tobacco mild green mosaic virus	• TMGMV has been occasionally detected in feces, potentially due to indirect tobacco exposure. • While structurally stable, it is not commonly found in food products. • This limits its practicality as a routine biomarker.	• TMGMV is primarily linked to tobacco use or contamination. • Not a part of typical food systems. • Exposure may occur through indirect ingestion of residues.	• TMGMV is rarely detected in wastewater or stool. • Exposure sources are unclear and likely not dietary. • Insufficient evidence supports its use as a biomarker.
Youcai mosaic virus	• YoMV has demonstrated strong stability and has been found in individuals consuming Brassica-rich diets. • It may serve as a biomarker in populations with frequent intake of leafy greens. • However, its use remains regionally specific and underexplored.	• YoMV is found in Brassica vegetables common in Asian cuisine. • Linked to consumption of bok choy, mustard greens, and similar crops. • Geographically limited to regions with Brassica-rich diets.	• YoMV is geographically specific and not well-studied globally. • May be overlooked in fecal surveys without targeted detection. • More data are needed to confirm consistency across regions.

6.49. Remarks and conclusions on the use of tobamoviruses as human fecal biomarkers

Normalization is an essential component of pathogen wastewater surveillance programs. Evidence consistently supports the use of matrix-endogenous biomarkers over alternative methods such as flow measurement, pharmaceuticals, or wastewater constituents like ammonia, particularly for highly transmissible diseases (e.g., SARS-CoV-2, Influenza A & B, RSV, mpox, etc.). The use of highly persistent, high-concentration non-human pathogens such as tobamoviruses appears preferable for WEM applications instead of phage, bacteria, or non-human-specific biomarkers, which may be subject to poorly understood environmental, seasonal, or geographical dynamics. Even in the case of bacteria or phages strongly associated with human microbiomes, the risk of the biomarkers undergoing growth or multiplication during their hours- to day-long transit time in centralized wastewater conveyance systems risks muddying the signal and making interpretation of measured pathogen signals normalized by these sub-optimal biomarkers exceedingly difficult or even impossible.

While tobamoviruses are not without their flaws, until an alternative, globally validated normalization biomarker are identified and thoroughly investigated, PMMoV and TBRFV will continue to be major components of numerous impactful and influential wastewater surveillance programs throughout the world. Despite the extreme environmental robustness and resilience of tobamoviruses being an advantage in the WEM context, there have been some concerns concerning their usefulness as a pathogen surrogate in studies investigating the effectiveness of disinfection and sanitation performance, particularly for drinking water disinfection and wastewater treatment, as researchers have argued that tobamoviruses may in fact be more conserved and stable than any pathogenic virion of interest (Canh et al., 2022; Fauquet et al., 2005; Hill, 2023; Kuroda et al., 2015; Momba et al., 2019; Wang et al., 2022). Some evidence exists that tobamoviruses and PMMoV-associated RNA may survive free chlorine-based drinking water disinfection processes (Shirakawa et al., 2023; Shirasaki et al., 2020), however the measured concentrations are significantly lower than those measured in wastewaters (Canh et al., 2022). As a result, while it is possible that tobamoviruses may enter the human body via drinking water, unless the water consumed is raw (untreated), the ingested tobamovirus RNA will represent a negligeable contribution (<0.1 – 0.5%) of the measured viral concentration in wastewaters. However, if raw water that has been agriculturally impacted was the only available drinking water source (either surface water or groundwater), it's possible that tobamovirus RNA or full virions could be ingested, leading to larger contribution to the measured viral concentration in wastewaters (Canh et al., 2019; Sassi et al., 2018). Additionally, it's important to note that due to the robustness and survival of PMMoV RNA to wastewater treatment, tobamoviruses in general are likely to be poor choices as human-associated biomarkers in any WEM program investigating pathogenic bacteria or viruses because of the ubiquitous nature of tobamoviruses in the natural environment (Haramoto

et al., 2013; Rosario et al., 2009c), breaking any link to human-associated shedding of DNA or RNA corresponding to pathogenic bacteria or viruses.

Of the surveyed tobamoviruses, a total of four (TMV, PMMoV, TBRFV and CGMMV) have documented uses as environmental and fecal biomarkers. However, the potential of other tobamovirus targets, primarily identified through their presence in human feces and wastewater is high. Based on the findings, it is highly recommended that future research be performed on the following 11 tobamoviruses to systematically establish their global prevalence in wastewater streams to adequately evaluate their potential use as environmental and fecal biomarkers: TMV, PMMoV, TBRFV, CGMMV, CMMoV, PMMV, SFBV, TMGMV, BPMM, YMoV and RCNaV. It is also possible that a new, specially designed RT-qPCR probe-based assay with degenerate bases in the forward and reverse primers, focusing on the tobamoviruses of interest (as identified by their presence in human feces) may also improve the seasonal and geographical stability and overall prevalence of tobamoviruses as human-associated normalization biomarkers for WEM applications. Of the 15 tobamoviruses identified as potentially useful as environmental and fecal biomarkers, two key characteristics permeate: i) the viruses must cause mild or asymptomatic infections in cultivars to avoid culling or causing too much damage to the cultivars to limit its consumption, and ii) the viruses must infect cultivars which are of nutritional and/or economic value and have a significant role in human consumption. Future research efforts should be aimed at better understanding the seasonality and geographic distribution of tobamoviruses of interest as potential environmental and fecal biomarkers. Studies investigating the distribution of different tobamoviruses in stool should also be performed to better grasp the global distribution of tobamoviruses in foodstuffs, as limited studies exist on this topic. This would in turn help further elucidate if the presence of certain tobamoviruses are biased towards a smaller subset of the population due to its presence in a limited number of high-titer foodstuffs attributable to a specific cultural group or restricted food distribution network, or instead if they are representative of the population at large, characterized by an abundance of diverse, widely-available commercial foodstuffs.

6.50. Limitations and 2025 field updates

This chapter presents a scoping review of tobamoviruses and their potential role as human-associated fecal biomarkers for use as WEM normalization. Since the time of writing, a few limitations were identified: 1) The ICTV has recently voted to rename all species within the tobamovirus genus to standardize the naming convention, which means all names used in the review are now the “old” names; and 2) It’s very likely that new tobamoviruses will be discovered, described and formally identified, which will impact the timeliness of this review over time.

6.51. Declaration of competing interests

The authors declare that no known competing financial interests or personal relationships influenced the work reported in this manuscript.

6.52. Ethical considerations

This study did not involve human participants or animals and did not require ethical approval.

6.53. Funding

This research was supported by the Province of Ontario's Wastewater Surveillance Initiative (WSI).

6.54. Acknowledgments

The authors have no additional acknowledgements to declare.

6.55. References

Adams, M.J., Adkins, S., Bragard, C., Gilmer, D., Li, D., MacFarlane, S.A., Wong, S.M., Melcher, U., Ratti, C., Ryu, K.H., 2017. ICTV virus taxonomy profile: Virgaviridae. J. Gen. Virol. 98, 1999–2000. https://doi.org/10.1099/JGV.0.000884

Adkins, S., D'Elia, T., Fillmer, K., Pongam, P., Baker, C.A., 2018. Biological and genomic characterization of a novel tobamovirus infecting hoya spp. Plant Dis. 102, 2571–2577. https://doi.org/10.1094/pdis-04-18-0667-re

Adkins, S., Kamenova, I., Achor, D., Lewandowski, D.J., 2003. Biological and Molecular Characterization of a Novel Tobamovirus with a Unique Host Range. Plant Dis. 87, 1190–1196. https://doi.org/10.1094/PDIS.2003.87.10.1190

Adkins, S., Kamenova, I., Rosskopf, E.N., Lewandowski, D.J., 2007. Identification and characterization of a novel tobamovirus from tropical soda apple in Florida. Plant Dis. 91, 287–293. https://doi.org/10.1094/PDIS-91-3-0287

Aguado-García, Y., Taboada, B., Morán, P., Rivera-Gutiérrez, X., Serrano-Vázquez, A., Iša, P., Rojas-Velázquez, L., Pérez-Juárez, H., López, S., Torres, J., Ximénez, C., Arias, C.F., 2020. Tobamoviruses can be frequently present in the oropharynx and gut of infants during their first year of life. Sci. Rep. 10, 1–11. https://doi.org/10.1038/s41598-020-70684-w

Aguilar, I., Sanchez, F., Martin, A.M., Martinez-Herrera, D., Ponz, F., 1996. Nucleotide sequence of Chinese rape mosaic virus (oilseed rape mosaic virus), a crucifer tobamovirus infectious on Arabidopsis thaliana. Plant Mol. Biol. 30, 191–197. https://doi.org/10.1007/BF00017814

Ainsworth, G.C., 1935. Mosaic Diseases of the Cucumber. Ann. Appl. Biol. 22, 55–67. https://doi.org/10.1111/j.1744-7348.1935.tb07708.x

Algradi, A.M., Liu, Y., Yang, B.Y., Kuang, H.X., 2021. Review on the genus Brugmansia: Traditional usage, phytochemistry, pharmacology, and toxicity. J. Ethnopharmacol. 279, 113910. https://doi.org/10.1016/j.jep.2021.113910

Allard, H.A., 1916. The mosaic disease of tomatoes and petunias. Phytopathology 6, 328–335.

Alonso, E., Garcia-Luque, I., de la Cruz, A., Wicke, B., Avila-Rincon, M.J., Serra, M.T., Castresana, C., Diaz-Ruiz, J.R., 1991. Nucleotide sequence of the genomic RNA of pepper mild mottle virus, a resistance-breaking tobamovirus in pepper. J. Gen. Virol. 72, 2875–2884. https://doi.org/10.1099/0022-1317-72-12-2875

Antignus, Y., Wang, Y., Pearlsman, M., Lachman, O., Lavi, N., Gal-On, A., 2001. Biological and molecular characterization of a new cucurbit-infecting Tobamovirus. Phytopathology 91, 565–571. https://doi.org/10.1094/PHYTO.2001.91.6.565

Bačnik, K., Kutnjak, D., Pecman, A., Mehle, N., Tušek Žnidarič, M., Gutiérrez Aguirre, I., Ravnikar, M., 2020. Viromics and infectivity analysis reveal the release of infective plant viruses from wastewater into the environment. Water Res. 177. https://doi.org/10.1016/j.watres.2020.115628

Bald, J.G., Solberg, R.A., 1961. Apparent Release of Tobacco Mosaic Virus in Living Infected Cells. Nature 190, 651–652. https://doi.org/10.1038/190651a0

Balique, F., Lecoq, H., Raoult, D., Colson, P., 2015. Can plant viruses cross the kingdom border and be pathogenic to humans? Viruses 7, 2074–2098. https://doi.org/10.3390/v7042074

Been, F., Rossi, L., Ort, C., Rudaz, S., Delémont, O., Esseiva, P., 2014. Population normalization with ammonium in wastewater-based epidemiology: Application to illicit drug monitoring. Environ. Sci. Technol. 48, 8162–8169. https://doi.org/10.1021/es5008388

Beijerinck, M.W., 1898. Over een contagium vivum fluidum als oorzaak van de vlekzickte der tabaksbladen. Versle. Gewone Vergad. Wis-Natuurkd. Afd. K. Akad. Wet. Amsterdam 7, 229–235.

Benchling, 2024. Benchling [Biology Software].

Bendahmane, M., Beachy, R.N., 1999. Control of tobamovirus infections via pathogen-derived resistance. Adv. Virus Res. 53, 369–386. https://doi.org/10.1016/s0065-3527(08)60357-7

Benschop, K.S.M., van der Avoort, H.G., Jusic, E., Vennema, H., van Binnendijk, R., Duizer, E., 2017. Polio and measles down the drain: Environmental enterovirus surveillance in the Netherlands, 2005 to 2015. Appl. Environ. Microbiol. 83, 1–12. https://doi.org/10.1128/AEM.00558-17

Bloomer, A.C., Champness, J.N., Bricogne, G., Staden, R., Klug, A., 1978. Protein disk of tobacco mosaic virus at 2.8 resolution showing the interactions within and between subunits. Nature 276, 362–368. https://doi.org/10.1038/276362a0

Bofill-Mas, S., Rusiñol, M., Fraile, J., Garrido, T., Munné, A., Girones, R., 2016. Specific viruses present in polluted groundwater are indicative of the source of nitrates and faecal contamination in agricultural areas. Exp. from Ground, Coast. Transitional Water Qual. Monit. EU Water Framew. Dir. Implement. Catalan River Basin Dist. (Part II) 1–24.

Bos, L., 1999. Beijerinck's work on tobacco mosaic virus: Historical context and legacy. Philos. Trans. R. Soc. B Biol. Sci. 354, 675–685. https://doi.org/10.1098/rstb.1999.0420

Brumfield, K.D., Leddy, M., Usmani, M., Cotruvo, J.A., Tien, C.T., Dorsey, S., Graubics, K., Fanelli, B., Zhou, I., Registe, N., Dadlani, M., Wimalarante, M., Jinasena, D., Abayagunawardena, R., Withanachchi, C., Huq, A., Jutla, A., Colwell, R.R., 2022. Microbiome Analysis for Wastewater Surveillance during COVID-19. MBio 13. https://doi.org/10.1128/mbio.00591-22

Brunt, A.A., Phillips, S., Jones, R.A.C., Kenten, R.H., 1982a. Viruses detected in Ullucus tuberosus (Basellaceae) from Peru and Bolivia. Ann. Appl. Biol. 101, 65–71. https://doi.org/10.1111/j.1744-7348.1982.tb00801.x

Brunt, A.A., Phillips, S., Jones, R.A.C., Kenten, R.H., 1982b. Viruses detected in Ullucus tuberosus (Basellaceae) from Peru and Bolivia. Ann. Appl. Biol. 101, 65–71. https://doi.org/10.1111/j.1744-7348.1982.tb00801.x

Canada Food Inspection Agency, 2020. Overview: Importing fresh fruit or vegetables [WWW Document]. Canada.ca. URL https://inspection.canada.ca/importing-food-plants-or-animals/food-

imports/food-specific-requirements/fresh-fruit-or-vegetables/eng/1541613882667/1541613882890 (accessed 2.28.24).

Canh, V.D., Furumai, H., Katayama, H., 2019. Removal of pepper mild mottle virus by full-scale microfiltration and slow sand filtration plants. npj Clean Water 2, 1–7. https://doi.org/10.1038/s41545-019-0042-1

Canh, V.D., Lien, N.T., Nga, T.T.V., 2022. Evaluation of the suitability of pepper mild mottle virus (PMMoV) as an indicator virus for water safety and quality. J. Sci. Technol. Civ. Eng. - HUCE 16, 76–88. https://doi.org/10.31814/stce.huce(nuce)2022-16(2)-07

Capoor, S.P., 1962. Southern Sunn Hemp mosaic virus: a strain of Tobacco mosaic virus.

Capoor, S.P., 1950. A mosaic disease of Sunn Hemp in Bombay. Curr. Sci. 19.

Capoor, S.P., Varma, P.M., 1948. Yellow mosaic of Phaseolus lunatus L. Curr. Sci. 17, 152–153 pp.

Capoor, S.P., Varma, P.M., Uppal, B.N., 1947. A mosaic disease of Vigna catjang Walp. Curr. Sci. 16, 151.

Castello, J.D., Lakshman, D.K., Tavantzis, S.M., Rogers, S.O., Bachand, G.D., Jagels, R., Carlisle, J., Liu, Y., 1995. Detection of infectious tomato mosaic tobamovirus in fog and clouds. Phytopathology. https://doi.org/10.1094/Phyto-85-1409

Castiglioni, S., Bijlsma, L., Covaci, A., Emke, E., Hernández, F., Reid, M., Ort, C., Thomas, K. V., Van Nuijs, A.L.N., De Voogt, P., Zuccato, E., 2013. Evaluation of uncertainties associated with the determination of community drug use through the measurement of sewage drug biomarkers. Environ. Sci. Technol. 47, 1452–1460. https://doi.org/10.1021/es302722f

Chai, A.L., Chen, L.D., Li, B.J., Xie, X.W., Shi, Y.X., 2018. First report of a mixed infection of Tomato mottle mosaic virus and Tobacco mild green mosaic virus on eggplants in China. Plant Dis. 102, 2668.

Charudattan, R., Hiebert, E., Pettersen, M.S., Horrell, J.R., Elliott, M.S., DeValerio, J.T., Maia, G.S., de Oliveira, T.B.C.B., 2024. Host-virus interaction between tobacco mild green mosaic virus strain U2 and tropical soda apple resulting in systemic hypersensitive necrosis and the host range, survival, spread, and molecular characterization of the virus. Pest Manag. Sci. 80, 176–191. https://doi.org/10.1002/ps.7802

Chavan, R.R., Cohen, D., Blouin, A.G., Pearson, M.N., 2012. Characterization of the complete genome of ribgrass mosaic virus isolated from Plantago major L. from New Zealand and Actinidia spp. from China. Arch. Virol. 157, 1253–1260. https://doi.org/10.1007/s00705-012-1292-0

Chen, C., Du, M., Peng, D., Li, W., Xu, J., Yang, X., Zhou, X., 2022. A Distinct Tobamovirus Associated With Trichosanthes kirilowii Mottle Mosaic Disease. Front. Microbiol. 13, 1–11. https://doi.org/10.3389/fmicb.2022.927230

Chen, J., Feng, C., Guo, X., Zhou, Y., Gu, T., Zhuang, X., Cheng, L., Zhang, K., 2022. Development of polyclonal antibodies-based serological methods for detection of the rehmannia mosaic virus in field plants. Front. Sustain. Food Syst. 6. https://doi.org/10.3389/fsufs.2022.1013470

Chessin, M., Juretiž, N., Miličić, D., Perryman, J., Giri, L., 1980. A Distinctive Strain of Ribgrass Mosaic Virus from Montana, USA. J. Phytopathol. 97, 295–301. https://doi.org/10.1111/j.1439-0434.1980.tb03698.x

Chettleburgh, C., Ma, S.X., Swinwood-Sky, M., McDougall, H., Kireina, D., Taggar, G., McBean, E., Parreira, V., Goodridge, L., Habash, M., 2023. Evaluation of four human-associated fecal biomarkers in wastewater in Southern Ontario. Sci. Total Environ. 904, 166542. https://doi.org/10.1016/j.scitotenv.2023.166542

Choi, B.C.K., 2012. The Past, Present, and Future of Public Health Surveillance. Scientifica (Cairo). 2012, 1–26. https://doi.org/10.6064/2012/875253

Choi, G.-S., Kim, J.-H., Ryu, K.-H., Choi, J.-K., Chae, S.-Y., Kim, J.-S., Chung, B.-N., Kim, H.-R., Choi, Y.-M., 2002. First Report of Tobacco mild green mosaic virus Infecting Pepper in Korea. Plant Pathol. J. 18, 323–327. https://doi.org/10.5423/PPJ.2002.18.6.323

Clinton, G.P., 1909. Tomato calico, lima bean, string bean, and muskmelon chlorosis: peach yellows, tobacco and tomato mosaic. Annu. Rep. Connect. Agric. Exp. Stn. 8.

Colson, P., Richet, H., Desnues, C., Balique, F., Moal, V., Grob, J.J., Berbis, P., Lecoq, H., Harlé, J.R., Berland, Y., Raoult, D., 2010. Pepper mild mottle virus, a plant virus associated with specific immune responses, fever, abdominal pains, and pruritus in humans. PLoS One 5, 1–12. https://doi.org/10.1371/JOURNAL.PONE.0010041

Csilléry, G., Ruskó, J., 1980. The control of a new Tobamovirus strain by a resistance linked to anthocyanin deficiency in pepper (Capsicum Annuum). Synopses IVth Meet. Eucarpia Capsicum Work. Group, Wageningen 40–43.

Csilléry, G., Tobias, I., Rusko, J., 1983. A new pepper strain of tomato mosaic virus. Acta Phytopathol. Acad. Sci. Hungaricae 18, 195–200.

D'Aoust, P.M., Mercier, É., Montpetit, D., Jia, J., Alexandrov, I., Neault, N., Baig, A.T., Mayne, J., Zhang, X., Alain, T., Langlois, M.-A., Servos, M.R., MacKenzie, M., Figeys, D., MacKenzie, A.E., Graber, T.E., Delatolla, R., 2021. Quantitative analysis of SARS-CoV-2 RNA from wastewater solids in communities with low COVID-19 incidence and prevalence. Water Res. 188, 116560. https://doi.org/10.1016/j.watres.2020.116560

Daryono, B.S., Somowiyarjo, S., Natsuaki, K.T., 2005. Biological and molecular characterization of melon-infecting kyuri green mottle mosaic virus in Indonesia. J. Phytopathol. 153, 588–595. https://doi.org/10.1111/j.1439-0434.2005.01024.x

Daughton, C.G., 2018. Monitoring wastewater for assessing community health: Sewage Chemical-Information Mining (SCIM). Sci. Total Environ. 619–620, 748–764. https://doi.org/10.1016/j.scitotenv.2017.11.102

Deb, L., Dutta, P., Gogoi, J., 2023. Diseases of Sunn hemp (Crotalaria juncea L.) and their Integrated Management. Dis. Commer. Crop. THeir Integr. Manag. 130–146. https://doi.org/10.1201/9781032627908-11

Dombrovsky, A., Tran-Nguyen, L.T.T., Jones, R.A.C., 2017. Cucumber green mottle mosaic virus: Rapidly Increasing Global Distribution, Etiology, Epidemiology, and Management. Annu. Rev. Phytopathol. 55, 231–256. https://doi.org/10.1146/annurev-phyto-080516-035349

Dong, J.L., Li, Y., Ding, W.L., Wang, R., 2017. First report of broad bean wilt virus 2 and Youcai mosaic virus infecting woolly foxglove (Digitalis lanata). J. Plant Pathol. 99.

Edwardson, J.R., Zettler, F.W., 1986. Odontoglossum Ringspot Virus. Plant Viruses 233–247. https://doi.org/10.1007/978-1-4684-7026-0_12

Fauquet, C.M., Mayo, M.A., Maniloff, J., Desselberger, U., Ball, L.A., 2005. Virus taxonomy: VIIIth report of the International Committee on Taxonomy of Viruses. Academic Press.

Feldman, J.M., Oremianer, S., 1972. An Unusual Strain of Tobacco mosaic virus from Pepper. J. Phytopathol. 75, 250–267. https://doi.org/10.1111/j.1439-0434.1972.tb02622.x

Feng, L., Zhang, W., Li, X., 2018. Monitoring of regional drug abuse through wastewater-based epidemiology—A critical review. Sci. China Earth Sci. 61, 239–255. https://doi.org/10.1007/s11430-017-9129-x

Feng, S., Roguet, A., McClary-Gutierrez, J.S., Newton, R.J., Kloczko, N., Meiman, J.G., McLellan, S.L., 2021. Evaluation of Sampling, Analysis, and Normalization Methods for SARS-CoV-2 Concentrations in Wastewater to Assess COVID-19 Burdens in Wisconsin Communities. ACS ES&T Water 1, 1955–1965. https://doi.org/10.1021/acsestwater.1c00160

Fillhart, R.C., Bachand, G.D., Castello, J.D., 1998. Detection of infectious tobamoviruses in forest soils. Appl. Environ. Microbiol. 64, 1430–1435. https://doi.org/10.1128/aem.64.4.1430-1435.1998

Fillhart, R.C., Bachand, G.D., Castello, J.D., 1997. Airborne transmission of tomato mosaic Tobamovirus and its occurrence in red spruce in the northeastern United States. Can. J. For. Res. 27, 1176–1181. https://doi.org/10.1139/x97-035

Fillmer, K., Adkins, S., Pongam, P., D'Elia, T., 2016. The complete nucleotide sequence and genomic characterization of tropical soda apple mosaic virus. Arch. Virol. 161, 2317–2320. https://doi.org/10.1007/s00705-016-2888-6

Francki, R.I.B., Hu, J., Palukaitis, P., 1986. Taxonomy of Cucurbit-Infecting Tobamoviruses as Determined by Serological and Molecular Hybridization Analyses. Intervirology 26, 156–163. https://doi.org/10.1159/000149695

Francki, R.I.B., Zaitlin, M., Grivell, C.J., 1971a. An unusual strain of tobacco mosaic virus from plumeria acutifolia. Aust. J. Biol. Sci. 24, 811–814. https://doi.org/10.1071/BI9710815

Francki, R.I.B., Zaitlin, M., Grivell, C.J., 1971b. An unusual strain of tobacco mosaic virus from plull1eria acutifolia. Aust. J. Biol. Sci. 24, 811–814. https://doi.org/10.1071/BI9710815

Fribourg, C.E., Koenig, R., Lesemann, D.E., 1987. A new tobamovirus from Passiflora edulis in Peru. Phytopathology 77, 486–491.

García-Arenal, F., 1988. Sequence and structure at the genome 3′ end of the U2-strain of tobacco mosaic virus, a histidine-accepting tobamovirus. Virology 167, 201–206. https://doi.org/10.1016/0042-6822(88)90070-0

García-Luque, I., Ferrero, M.L., Rodríguez, J.M., Alonso, E., de la Cruz, A., Sanz, A.I., Vaquero, C., Serra, M.T., Díaz-Ruíz, J.R., 1993. The nucleotide sequence of the coat protein genes and 3′ non-coding regions of two resistance-breaking tobamoviruses in pepper shows that they are different viruses. Arch. Virol. 131, 75–88. https://doi.org/10.1007/BF01379081

Gibbs, A., 1999. Evolution and origins of tobamoviruses. Philos. Trans. R. Soc. B Biol. Sci. 354, 593–602. https://doi.org/10.1098/rstb.1999.0411

Gibbs, A., 1986. The Plant Viruses, 1st ed. Springer US, Boston, MA. https://doi.org/10.1007/978-1-4684-7026-0

Gibbs, A.J., Harrison, B.D., Murant, A.F., 1970. CMI/AAB Descriptions of plant viruses. Commonwealth Mycological Institute and the Association of Applied Biologists.

Giesbers, A.K.J., Roenhorst, A., Schenk, M.F., Westenberg, M., Botermans, M., 2023. African eggplant-associated virus: Characterization of a novel tobamovirus identified from Solanum macrocarpon and assessment of its potential impact on tomato and pepper crops. PLoS One 18, 1–13. https://doi.org/10.1371/journal.pone.0277840

González-Mariño, I., Baz-Lomba, J.A., Alygizakis, N.A., Andrés-Costa, M.J., Bade, R., Bannwarth, A., Barron, L.P., Been, F., Benaglia, L., Berset, J.D., Bijlsma, L., Bodík, I., Brenner, A., Brock, A.L., Burgard, D.A., Castrignanò, E., Celma, A., Christophoridis, C.E., Covaci, A., Delémont, O., Devoogt, P., Devault, D.A., Dias, M.J., Emke, E., Esseiva, P., Fatta-Kassinos, D., Fedorova, G., Fytianos, K., Gerber, C., Grabic, R., Gracia-Lor, E., Grüner, S., Gunnar, T., Hapeshi, E., Heath, E., Helm, B., Hernández, F., Kankaanpaa, A., Karolak, S., Kasprzyk-Hordern, B., Krizman-Matasic, I., Lai, F.Y., Lechowicz, W., Lopes, A., de Alda, M.L., López-García, E., Löve, A.S.C., Mastroianni, N., McEneff, G.L., Montes, R., Munro, K., Nefau, T., Oberacher, H., O'brien, J.W., Oertel, R., Olafsdottir, K., Picó, Y., Plósz, B.G., Polesel, F., Postigo, C., Quintana, J.B., Ramin, P., Reid, M.J., Rice, J., Rodil, R., Salgueiro-Gonzàlez, N., Schubert, S., Senta, I., Simões, S.M., Sremacki, M.M., Styszko, K., Terzic, S., Thomaidis, N.S., Thomas, K. V., Tscharke, B.J., Udrisard, R., van Nuijs, A.L.N., Yargeau, V., Zuccato, E., Castiglioni, S., Ort, C., 2020. Spatio-temporal assessment of illicit drug use at large scale: evidence from 7 years of international wastewater monitoring. Addiction 115, 109–120. https://doi.org/10.1111/add.14767

Gracia-Lor, E., Castiglioni, S., Bade, R., Been, F., Castrignanò, E., Covaci, A., González-Mariño, I., Hapeshi, E., Kasprzyk-Hordern, B., Kinyua, J., Lai, F.Y., Letzel, T., Lopardo, L., Meyer, M.R., O'Brien, J., Ramin, P., Rousis, N.I., Rydevik, A., Ryu, Y., Santos, M.M., Senta, I., Thomaidis, N.S., Veloutsou, S., Yang, Z., Zuccato, E., Bijlsma, L., 2017. Measuring biomarkers in wastewater as a new source of epidemiological information: Current state and future perspectives. Environ. Int. 99, 131–150. https://doi.org/10.1016/j.envint.2016.12.016

Gracia, O., Feldman, J.M., Pontis, R.E., Boninsegna, J., 1968. Some viruses affecting tomatoes and peppers in Argentina. Plant Dis. Report. 52, 674–677.

Graham, K.E., Loeb, S.K., Wolfe, M.K., Catoe, D., Sinnott-Armstrong, N., Kim, S., Yamahara, K.M., Sassoubre, L.M., Mendoza Grijalva, L.M., Roldan-Hernandez, L., Langenfeld, K., Wigginton, K.R., Boehm, A.B., 2021. SARS-CoV-2 RNA in Wastewater Settled Solids Is Associated with COVID-19 Cases in a Large Urban Sewershed. Environ. Sci. Technol. 55, 488–498. https://doi.org/10.1021/acs.est.0c06191

Grant, T.J., 1934. The host range and behavior of the ordinary Tobacco-mosaic virus. Phytopathology 24, 331–330 pp.

Greenleaf, W.H., Cook, A.A., Heyn, A.N.J., 1964. Resistance to Tobacco mosaic virus in Capsicum, with reference to the Samsun latent strain. Phytopathology 54, 1367–1371.

Gu, T., Feng, C., Hua, Y., Liu, D., Chen, H., He, Z., Xu, K., Zhang, K., 2024. Molecular Characterization and Pathogenicity of an Infectious cDNA Clone of Youcai Mosaic Virus on Solanum nigrum. Int. J. Mol. Sci. 25. https://doi.org/10.3390/ijms25031620

Gushgari, A.J., Driver, E.M., Steele, J.C., Halden, R.U., 2018. Tracking narcotics consumption at a Southwestern U.S. university campus by wastewater-based epidemiology. J. Hazard. Mater. 359, 437–444. https://doi.org/10.1016/j.jhazmat.2018.07.073

Hamada, Hiroyuki, Takeuchi, Shigeharu, Morita, Yasuaki, Sawada, H., Kiba, A., Hikichi, Y., Hamada, H, Sawada, · H, Kiba, · A, Hikichi, · Y, Takeuchi, S, Morita, Y, 2003. Characterization of Paprika mild mottle virus first isolated in Japan. J Gen Plant Pathol 69, 199–204.

Hamza, I.A., Jurzik, L., Überla, K., Wilhelm, M., 2011. Evaluation of pepper mild mottle virus, human picobirnavirus and Torque teno virus as indicators of fecal contamination in river water. Water Res. 45, 1358–1368. https://doi.org/10.1016/j.watres.2010.10.021

Haňcinský, R., Mihálik, D., Mrkvová, M., Candresse, T., Glasa, M., 2020. Plant viruses infecting solanaceae family members in the cultivated and wild environments: A review. Plants 9. https://doi.org/10.3390/plants9050667

Haramoto, E., Kitajima, M., Kishida, N., Konno, Y., Katayama, H., Asami, M., Akiba, M., 2013. Occurrence of pepper mild mottle virus in drinking water sources in Japan. Appl. Environ. Microbiol. 79, 7413–7418. https://doi.org/10.1128/AEM.02354-13

Harrison, B.D., Finch, J.T., Gibbs, A.J., Hollings, M., Shepherd, R.J., Valenta, V., Wetter, C., 1971. Sixteen groups of plant viruses. Virology 45, 356–363. https://doi.org/10.1016/0042-6822(71)90336-9

Harzing, A.W., Publish or Perish (version 8.0) (2021), (available at https://harzing.com/blog/2021/10/publish-or-perish-version-8).

Hata, A., Hanamoto, S., Ihara, M., Shirasaka, Y., Yamashita, N., Tanaka, H., 2018. Comprehensive Study on Enteric Viruses and Indicators in Surface Water in Kyoto, Japan, During 2014–2015 Season. Food Environ. Virol. 10, 353–364. https://doi.org/10.1007/s12560-018-9355-3

Heinze, C., Lesemann, D.E., Ilmberger, N., Willingmann, P., Adam, G., 2006. The phylogenetic structure of the cluster of tobamovirus species serologically related to ribgrass mosaic virus (RMV) and the sequence of streptocarpus flower break virus (SFBV). Arch. Virol. 151, 763–774. https://doi.org/10.1007/s00705-005-0640-8

Hellmér, M., Paxéus, N., Magnius, L., Enache, L., Arnholm, B., Johansson, A., Bergström, T., Norder, H., 2014. Detection of pathogenic viruses in sewage provided early warnings of hepatitis A virus and norovirus outbreaks. Appl. Environ. Microbiol. 80, 6771–6781. https://doi.org/10.1128/AEM.01981-14

Herrera‐Vásquez, J.A., Córdoba‐Sellés, M.C., Cebrián, M.C., Alfaro‐Fernández, A., Jordá, C., 2009. First report of Pepper mild mottle virus and Tobacco mild green mosaic virus infecting pepper in Panama. Plant Pathol. 58, 786–786. https://doi.org/10.1111/j.1365-3059.2009.02030.x

Hilf, M.E., Dawson, W.O., 1993. The tobamovirus capsid protein functions as a host-specific determinant of long-distance movement. Virology 193, 106–114. https://doi.org/10.1006/viro.1993.1107

Hill, T., 2023. Virus Removal and Characterization During Secondary Treatment at a Full-Scale Plant.

Holmes, F.O., 1941. A distinctive strain of tobacco mosaic virus from Plantago. Phytopathology 31, 1089–1098.

Hsu, S.Y., Bayati, M., Li, C., Hsieh, H.Y., Belenchia, A., Klutts, J., Zemmer, S.A., Reynolds, M., Semkiw, E., Johnson, H.Y., Foley, T., Wieberg, C.G., Wenzel, J., Johnson, M.C., Lin, C.H., 2022. Biomarkers selection for population normalization in SARS-CoV-2 wastewater-based epidemiology. Water Res. 223, 118985. https://doi.org/10.1016/j.watres.2022.118985

Hu, J.S., Ferreira, S., Wang, M., Xu, M.Q., 1993. Detection of Cymbidium Mosaic Virus, Odontoglossum Ringspot Virus, Tomato Spotted Wilt Virus, and Potyviruses Infecting Orchids in Hawaii. Plant Dis. 77, 464–468.

Hu, J.S., Ferreira, S., Xu, M.Q., Lu, M., Iha, M., Pflum, E., Wang, M., 1994. Transmission, movement and inactivation of cymbidium mosaic and odontoglossum ringspot viruses. Plant Dis. 78, 633–636.

Hutchison, J.M., Li, Z., Chang, C.N., Hiripitiyage, Y., Wittman, M., Sturm, B.S.M., 2022. Improving correlation of wastewater SARS-CoV-2 gene copy numbers with COVID-19 public health cases using readily available biomarkers. FEMS Microbes 3, 1–8. https://doi.org/10.1093/femsmc/xtac010

Ikeda, R., Watanabe, E., Watanabe, Y., Okada, Y., 1993. Nucleotide sequence of tobamovirus Ob which can spread systemically in N gene tobacco. J. Gen. Virol. 74, 1939–1944. https://doi.org/10.1099/0022-1317-74-9-1939

Ilmberger, N., Willingmann, P., Adam, G., Heinze, C., 2007. A subgroup 1 Tobamovirus isolated from Brugmansia sp. and its detection by RT-PCR. J. Phytopathol. 155, 326–332. https://doi.org/10.1111/j.1439-0434.2007.01235.x

Inouye, N., Leu, L.S., 1983. Survey on the viruses in orchids in Taiwan. Nogaku Kenkyu (Japan) 60.

Inouye, T., Inouye, N., Asatani, M., Mitsuhata, K., 1967. Studies on cucumber green mottle mosaic virus in Japan. Nogaku Kenkyu 51, 175–186.

Isaksson, F., Lundy, L., Hedström, A., Székely, A.J., Mohamed, N., 2022. Evaluating the Use of Alternative Normalization Approaches on SARS-CoV-2 Concentrations in Wastewater: Experiences from Two Catchments in Northern Sweden. Environ. - MDPI 9. https://doi.org/10.3390/environments9030039

Ishii, M., Martinez, A.P., 1973. Significant orchid diseases in Hawaii. Hawaii Orchid J. 2, 6–10.

Ivanovsky, D.I., 1892. On two diseases of tobacco plants. Agric. For. CCIXX 104–121.

Izadpanah, K., Thompson, M.R., Thornberry, H.H., 1968. Orchid Virus: Characterization of a Type of Tobacco ‐ mosaic Virus isolated from Cattleya Plants with Infectious Blossom Necrosis. J. Phytopathol. 63, 272 ‐ 286. https://doi.org/10.1111/j.1439-0434.1968.tb02393.x

Jensen, D.D., 1970. Virus diseases of orchids in The Netherlands. Netherlands J. Plant Pathol. 76, 135–139. https://doi.org/10.1007/BF01974319

Jensen, D.D., 1951. Mosaic or black streak disease of Cymbidium Orchids. Phytopathology 41.

Jensen, D.D., 1949. Breaking of Cattleya Orchid flowers by Orchid mosaic virus and its transmission by aphids. Phytopathology 39.

Jensen, D.D., Gold, A.H., 1951. A virus ring spot of Odontoglossum Orchid: symptoms, transmission, and electron microscopy. Phytopathology 41, 648–653.

Johnson, J., 1947. Virus attenuation and the separation of strains by specific hosts. Phytopathology 37, 822–837.

Ju, Y.Y., Byoung, E.M., Jang, K.C., Ki, H.R., 2002. Genome structure and production of biologically active in vitro transcripts of cucurbit-infecting Zucchini green mottle mosaic virus. Phytopathology 92, 156–163. https://doi.org/10.1094/phyto.2002.92.2.156

Kado, C.I., van Regenmortel, M.H.V., Knight, C.A., 1968. Studies on some strains of tobacco mosaic virus in orchids. I. Biological, chemical, and serological studies. Virology 34, 17–24. https://doi.org/10.1016/0042-6822(68)90004-4

Kashiwazaki, S., Shimazu, K., Tsuchizaki, T., 1990. Serological properties of wasabi strain of tobacco mosaic virus. Japanese J. Phytopathol. 56, 257–260. https://doi.org/10.3186/jjphytopath.56.257

Kashiwazaki, S., Yamashita, S., Doi, Y., 1982. Two hibiscus viruses: hibiscus yellow mosaic virus and hibiscus chlorotic ringspot virus (in Japanese). Ann. Phytopath. Soc. Japan 48.

Kerchner, A., Farkas, Á., 2020a. Worldwide poisoning potential of Brugmansia and Datura. Forensic Toxicol. 38, 30–41. https://doi.org/10.1007/s11419-019-00500-2

Kerchner, A., Farkas, Á., 2020b. Worldwide poisoning potential of Brugmansia and Datura. Forensic Toxicol. 38, 30–41. https://doi.org/10.1007/s11419-019-00500-2

Kim, N.R., Hong, J.S., Song, Y.S., Chung, B.N., Park, J.W., Ryu, K.H., 2012. The complete genome sequence of a member of a new species of tobamovirus (rattail cactus necrosis-associated virus) isolated from Aporcactus flagelliformis. Arch. Virol. 157, 185–187. https://doi.org/10.1007/s00705-011-1142-5

Kitajima, M., Sassi, H.P., Torrey, J.R., 2018. Pepper mild mottle virus as a water quality indicator. npj Clean Water 1. https://doi.org/10.1038/s41545-018-0019-5

Knight, C.A., 1942. Effect of artificial light on the symptoms produced by two yellow mosaic viruses. Arch. Gesamte Virusforsch. 2, 260–267. https://doi.org/10.1007/BF01242576

Ko, N.J., 1982. Occurrence and diagnosis of Odontoglossum ringspot virus in Taiwan. Bull. Orchid Soc. Rep. China 5, 319.

Koenig, R., 1986. Plant viruses in rivers and lakes. Adv. Virus Res. 31, 321–333. https://doi.org/10.1016/S0065-3527(08)60267-5

Koh, S.H., Li, H., Sivasithamparam, K., Admiraal, R., Jones, M.G.K., Wylie, S.J., 2018. Low root-to-root transmission of a tobamovirus, yellow tailflower mild mottle virus, and resilience of its virions. Plant Pathol. 67, 651–659. https://doi.org/10.1111/ppa.12758

Köhler, E., Hauschild, I., 1947. Betrachtungen und Versuche zum Problem der "erworbenen Immumtät" gegen Virusinfektionem bei Pflanzen. Züchter 17–18, 97–105.

Kubota, K., Usugi, T., Tomitaka, Y., Matsushita, Y., Higashiyama, M., Kosaka, Y., Tsuda, S., 2012. Characterization of Rehmannia mosaic virus isolated from chili pepper (Capsicum annuum) in Japan. J. Gen. Plant Pathol. 78, 43–48. https://doi.org/10.1007/s10327-011-0345-7

Kumar, A., Abdul Kader Jailani, A., Roy, A., Mandal, B., 2017. The occurrence, biology and genomic properties of tobamoviruses infecting crop plants in India. A Century Plant Virol. India 429–444. https://doi.org/10.1007/978-981-10-5672-7_19

Kumar, A., Mandal, B., 2014. Plumeria mosaic virus isolate Plu-Ind-1, complete genome - Nucleotide - NCBI [WWW Document]. NCBI Genome Proj. - Direct Submiss. URL https://www.ncbi.nlm.nih.gov/nuccore/NC_026816.1 (accessed 3.27.24).

Kumar, A., Solanki, V., Katiyar, A., Mandal, B., 2022. Host biology and genomic properties of Plumeria mosaic virus, a tobamovirus discovered in a temple tree in India co-infecting with frangipani mosaic virus. Front. Microbiol. 13, 1–13. https://doi.org/10.3389/fmicb.2022.1030042

Kumar, A., Solanki, V., Mandal, B., 2013. Frangipani mosaic virus and Plumeria mosaic virus: identification and comparison of two tobamovirus infecting frangipani in India, in: International Conference of Indian Virological Society (IVS) Held at Amity University, Noida.

Kuroda, K., Nakada, N., Hanamoto, S., Inaba, M., Katayama, H., Do, A.T., Nga, T.T.V., Oguma, K., Hayashi, T., Takizawa, S., 2015. Pepper mild mottle virus as an indicator and a tracer of fecal pollution in water environments: Comparative evaluation with wastewater-tracer pharmaceuticals in Hanoi, Vietnam. Sci. Total Environ. 506–507, 287–298. https://doi.org/10.1016/j.scitotenv.2014.11.021

Kwon, S.-J., Kim, Y.-B., Back, C.-K., Chung, B.-N., 2017. First Report of a Mixed Infection of Youcai mosaic virus and Rehmannia mosaic virus in Rehmannia glutinosa in Korea. Plant Dis. 102, 462. https://doi.org/10.1094/PDIS-07-17-1128-PDN

Ladipo, J.L., Koenig, R., Lesemann, D.E., 2003. Nigerian tobacco latent virus: A new Tobamovirus from tobacco in Nigeria. Eur. J. Plant Pathol. 109, 373–379. https://doi.org/10.1023/A:1023557723943

Lanter, J.M., 1982. Persistence of Tomato Mosaic Virus in Tomato Debris and Soil Under Field Conditions. Plant Dis. 66, 552. https://doi.org/10.1094/PD-66-552

Lartey, R.., Hartson, S.., Pennington, R.., J.L, S., Melcher, U., 1993. Occurence of Vein clearing on Tabacco and Turnip. Plant Dis.

Lartey, R.T., Lane, L.C., Melcher, U., 1994. Electron microscopic and molecular characterization of turnip vein-clearing virus. Arch. Virol. 138, 287–298. https://doi.org/10.1007/BF01379132

Lartey, R.T., Voss, T.C., Melcher, U., 1995. Completion of a cDNA sequence from a tobamovirus pathogenic to crucifers. Gene 166, 331–332. https://doi.org/10.1016/0378-1119(95)00674-5

Lewandowski, D.J., Dawson, W.O., 2000. Functions of the 126- and 183-kDa proteins of tobacco mosaic virus. Virology 271, 90–98. https://doi.org/10.1006/viro.2000.0313

Li, H., Zhang, C., Luo, H., Jones, M.G.K., Sivasithamparam, K., Koh, S.H., Ong, J.W.L., Wylie, S.J., 2016. Yellow tailflower mild mottle virus and Pelargonium zonate spot virus co-infect a wild plant of red-striped tailflower in Australia. Plant Pathol. 65, 503–509. https://doi.org/10.1111/ppa.12416

Li, R., Gao, S., Fei, Z., Ling, K.-S., 2013. Complete Genome Sequence of a New Tobamovirus Naturally Infecting Tomatoes in Mexico. Genome Announc. 1, 2008–2010. https://doi.org/10.1128/genomeA.00794-13

Li, Y., Wang, Y., Hu, J., Xiao, L., Tan, G., Lan, P., Liu, Y., Li, F., 2017. The complete genome sequence, occurrence and host range of Tomato mottle mosaic virus Chinese isolate. Virol. J. 14, 1–9. https://doi.org/10.1186/s12985-016-0676-2

Li, Z., Yang, S., Qin, B., Xie, H., Cui, L., Su, Q., Cai, J., Gu, Q., 2018. First Report of Natural Infection of Zucchini Green Mottle Mosaic Virus on Bottle Gourd in Guangxi, China. Plant Dis. 102, 2384. https://doi.org/10.1094/PDIS-02-18-0341-PDN

Lim, M.A., Hong, J.S., Song, Y.S., Ryu, K.H., 2010. The complete genome sequence and genome structure of frangipani mosaic virus. Arch. Virol. 155, 1543–1546. https://doi.org/10.1007/s00705-010-0766-1

Lim, T.K., 2012. Edible Medicinal And Non-Medicinal Plants, Edible Medicinal and Non-Medicinal Plants: Volume 4, Fruits. Springer Netherlands, Dordrecht. https://doi.org/10.1007/978-94-007-4053-2

Lister, R.M., Thresh, J.M., 1955. A Mosaic Disease of Leguminous Plants caused by a Strain of Tobacco Mosaic Virus. Nature 175, 1047–1048. https://doi.org/10.1038/1751047a0

Liu, F.X., Han, Y.C., Li, W.D., Shi, X.Q., Xu, W., Lin, M.G., 2013. Incidence of Cymbidium mosaic virus and Odontoglossum ringspot virus affecting Oncidium orchids in Hainan Island, China. Crop Prot. 54, 176–180. https://doi.org/10.1016/j.cropro.2013.08.013

Liu, M., Lau, A.K., Lo, K. V., 1999. Ultrafiltration tests for the reutilization of greenhouse wastewater. J. Environ. Sci. Heal. - Part B Pestic. Food Contam. Agric. Wastes 34, 1101–1110. https://doi.org/10.1080/03601239909373247

Lockhart, B.E., Swenson, A.S., Olszewski, N.E., Voth, P., 2008. Characterization of a strain of Turnip vein-clearing virus causing red ringspot of penstemon. Plant Dis. 92, 725–729. https://doi.org/10.1094/PDIS-92-5-0725

Lopez-Roblero, A., Martínez Cano, D.J., Diego-García, E., Guillén-Navarro, G.K., Iša, P., Zarza, E., 2024. Metagenomic analysis of plant viruses in tropical fresh and wastewater. Environ. DNA 6, 1–13. https://doi.org/10.1002/edn3.416

Lorenzo, M., Picó, Y., 2019. Wastewater-based epidemiology: current status and future prospects. Curr. Opin. Environ. Sci. Heal. 9, 77–84. https://doi.org/10.1016/j.coesh.2019.05.007

Luria, N., Smith, E., Reingold, V., Bekelman, I., Lapidot, M., Levin, I., Elad, N., Tam, Y., Sela, N., Abu-Ras, A., Ezra, N., Haberman, A., Yitzhak, L., Lachman, O., Dombrovsky, A., 2017. A new israeli Tobamovirus isolate infects tomato plants harboring Tm-22 resistance genes. PLoS One 12, 1–19. https://doi.org/10.1371/journal.pone.0170429

Luria, N., Smith, E., Sela, N., Lachman, O., Bekelman, I., Koren, A., Dombrovsky, A., 2018. A local strain of Paprika mild mottle virus breaks L 3 resistance in peppers and is accelerated in Tomato brown rugose fruit virus-infected Tm-2 2-resistant tomatoes. Virus Genes 54, 280–289. https://doi.org/10.1007/s11262-018-1539-2

Lutgen, H., Olmedo-Velarde, A., Kong, A.T., Melzer, M.J., 2023. First Report of Plumeria Mosaic Virus Infecting Plumeria spp. in the United States. Plant Dis. 107, 1956. https://doi.org/10.1094/PDIS-09-22-2019-PDN

Maal-Bared, R., Qiu, Y., Li, Q., Gao, T., Hrudey, S.E., Bhavanam, S., Ruecker, N.J., Ellehoj, E., Lee, B.E., Pang, X., 2023. Does normalization of SARS-CoV-2 concentrations by Pepper Mild Mottle Virus improve correlations and lead time between wastewater surveillance and clinical data in Alberta (Canada): comparing twelve SARS-CoV-2 normalization approaches. Sci. Total Environ. 856, 158964. https://doi.org/10.1016/j.scitotenv.2022.158964

Magne, A., Gerard, D., Hirth, L., Laustriat, G., 1977. Fluorescence study of tobacco mosaic virus protein. BBA - Protein Struct. 495, 189–194. https://doi.org/10.1016/0005-2795(77)90375-0

Malla, B., Makise, K., Nakaya, K., Mochizuki, T., Yamada, T., Haramoto, E., 2019. Evaluation of Human- and Animal-Specific Viral Markers and Application of CrAssphage, Pepper Mild Mottle Virus, and Tobacco Mosaic Virus as Potential Fecal Pollution Markers to River Water in Japan. Food Environ. Virol. 11, 446–452. https://doi.org/10.1007/s12560-019-09398-w

Martelli, G.P., Quacquarelli, A., 1983. The present status of tomato and pepper viruses. Acta Hortic. 39–64. https://doi.org/10.17660/actahortic.1983.127.3

Mayer, A., 1886. Ueber die Mosaikkrankheit des Tabaks. Die Landwirtsch. Versuchs-Stationen 32, 451–467.

Mazumder, P., Dash, S., Honda, R., Sonne, C., Kumar, M., 2022. Sewage surveillance for SARS-CoV-2: Molecular detection, quantification, and normalization factors. Curr. Opin. Environ. Sci. Heal. 28, 100363. https://doi.org/10.1016/j.coesh.2022.100363

McCreight, J.D., 2017. Book: Genetics and Genomics of Cucurbitaceae.

McKinney, H H, 1952. Two strains of Tobacco-mosaic virus, one of which is seed-borne in an etch-immune pungent Pepper. Plant Dis. Report. 36.

McKinney, H. H., 1952. Two strains of tobacco-mosaic virus, one of which is seed-borne in an etch-immune pungent pepper. Plant Dis. Report. 36, 184–187.

McKinney, H.H., 1929. Mosaic diseases in the Canary Islands, West Africa and Gibraltar. J. Agric. Res. 39, 557–578.

Mehle, N., Ravnikar, M., 2012. Plant viruses in aqueous environment - Survival, water mediated transmission and detection. Water Res. 46, 4902–4917. https://doi.org/10.1016/j.watres.2012.07.027

Mercier, E., D'Aoust, P.M., Thakali, O., Hegazy, N., Jia, J.J., Zhang, Z., Eid, W., Plaza-Diaz, J., Kabir, M.P., Fang, W., Cowan, A., Stephenson, S.E., Pisharody, L., MacKenzie, A.E., Graber, T.E., Wan, S., Delatolla, R., 2022. Municipal and neighbourhood level wastewater surveillance and subtyping of an influenza virus outbreak. Sci. Rep. 12, 2022.06.28.22276884. https://doi.org/10.1038/s41598-022-20076-z

Metcalf, T.G., Melnick, J.L., Estes, M.K., 1995. Environmental virology: From detection of virus in sewage and water by isolation to identification by molecular biology - A trip of over 50 years. Annu. Rev. Microbiol. 49, 461–487. https://doi.org/10.1146/annurev.mi.49.100195.002333

Milbrath, G.M., 1971. Etiology and epidemiology of viruses of native cactus species in Arizona. University of Arizona.

Min, B.E., Chung, B.N., Kim, M.J., Ha, J.H., Lee, B.Y., Ryu, K.H., 2006. Cactus mild mottle virus is a new cactus-infecting tobamovirus. Arch. Virol. 151, 13–21. https://doi.org/10.1007/s00705-005-0617-7

Min, B.E., Song, Y.S., Ryu, K.H., 2009. Complete sequence and genome structure of cactus mild mottle virus. Arch. Virol. 154, 1371–1374. https://doi.org/10.1007/s00705-009-0435-4

Mise, K., Kamiya, H., Takano, Y., Fujita, Y., Kaido, M., Okuno, T., Furusawa, I., 1996. Sunn-hemp mosaic virus SH8TP2 RNA, complete genome - Nucleotide - NCBI [WWW Document]. NCBI Genome Proj. - Direct Submiss. URL https://www.ncbi.nlm.nih.gov/nuccore/D84000.1 (accessed 3.27.24).

Mizumoto, H., Morikawa, Y., Ishibashi, K., Kimura, K., Matsumoto, K., Tokunaga, M., Kiba, A., Ishikawa, M., Okuno, T., Hikichi, Y., 2014. Functional characterization of the mutations in Pepper mild mottle virus overcoming tomato tm-1 mediated resistance. Mol. Plant Pathol. 15, 479–487. https://doi.org/https://doi.org/10.1111/mpp.12107

Momba, M., Ebdon, J., Kamika, I., Verbyla, M., 2019. Using indicators to assess microbial treatment and disinfection efficacy, in: Farnleitner, A., Blanch, A. (Eds.), Water and Sanitation for the 21st Century: Health and Microbiological Aspects of Excreta and Wastewater Management (Global Water Pathogen Project). Michigan State University. https://doi.org/10.14321/waterpathogens.9

Murakishi, H.H., 1958. Host range, symptomatology, physical properties, and cross-protection studies of Orchid virus isolates. Serological and morphological relationships among Orchid viruses. Phytopathology 48.

Murcia Bermudez, J.M., Singh, N., Chamberland, M., Poudel-Ward, B., 2024. First Report of Rattail Cactus Necrosis-Associated Virus Infecting Prickly Pear (Opuntia macrocentra) in the United States. Plant Dis. 100, 2024. https://doi.org/10.1094/PDIS-07-23-1344-PDN

Nefzaoui, A., 2009. Cactus: A crop to meet the challenges of climate change in dry areas. Ann. Arid Zone 48, 1–18.

Offei, S.K., Ibidapo, O., Brunt, A.A., Coutts, R.H.A., 1995. Further evidence for the recognition of Ullucus Mild Mottle Virus as a Distinct Tobamovirus. J. Phytopathol. 143, 543–545. https://doi.org/10.1111/j.1439-0434.1995.tb00660.x

Ojinaga, M., Guirao, P., Larregla, S., 2022. A Survey of Main Pepper Crop Viruses in Different Cultivation Systems for the Selection of the Most Appropriate Resistance Genes in Sensitive Local Cultivars in Northern Spain. Plants 11. https://doi.org/10.3390/plants11060719

Okada, Y., 2000. Tobacco mosaic virus: pioneering research for a century. Tanpakushitsu Kakusan Koso. 45, 1757–1765. https://doi.org/10.2307/3870861

Ong, S.N., Taheri, S., Othman, R.Y., Teo, C.H., 2020. Viral disease of tomato crops (Solanum lycopesicum L.): an overview. J. Plant Dis. Prot. 127, 725–739. https://doi.org/10.1007/s41348-020-00330-0

Orita, H., Sakai, J.I., Kubota, K., Okuda, M., Tanaka, Y., Hanada, K., Imamura, Y., Nishiguchi, M., Karasev, A. V., Miyata, S.I., Iwanami, T., 2007. Molecular and serological characterization of cucumber mottle virus, a new cucurbit-infecting tobamo-like virus. Plant Dis. 91, 1574–1578. https://doi.org/10.1094/PDIS-91-12-1574

Oshima, N., Harrison, B.D., 1975. Ribgrass mosaic virus. C. Descr. plant viruses 152.

Pappu, H.R., Druffel, K.B., 2007. First Report of Streptocarpus flower break virus in Streptocarpus in the United States. Plant Dis. 91, 1361. https://doi.org/10.1094/PDIS-91-10-1361A

Pares, R.D., Gunn, L. V., Keskula, E.N., 1996. The role of infective plant debris, and its concentration in soil, in the ecology of tomato mosaic tobamovirus - A non-vectored plant virus. J. Phytopathol. 144, 147–150. https://doi.org/10.1111/j.1439-0434.1996.tb01505.x

Polo, D., Quintela-Baluja, M., Corbishley, A., Jones, D.L., Singer, A.C., Graham, D.W., Romalde, J.L., 2020. Making waves: Wastewater-based epidemiology for COVID-19 – approaches and challenges for surveillance and prediction. Water Res. 186, 116404. https://doi.org/10.1016/j.watres.2020.116404

Preissel, U., Preissel, H.-G., 2002. Brugmansia and datura : angel's trumpets and thorn apples, Firefly Gardener's Guide Series. Firefly Books.

Pruden, A., 2014. Balancing water sustainability and public health goals in the face of growing concerns about antibiotic resistance. Environ. Sci. Technol. 48, 5–14. https://doi.org/10.1021/es403883p

Ranjan, P., Ranjan, J.K., Misra, R.L., Dutta, M., Singh, B., 2016. Cacti: notes on their uses and potential for climate change mitigation. Genet. Resour. Crop Evol. 63, 901–917. https://doi.org/10.1007/s10722-016-0394-z

Rao, G.P., Reddy, M.G., 2020. Overview of yield losses due to plant viruses, Applied Plant Virology: Advances, Detection, and Antiviral Strategies. INC. https://doi.org/10.1016/B978-0-12-818654-1.00038-4

Rast, A.T.B., 1979. Mededelingen van de Faculteit Landbouwwetenschappen, Rijksuniversiteit Gent. Rijkuniversitet te Gent.

Raychaudhuri, S.P., Pathanian, P.S., 1950. A mosaic disease of Crotalaria mucronata Desv.(C. striata DC.). Curr. Sci. 19.

Rhee, S.J., Hong, J.S., Lee, G.P., 2014. Infectivity and complete nucleotide sequence of cucumber fruit mottle mosaic virus isolate Cm cDNA. Arch. Virol. 159, 1807–1811. https://doi.org/10.1007/s00705-014-1990-x

Rhie, M.J., Min, B.E., Hong, J.S., Song, Y.S., Ryu, K.H., 2007. Brief Report Complete genome sequence supports Bell pepper mottle virus as a species of the genus Tobamovirus 1401–1407. https://doi.org/10.1007/s00705-007-0950-0

Rivarez, M.P.S., Pecman, A., Bačnik, K., Maksimović, O., Vučurović, A., Seljak, G., Mehle, N., Gutiérrez-Aguirre, I., Ravnikar, M., Kutnjak, D., 2023. In-depth study of tomato and weed viromes reveals undiscovered plant virus diversity in an agroecosystem. Microbiome 11, 1–24. https://doi.org/10.1186/s40168-023-01500-6

Rodríguez, Y., Rangel, E., Centeno, F., Mendoza, O., Parra, A., 2004. Detection of viral diseases affecting sweet pepper in Counties Iribarren, Jiménez and Torres of Lara State, Venezuela, using ELISA technique. Univ. del Zulia 21, 105–115.

Roldan-Hernandez, L., Graham, K.E., Duong, D., Boehm, A.B., 2022. Persistence of Endogenous SARS-CoV-2 and Pepper Mild Mottle Virus RNA in Wastewater-Settled Solids. ACS Environ. Sci. Technol. Water. https://doi.org/10.1021/acsestwater.2c00003

Rosario, K., Nilsson, C., Lim, Y.W., Ruan, Y., Breitbart, M., 2009a. Metagenomic analysis of viruses in reclaimed water. Environ. Microbiol. 11, 2806–2820. https://doi.org/10.1111/j.1462-2920.2009.01964.x

Rosario, K., Symonds, E.M., Sinigalliano, C., Stewart, J., Breitbart, M., 2009b. Pepper mild mottle virus as an indicator of fecal pollution. Appl. Environ. Microbiol. 75, 7261–7267. https://doi.org/10.1128/AEM.00410-09

Rosario, K., Symonds, E.M., Sinigalliano, C., Stewart, J., Breitbart, M., 2009c. Pepper mild mottle virus as an indicator of fecal pollution. Appl. Environ. Microbiol. 75, 7261–7267. https://doi.org/10.1128/AEM.00410-09

Rothman, J.A., Whiteson, K.L., 2022. Sequencing and Variant Detection of Eight Abundant Plant-Infecting Tobamoviruses across Southern California Wastewater. Microbiol. Spectr. 10. https://doi.org/10.1128/spectrum.03050-22

Ryu, K.H., Min, B.E., Choi, G.S., Choi, S.H., Kwon, S.B., Noh, G.M., Yoon, J.Y., Choi, Y.M., Jang, S.H., Lee, G.P., Cho, K.H., Park, W.M., 2000. Zucchini green mottle mosaic virus is a new

tobamovirus; comparison of its coat protein gene with that of kyuri green mottle mosaic virus. Arch. Virol. 145, 2325–2333. https://doi.org/10.1007/s007050070023

Ryu, K.H., Park, W.M., 1995. The complete nucleotide sequence and genome organization of odontoglossum ringspot tobamovirus RNA. Arch. Virol. 140, 1577–1587. https://doi.org/10.1007/BF01322531

Salem, N., Mansour, A., Ciuffo, M., Falk, B.W., Turina, M., 2016. A new tobamovirus infecting tomato crops in Jordan. Arch. Virol. 161, 503–506. https://doi.org/10.1007/s00705-015-2677-7

Salem, N.M., Cao, M.J., Odeh, S., Turina, M., Tahzima, R., 2020. First report of tobacco mild green mosaic virus and tomato brown rugose fruit virus infecting Capsicum annuum in Jordan. Plant Dis. 104, 601.

Sammons, I.M., Chessin, M., 1961. Cactus virus in the United States. Nature 191, 517–518. https://doi.org/10.1038/191517b0

Sassi, H.P., Tuttle, K.D., Betancourt, W.Q., Kitajima, M., Gerba, C.P., 2018. Persistence of Viruses by qPCR Downstream of Three Effluent-Dominated Rivers in the Western United States. Food Environ. Virol. 10, 297–304. https://doi.org/10.1007/s12560-018-9343-7

Scholthof, K.-B.G., 2008. Tobacco Mosaic Virus: The Beginning of Plant Virology [WWW Document]. APS Educ. Contrib. Content. URL https://www.apsnet.org/edcenter/apsnetfeatures/Pages/TMV.aspx (accessed 11.24.24).

Scholthof, K.B.G., 2023. The Past Is Present: Coevolution of Viruses and Host Resistance Within Geographic Centers of Plant Diversity. Annu. Rev. Phytopathol. 61, 119–136. https://doi.org/10.1146/annurev-phyto-021621-113819

Scholthof, K.B.G., 2004. Tobacco Mosaic Virus: A model system for plant biology. Annu. Rev. Phytopathol. 42, 13–34. https://doi.org/10.1146/annurev.phyto.42.040803.140322

Scholthof, K.B.G., Adkins, S., Czosnek, H., Palukaitis, P., Jacquot, E., Hohn, T., Hohn, B., Saunders, K., Candresse, T., Ahlquist, P., Hemenway, C., Foster, G.D., 2011. Top 10 plant viruses in molecular plant pathology. Mol. Plant Pathol. 12, 938–954. https://doi.org/10.1111/j.1364-3703.2011.00752.x

Scott-Brown, A.S., D'Elia, T., Devey, D.S., Funderburk, J.E., Adkins, S., 2020a. Genome characterization of brugmansia latent virus, a novel tobamovirus. Arch. Virol. 165, 2389–2392. https://doi.org/10.1007/s00705-020-04718-z

Scott-Brown, A.S., D'Elia, T., Devey, D.S., Funderburk, J.E., Adkins, S., 2020b. Genome characterization of brugmansia latent virus, a novel tobamovirus. Arch. Virol. 165, 2389–2392. https://doi.org/10.1007/s00705-020-04718-z

Shen, J., Liu, Y., Wang, X., Bai, J., Lin, L., Luo, F., Zhong, H., 2023. A Comprehensive Review of Health-Benefiting Components in Rapeseed Oil. Nutrients 15, 1–14. https://doi.org/10.3390/nu15040999

Sherchan, S.P., Malla, B., Haramoto, E., 2023. First quantitative detection of tomato brown rugose fruit virus in wastewater in Louisiana. Sci. Total Environ. 888, 164001. https://doi.org/10.1016/j.scitotenv.2023.164001

Shirakawa, D., Shirasaki, N., Hu, Q., Matsushita, T., Matsui, Y., Takagi, H., Oka, T., 2023. Investigation of removal and inactivation efficiencies of human sapovirus in drinking water treatment processes by applying an in vitro cell-culture system. Water Res. 236. https://doi.org/10.1016/j.watres.2023.119951

Shirasaki, N., Matsushita, T., Matsui, Y., Koriki, S., 2020. Suitability of pepper mild mottle virus as a human enteric virus surrogate for assessing the efficacy of thermal or free-chlorine disinfection processes by using infectivity assays and enhanced viability PCR. Water Res. 186, 116409. https://doi.org/10.1016/j.watres.2020.116409

Shirasaki, N., Matsushita, T., Matsui, Y., Yamashita, R., 2018. Evaluation of the suitability of a plant virus, pepper mild mottle virus, as a surrogate of human enteric viruses for assessment of the efficacy of coagulation–rapid sand filtration to remove those viruses. Water Res. 129, 460–469.

Shrestha, Sadhana, Shrestha, Shankar, Shindo, J., Sherchand, J.B., Haramoto, E., 2018. Virological Quality of Irrigation Water Sources and Pepper Mild Mottle Virus and Tobacco Mosaic Virus as Index of Pathogenic Virus Contamination Level. Food Environ. Virol. 10, 107–120. https://doi.org/10.1007/s12560-017-9324-2

Silver, S., Quan, S., Deom, C.M., 1996. Completion of the nucleotide sequence of sunn-hemp mosaic virus: A tobamovirus pathogenic to legumes. Virus Genes 13, 83–85. https://doi.org/10.1007/BF00576982

Singer, A.C., Järhult, J.D., Grabic, R., Khan, G.A., Fedorova, G., Fick, J., Lindberg, R.H., Bowes, M.J., Olsen, B., Söderström, H., 2013. Compliance to Oseltamivir among Two Populations in Oxfordshire, United Kingdom Affected by Influenza A(H1N1)pdm09, November 2009 - A Waste Water Epidemiology Study. PLoS One 8, 2–9. https://doi.org/10.1371/journal.pone.0060221

Smith, E., Dombrovsky, A., 2020. Aspects in Tobamovirus Management in Intensive Agriculture, in: Plant Diseases - Current Threats and Management Trends. https://doi.org/10.5772/intechopen.87101

Solis, I., Garcia-Arenal, F., 1990. The complete nucleotide sequence of the genomic RNA of the tobamovirus tobacco mild green mosaic virus. Virology 177, 553–558. https://doi.org/10.1016/0042-6822(90)90520-2

Solovyev, A.G., Makarov, V. V., 2016. Helical capsids of plant viruses: Architecture with structural lability. J. Gen. Virol. 97, 1739–1754. https://doi.org/10.1099/jgv.0.000524

Song, Y.S., Min, B.E., Hong, J.S., Rhie, M.J., Kim, M.J., Ryu, K.H., 2006. Molecular evidence supporting the confirmation of Maracuja mosaic virus as a species of the genus Tobamovirus and production of an infectious cDNA transcript. Arch. Virol. 151, 2337–2348. https://doi.org/10.1007/s00705-006-0823-y

Song, Y.S., Ryu, K.H., 2011. The complete genome sequence and genome structure of passion fruit mosaic virus. Arch. Virol. 156, 1093–1095. https://doi.org/10.1007/s00705-011-0961-8

Srinivasan, K.G., Min, B.E., Ryu, K.H., Adkins, S., Wong, S.M., 2005. Determination of complete nucleotide sequence of Hibiscus latent Singapore virus : Evidence for the presence of an internal poly (A) tract ∗ Brief Report 153–166. https://doi.org/10.1007/s00705-004-0404-x

Svobodová, J., 1959. A New Strain of Tobacco Mosaic Virus Caused by Influencing the Metabolism of the Host. Biol. Plant. 1, 113–122. https://doi.org/10.1007/bf02927046

Symonds, E.M., Breitbart, M., Paul, J.H., Griffin, D.W., 2008. Viruses in Raw Sewage and Their Potential to Indicate Fecal Pollution in Coastal Environments. Coll. Mar. Sci. Master of, 73.

Taboada, B., Morán, P., Serrano-Vázquez, A., Iša, P., Rojas- Velázquez, L., Pérez-Juárez, H., López, S., Torres, J., Ximenez, C., Arias, C.F., 2021. The gut virome of healthy children during the first year of life is diverse and dynamic. PLoS One 16, 1–18. https://doi.org/10.1371/journal.pone.0240958

Tandukar, S., Sherchan, S.P., Haramoto, E., 2020. Applicability of crAssphage, pepper mild mottle virus, and tobacco mosaic virus as indicators of reduction of enteric viruses during wastewater treatment. Sci. Rep. 10, 1–8. https://doi.org/10.1038/s41598-020-60547-9

Tang, J., Lilly, S.T., Thompson, J.R., 2024. First Report of Streptocarpus Flower Break Virus in Streptocarpus Hybrids in Aotearoa New Zealand. Plant Dis. 106, 1–2. https://doi.org/10.1094/PDIS-06-23-1093-PDN

Tóbiás, I., Rast, A.T.B., Maat, D.Z., 1982. Tobamoviruses of pepper, eggplant and tobacco: Comparative host reactions and serological relationships. Netherlands J. Plant Pathol. 88, 257–268. https://doi.org/10.1007/BF02000131

Tomita, R., Sekine, K.-T., Mizumoto, H., Sakamoto, M., Murai, J., Kiba, A., Hikichi, Y., Suzuki, K., Kobayashi, K., 2011. Genetic Basis for the Hierarchical Interaction Between Tobamovirus spp. and L Resistance Gene Alleles from Different Pepper Species. Mol. Plant-Microbe Interact. 24, 108–117. https://doi.org/10.1094/MPMI-06-10-0127

Ugaki, M., Tomiyama, M., Kakutani, T., Hidaka, S., Kiguchi, T., Nagata, R., Sato Motoyoshi, T.F., Nishiguchi, M., 1991. The complete nucleotide sequence of cucumber green mottle mosaic virus (SH strain) genomic RNA. J. Gen. Virol. 72, 1487–1495. https://doi.org/10.1099/0022-1317-72-7-1487

USDA, 2022. EXPLORING THE POTENTIAL OF PASSION FRUIT IN SUBTROPICAL NORTH AMERICA | National Agricultural Library [WWW Document]. Natl. Agric. Libr. URL https://www.nal.usda.gov/research-tools/food-safety-research-projects/exploring-potential-passion-fruit-subtropical-north (accessed 2.28.24).

Van Regenmortel, M.H.V., Fraenkel-Conrat, H., 1996. The Plant Viruses, The Plant Viruses. Springer US, Boston, MA. https://doi.org/10.1007/978-1-4899-1772-0

Vänninen, I., 2019. New developments and challenges of cucumber production in western and northern European countries, in: VI International Symposium on Cucurbits 1294. pp. 35–52.

Verhoeven, J.T.J., Bouwen, I., Roenhorst, J.W., 1995. A new flower breaking tobamovirus of Streptocarpus. Eur. J. Plant Pathol. 101, 311–318. https://doi.org/10.1007/BF01874787

Verma, S., Khan, M., Li, L., Haak, L., Pagilla, K., 2023. Tomato Brown Rugose Fruit Virus (ToBRFV): A Better Indicator of Viral Load and Treatment Efficacy of Wastewater Treatment (preprint). Res. Sq. 1–21.

Vitale, D., Morales Suárez-Varela, M., Picó, Y., 2021. Wastewater-based epidemiology, a tool to bridge biomarkers of exposure, contaminants, and human health. Curr. Opin. Environ. Sci. Heal. 20, 100229. https://doi.org/10.1016/j.coesh.2021.100229

Wang, L., Piedra, P.A., Avadhanula, V., Durigon, E.L., Machablishvili, A., López, M.R., Thornburg, N.J., Peret, T.C.T., 2019. Duplex real-time RT-PCR assay for detection and subgroup-specific identification of human respiratory syncytial virus. J. Virol. Methods 271, 113676. https://doi.org/10.1016/j.jviromet.2019.113676

Wang, R., Alamin, M., Tsuji, S., Hara-Yamamura, H., Hata, A., Zhao, B., Ihara, M., Honda, R., 2022. Removal performance of SARS-CoV-2 in wastewater treatment by membrane bioreactor, anaerobic-anoxic-oxic, and conventional activated sludge processes. Sci. Total Environ. 851, 158310. https://doi.org/10.1016/j.scitotenv.2022.158310

Wang, X., Larrea-Sarmiento, A., Olmedo-Velarde, A., Kong, A., Borth, W., Suzuki, J.Y., Wall, M.M., Melzer, M., Hu, J., 2023. First detection and complete genome sequence of a new tobamovirus naturally infecting Hibiscus rosa-sinensis in Hawaii. Arch. Virol. 168, 1–4. https://doi.org/10.1007/s00705-022-05634-0

Wei, K., Gibbs, A., MacKenzie, A., 2012. Clitoria yellow mottle virus: A tobamovirus from Northern Australia. Australas. Plant Dis. Notes 7, 59–61. https://doi.org/10.1007/s13314-012-0048-8

Wetter, C., 1986. Ribgrass Mosaic Virus, in: Van Regenmortel, M.H. V, Fraenkel-Conrat, H. (Eds.), The Plant Viruses: The Rod-Shaped Plant Viruses. Springer US, Boston, MA, pp. 221–232. https://doi.org/10.1007/978-1-4684-7026-0_11

Wetter, C., 1984. Pepper Mild Mottle Virus, a Tobamovirus Infecting Pepper Cultivars in Sicily. Phytopathology. https://doi.org/10.1094/phyto-74-405

Wetter, C., 1975. Tobacco mosaic virus and para-tobacco mosaic virus in cigarettes. Naturwissenschaften 62, 533.

Wetter, C., Dore, I., Bernard, M., 1987. Bell Pepper Mottle Virus, a Distinct Tobamovirus Infecting Pepper. J. Phytopathol. 119, 333–344. https://doi.org/https://doi.org/10.1111/j.1439-0434.1987.tb04404.x

Wetter, C., Paul, H.L., 1967. Serologische und physikalische Eigenschaften von Sammons' Opuntia Virus. J. Phytopathol. 60, 92–95. https://doi.org/10.1111/j.1439-0434.1967.tb02979.x

Wolfe, M.K., Archana, A., Catoe, D., Coffman, M.M., Dorevich, S., Graham, K.E., Kim, S., Grijalva, L.M., Roldan-Hernandez, L., Silverman, A.I., Sinnott-Armstrong, N., Vugia, D.J., Yu, A.T., Zambrana, W., Wigginton, K.R., Boehm, A.B., 2021. Scaling of SARS-CoV-2 RNA in Settled Solids from Multiple Wastewater Treatment Plants to Compare Incidence Rates of Laboratory-Confirmed COVID-19 in Their Sewersheds. Environ. Sci. Technol. Lett. https://doi.org/10.1021/acs.estlett.1c00184

Wylie, S.J., Li, H., Jones, M.G.K., 2014. Yellow tailflower mild mottle virus: A new tobamovirus described from Anthocercis littorea (Solanaceae) in Western Australia. Arch. Virol. 159, 791–795. https://doi.org/10.1007/s00705-013-1891-4

Wylie, S.J., Zhang, C., Long, V., Roossinck, M.J., Koh, S.H., Jones, M.G.K., Iqbal, S., Li, H., 2015. Differential responses to virus challenge of laboratory and wild accessions of Australian species of Nicotiana, and comparative analysis of RDR1 gene sequences. PLoS One 10, 1–22. https://doi.org/10.1371/journal.pone.0121787

Xiaoqiong, G., 2018. Viral Metagenomics Analysis of Surface Water and Wastewater in Singapore.

Yang, Z., Xu, G., Reboud, J., Kasprzyk-Hordern, B., Cooper, J.M., 2017. Monitoring Genetic Population Biomarkers for Wastewater-Based Epidemiology. Anal. Chem. 89, 9941–9945. https://doi.org/10.1021/acs.analchem.7b02257

Yasui, M., Iso, H., Torii, S., Matsui, Y., Katayama, H., 2021. Applicability of pepper mild mottle virus and cucumber green mottle mosaic virus as process indicators of enteric virus removal by membrane processes at a potable reuse facility. Water Res. 206, 117735. https://doi.org/10.1016/j.watres.2021.117735

Yoon, J.Y., Min, B.E., Choi, S.H., Ryu, K.H., 2001. Completion of nucleotide sequence and generation of highly infectious transcripts to cucurbits from full-length cDNA clone of Kyuri green mottle mosaic virus. Arch. Virol. 146, 2085–2096. https://doi.org/10.1007/s007050170022

Yoshida, T., Kitazawa, Y., Komatsu, K., Neriya, Y., Ishikawa, K., Fujita, N., Hashimoto, M., Maejima, K., Yamaji, Y., Namba, S., 2014. Complete nucleotide sequence and genome structure of a Japanese isolate of hibiscus latent Fort Pierce virus, a unique tobamovirus that contains an internal poly(A) region in its 3′ end. Arch. Virol. 159, 3161–3165. https://doi.org/10.1007/s00705-014-2175-3

Zaitlin, M., Schlechtman, A.M., Bald, J.G., Wildman, S.G., 1954. Detection of virus in Cattleya Orchids by serological methods. Phytopathology 44, 314–318 pp.

Zamfir, A.D., Babalola, B.M., Fraile, A., McLeish, M.J., García-Arenal, F., 2023. Tobamoviruses Show Broad Host Ranges and Little Genetic Diversity Among Four Habitat Types of a Heterogeneous Ecosystem. Phytopathology 113, 1697–1707. https://doi.org/10.1094/PHYTO-11-22-0439-V

Zhan, Q., Babler, K.M., Sharkey, M.E., Amirali, A., Beaver, C.C., Boone, M.M., Comerford, S., Cooper, D., Cortizas, E.M., Currall, B.B., Foox, J., Grills, G.S., Kobetz, E., Kumar, N., Laine, J., Lamar, W.E., Mantero, A.M.A., Mason, C.E., Reding, B.D., Robertson, M., Roca, M.A., Ryon, K., Schürer, S.C., Shukla, B.S., Solle, N.S., Stevenson, M., Tallon Jr, J.J., Thomas, C., Thomas, T., Vidović, D., Williams, S.L., Yin, X., Solo-Gabriele, H.M., 2022. Relationships between SARS-CoV-2 in Wastewater and COVID-19 Clinical Cases and Hospitalizations, with and without Normalization against Indicators of Human Waste. ACS ES&T Water. https://doi.org/10.1021/acsestwater.2c00045

Zhang, S., Griffiths, J.S., Marchand, G., Bernards, M.A., Wang, A., 2022. Tomato brown rugose fruit virus: An emerging and rapidly spreading plant RNA virus that threatens tomato production worldwide. Mol. Plant Pathol. 23, 1262–1277. https://doi.org/10.1111/mpp.13229

Zhang, S.B., Liu, J., Zhao, Z.B., Zheng, L.M., Zhang, D.Y., Liu, Y., Du, J., Peng, J., Yan, F., Li, F., Xie, Y., Cheng, Z.B., 2015. First Report of Pepper (Capsicum annuum) as a Natural Host Plant for Youcai mosaic virus. Plant Dis. 100, 541. https://doi.org/10.1094/PDIS-07-15-0795-PDN

Zhang, T., Breitbart, M., Lee, W.H., Run, J.Q., Wei, C.L., Soh, S.W.L., Hibberd, M.L., Liu, E.T., Rohwer, F., Ruan, Y., 2006. RNA viral community in human feces: Prevalence of plant pathogenic viruses. PLoS Biol. 4, 0108–0118. https://doi.org/10.1371/journal.pbio.0040003

Zhang, Z.C., Lei, C.Y., Zhang, L.F., Yang, X.X., Chen, R., Zhang, D.S., 2008. The complete nucleotide sequence of a novel Tobamovirus, Rehmannia mosaic virus. Arch. Virol. 153, 595–599. https://doi.org/10.1007/s00705-007-0002-9

Zhenchen, Z., Lifang, Z., Qi, Q., Yongjiang, W., Xiulan, J., 2004. Identification of viral pathogens of Rehmannia glutinosa disease in Henan Province (in Chinese). Acta Phytopathol. Sin.

Zheng, Y.X., Shen, B.N., Chen, C.C., Jan, F.J., 2010. Odontoglossum ringspot virus causing flower crinkle in Phalaenopsis hybrids. Eur. J. Plant Pathol. 128, 1–5. https://doi.org/10.1007/s10658-010-9630-0

Zhou, W.P., Li, Y.Y., Li, F., Tan, G.L., 2020. First report of natural infection of tomato by pepper mild mottle virus in China. J. Plant Pathol. 650201. https://doi.org/10.1007/s42161-020-00688-y

Chapter 7 – Globally Validated PMMoV Assay for Wastewater & Environmental Surveillance Data Normalization

Context

This manuscript presented in this chapter of the doctoral dissertation is titled *Globally validated PCR assay for pepper mild mottle virus in wastewater*, by Patrick M. D'Aoust, Tyson E. Graber, Chandler H. Wong, Tram B. Nguyen, Shen Wan, Elizabeth M. Renouf, Raul Gonzalez, Parthenopi Karaolia, Bilge Alpaslan Kocamemi, Anna Maria, Cresten Mansfeldt, Despo Fatta-Kassinos, Dominic Frigon, Sukriye Celikkol, Kevin Murmane, Colleen C. Naughton, Masaaki Kitajima, Anna J. Székely, Syeda Tasneem Towhid, Emanuel Wyler, Ryan Ziels and Robert Delatolla, and is in preparation for submittal to the *Journal of Virological Methods*. This manuscript addresses the development of a globally validated assay for *PMMoV*, a key biomarker for normalizing RNA concentrations in wastewater surveillance. Analyzing 116 samples from 12 countries, the study identified a conserved genomic region (nt 2776-3023) to design the P17 PMMoV assay, ensuring reliable performance across diverse diets and environmental conditions, with enhanced sensitivity for consistent surveillance data.

Abstract

Pepper mild mottle virus (PMMoV) RNA has become one of the most commonly used human-feces-associated biomarkers to normalize wastewater-measured RNA concentrations of respiratory viruses and other pathogens for wastewater and environmental monitoring (WEM). The SARS-CoV-2 pandemic led to the significant growth of WEM programs and highlighted the critical need for normalization of wastewater surveillance measurements to continue improving the usability of WEM data and decrease the impacts of sewerage effluent dynamics and major weather events on WEM measurements. As a result, since the adoption of PMMoV as a human-feces-associated biomarker in 2006, over 250 WEM studies have used PMMoV RNA to normalize WEM measurements. Due to highly diverse diets, varying amounts and different strains of PMMoV may be encountered in global wastewaters. To address variations in wastewater-measured PMMoV RNA concentrations caused by different diets and the presence of different strains, we tested 116 samples from 12 countries and identified nucleotides 2776-3023 (in ORF1) to be the most persistent locus of the PMMoV genome across wastewater from geographically distinct locales with diverse diets. Finally, we propose a new, highly sensitive and specific (ALOQ = 4.9 copies/reaction, ALOD = 3.4 copies/reaction) called the P17 PMMoV assay to facilitate the use of PMMoV as a biomarker across the world, validated to be sensitive despite varying diets and environmental conditions.

7.1. Introduction

Wastewater and environmental monitoring (WEM) has emerged as a robust & accepted method for tracking viral infection and disease outbreaks in sewered and urbanized communities. Tracked pathogens now typically include SARS-CoV-2 (Ahmed et al., 2020), the seasonal influenza A & B viruses (Mercier et al., 2022; Wolfe et al., 2022), highly pathogenic avian influenza subtypes (such as H5N1) (Wolfe et al., 2024), respiratory syncytial virus (Hughes et al., 2022; Toribio-Avedillo et al., 2023; Zambrana et al., 2024), mpox (Adams et al., 2024; Wolfe et al., 2023; Wong et al., 2023), norovirus (Boehm et al., 2023b; Dunkin et al., 2018), rotavirus (Atabakhsh et al., 2020; Elmahdy et al., 2020; He et al., 2008; Hotta et al., 2024), enteroviruses (Bisseux et al., 2020; Brinkman et al., 2017), hepatitis (Fantilli et al., 2023), and human metapneumovirus (Boehm et al., 2023a).

Normalization of measured viral/pathogen RNA or DNA concentrations has become increasingly important in improving the interpretation and applicability of WEM by public health professionals as it can provide a more accurate representation of trends over time, by improving the correlation between wastewater-measured levels of viral/pathogen RNA or DNA and reported clinical cases in a community (D'Aoust et al., 2021a; Daughton, 2020; Maal-Bared et al., 2023; Mazumder et al., 2022; Pang et al., 2022; Wu et al., 2022). Due to the presence of genetic material from SARS-CoV-2, influenza viruses and many other pathogens in feces and fecal-associated solids (solids present in the wastewater matrix that are fecal in nature and/or originate from feces) (D'Aoust et al., 2021b; Graham et al., 2021; Roldan-Hernandez et al., 2022), WEM studies have concentrated on normalizing viral/pathogen RNA or DNA concentrations through the use of biomarkers linked to human feces. Normalization methods in the WEM context typically adjust or apply a modifier or factor to viral/pathogen DNA/RNA concentration measurements to minimize the effects of sewershed size (Holm et al., 2022) and rainfall- or snowmelt-induced dilution (Bertels et al., 2022; Mercier et al., 2024). The normalization biomarker chosen should not co-vary with the target nucleic acid/pathogen of interest and be consistently shed (over the sampling period) by the targeted population, on an aggregated per capita basis (Malla et al., 2024; Mazumder et al., 2022; Polo et al., 2020).

Proposed biomarkers include tobamovirus RNAs (D'Aoust et al., 2021b; Kitajima et al., 2018; Lopez-Roblero et al., 2024; Nash et al., 2024; Rosario et al., 2009a; Rothman and Whiteson, 2022; Sherchan et al., 2023; Symonds et al., 2018). Tobamoviruses are a genus comprised of 43 individual plant viruses belonging to the Virgaviridae family, typically characterized by rod-shaped virions and positive-sense, single-stranded RNA (Adams et al., 2017; Gibbs, 1999). Named after the type species tobacco mosaic virus (TMV), these viruses may cause significant agricultural damage and cause crop yield losses by infecting a wide variety of cultivars including amaranths, brassicas, cucurbits, legumes, ornamental plants, and

solanums (Rao and Reddy, 2020; Smith and Dombrovsky, 2020). As a result, tobamoviruses are commonly present in numerous cultivars grown all around the world, where they are often inadvertently consumed by humans via symptomless fruits and vegetables or infected transformed/processed foodstuffs, leading to their subsequent excretion through stool and urine. As a result, RNA from these tobamoviruses is routinely detected in wastewater. Their exceptional environmental stability and resilience, owing to strong protein-protein interactions at the capsid level (Bloomer et al., 1978; Solovyev and Makarov, 2016), allow them to remain infectious in traditionally difficult environments such as wastewater, soil, water, and clouds for extended periods (Bačnik et al., 2020; Castello et al., 1995; Cervantes-Avilés et al., 2021; Fillhart et al., 1998; Kitajima et al., 2018; Mehle and Ravnikar, 2012). Due to the high degree of persistence of tobamovirus in multiple different environmental contexts, it's unsurprising that tobamoviruses have been identified as the most common group of viruses found in human feces (Rothman and Whiteson, 2022; Zhang et al., 2006), and identified pepper mild mottle virus (PMMoV) as the single most commonly encountered virus in human feces, leading to investigations as a biomarker in surface and wastewaters (Haramoto et al., 2013; Rosario et al., 2009a; Symonds et al., 2018).

It has been demonstrated that the normalization of viral/pathogen RNA concentration measurements in the solids fraction of wastewater with RNA concentration measurements of PMMoV in large sewered and urbanized locations can significantly improve the relevance and usability of data sets by public health officials (D'Aoust et al., 2021a; Graham et al., 2021; Wade et al., 2022; Wolfe et al., 2021). However, it is important to note that there is no consensus among all researchers in the field in regards to the 'correct' method to normalize infectious disease RNA measurements in wastewater, and the use of PMMoV as a normalization biomarker has been criticized, owing to both weak and strong correlations observed between PMMoV-normalized viral/pathogen RNA or DNA concentration and reported clinical cases, as compared to other biomarkers or normalizers (Maal-Bared et al., 2023; Malla et al., 2024; Zheng et al., 2022). It has been hypothesized that sewershed size and local diets in smaller sewersheds in particular may be the cause of the lack of improvement in correlation in PMMoV-normalized viral/pathogen RNA or DNA concentration measurements in some studies (Holm et al., 2022).

Despite the demonstrated benefits of PMMoV-normalization, a significant issue however persists: the most used assay to quantify PMMoV RNA in wastewater – a probe-based RT-qPCR assay originally developed by Zhang et al. and modified by Haramoto et al. (Haramoto et al., 2013; Zhang et al., 2006) has not undergone systemic validation to confirm its status as the most sensitive and reliable method for PMMoV RNA quantification in wastewater across different regions of the world. The closest approximation to this proposed experiment has been interlaboratory/multi-lab studies conducted in the United States, Japan, and Canada, where quantification of PMMoV RNA in wastewater was performed

(Antkiewicz et al., 2024; Chettleburgh et al., 2023; Chik et al., 2021; Davis et al., 2023; Endo et al., 2024). However, without a standardized sample concentration and nucleic extraction methodology between all labs, the data generated by the different participating labs has never been fully comparable. A lack of reproducibility and local variations likely caused by diverging sewershed sizes, local dietary trends, and differences in sampling and analysis methodologies have therefore led to diverging opinions about the usefulness of normalization methods and chosen biomarkers. Without formal validation, there remains uncertainty about this assay's effectiveness across different geographical regions, potentially limiting the comparability and accuracy of PMMoV-normalized global wastewater surveillance efforts.

As a result of this perceived limitation and lack of consensus on the use of PMMoV as a normalizing biomarker, our goal in this study was to design a universal RT-qPCR assay for the quantification of PMMoV RNA with high analytical sensitivity in geographically diverse wastewater settings. We first designed a series of overlapping PCR primers spanning the ~6.4 kilobase (kb) RNA genome of PMMoV (GenBank accession number NC_003630.1) and tested 116 wastewater samples from 12 different countries to identify any differences in the persistence of genomic regions within and across sample collection sites. We identified a genomic region located in the replication-associated protein CDS (coding DNA sequence) to be the most preserved region across all tested genomic regions and sampling sites. Using this information, we designed and validated a universal TaqMan probe-based RT-qPCR assay for the quantification of PMMoV RNA in WEM applications. This assay improves the analytical sensitivity of the currently widely-used iteration, and its adoption should improve the interoperability of WEM datasets.

7.2. Materials and methods

7.2.1. Wastewater sample collection and preservation

To investigate the persistence and RNA concentrations of the different genomic regions of PMMoV, and to compare the “benchmark” and the universal PMMoV assays across samples from around the world that were extracted using the same method, a total of 116 wastewater samples were collected from 12 different countries. To ensure minimal degradation during transport, we sent sample transport packages to participating locations to eliminate any potential issues with cold-chain management following sample collection and transport. Each sampling package contained 15 mL sample transport tubes prefilled with 2 mL of DNA/RNA Shield (Zymo Research, Irvine, United States) and was shipped to all collaborators. Samples were collected (8 mL of either pre- or post-grit influent wastewater, or primary clarified sludge) from both smaller and larger water resource recovery facilities (WRRFs) in cities located in Canada, Australia, Bangladesh, Cyprus, Finland, Germany, Ireland, Japan, Spain, Sweden, Turkey, and the United

States (Figure 7-1). Samples were immediately pipetted into the provided transport tubes, vortexed, and shipped to our lab in Ottawa, Canada, at ambient temperature.

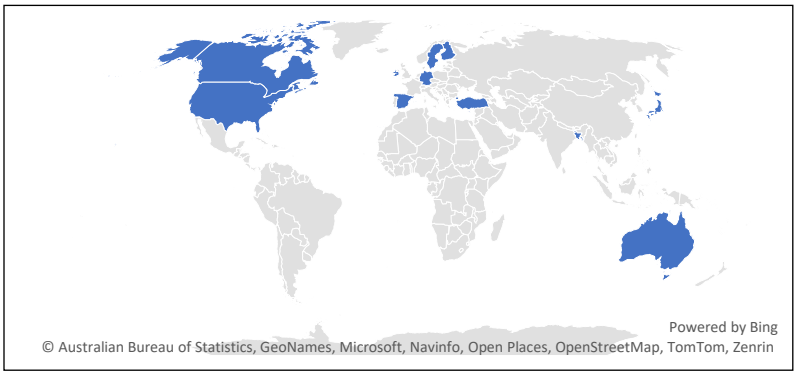


Figure 7-1. A map highlighting the countries (in blue) in which wastewater samples were harvested in this study.

7.2.2. Nucleic acid extraction

Upon receipt in Ottawa, the sample tubes were immediately refrigerated at 4°C, and nucleic acid extraction was performed within 7 days. Briefly, sample tubes were vortexed to fully homogenize the samples, and RNA was extracted from 140 µL of the 8 mL sample using the QIAamp Viral RNA Mini Kit (Qiagen, Germantown, USA) using a QIAcube Connect automated extraction platform, as per the manufacturer's recommendations. Samples were eluted with 100 µL of RNase- and free, DNase-free PCR-grade water. Samples were either analyzed by RT-qPCR immediately or stored at -80°C until analysis.

7.2.3. Primer design for PCR panel overlapping the PMMoV genome

To assess the relative persistence of the different genomic regions of PMMoV in wastewater, a primary screen using SYBR Green RT-qPCR was performed with a panel of 35 overlapping amplicons. To this end, the panel was created using the "Overlapping Primers" function of The PCR Suite (van Baren and Heutink, 2004), a software extension of Primer3 (Rozen and Skaletsky, 2000; Untergasser et al., 2012) Using the PMMoV genome reference sequence (GenBank accession number NC_003630.1), forward and reverse primers were designed using the default parameters (product size range of 250-450 base pairs (bp) & overlap size range of 40-90 bp), covering approximately 96.3% of the PMMoV reference genome, and named incrementally from genomic regions 2 to 36. Genomic region 1 (starting at the 5' end of the PMMoV genome) was excluded due to highly repetitive patterns (the pattern CAA repeats at least 17 times in the first 180 bp), making quantification more difficult. Genomic region 37 (ending at the 3' end of the PMMoV genome) was also excluded due to the presence of a homopolymer repeat (7 C's) near the 3' end of the

PMMoV genome, also making PCR quantification more difficult. The generated PCR forward and reverse primers are provided below in Table 7-1. The amplicons' characteristics are also provided below in Table 7-2.

Table 7-1. List of forward and reverse primers developed for the panel of 35 overlapping SYBR Green PCR assays used to evaluate the relative persistence of the PMMoV genome.

Primer/probe name	Sequence	Primer/probe name	Sequence
reg2_PMMoV_for	TCGGAGACTGTACGAATCAGC	**reg20_PMMoV_for**	GCACCTGTTGGTCTCATTGTC
reg2_PMMoV_rev	AGGGGATCTGCATCATCAAG	**reg20_PMMoV_rev**	TTGCATGTCAGAAACATCTCC
reg3_PMMoV_for	CACAGTCTCGCAGGTGGAC	**reg21_PMMoV_for**	AGAATCGGTGTACAAAGGTG
reg3_PMMoV_rev	ACACTACTGATTGCGGATCG	**reg21_PMMoV_rev**	ATCATCGCGACCAAATTTTC
reg4_PMMoV_for	AATACCGCCATATCAAAAGC	**reg22_PMMoV_for**	TGTGATCAGGACTGCTGCTG
reg4_PMMoV_rev	AGAAGAAAGCGCCTATGTCG	**reg22_PMMoV_rev**	CTGGCCAATTGTTGACTTCTC
reg5_PMMoV_for	CTGCTATGCTGCCTTCCAC	**reg23_PMMoV_for**	CTTTCAAGGGCGAGTTTGG
reg5_PMMoV_rev	CCTTGAAAACTTACAAAACCAAG	**reg23_PMMoV_rev**	AAGCGCATTGATTTTCTTGC
reg6_PMMoV_for	AAGACTTACTTCCCCGCTTC	**reg24_PMMoV_for**	CGAAACAGCGTTTGGATCTTAG
reg6_PMMoV_rev	CCATATCTTTCATCTTTGGAAACC	**reg24_PMMoV_rev**	CGACTGCACAATGAAATTCG
reg7_PMMoV_for	GCGATGATGAATAGCGAAAG	**reg25_PMMoV_for**	GATCTGGACTCTAATGTTCCTATGG
reg7_PMMoV_rev	ATCCACATCCCACTCTGAGC	**reg25_PMMoV_rev**	ACATCACCGCTTTTCCTCTG
reg8_PMMoV_for	CGCCAATGTATTATCGTTCG	**reg26_PMMoV_for**	TTTGGAAACACGGGCATC
reg8_PMMoV_rev	CAGCAGTAATCTCATCCCAGAC	**reg26_PMMoV_rev**	TTTGCGCCCTGTTGAATATC
reg9_PMMoV_for	CCATGCTCAAGGATGACCTC	**reg27_PMMoV_for**	AGGTGCCTTTTGTGGTGATG
reg9_PMMoV_rev	GCATTTCCACCGAAGACTTG	**reg27_PMMoV_rev**	TGTGTTTTGCACCGAGTTTC
reg10_PMMoV_for	AAAGTACCTGATTTGTATGTAACTTTCC	**reg28_PMMoV_for**	TTTTGCGGTAGGTACATAATTCAC
reg10_PMMoV_rev	GCTGCCACCAATGGATCTAC	**reg28_PMMoV_rev**	AAACAAACGAACCAAGAGGTG
reg11_PMMoV_for	CAGTGACAAGTTTGATGTTGATG	**reg29_PMMoV_for**	TGCGTACTATACACATTTGAACG
reg11_PMMoV_rev	TTCGAACCACTTCCTTGATTG	**reg29_PMMoV_rev**	TCGTACCGTCTTGACCGAAG
reg12_PMMoV_for	CAAAGGAGGAAGGTTCGTTG	**reg30_PMMoV_for**	CAATTTGTCTGCCGCTGAG
reg12_PMMoV_rev	ATCGCATGCATCTGTTTACG	**reg30_PMMoV_rev**	TTGTCGGGTAGGTTCCACTC
reg13_PMMoV_for	AATCGAGTCGTTGCAGCAG	**reg31_PMMoV_for**	GGTGTAAAGCTTGTTAAGGATGG
reg13_PMMoV_rev	AGGCACACGTCGTAGACTCC	**reg31_PMMoV_rev**	TTGCCAAACTTTTCTCTCAGC
reg14_PMMoV_for	GCGGTATCAAACCTGAAGAAG	**reg32_PMMoV_for**	AACCAGTGCAGCTAAGAAACG
reg14_PMMoV_rev	AAAGATTCGGAGCTCACTGC	**reg32_PMMoV_rev**	TCTGTCAGCCATTGGAACTG
reg15_PMMoV_for	GATGGCGAGAACATTGTGTG	**reg33_PMMoV_for**	GGAGGACCCGTTGAACTTAC
reg15_PMMoV_rev	CGCCACGATTAAACCAGAAC	**reg33_PMMoV_rev**	TTGATTGGCACTGGAAACTG
reg16_PMMoV_for	ACCAGGAAAACAGGCTGCTG	**reg34_PMMoV_for**	TTAGAATTGGGCAGAACTCG
reg16_PMMoV_rev	ACAAAAGCCTCGGAGCATAG	**reg34_PMMoV_rev**	CACGGCATTATATCGGAAAAC
reg17_PMMoV_for	AGGCTGTTTCTGGATGAAGG	**reg35_PMMoV_for**	CAGCAGTTCTCTGATGTGTGG
reg17_PMMoV_rev	TGCCCTTCGTACTTCTGATTC	**reg35_PMMoV_rev**	ACCGTCGCATCGTCTACC
reg18_PMMoV_for	TTGAAACTCGCAGAACAACG	**reg36_PMMoV_for**	CCGCAAAATCCTACAACTGC
reg18_PMMoV_rev	TCGAGAGCAGCAATGACTTG	**reg36_PMMoV_rev**	TAATTGCGTTCCATCCCAAC
reg19_PMMoV_for	AGGTGCAGCGGTAATGAATC		
reg19_PMMoV_rev	CGACTGCATCTAGCACAACTG		

Table 7-2. Overlapping SYBR Green PCR amplicon characteristics (amplicon size, GC content, location, and genomic feature(s) intersecting the amplicon).

Overlapping PCR assay genomic region	Amplicon size (bp)	GC content (%)	Nucleotide	Genomic feature(s) intersecting the amplicon
reg 2	218	49.08	153-370	Replication-associated protein (ORF1, ORF2)
reg 3	295	44.07	310-604	Replication-associated protein (ORF1, ORF2)
reg 4	278	44.6	543-820	Replication-associated protein (ORF1, ORF2)
reg 5	265	38.11	738-1002	Replication-associated protein (ORF1, ORF2)
reg 6	271	37.27	913-1183	Replication-associated protein (ORF1, ORF2)
reg 7	300	42.00	1105-1404	Replication-associated protein (ORF1, ORF2)
reg 8	224	45.54	1320-1543	Replication-associated protein (ORF1, ORF2)
reg 9	240	39.58	1457-1698	Replication-associated protein (ORF1, ORF2)
reg 10	221	39.82	1627-1847	Replication-associated protein (ORF1, ORF2)
reg 11	248	44.35	1776-2023	Replication-associated protein (ORF1, ORF2)
reg 12	208	44.71	1952-2159	Replication-associated protein (ORF1, ORF2)
reg 13	231	44.59	2091-2321	Replication-associated protein (ORF1, ORF2)
reg 14	245	45.71	2233-2477	Replication-associated protein (ORF1, ORF2)
reg 15	291	46.39	2416-2706	Replication-associated protein (ORF1, ORF2)
reg 16	219	44.29	2643-2861	Replication-associated protein (ORF1, ORF2)
reg 17	248	45.16	2776-3023	Replication-associated protein (ORF1, ORF2)
reg 18	213	46.48	2951-3163	Replication-associated protein (ORF1, ORF2)
reg 19	272	47.43	3075-3346	Replication-associated protein (ORF1, ORF2)
reg 20	229	41.48	3276-3504	Replication-associated protein (ORF1, ORF2)
reg 21	297	41.41	3435-3731	Replication-associated protein (ORF1)
reg 22	256	38.67	3666-3921	Replication-associated protein (ORF1)
reg 23	213	41.31	3862-4074	Replication-associated protein (ORF1)
reg 24	285	37.19	3989-4273	Replication-associated protein (ORF1)
reg 25	227	41.85	4186-4412	Replication-associated protein (ORF1)
reg 26	244	43.44	4322-4565	Replication-associated protein (ORF1)
reg 27	218	39.91	4488-4705	Replication-associated protein (ORF1)

reg 28	232	40.52	4615-4846	Replication-associated protein (ORF1)
reg 29	238	39.92	4776-5013	Replication-associated protein & movement protein (ORF1, ORF3)
reg 30	204	42.65	4953-5156	Movement protein (ORF3)
reg 31	243	44.03	5080-5322	Movement protein (ORF3)
reg 32	292	39.38	5235-5526	Movement protein (ORF3)
reg 33	257	40.86	5458-5714	Movement protein & capsid protein (ORF3, ORF4)
reg 34	283	43.11	5630-5912	Movement protein & capsid protein (ORF3, ORF4)
reg 35	221	47.51	5823-6043	Capsid protein (ORF4)
reg 36	293	48.81	5982-6274	Capsid protein & 3'-end noncoding region (ORF4)

7.2.4. Primer and probe design for the universal PMMoV assay

For the design of the universal probe-based assay to detect and quantify PMMoV RNA in wastewater, the reference sequence of PMMoV (GenBank accession number NC_003630.1) was analyzed. Based on results from our preliminary PCR screening, the assay was designed to target the first open reading frame (ORF1), encoding the replication-associated protein of PMMoV. Optimal oligonucleotide primers and probe pairs were designed using Primer3 Plus (Untergasser et al., 2012). Within the selected genomic region, several RT-qPCR assays were considered, synthesized, and evaluated for use in the P17 assay (data not shown), and the most sensitive assay was selected. The proposed primers and probes were checked in NCBI BLAST for specificity to PMMoV as it was possible that region 17 was over-represented in samples due to the presence of other similar nucleotide sequences (Altschul et al., 1990). The nucleotide sequences of the benchmark PMMoV assay (Haramoto et al., 2013; Zhang et al., 2006) and the universal PMMoV assay, along with their amplicon characteristics are shown below in Table 7-3. All primers and probes used in this study were synthesized by from Life Technologies (Waltham, USA). The universal assay developed in this study will be referred to as the P17 assay from this point on.

Table 7-3. Oligonucleotide sequences of the benchmark PMMoV and P17 qRT-PCR assays.

Assay	Primer/probe	Sequence (5'-3')	Genomic feature	Location (nt)	Length (bp)	Tm value (°C)	Amplicon length (bp)	Amplicon GC%
Benchmark PMMoV (Haramoto et al., 2013; Zhang et al., 2006)	PMMV-FP1-rev	GAGTGGTTTGACCTTAACGTTTGA	ORF1/Replication-associated protein	1878-1901	24	55.6	68	48.53
	PMMV-RP1	TTGTCGGTTGCAATGCAAGT		1945-1926	20	55.7		
	PMMV-Probe1	FAM-CCTACCGAAGCAAATG-MGB-NFQ		1906-1921	16	46.1		
P17 *(this study)*	P17_f	TGGAGACACCCAGCAGATTCCT	ORF1/Replication-associated protein	2865-2886	22	59.1	98	45.92
	P17_r	TGCGAGTTTCAACAGCATCGACCT		2962-2939	24	61.1		
	P17_p	FAM-TCAACAGAGTTGCAACTTTTCCCT-MGB-NFQ		2891-2914	24	57.0		

7.2.5. PCR controls

In this study, RNA extracted from a commercially available hot sauce was used as a PMMoV reference standard as it is known to yield high levels of PMMoV RNA (Cantillon and Roberts, 2022). Briefly, 0.50 mL of Triton-X 100 was added to 0.75 mL of Tabasco® regular hot sauce and vortexed for 30 seconds. The mixture was then allowed to incubate at room temperature for 5 minutes, before proceeding with nucleic acid extraction using the QIAamp Viral RNA Mini Kit (Qiagen, Germantown, USA), as

described above. The total RNA concentration was quantified using a ThermoFisher QuantStudio Absolute Q Digital PCR instrument (Waltham, USA).

7.2.6. Quantification of PMMoV RNA in wastewater by RT-qPCR

To assess the relative persistence of the PCR loci across the PMMoV genome, samples were analyzed using the panel of 35 overlapping RT-qPCR assays designed in this study using SYBR Green technology. The PMMoV signal of all 116 samples was measured using each of the overlapping assays using a singleplex one-step RT-qPCR reaction. To compare the benchmark and P17 PMMoV assays, the RT-qPCR signal from 29 samples and one positive control (cf. Section 7.2.5) was measured in technical triplicate using singleplex one-step RT-qPCR. All primers, probes (if applicable), cycling conditions, and reagent concentrations used in this study are described below, in Table 7-4.

Table 7-4. Summary of the RT-qPCR testing conditions for the SYBR Green overlapping assays, and the PMMoV probe-based assays during this study.

Targeted region	**PMMoV SYBR Green overlapping assays**	**Benchmark PMMoV assay**	**P17 assay**
RNA template volume (µL)	1.5 µL	1.5 µL	1.5 µL
Total qPCR reaction volume (µL)	10 µL	10 µL	10 µL
Supermix used	iTaq universal SYBR® Green reaction mix (Bio-Rad)	TaqMan™ Fast Virus 1-Step Master Mix (ABI)	TaqMan™ Fast Virus 1-Step Master Mix (ABI)
qPCR conditions	*(All targets)*	*(All targets)*	*(All targets)*
	Rev. transcript.: 50°C for 5:00	*Rev. transcript.: 50°C for 5:00*	*Rev. transcript.: 50°C for 5:00*
	Initial denat.: 95°C for 1:00	*Initial denat.: 95°C for 0:20*	*Initial denat.: 95°C for 0:20*
	Denaturation: 95°C for 0:10	*Denaturation: 95°C for 0:03*	*Denaturation: 95°C for 0:03*
	Anneal/ext.: 60°C for 0:45	*Anneal/ext.: 60°C for 0:30*	*Anneal/ext.: 60°C for 0:30*
Primers and probe/dye/RT in reaction	*500 µM (primers)* *5 µL iTaq SG reaction mix* *0.125 µL iScript RT*	*500 µM (primers)* *125 µM (probe)* *2.5 µL 4x TaqMan™ FV1S MM*	*500 µM (primers)* *125 µM (probe)* *2.5 µL 4x TaqMan™ FV1S MM*

7.2.7. Assay limits of detection and quantification

We used generally accepted methods (Forootan et al., 2017) to determine the assay limits of detection (ALOD, ⩾ 95% detection) and assay limits of quantification (ALOQ, CV = 35%) of the P17 assay. The standard material used to perform serial dilutions was RNA extracted from a commercially available hot sauce described above (previously quantified aliquots with the following concentrations were used: 70.9, 17.8, 8.9, 4.4, and 2.2 copies/µL). Meanwhile, the ALOD and ALOQ values of the benchmark PMMoV assay were previously determined to be 6.8 copies/reaction and 8.2 copies/reaction, respectively (data not shown).

7.2.8. Statistical analysis

All descriptive statistics, mean, standard deviation and variance calculations were performed using Microsoft® Excel® 365 (version 2405). Linear regressions, correlation and significance values and the generation of best-fit lines were performed using GraphPad Prism (version 9.5.1).

7.3. Results and discussion

7.3.1. Concentrations and persistence of PMMoV locus in global wastewaters

To determine which genomic region would be most suitable for the development of a universal RT-qPCR assay, the panel of 35 overlapping SYBR Green RT-qPCR assays spanning most of the PMMoV genome was tested on all 116 collected samples in this study, to determine which region of the PMMoV genome was detected most strongly in wastewater. Results from this preliminary screening are shown in Figure 7-2. Despite all overlapping RT-qPCR assays being run using identical PCR conditions and having similar amplicon sizes, statistically significant differences in mean Ct values across all 116 samples were observed ($p < 0.001$), with the highest RNA concentrations measured in genomic regions 17 and 31 (in red), and the lowest RNA concentrations measured in genomic regions 28, 34 and 36. These findings are congruent with the structural characteristics of PMMoV: In typical tobamovirus organization, PMMoV is rod-shaped, measuring approximately 18 nm in width and 300 nm in length. Its exterior is composed of several dozen identical copies of the capsid protein, stacked in a helical fashion to create a rod/tube, with a gap of approximately 4 nm in the center. The capsid proteins are held together in a helical structure due to strong electrostatic interactions and the formation of hydrophobic girdles, giving the virus significant rigidity (Bloomer et al., 1978; Solovyev and Makarov, 2016). As a result, much of the viral genomic RNA remains protected within the inner portion of the capsids in the center of the rod, explaining the extreme environmental persistence of PMMoV (and tobamoviruses in general) (Fillhart et al., 1998; Mehle and Ravnikar, 2012; Pares et al., 1996; Sassi et al., 2018; Smith and Dombrovsky, 2020). It is hypothesized that the lower Ct values (indicating higher PMMoV RNA concentrations) measured in genomic regions 17 and 31 are due to these regions being located within structurally protected areas of PMMoV's genome. Conversely, higher Ct values (indicating lower PMMoV RNA concentrations) in the capsid-encoding portion of the genome may be attributed to a higher nucleotide mutation rate in the capsid. This higher mutational propensity is a known mechanism by which tobamoviruses overcome host resistance. region (Spiegelman and Dinesh-Kumar, 2023). As a result, the assays quantifying RNA in genomic regions 33 to 36 were on average 4.58 (influent wastewater) and 4.19 (primary sludge) Ct values higher than the global average Ct value for all genomic regions, indicating significantly lower PMMoV RNA concentrations in

these genomic regions. A macro-analysis investigating the variance in Ct values of each individual PMMoV genomic region revealed the following: the locus with the lowest variance are regions 35, 18, 17, 26 and 27 of the PMMoV genome, and the locus with the highest variance are regions 32, 28, 8, 6 and 29 (Table S6). Since all the samples were tested with panel of PCR assays, effects caused by the type of sample were eliminated. It's therefore hypothesized that large differences in variance observed here are indeed caused by marked propensities for degradation due to less stable RNA secondary structures or rapid mutational turnover. Genomic regions with higher variances are therefore less desirable to develop a universal assay in.

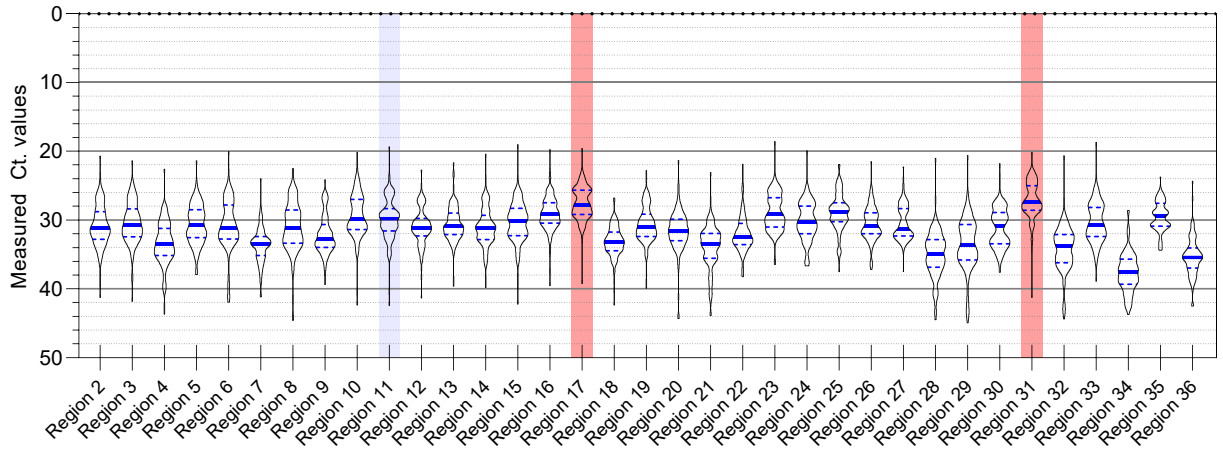


Figure 7-2. A summary graph of measured cycle threshold (Ct) values for all 35 targets within the PMMoV genome, highlighting in blue the benchmark PMMoV assay's location, and in red, two potential regions of interest for the development of a universal probe-based assay. The solid blue lines indicate the median values for the Ct values of each genomic region, and the dashed blue lines indicate the quartiles of the Ct values of each genomic region. A minimum of 116 samples were analyzed per genomic region. Including reruns, a total of 4,066 analyses were performed across all regions of the PMMoV genome.

7.3.2. Effects of geographical location on PMMoV RNA concentrations in wastewaters

A closer analysis of the geographical effects on the measured PMMoV RNA concentrations in genomic regions showed a trend that measured RNA concentrations were generally highest in genomic regions 17 and 31 in the four grouped geographical regions (Americas, Europe, Oceania, and Asia) (Figure 7-3). This trend is not observed in samples collected from Oceania, with genomic region 31 not showing the same high RNA concentrations.

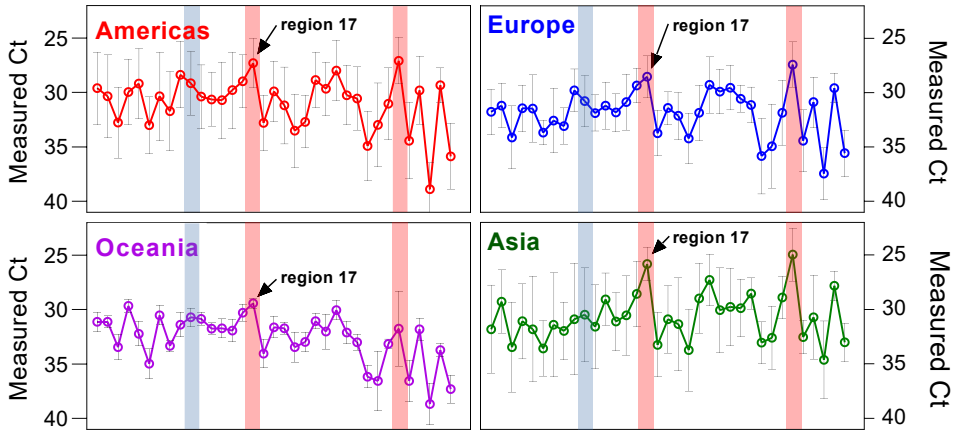


Figure 7-3. A graph demonstrating the variance in measured cycle threshold (Ct) values for all 35 'genomic regions' within the PMMoV genome, organized per geographical region of the world (Americas, Europe, Oceania and Asia) of the analyzed samples. Regions 11 (blue), 17 and 31 (red) are highlighted.

To better understand the influence of geography, Figure 7-4 (below) provides a more granular examination of PMMoV RNA concentrations in wastewater across the 12 sampled countries in this study (all 35 PMMoV genomic regions were consolidated). The descriptive statistics for the measured Ct values, separated by geographical location of the wastewater samples, are also given below in Table 7-5. The highest number of samples came from Canada, and incidentally, the lowest measured Ct values (correlating to the highest PMMoV RNA concentrations in wastewater) were observed in Canada and Japan. It is hypothesized that the higher PMMoV RNA concentrations measured in Canadian and Japanese samples may be simply explained by the higher number of primary sludge samples obtained from these countries. Based on extensive observations in previous studies and in literature, it's expected that PMMoV RNA concentrations in primary sludge will be more elevated than in influent wastewater, particularly if the analyzed samples have the same extraction protocol (D'Aoust et al., 2021b; Kitamura et al., 2021). Due to the dietary route required for PMMoV, samples with higher fecal content will generally have higher PMMoV RNA as well. Overall, measured PMMoV RNA concentrations in any given sampling location were within two standard deviations from any other sampling location, indicating relative similarity in the RNA concentrations along all sampling locations. These findings do not necessarily point to major changes or differences in diet throughout the world, and it is hypothesized that PMMoV RNA concentrations in wastewater samples could instead correlate with fecal strength of the wastewater, as tested samples were not all collected from the same sampling site over time and do not provide a longitudinal perspective to PMMoV RNA concentrations in wastewater. Furthermore, samples in this study were volume-normalized in terms of the quantity of wastewater which from which nucleic acids were extracted, complicating further the interpretation. These results however demonstrate show the ubiquity of PMMoV RNA in wastewaters

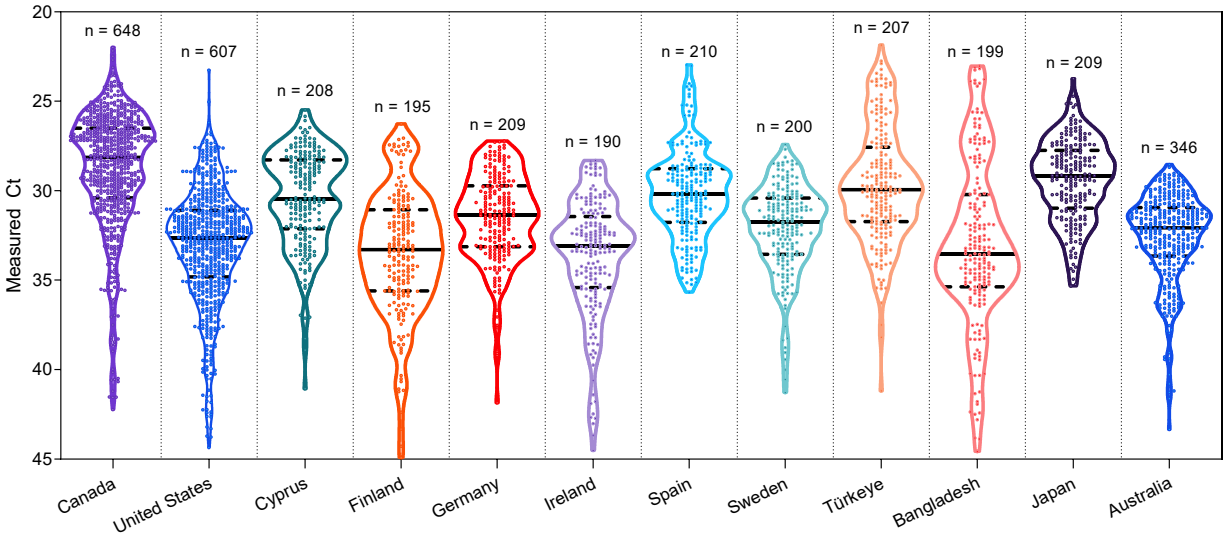


Figure 7-4. A graph showing the distribution of PMMoV RNA concentration (inferred from Ct values) in wastewaters from the 12 sampled countries in this study. Solid lines indicate the average, and the dashed lines indicate the 1st and 3rd quartiles. Lower Ct values indicate a higher PMMoV RNA concentration. In this graph, measurements from all PMMoV genomic regions were consolidated on a per country basis.

around the world, similar to findings reported by others (Hamza et al., 2011; Roldan-Hernandez et al., 2022; Rosario et al., 2009b; Sassi et al., 2018). Variations in concentrations are expected to be caused by variations in fecal strength/content among the sampled sites and samples rather than intrinsic day-to-day changes in PMMoV RNA concentrations in wastewater.

Table 7-5. This table presents the descriptive statistics for the measured Ct values (representative of the concentration of PMMoV RNA in wastewater samples) in all tested wastewater samples (all PMMoV genomic locations combined), separated by geographical location. This table provides the number of measurements performed (n), the mean values, the standard deviation, the 1st and 3rd quartiles and the variance of the measured Ct values. In this table, measurements from all PMMoV genomic regions were consolidated on a per country basis.

Country of origin of samples	**n**	**Mean Ct**	**Standard deviation**	**1st quartile**	**3rd quartile**	**Variance**
Canada	648	28.8	3.4	26.5	30.4	11.2
United States	607	33.1	3.3	31.1	34.8	12.3
Cyprus	208	30.4	2.7	28.3	32.1	11.3
Finland	195	33.5	3.5	31.1	35.6	17.5
Germany	209	31.5	2.5	29.7	33.1	10.4
Ireland	190	33.7	3.3	31.5	35.4	16.4
Spain	210	30.2	2.5	28.8	31.7	10.4
Sweden	200	32.1	2.5	30.4	33.5	11.1

Türkeye	207	29.7	3.3	27.6	31.7	14.6
Bangladesh	199	33.0	4.6	30.2	35.3	26.0
Japan	209	29.4	2.2	27.8	30.9	8.9
Australia	346	32.6	2.5	31.0	33.6	8.9

7.3.3. Effects of sample type of PMMoV RNA concentrations in wastewaters

Of the 116 surveyed samples, 102 were pre- or post-grit influent wastewater and 14 were primary sludge. When comparing the general trends of PMMoV RNA concentrations measured in both types of samples, it was observed that the primary sludge samples yielded higher RNA concentrations of PMMoV in all surveyed genomic regions of PMMoV except region 31. On average, PMMoV measurements obtained in primary sludge were approximately 2.02 Ct values higher than those obtained in influent wastewater (305.3% higher RNA concentration) (Figure 7-5).

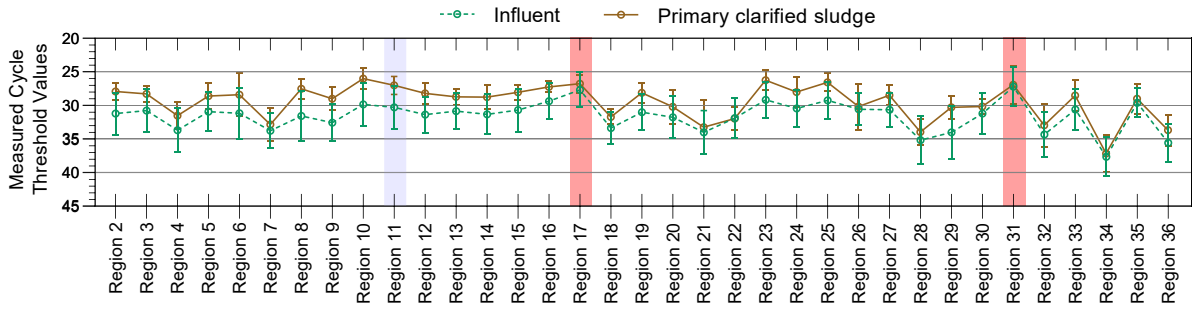


Figure 7-5. A comparison of measured PMMoV RNA concentration (displayed as Ct values) comparing pre- and post-grit and primary sludge samples across the 35 genomic region within the PMMoV genome. Lower Ct values indicate a high measured concentration of PMMoV RNA in the sample. Data points and error bars represent the mean and standard deviation of the agglomorated Ct measurements across all tested samples in the study. Three regions are highlighted as genomic regions of interest: in blue the benchmark PMMoV's assay location (region 11), and in red, two potential regions of interest (regions 17 and 31).

7.3.4. Effects of sewershed population size on PMMoV RNA concentrations in wastewaters

An analysis of the effects of sewershed population size on measured PMMoV RNA concentrations did not reveal any significant overarching trends. In all tested samples for which sufficient metadata was available, sewershed population size did not strongly correlate with PMMoV RNA concentrations. Of the 116 tested samples, sufficient metadata was available for at least 75. Linear regressions were performed on the three PMMoV genomic regions of interest (regions 11, 17, and 31), and the results are shown in Figure 7-6. In this figure, three x-y plots display the relationship between the population size contributing to tested

sewersheds (x-axis) and the corresponding Ct values measured (y-axis). Regions 11 and 17 exhibited negligible or weak relationships, with r^2 values of 0.001 (p = 0.409) and 0.028 (p = 0.153), respectively, indicating no significant trends. However, Region 31 demonstrated a moderate relationship, with an r^2 value of 0.131 and a statistically significant p-value (p = 0.031). These results suggest that while sewershed population size does not generally correlate with PMMoV RNA concentrations, some genomic regions, such as Region 31, may exhibit weak but statistically significant associations that warrant further investigation into potential underlying factors.

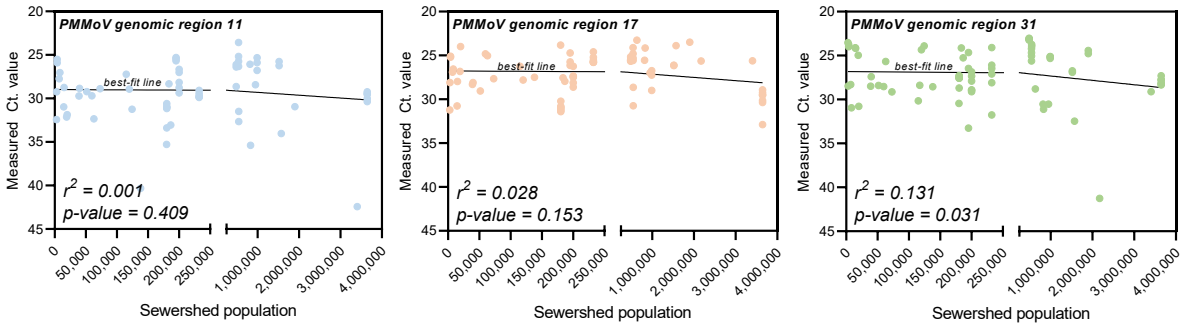


Figure 7-6. Three panels illustrating the relationship between sewershed population size and measured PMMoV RNA concentrations across three genomic regions of interest (regions 11, 17, and 31). Linear regression analyses were performed independently for each region, comparing sewershed population size with measured Ct values. The results indicate that no strong linear relationships exist between sewershed population size and PMMoV RNA concentrations.

7.3.5. Description of the universal PMMoV RT-qPCR assay

Based on the observed RT-qPCR measurements using the overlapping SYBR Green RT-qPCR assays described above, we identified the most conserved genomic regions of the PMMoV genome between individual sites, and across all sample sites: region 17, located at nucleotides 2776-3023. Within region 17, several RT-qPCR assays were considered, synthesized, and evaluated for use in the universal TaqMan RT-qPCR assay *(data not shown)*, and the most sensitive assay was selected. The proposed primers and probes were verified in NCBI BLAST for specificity to PMMoV as it was possible that region 17 was over-represented in samples due to the presence of other similar nucleotide sequences occurring in the natural environment (Altschul et al., 1990).

The primers and probe for the P17 assay were aligned with 45 full-genome sequences of PMMoV to highlight any nucleotide mismatches (Figure 7-7), and it was observed that the selected genomic region for the P17 PMMoV assay did not contain nucleotide mismatches likely to cause important effects on PCR efficiency with any of the main full-genome sequences of PMMoV, such as mismatches at the 3' end. Almost all noted mismatches are expected to be well tolerated to their distance from the 3' end of the oligos, and most mismatches were a single nucleotide along the entire oligo. The same alignment was performed between the primers and probe of the benchmark assay and 45 full-genome sequences, and it was also observed that no nucleotide mismatches were likely to cause important effects on PCR efficiency.

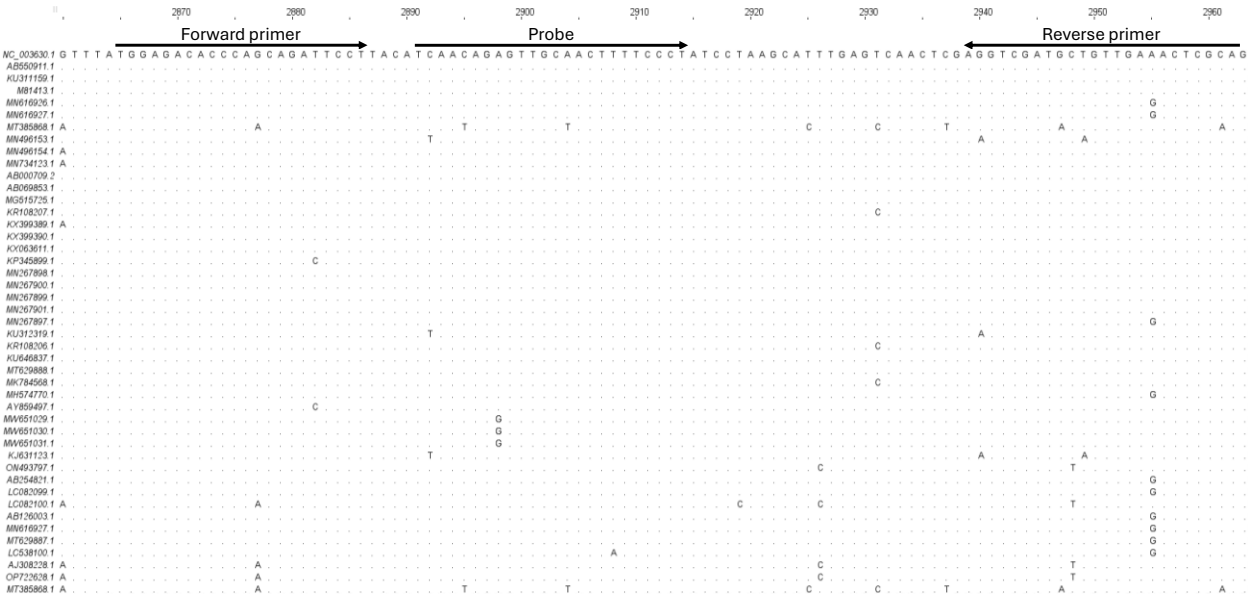


Figure 7-7. Alignment of the primers and probe of the P17 PMMoV assay proposed in this study. The primers and probe are aligned with 45 full-genome sequences of PMMoV to highlight any nucleotide mismatches.

The alignment of the benchmark assay and the full-genome sequences is shown below in Figure 7-8. The genomic locations of the benchmark and P17 assays (Figure 7-9) were also briefly assessed to determine if their location within the PMMoV genome could potentially have an impact on the PCR efficiency or the persistence of RNA, due to the assays being in different genomic features. The reference PMMoV genome is a relatively simple and small genome at 6357 nucleotides long, containing four open reading frames (ORFs) that encode four proteins. The viral RNA encodes two large replication-associated proteins (ORF1: 183.0 kDa, ORF2: 126.0 kDa, RAP), a movement protein (ORF3: 30.0 kDa, MP), and a

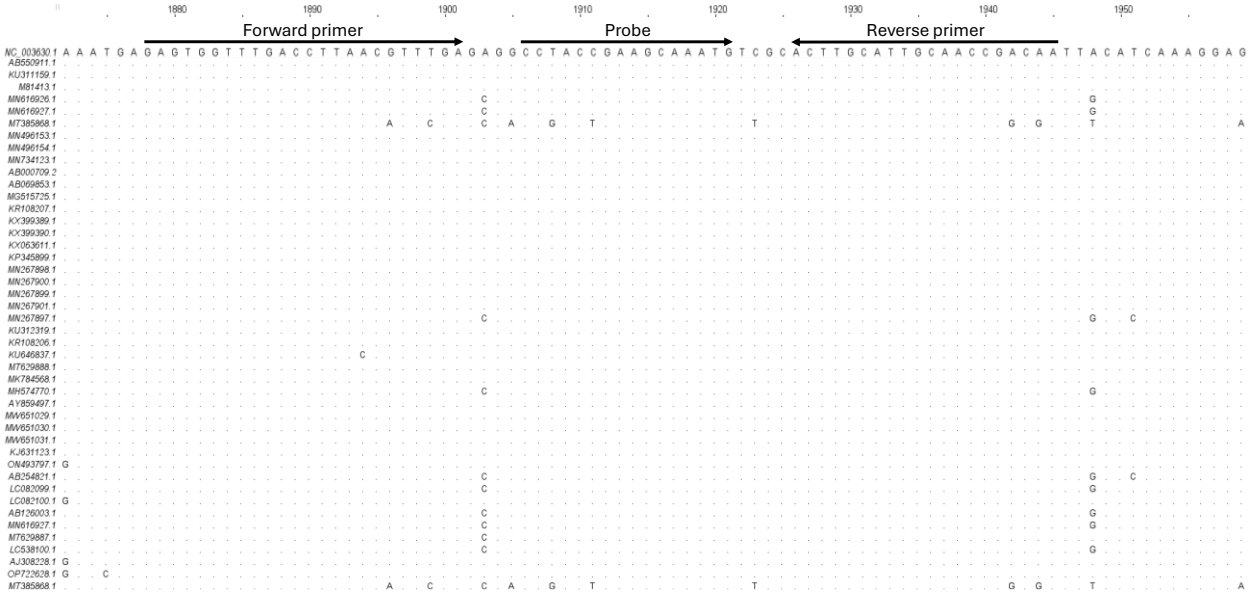


Figure 7-8. Alignment of the primers and probe of the "benchmark" PMMoV assay proposed in this study. The primers and probe are aligned with 45 full-genome sequences of PMMoV to highlight any nucleotide mismatches.

capsid/coat protein (ORF4: 17.3 kDa, CP) (Adams et al., 2017; Gibbs, 1999). In this case, both assays are located in the ORF1 (and ORF2), before the leaky stop codon at nucleotide 3423 that allows for RNA translation readthrough (Luria et al., 2018). The presence of both assays in the ORF1/ORF2 region of PMMoV is somewhat expected, due to the genomic structure of PMMoV and genomic RNA protection conferred by the exterior capsid proteins.

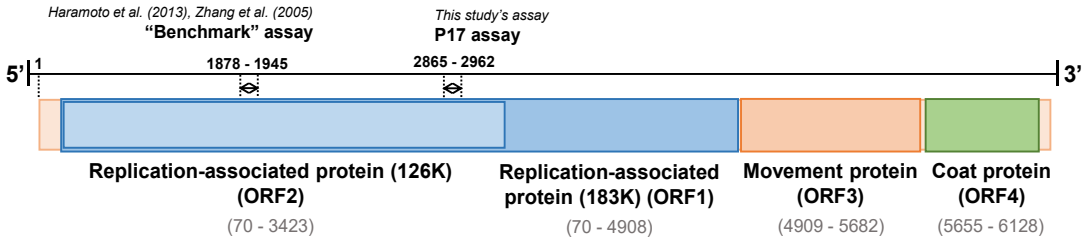


Figure 7-9. Genomic map of the 6.4 kb genome of PMMoV, highlighting the four major ORFs, and the location of the benchmark and P17 PMMoV assays.

7.3.6. Evaluating the P17 PMMoV assay

As a result of the findings above, total RNA was extracted from 29 wastewater samples and a hot pepper sauce control were analyzed using both the benchmark and P17 assays. All samples were run in PCR technical triplicates. It was observed that in 56.7% (17/30) of the tested samples, the P17 assay was slightly more sensitive than the benchmark assay (Table 7-6). In one sample, the P17 assay reported no detects in all technical replicates while the benchmark assay reported an average Ct value of 39.72 ± 0.02). PMMoV RNA concentrations measured using the P17 assay were on average 10.7% greater (i.e., 0.15 Ct lower) than the benchmark assay. This change/improvement was significant in 30.0% (9/30) of tested samples (changes/improvements were considered significant improvements when the average ΔCt between the two assays exceeded the summed standard deviations of each assay). The P17 assay's ALOD and ALOQ were determined to be 3.4 copies/reaction and 4.9 copies/reaction, respectively, while those of the benchmark assay were previously calculated (unpublished) to be 6.8 copies/reaction and 8.2 copies/reaction, respectively. Extraction, process, and assay blanks run throughout the experiment were negative (>= 45 Ct) using either assay. These results confirm that the P17 assay exhibits diagnostic sensitivity and specificity equivalent to the benchmark assay, effectively detecting PMMoV RNA in both wastewater and hot sauce extracts while maintaining non-detects in negative samples.

Table 7-6. Validation of the benchmark and P17 PMMoV assays. This table provides shows a summary of PMMoV RNA measurements in 29 samples and one control, comparing both PMMoV assays. The RNA concentrations are expressed and compared as Ct values.

Sample	*Sample ID*	*Location*	*Benchmark PMMoV assay (Ct)*	*P17 PMMoV assay (Ct)*	*Significant improvement? (Y/N)*
Pepper mild mottle virus (in wastewater)	BD-DH-01	Dhaka (BD)	34.93 ± 0.16	34.84 ± 0.32	N
	BD-GP-02	Gazipur (BD)	34.68 ± 0.10	34.37 ± 0.43	N
	BD-KG-03	Kereniganj (BD)	37.51 ± 0.23	36.74 ± 0.41	Y
	BD-UT-04	Uttara (BD)	33.16 ± 0.06	32.88 ± 0.23	N
	BD-JU-05	Manikganj (BD)	31.73 ± 0.29	31.14 ± 0.03	Y
	BD-HJ-06	Narayanganj (BD)	39.72 ± 0.02	*n.d.*	*N*
	SP-GN-01	Granada (ES)	29.59 ± 0.24	28.92 ± 0.03	Y
	SP-GN-02	Granada (ES)	30.54 ± 0.14	30.27 ± 0.11	Y
	SP-GN-03	Granada (ES)	30.68 ± 0.08	30.22 ± 0.08	Y
	SP-GN-04	Granada (ES)	30.44 ± 0.05	29.88 ± 0.17	Y
	SP-GN-05	Granada (ES)	29.84 ± 0.06	29.14 ± 0.04	Y
	SP-GN-06	Granada (ES)	30.25 ± 0.12	29.63 ± 0.10	Y
	Woodland 3-7-22	Woodland (US)	31.13 ± 0.04	31.48 ± 0.13	N
	Winters 3-1-22	Winters (US)	28.73 ± 0.04	29.20 ± 0.09	N
	Esparto 3-11-22	Esparto (US)	30.06 ± 0.42	29.82 ± 0.44	N
	Modesto 3-3-22	Modesto (US)	30.15 ± 0.03	30.59 ± 0.04	N
	JR 1028	Virginia (US)	32.35 ± 0.15	32.22 ± 0.19	N
	AT 1110	Virginia (US)	33.89 ± 0.26	33.89 ± 0.36	N
	VIP 1010	Virginia (US)	33.24 ± 0.17	33.84 ± 0.33	N
	AB 0955	Virginia (US)	33.53 ± 0.27	33.71 ± 0.25	N
	S0077	Limassol (CY)	32.86 ± 0.19	32.92 ± 0.20	N
	S0075	Vathia Gonia (CY)	32.97 ± 0.11	32.81 ± 0.18	N
	S0072	Anthapoli (CY)	33.45 ± 0.23	34.18 ± 0.22	N
	S0161	Agva (TR)	28.09 ± 0.13	28.54 ± 0.21	N
	S0162	Dogan (TR)	29.69 ± 0.28	29.73 ± 0.51	N
	S0157	Tuzla (TR)	30.11 ± 0.30	30.03 ± 0.68	N
	S0159	Pasakoy (TR)	27.85 ± 0.44	28.08 ± 0.60	N
	S0158	Amboli (TR)	23.80 ± 0.52	23.82 ± 0.49	N
	S0160	Paşabahçe (TR)	27.80 ± 0.27	27.10 ± 0.17	Y
Hot pepper sauce	Pep_Sauce 1	*Multiple locations*[†]	31.67 ± 0.08	30.46 ± 0.14	Y

[a] This number is the amplification cycle number where the measured fluorescence on the quantitative PCR unit crossed the threshold of baseline, called the cycle threshold (Ct). If no amplification was measured within 45 cycles, the mention *n.d.* (not detected) is given. All sample analysis results shown in this table were tested as technical triplicates. The ΔCt is measured as the difference between the two compared assays' mean Ct values. A significant improvement in the P17 PMMoV assay over the benchmark PMMoV assay is demonstrated when the average ΔCt between the two assays exceeds the summed standard deviations of each assay.

[†] The exact growing locations of the peppers used in the fabrication of the hot sauce are not fully disclosed, however growing locations include a location in the United States and locations in Central America, South America, and Africa (Narishkin et al., 2023).

Within the confines of our experiments, the P17 assay appeared slightly more sensitive (higher measured RNA concentrations in the same samples) compared to the "benchmark assay. This result is at first surprising as the "benchmark" assay's amplicon is significantly shorter (68 bp, GC% = 48.53) than the P17 assay's (98 bp, GC% = 45.92), which should, in theory, lead to higher sensitivity. It is hypothesized that the universal assay locus might have a lower tendency to form RNA secondary structures, which could enhance reverse transcription (RT) efficiency and contribute to the higher sensitivity observed in the universal assay.

Beyond these results, the authors note that in addition to globally validating the P17 PMMoV assay, they have also done so for the benchmark PMMoV assay, allowing increased interoperability of existing WEM data sets where PMMoV was analyzed using the benchmark assay. Furthermore, this study also provides ready-built overlapping PCR assays spanning >96% of the PMMoV genome, which provides a

simple, validated pathway for future studies to rapidly sequence the PMMoV genome via readily available short-read next-generation sequencing technologies, even in degraded or fragmented genomes found from environmental samples.

With these results in mind, the authors wish to point out one important caveat and limitation to the study was the lack of normalization of measured RNA concentrations in wastewater by the mass of solids present in the samples. Due to the nature of the samples and the method of preservation using Zymo's DNA/RNA shield solution, the mass of salts imparted by the storage solution masked the mass (and concentration) of solids present endogenously in the samples. It has been shown in the past that mass-normalization can be helpful in improving interpretation and usability of WEM data for pathogens of interest such as SARS-CoV-2 or influenza, but not specifically for PMMoV.

7.4. Conclusion

This study has successfully developed a globally applicable assay for the detection and quantification of PMMoV RNA in wastewater, a critical biomarker for WEM. Through the analysis of wastewater samples spanning diverse geographical sites in 12 countries, we identified a highly conserved locus within the PMMoV genome that enables more consistent and sensitive RNA detection and quantification in wastewater. This study also demonstrates that PMMoV RNA concentrations in wastewater throughout the world are similar despite geographical and dietary differences, and that the size and population of sampled sewersheds do not appear to have a strong relationship with the measured PMMoV RNA concentrations. The P17 PMMoV RT-qPCR assay performs as well or better than the widely used benchmark assay, thus potentially offering improved sensitivity in real-world wastewater samples. This new assay provides a valuable tool for enhancing the sensitivity of future WEM data sets and supports the broader adoption of PMMoV as a normalization biomarker in global wastewater surveillance.

CRediT authorship contribution statement

Patrick M. D'Aoust contributed to Writing – original draft, Conceptualization, Visualization, Methodology, Investigation, Formal analysis, and Data Curation. **Chandler H. Wong** contributed to Methodology and Investigation. **Tram B. Nguyen** contributed to Methodology and Investigation. **Tyson E. Graber** contributed to Supervision, Conceptualization, Methodology, Investigation, and Writing – review & editing. **Robert Delatolla** contributed to Supervision, Conceptualization, and Writing – review & editing. **Shen Wan, Elizabeth M. Renouf, Raul Gonzalez, Parthenopi Karaolia, Bilge Alpaslan Kocamemi, Anna Maria, Cresten Mansfeldt, Despo Fatta-Kassinos, Dominic Frigon, Sukriye Celikkol, Kevin Murmane, Colleen C. Naughton, Masaaki Kitajima, Anna J. Székely, Syeda Tasneem Towhid, Emanuel Wyler, and Ryan Ziels** contributed to Sample collection and Writing – review & editing.

7.5. Limitations and 2025 field updates

This chapter develops a new PMMoV detection and quantification assay and compares to the existing benchmark PMMoV assay with several global samples. Since the time of writing, a few limitations have been identified: 1) In order to limit sample integrity or degradation issues caused by potential cold-chain breakdowns, samples were shipped from collaborators using DNA/RNA shield, which limited the volume of received samples to less than 15 mL total volume. As a result, the mass and solids content of the samples could not be reliably recorded and were excluded from the analysis. The volume of received wastewater was too low to obtain representative, replicate measurements. Additionally, the use of DNA/RNA Shield - a solution with a high concentration of salts and other solutes—partially masked the original solids measurements, further complicating accurate assessment. The interpretation of the results could differ when normalizing or standardizing the PMMoV RNA concentrations for the mass of solids present in the samples; and 2) The use of PMMoV as a biomarker continues to be debated for some researchers (Goitom et al., 2024; Rosengart et al., 2022) as it is argued that the use of PMMoV may not be a good normalizer in certain WEM contexts. Finally, the relevance of the findings in this study may decrease if the usage of PMMoV diminishes over time, or when a more effective normalization biomarker arises.

7.6. Declaration of competing interest

The authors declare that they have no known competing financial or personal interests that could have appeared to influence the work or results reported in this manuscript.

7.7. Ethical considerations

This study did not involve human participants or animals and did not require ethical approval.

7.8. Funding

This research was supported by the Province of Ontario's Wastewater Surveillance Initiative (WSI).

7.9. Acknowledgments

The authors would like to acknowledge the invaluable help and assistance provided by all wastewater and water operators, municipal staff, administrative staff, and laboratory support members which made this study possible by helping us gather samples from global locations.

7.10. References

Adams, C., Kirby, A.E., Bias, M., Riser, A., Wong, K.K., Mercante, J.W., Reese, H., 2024. Detecting Mpox Cases Through Wastewater Surveillance — United States, August 2022–May 2023. MMWR. Morb. Mortal. Wkly. Rep. 73, 37–43. https://doi.org/10.15585/MMWR.MM7302A3

Adams, M.J., Adkins, S., Bragard, C., Gilmer, D., Li, D., MacFarlane, S.A., Wong, S.M., Melcher, U., Ratti, C., Ryu, K.H., 2017. ICTV virus taxonomy profile: Virgaviridae. J. Gen. Virol. 98, 1999–2000. https://doi.org/10.1099/JGV.0.000884

Ahmed, W., Angel, N., Edson, J., Bibby, K., Bivins, A., O'Brien, J.W., Choi, P.M., Kitajima, M., Simpson, S.L., Li, J., Tscharke, B., Verhagen, R., Smith, W.J.M., Zaugg, J., Dierens, L., Hugenholtz, P., Thomas, K. V., Mueller, J.F., 2020. First confirmed detection of SARS-CoV-2 in untreated wastewater in Australia: A proof of concept for the wastewater surveillance of COVID-19 in the community. Sci. Total Environ. 728, 138764. https://doi.org/10.1016/j.scitotenv.2020.138764

Altschul, S.F., Gish, W., Miller, W., Myers, E.W., Lipman, D.J., 1990. Basic local alignment search tool. J. Mol. Biol. 215, 403–410. https://doi.org/10.1016/S0022-2836(05)80360-2

Antkiewicz, D.S., Janssen, K.H., Roguet, A., Pilch, H.E., Fahney, R.B., Mullen, P.A., Knuth, G.N., Everett, D.G., Doolittle, E.M., King, K., Wood, C., Stanley, A., Hemming, J.D.C., Shafer, M.M., 2024. Wastewater-based protocols for SARS-CoV-2: insights into virus concentration, extraction, and quantitation methods from two years of public health surveillance. Environ. Sci. Water Res. Technol. 10. https://doi.org/10.1039/d3ew00958k

Atabakhsh, P., Kargar, M., Doosti, A., 2020. Molecular detection and genotyping of group A rotavirus in two wastewater treatment plants, Iran. Brazilian J. Microbiol. 51, 197–203. https://doi.org/10.1007/s42770-019-00131-0

Bertels, X., Demeyer, P., Van den Bogaert, S., Boogaerts, T., van Nuijs, A.L.N., Delputte, P., Lahousse, L., 2022. Factors influencing SARS-CoV-2 RNA concentrations in wastewater up to the sampling stage: A systematic review. Sci. Total Environ. 820, 153290. https://doi.org/10.1016/j.scitotenv.2022.153290

Bisseux, M., Didier, D., Audrey, M., Christine, A., Hélène, P.L., Jean-Luc, B., Cécile, H., 2020. Monitoring of enterovirus diversity in wastewater by ultra-deep sequencing: An effective complementary tool for clinical enterovirus surveillance. Water Res. 169. https://doi.org/10.1016/j.watres.2019.115246

Bloomer, A.C., Champness, J.N., Bricogne, G., Staden, R., Klug, A., 1978. Protein disk of tobacco mosaic virus at 2.8 resolution showing the interactions within and between subunits. Nature 276, 362–368. https://doi.org/10.1038/276362a0

Boehm, A.B., Hughes, B., Duong, D., Chan-Herur, V., Buchman, A., Wolfe, M.K., White, B.J., 2023a. Wastewater concentrations of human influenza, metapneumovirus, parainfluenza, respiratory syncytial virus, rhinovirus, and seasonal coronavirus nucleic-acids during the COVID-19 pandemic: a surveillance study. The Lancet Microbe 4, e340–e348. https://doi.org/10.1016/S2666-5247(22)00386-X

Boehm, A.B., Wolfe, M.K., White, B.J., Hughes, B., Duong, D., Banaei, N., Bidwell, A., 2023b. Human norovirus (HuNoV) GII RNA in wastewater solids at 145 United States wastewater treatment plants: comparison to positivity rates of clinical specimens and modeled estimates of HuNoV GII shedders. J. Expo. Sci. Environ. Epidemiol. 3–10. https://doi.org/10.1038/s41370-023-00592-4

Brinkman, N.E., Fout, G.S., Keely, S.P., 2017. Retrospective Surveillance of Wastewater To Examine Seasonal Dynamics of Enterovirus Infections. mSphere 2. https://doi.org/10.1128/msphere.00099-17

Castello, J.D., Lakshman, D.K., Tavantzis, S.M., Rogers, S.O., Bachand, G.D., Jagels, R., Carlisle, J., Liu, Y., 1995. Detection of infectious tomato mosaic tobamovirus in fog and clouds. Phytopathology. https://doi.org/10.1094/Phyto-85-1409

Cervantes-Avilés, P., Moreno-Andrade, I., Carrillo-Reyes, J., 2021. Approaches applied to detect SARS-CoV-2 in wastewater and perspectives post-COVID-19. J. Water Process Eng. 40. https://doi.org/10.1016/j.jwpe.2021.101947

Chettleburgh, C., Ma, S.X., Swinwood-Sky, M., McDougall, H., Kireina, D., Taggar, G., McBean, E., Parreira, V., Goodridge, L., Habash, M., 2023. Evaluation of four human-associated fecal biomarkers in wastewater in Southern Ontario. Sci. Total Environ. 904, 166542. https://doi.org/10.1016/j.scitotenv.2023.166542

Chik, A.H.S., Glier, M.B., Servos, M., Mangat, C.S., Pang, X.L., Qiu, Y., D'Aoust, P.M., Burnet, J.B., Delatolla, R., Dorner, S., Geng, Q., Giesy, J.P., McKay, R.M., Mulvey, M.R., Prystajecky, N., Srikanthan, N., Xie, Y., Conant, B., Hrudey, S.E., 2021. Comparison of approaches to quantify SARS-CoV-2 in wastewater using RT-qPCR: Results and implications from a collaborative inter-laboratory study in Canada. J. Environ. Sci. 107, 218–229. https://doi.org/10.1016/j.jes.2021.01.029

D'Aoust, P.M., Graber, T.E., Mercier, E., Montpetit, D., Alexandrov, I., Neault, N., Baig, A.T., Mayne, J., Zhang, X., Alain, T., Servos, M.R., Srikanthan, N., MacKenzie, M., Figeys, D., Manuel, D., Jüni, P., MacKenzie, A.E., Delatolla, R., 2021a. Catching a resurgence: Increase in SARS-CoV-2 viral RNA identified in wastewater 48 h before COVID-19 clinical tests and 96 h before hospitalizations. Sci. Total Environ. 770, 145319. https://doi.org/10.1016/j.scitotenv.2021.145319

D'Aoust, P.M., Mercier, É., Montpetit, D., Jia, J., Alexandrov, I., Neault, N., Baig, A.T., Mayne, J., Zhang, X., Alain, T., Langlois, M.-A., Servos, M.R., MacKenzie, M., Figeys, D., MacKenzie, A.E., Graber, T.E., Delatolla, R., 2021b. Quantitative analysis of SARS-CoV-2 RNA from wastewater solids in communities with low COVID-19 incidence and prevalence. Water Res. 188, 116560. https://doi.org/10.1016/j.watres.2020.116560

Daughton, C.G., 2020. Wastewater surveillance for population-wide Covid-19: The present and future. Sci. Total Environ. 736, 139631. https://doi.org/10.1016/j.scitotenv.2020.139631

Davis, A., Keely, S.P., Brinkman, N.E., Bohrer, Z., Ai, Y., Mou, X., Chattopadhyay, S., Hershey, O., Senko, J., Hull, N., Lytmer, E., Quintero, A., Lee, J., 2023. Evaluation of intra- and inter-lab variability in quantifying SARS-CoV-2 in a state-wide wastewater monitoring network. Environ. Sci. Water Res. Technol. 9, 1053–1068. https://doi.org/10.1039/d2ew00737a

Dunkin, N., Weng, S.C., Coulter, C.G., Jacangelo, J.G., Schwab, K.J., 2018. Impacts of virus processing on human norovirus GI and GII persistence during disinfection of municipal secondary wastewater effluent. Water Res. 134, 1–12. https://doi.org/10.1016/j.watres.2018.01.053

Elmahdy, E.M., Shaheen, M.N.F., Rizk, N.M., Saad-Hussein, A., 2020. Quantitative Detection of Human Adenovirus and Human Rotavirus Group A in Wastewater and El-Rahawy Drainage Canal Influencing River Nile in the North of Giza, Egypt. Food Environ. Virol. 12, 218–225. https://doi.org/10.1007/s12560-020-09429-x

Endo, N., Hisahara, A., Kameda, Y., Mochizuki, K., Kitajima, M., Yasojima, M., Daigo, F., Takemori, H., Nakamura, M., Matsuda, R., Iwamoto, R., Nojima, Y., Ihara, M., Tanaka, H., 2024. Enabling quantitative comparison of wastewater surveillance data across methods through data standardization without method standardization. Sci. Total Environ. 953. https://doi.org/10.1016/j.scitotenv.2024.176073

Fantilli, A., Cola, G. Di, Castro, G., Sicilia, P., Cachi, A.M., de los Ángeles Marinzalda, M., Ibarra, G., López, L., Valduvino, C., Barbás, G., Nates, S., Masachessi, G., Pisano, M.B., Ré, V., 2023. Hepatitis A virus monitoring in wastewater: A complementary tool to clinical surveillance. Water Res. 241. https://doi.org/10.1016/j.watres.2023.120102

Fillhart, R.C., Bachand, G.D., Castello, J.D., 1998. Detection of infectious tobamoviruses in forest soils. Appl. Environ. Microbiol. 64, 1430–1435. https://doi.org/10.1128/aem.64.4.1430-1435.1998

Forootan, A., Sjöback, R., Björkman, J., Sjögreen, B., Linz, L., Kubista, M., 2017. Methods to determine limit of detection and limit of quantification in quantitative real-time PCR (qPCR). Biomol. Detect. Quantif. 12, 1–6. https://doi.org/10.1016/j.bdq.2017.04.001

Gibbs, A., 1999. Evolution and origins of tobamoviruses. Philos. Trans. R. Soc. B Biol. Sci. 354, 593–602. https://doi.org/10.1098/rstb.1999.0411

Goitom, E., Ariano, S., Gilbride, K., Yang, M.I., Edwards, E.A., Peng, H., Dannah, N., Farahbakhsh, F., Hataley, E., Sarvi, H., Sun, J., Waseem, H., Oswald, C., 2024. Identification of environmental and methodological factors driving variability of Pepper Mild Mottle Virus (PMMoV) across three wastewater treatment plants in the City of Toronto. Sci. Total Environ. 932, 172917. https://doi.org/10.1016/j.scitotenv.2024.172917

Graham, K.E., Loeb, S.K., Wolfe, M.K., Catoe, D., Sinnott-Armstrong, N., Kim, S., Yamahara, K.M., Sassoubre, L.M., Mendoza Grijalva, L.M., Roldan-Hernandez, L., Langenfeld, K., Wigginton, K.R., Boehm, A.B., 2021. SARS-CoV-2 RNA in Wastewater Settled Solids Is Associated with COVID-19 Cases in a Large Urban Sewershed. Environ. Sci. Technol. 55, 488–498. https://doi.org/10.1021/acs.est.0c06191

Haramoto, E., Kitajima, M., Kishida, N., Konno, Y., Katayama, H., Asami, M., Akiba, M., 2013. Occurrence of pepper mild mottle virus in drinking water sources in Japan. Appl. Environ. Microbiol. 79, 7413–7418. https://doi.org/10.1128/AEM.02354-13

He, X.Q., Cheng, L., Li, W., Xie, X.M., Ma, M., Wang, Z.J., 2008. Detection and distribution of rotavirus in municipal sewage treatment plants (STPs) and surface water in Beijing. J. Environ. Sci. Heal. - Part A Toxic/Hazardous Subst. Environ. Eng. 43, 424–429. https://doi.org/10.1080/10934520701795731

Holm, R.H., Nagarkar, M., Yeager, R.A., Talley, D., Chaney, A.C., Rai, J.P., Mukherjee, A., Rai, S.N., Bhatnagar, A., Smith, T., 2022. Surveillance of RNase P, PMMoV, and CrAssphage in wastewater as indicators of human fecal concentration across urban sewer neighborhoods, Kentucky. FEMS Microbes 3, 1–12. https://doi.org/10.1093/femsmc/xtac003

Hotta, C., Fujinuma, Y., Ogawa, Takashi, Akita, M., Ogawa, Tomoko, 2024. Surveillance of Wastewater to Monitor the Prevalence of Gastroenteritis Viruses in Chiba Prefecture (2014–2019). J. Epidemiol. 34, 195–202. https://doi.org/10.2188/jea.JE20220305

Hughes, B., Duong, D., White, B.J., Wigginton, K.R., Chan, E.M.G.G., Wolfe, M.K., Boehm, A.B., 2022. Respiratory Syncytial Virus (RSV) RNA in Wastewater Settled Solids Reflects RSV Clinical Positivity Rates. Environ. Sci. Technol. Lett. 9, 173–178. https://doi.org/10.1021/acs.estlett.1c00963

Kitajima, M., Sassi, H.P., Torrey, J.R., 2018. Pepper mild mottle virus as a water quality indicator. npj Clean Water 1. https://doi.org/10.1038/s41545-018-0019-5

Lopez-Roblero, A., Martínez Cano, D.J., Diego-García, E., Guillén-Navarro, G.K., Iša, P., Zarza, E., 2024. Metagenomic analysis of plant viruses in tropical fresh and wastewater. Environ. DNA 6, 1–13. https://doi.org/10.1002/edn3.416

Maal-Bared, R., Qiu, Y., Li, Q., Gao, T., Hrudey, S.E., Bhavanam, S., Ruecker, N.J., Ellehoj, E., Lee, B.E., Pang, X., 2023. Does normalization of SARS-CoV-2 concentrations by Pepper Mild Mottle Virus improve correlations and lead time between wastewater surveillance and clinical data in Alberta (Canada): comparing twelve SARS-CoV-2 normalization approaches. Sci. Total Environ. 856, 158964. https://doi.org/10.1016/j.scitotenv.2022.158964

Malla, B., Shrestha, S., Sthapit, N., Hirai, S., Raya, S., Rahmani, A.F., Angga, M.S., Siri, Y., Ruti, A.A., Haramoto, E., 2024. Beyond COVID-19: Wastewater-based epidemiology for multipathogen surveillance and normalization strategies. Sci. Total Environ. 946, 174419. https://doi.org/10.1016/j.scitotenv.2024.174419

Mazumder, P., Dash, S., Honda, R., Sonne, C., Kumar, M., 2022. Sewage surveillance for SARS-CoV-2: Molecular detection, quantification, and normalization factors. Curr. Opin. Environ. Sci. Heal. 28, 100363. https://doi.org/10.1016/j.coesh.2022.100363

Mercier, E., D'Aoust, P.M., Renouf, E., Tomalty, E., Addo, F.G., Nguyen, T.B., Wong, C.H., Ramsay, N., Tian, X., Hegazy, N., Kabir, M.P., Jia, J.-J., Wan, S., Pisharody, L., Szulc, P., Mackenzie, A.E., Delatolla, R., 2024. Effective Method to Mitigate Impact of Rain or Snowmelt Sewer Flushing Events on Wastewater-Based Surveillance Measurements. SSRN Prepr. https://doi.org/10.2139/SSRN.4895052

Mercier, E., D'Aoust, P.M., Thakali, O., Hegazy, N., Jia, J.J., Zhang, Z., Eid, W., Plaza-Diaz, J., Kabir, M.P., Fang, W., Cowan, A., Stephenson, S.E., Pisharody, L., MacKenzie, A.E., Graber, T.E., Wan, S., Delatolla, R., 2022. Municipal and neighbourhood level wastewater surveillance and subtyping of an influenza virus outbreak. Sci. Rep. 12, 2022.06.28.22276884. https://doi.org/10.1038/s41598-022-20076-z

Nash, D., Ellmen, I., Knapp, J.J., Menon, R., Overton, A.K., Cheng, J., Lynch, M.D.J., Nissimov, J.I., Charles, T.C., 2024. Brown Rugose Fruit Virus (ToBRFV) Genome Reveals Widespread Province of Ontario , Canada.

Pang, X., Gao, T., Ellehoj, E., Li, Q., Qiu, Y., Maal-Bared, R., Sikora, C., Tipples, G., Diggle, M., Hinshaw, D., Ashbolt, N.J., Talbot, J., Hrudey, S.E., Lee, B.E., 2022. Wastewater-Based Surveillance Is an Effective Tool for Trending COVID-19 Prevalence in Communities: A Study of 10 Major Communities for 17 Months in Alberta. ACS ES T Water 2, 2243–2254. https://doi.org/10.1021/ACSESTWATER.2C00143/ASSET/IMAGES/LARGE/EW2C00143_0004.JPEG

Polo, D., Quintela-Baluja, M., Corbishley, A., Jones, D.L., Singer, A.C., Graham, D.W., Romalde, J.L., 2020. Making waves: Wastewater-based epidemiology for COVID-19 – approaches and challenges for surveillance and prediction. Water Res. 186, 116404. https://doi.org/10.1016/j.watres.2020.116404

Rao, G.P., Reddy, M.G., 2020. Overview of yield losses due to plant viruses, Applied Plant Virology: Advances, Detection, and Antiviral Strategies. INC. https://doi.org/10.1016/B978-0-12-818654-1.00038-4

Roldan-Hernandez, L., Graham, K.E., Duong, D., Boehm, A.B., 2022. Persistence of Endogenous SARS-CoV-2 and Pepper Mild Mottle Virus RNA in Wastewater-Settled Solids. ACS Environ. Sci. Technol. Water. https://doi.org/10.1021/acsestwater.2c00003

Rosario, K., Symonds, E.M., Sinigalliano, C., Stewart, J., Breitbart, M., 2009. Pepper mild mottle virus as an indicator of fecal pollution. Appl. Environ. Microbiol. 75, 7261–7267. https://doi.org/10.1128/AEM.00410-09

Rosengart, A.L., Bidwell, A.L., Wolfe, M.K., Boehm, A.B., Townes, F.W., 2024. Spatio-Temporal Variability of the Pepper Mild Mottle Virus Biomarker in Wastewater. https://doi.org/10.1021/acsestwater.4c00866

Rothman, J.A., Whiteson, K.L., 2022. Sequencing and Variant Detection of Eight Abundant Plant-Infecting Tobamoviruses across Southern California Wastewater. Microbiol. Spectr. 10. https://doi.org/10.1128/spectrum.03050-22

Rozen, S., Skaletsky, H., 2000. Primer3 on the WWW for general users and for biologist programmers. Methods Mol. Biol. 132, 365–386. https://doi.org/10.1385/1-59259-192-2:365

Sherchan, S.P., Malla, B., Haramoto, E., 2023. First quantitative detection of tomato brown rugose fruit virus in wastewater in Louisiana. Sci. Total Environ. 888, 164001. https://doi.org/10.1016/j.scitotenv.2023.164001

Smith, E., Dombrovsky, A., 2020. Aspects in Tobamovirus Management in Intensive Agriculture, in: Plant Diseases - Current Threats and Management Trends. https://doi.org/10.5772/intechopen.87101

Solovyev, A.G., Makarov, V. V., 2016. Helical capsids of plant viruses: Architecture with structural lability. J. Gen. Virol. 97, 1739–1754. https://doi.org/10.1099/jgv.0.000524

Symonds, E.M., Nguyen, K.H., Harwood, V.J., Breitbart, M., 2018. Pepper mild mottle virus: A plant pathogen with a greater purpose in (waste)water treatment development and public health management. Water Res. 144, 1–12. https://doi.org/10.1016/j.watres.2018.06.066

Toribio-Avedillo, D., Gómez-Gómez, C., Sala-Comorera, L., Rodríguez-Rubio, L., Carcereny, A., García-Pedemonte, D., Pintó, R.M., Guix, S., Galofré, B., Bosch, A., Merino, S., Muniesa, M., 2023.

Monitoring influenza and respiratory syncytial virus in wastewater. Beyond COVID-19. Sci. Total Environ. 892. https://doi.org/10.1016/j.scitotenv.2023.164495

Untergasser, A., Cutcutache, I., Koressaar, T., Ye, J., Faircloth, B.C., Remm, M., Rozen, S.G., 2012. Primer3-new capabilities and interfaces. Nucleic Acids Res. 40, 1–12. https://doi.org/10.1093/nar/gks596

van Baren, M.J., Heutink, P., 2004. The PCR suite. Bioinformatics 20, 591–593. https://doi.org/10.1093/bioinformatics/btg473

Wade, M.J., Lo Jacomo, A., Armenise, E., Brown, M.R., Bunce, J.T., Cameron, G.J., Fang, Z., Farkas, K., Gilpin, D.F., Graham, D.W., Grimsley, J.M.S., Hart, A., Hoffmann, T., Jackson, K.J., Jones, D.L., Lilley, C.J., McGrath, J.W., McKinley, J.M., McSparron, C., Nejad, B.F., Morvan, M., Quintela-Baluja, M., Roberts, A.M.I., Singer, A.C., Souque, C., Speight, V.L., Sweetapple, C., Walker, D., Watts, G., Weightman, A., Kasprzyk-Hordern, B., 2022. Understanding and managing uncertainty and variability for wastewater monitoring beyond the pandemic: Lessons learned from the United Kingdom national COVID-19 surveillance programmes. J. Hazard. Mater. 424. https://doi.org/10.1016/j.jhazmat.2021.127456

Wolfe, M.K., Archana, A., Catoe, D., Coffman, M.M., Dorevich, S., Graham, K.E., Kim, S., Grijalva, L.M., Roldan-Hernandez, L., Silverman, A.I., Sinnott-Armstrong, N., Vugia, D.J., Yu, A.T., Zambrana, W., Wigginton, K.R., Boehm, A.B., 2021. Scaling of SARS-CoV-2 RNA in Settled Solids from Multiple Wastewater Treatment Plants to Compare Incidence Rates of Laboratory-Confirmed COVID-19 in Their Sewersheds. Environ. Sci. Technol. Lett. https://doi.org/10.1021/acs.estlett.1c00184

Wolfe, M.K., Duong, D., Bakker, K.M., Ammerman, M., Mortenson, L., Hughes, B., Arts, P., Lauring, A.S., Fitzsimmons, W.J., Bendall, E., Hwang, C.E., Martin, E.T., White, B.J., Boehm, A.B., Wigginton, K.R., 2022. Wastewater-Based Detection of Two Influenza Outbreaks. Environ. Sci. Technol. Lett. https://doi.org/10.1021/acs.estlett.2c00350

Wolfe, M.K., Duong, D., Shelden, B., Chan, E.M.G., Chan-Herur, V., Hilton, S., Paulos, A.H., Xu, X.R.S., Zulli, A., White, B.J., Boehm, A.B., 2024. Detection of Hemagglutinin H5 Influenza A Virus Sequence in Municipal Wastewater Solids at Wastewater Treatment Plants with Increases in Influenza A in Spring, 2024. Environ. Sci. Technol. Lett. 11, 526–532. https://doi.org/10.1021/acs.estlett.4c00331

Wolfe, M.K., Yu, A.T., Duong, D., Rane, M.S., Hughes, B., Chan-Herur, V., Donnelly, M., Chai, S., White, B.J., Vugia, D.J., Boehm, A.B., 2023. Use of Wastewater for Mpox Outbreak Surveillance in California. N. Engl. J. Med. https://doi.org/10.1056/nejmc2213882

Wong, C.H., Zhang, Z., Eid, W., Plaza-Diaz, J., Kabir, P., Wan, S., Jia, J.J., Mercier, E., Thakali, O., Pisharody, L., Hegazy, N., Stephenson, S.E., Fang, W., Nguyen, T.B., Ramsay, N.T., McKay, R.M., Corchis-Scott, R., MacKenzie, A.E., Graber, T.E., D' Aoust, P.M., Delatolla, R., 2023. Rapidly developed, optimized, and applied wastewater surveillance system for real-time monitoring of low-incidence, high-impact MPOX outbreak. J. Water Health 21, 1264–1276. https://doi.org/10.2166/WH.2023.145

Wu, F., Lee, W.L., Chen, H., Gu, X., Chandra, F., Armas, F., Xiao, A., Leifels, M., Rhode, S.F., Wuertz, S., Thompson, J., Alm, E.J., 2022. Making waves: Wastewater surveillance of SARS-CoV-2 in an endemic future. Water Res. 219, 118535. https://doi.org/10.1016/j.watres.2022.118535

Zambrana, W., Huang, C., Solis, D., Sahoo, M.K., Pinsky, B.A., Boehm, A.B., 2024. Spatial and temporal variation in respiratory syncytial virus (RSV) subtype RNA in wastewater and relation to clinical specimens. mSphere. https://doi.org/10.1128/msphere.00224-24

Zhang, T., Breitbart, M., Lee, W.H., Run, J.Q., Wei, C.L., Soh, S.W.L., Hibberd, M.L., Liu, E.T., Rohwer, F., Ruan, Y., 2006. RNA viral community in human feces: Prevalence of plant pathogenic viruses. PLoS Biol. 4, 0108–0118. https://doi.org/10.1371/journal.pbio.0040003

Zheng, X., Li, S., Deng, Y., Xu, X., Ding, J., Lau, F.T.K., In Yau, C., Poon, L.L.M., Tun, H.M., Zhang, T., 2022. Quantification of SARS-CoV-2 RNA in wastewater treatment plants mirrors the pandemic trend in Hong Kong. Sci. Total Environ. 844, 157121. https://doi.org/10.1016/j.scitotenv.2022.157121

Chapter 8 – Discussion and Conclusion

This dissertation has made transformative contributions to WEM, showcasing its effectiveness as a scalable and reliable tool for public health monitoring. These contributions are particularly significant in light of the COVID-19 pandemic, which highlighted an urgent need for innovative, community-wide health monitoring systems as traditional public health resources became overwhelmed. The first two studies in this dissertation served as pivotal benchmarks that informed subsequent research on the detection of SARS-CoV-2 RNA and other pathogens in wastewater across Canada. Early findings also played a crucial role in shaping and directing the Ontario Wastewater Surveillance Initiative (WSI) during its formative stages (Hrudey et al., 2022). This initiative evolved into the largest wastewater surveillance program in Canada and, at its peak, one of the most comprehensive wastewater monitoring efforts globally. Moreover, my research conclusively demonstrated the feasibility of wastewater surveillance for detecting traces of respiratory viruses in wastewater-associated solids, providing a robust framework for community health monitoring. The studies established a strong correlation between SARS-CoV-2 RNA concentrations in wastewater and clinical trends, confirming the reliability of wastewater-derived human health data as a valuable complement to traditional epidemiological metrics.

Notably, the first two studies of this research revealed that wastewater-based trends in SARS-CoV-2 RNA could serve as predictive indicators, offering early warnings of clinical surges and enabling proactive public health interventions. The third study in this dissertation further developed methodologies for SARS-CoV-2 surveillance in smaller rural communities operating facultative lagoons instead of mechanical wastewater treatment facilities. In the fourth study, we demonstrated that analyzing the relationship existing between SARS-CoV-2 RNA concentrations in wastewater to clinical cases (WC ratio) can potentially reveal fundamental changes in disease infection patterns. The fifth study of the dissertation then focused on the normalization of WEM measurements in wastewater with biomarkers by performing an extensive review of all known tobamoviruses and their potential use WEM signal normalizers. This was them followed by the sixth and final study of the dissertation, where PMMoV RNA concentrations were measured in samples from 12 different countries using a panel of overlapping PCR assays to determine the most preserved portions of the PMMoV genome, allowing us to propose a novel, globally validated RT-qPCR assay for PMMoV in wastewater. Throughout the dissertation, Chapters 2 through 7 collectively construct a cohesive narrative that systematically addresses critical gaps in knowledge, advancing the field and setting the stage for future innovations in WEM.

8.1. Optimization of sampling, detection and normalization of SARS-CoV-2 RNA in wastewater

Chapter 2 provided a comprehensive examination of methodologies to optimize the detection and quantification of SARS-CoV-2 RNA in wastewater solids and was the first study in Canada to do so, with a focus on PCS and PGS. The study established that PCS is the superior sample type for detecting viral RNA, with detection rates for SARS-CoV-2 N1 RNA reaching 92.7% in PCS compared to 79.2% in PGS. Similarly, N2 RNA detection rates were 90.6% for PCS and 82.3% for PGS, as shown in a three-month sampling period across 24 paired samples. The improved performance of PCS was attributed to its stability, higher solids content, and reduced susceptibility to variability caused by wastewater flowrate fluctuations and biochemical changes at the wastewater resource recovery facilities. Conversely, PGS samples exhibited greater variability and lower detection rates, likely due to lower solids content. The study also compared RT-qPCR and RT-ddPCR for quantifying SARS-CoV-2 RNA in PCS and PGS samples. Surprisingly, RT-qPCR demonstrated superior sensitivity, with detection limits of 2 copies/reaction for N1 and N2 regions, compared to 5 copies/reaction for RT-ddPCR. Quantitative results for PGS showed mean values of 133.4 ± 9.0 N1 gene copies/100 µL for RT-ddPCR and 167.1 ± 25.6 N1 gene copies/100 µL for RT-qPCR. For PCS, RT-qPCR detected 130.4 ± 20.8 N1 copies/100 µL, significantly outperforming RT-ddPCR, which detected only 33.5 ± 5.8 N1 copies/100 µL. The reduced performance of RT-ddPCR was attributed to the inhibition effects of the PCS matrix, which likely concentrated inhibitors in the small reaction droplets used in digital PCR. This finding contradicted theoretical expectations that RT-ddPCR would be less prone to inhibition, underscoring the importance of selecting appropriate molecular methods based on sample matrix composition. A significant contribution of this chapter was the validation of Pepper Mild Mottle Virus (PMMoV) as a reliable normalization biomarker. PMMoV exhibited low variability, with a Ct variance of 1.18 compared to 5.32 for the 16S rRNA biomarker and 5.12 for the 18S rRNA biomarker. When applied to SARS-CoV-2 RNA data, PMMoV normalization improved the signal-to-noise ratio, reducing the standard deviation of longitudinal data points and enhancing the ability to detect trends. PMMoV-normalized N1 and N2 signals in PCS showed strong correlations with epidemiological metrics, particularly the 7-day rolling average percent positivity ($R = 0.82$ for N1 in Ottawa, $p < 0.01$) and active cases ($R = 0.76$ for N1 in Gatineau, $p < 0.01$). During the studied period, RNA concentrations of the SARS-CoV-2's N1 region in PCS ranged from 1.7×10^3 to 7.8×10^4 copies/L in Ottawa and 6.6×10^4 to 3.8×10^5 copies/L in Gatineau. Without normalization, these data sets showed considerable variability, which was mitigated by PMMoV normalization. In contrast, mass-flux normalization did not significantly reduce variability, as solids flux in the primary clarifier stream was well-controlled and less variable than anticipated.

8.2. Predictive value and correlation of wastewater surveillance metrics

Once sensitive and reproducible methodologies to quantify SARS-CoV-2 RNA concentrations in wastewater were developed, we began investigating the ability of WEM to track and predict COVID-19 prevalence via conventional clinical metrics in Chapter 3. A significant finding of this study was the strong temporal and quantitative correlation between the PMMoV-normalized wastewater viral signal and new daily COVID-19 cases (N1: $r = 0.673$, $p < 0.001$; N2: $r = 0.648$, $p < 0.001$) as well as clinical testing percent positivity (N1: $r = 0.468$, $p < 0.001$; N2: $r = 0.404$, $p < 0.001$). These correlations confirmed that wastewater surveillance could serve as a reliable complement to clinical data, providing community-level insights into disease dynamics. Beyond mere complement to clinical data, time-step correlation analyses revealed that increases in SARS-CoV-2 RNA levels in PCS preceded rises in new daily cases and percent positivity by two days ($r = 0.703–0.721$, $p < 0.001$), demonstrating the predictive ability of WEM. Furthermore, wastewater signals were shown to predict hospitalizations with a lead time of four days (N1: $r = 0.741$, $p < 0.001$; N2: $r = 0.767$, $p < 0.001$). These findings support the use of WEM as an early warning system, offering public health resources critical lead time to respond to surges in infections. This study also attempted to compare data normalization approaches by comparing PMMoV, 16S and 18S biomarkers. The PMMoV normalization approach emerged as a key methodological advancement in this study. PMMoV demonstrated low temporal variability, with Ct values consistently showing lower variance compared to other normalization biomarkers or SARS-CoV-2 targets. This stability allowed the normalized SARS-CoV-2 RNA signal to better account for variability in wastewater composition, sample handling, and storage, thereby improving the interpretability and reliability of longitudinal data. It's believed that PMMoV-normalization reduced in SARS-CoV-2 RNA variations induced by the fecal content of wastewater-associated solids.

8.3. Extending wastewater surveillance to rural and small communities

Chapter 4 focused on adapting WEM methodologies for small and rural communities operating facultative lagoons as their wastewater treatment facility, addressing challenges caused by passive, low operational intensity wastewater treatment infrastructure. By comparing SARS-CoV-2 and PMMoV RNA concentration measurements in samples from upstream pumping stations and downstream lagoon systems, the study established that upstream sampling yielded stronger and more reliable SARS-CoV-2 RNA signals. Upstream samples exhibited detection rates of 92.7% (N1) and 90.6% (N2), whereas downstream lagoon samples had significantly lower detection rates, often affected by RNA degradation and dilution due to extended retention times in lagoons. The SARS-CoV-2 RNA concentrations in lagoon samples showed considerable variability, with coefficients of variation (%CV) exceeding 40%, compared to 29–32% for

upstream pumping station samples. This instability in lagoon systems was attributed to environmental and operational factors such as potential UV degradation of RNA and virions, and the use of coagulants for phosphorus control, impacting solid-liquid partitioning dynamics and making upstream pumping stations the preferred sampling location for rural WEM. The study highlighted that upstream samples not only demonstrated higher overall RNA concentrations but also provided more consistent correlations with community-level epidemiological data, such as active case counts and percent positivity.

8.4. WC ratio as a public health metric

Chapter 5 investigates the WC ratio as a novel method for integrating wastewater surveillance data with clinical epidemiological metrics. This analysis highlights its ability to identify underreported cases, track shifts in disease dynamics, and detect the emergence of SARS-CoV-2 variants of concern (VOCs) during the COVID-19 pandemic. The chapter demonstrates how the WC ratio responded to key epidemiological events, such as a change in clinical testing strategies in Ottawa in October 2020, which led to a 23.2% decrease in testing volume and a 16.8% drop in reported COVID-19 cases. Simultaneously, wastewater SARS-CoV-2 signal increased by 55.9%, resulting in a 189% surge in the WC ratio. This significant increase underscored the WC ratio's potential to highlight testing gaps and underreported infections in communities. Later in the study, the WC ratio's capacity to monitor the emergence of SARS-CoV-2 variants and their impact on disease dynamics is highlighted. During the onset of the Alpha variant (B.1.1.7), the WC ratio in Ottawa decreased by 56.3%, a shift attributed to the variant's increased transmissibility and potential changes in fecal shedding patterns. Similarly, the Delta variant (B.1.617.2) led to a modest 18.7% reduction in the WC ratio, likely dampened by higher vaccination rates (>60%) that reduced disease transmission and viral shedding. The Omicron variant (B.1.1.529), characterized by more significant immune escape capabilities, caused a more significant 41.9% decrease, reflecting its rapid spread despite high community immunization rates. These findings highlight the WC ratio's sensitivity to epidemiological shifts and its adaptability in diverse immunization contexts. The findings from this study show that actively monitoring the WC ratio during periods of increased infection can yield informative insights into disease dynamics.

8.5. The role of tobamoviruses in wastewater and environmental surveillance

Chapter 6 of this dissertation performs an extensive review of all known tobamoviruses as potential biomarkers for normalizing pathogen detection in WEM. We have examined the characteristics of these viruses, focusing particularly on their stability, prevalence, and association with human consumption through dietary sources to determine if they had previously been used in WEM and, if not, might be good

candidates for use in WEM. Out of the 43 identified tobamoviruses, only four (TMV, PMMoV, TBRFV, and CGMMV were recognized and employed as environmental and fecal biomarkers in WEM initiatives. The rationale for their selection stems from their prevalence and potential robustness in environmental conditions, their consistent detection in human feces, which directly correlates with dietary intake, and their utility in providing a reliable baseline for normalizing pathogen signals in wastewater. Normalization using endogenous biomarkers (frequently found in human foodstuffs, which are readily shed in stool) like tobamoviruses helps in adjusting for various confounding factors such as daily wastewater flow variations or changes in population size, thereby enhancing the accuracy of pathogen concentration estimates relative to clinical health outcomes. To advance the field, we conclude the review by suggesting a broader investigation into the remaining tobamoviruses to assess their potential as normalization agents. This includes evaluating viruses like CMMoV, PMMV, and others which might offer similar stability and prevalence in wastewater systems. The development of more inclusive, possibly degenerate primer-based RT-qPCR assays is proposed to capture a wider range of tobamoviruses, thereby increasing the robustness of biomarkers used across diverse environmental and dietary contexts. Despite this, PMMoV and TBRFV have become the most common tobamovirus WEM normalizers, the potential of other tobamoviruses should not be overlooked.

8.6. The development of a universal, globally validated PMMoV RT-qPCR assay

Chapter 7 presents a comprehensive study aimed at the development and validation of a globally applicable RT-qPCR assay for PMMoV, a key biomarker in WEM. The research begins with a systematic evaluation of 35 overlapping RT-qPCR assays across 116 samples collected from 12 countries, identifying genomic regions with the highest RNA concentrations and lowest variability, crucial for assay optimization. Genomic region 17 emerged as the most suitable due to its structural protection and lower susceptibility to degradation and mutational turnover, likely a result of PMMoV's robust nucleocapsid organization. Region 31 also showed promise, though its performance varied geographically, particularly in Oceania.

The study examined the influence of sample type, geographical location, and sewershed population size on PMMoV RNA concentrations. Results showed higher RNA concentrations in primary sludge compared to influent wastewater, highlighting the importance of sample type in assay sensitivity, even for biomarkers such as PMMoV. Geographically, PMMoV RNA concentrations were generally consistent, with slight elevations in samples from Canada and Japan, attributed to the prevalence of primary sludge samples. No strong correlation was found between RNA concentrations and sewershed population sizes, except for a weak association in Region 31, suggesting that fecal strength and sample type may be more influential factors.

A new universal RT-qPCR assay, termed the P17 assay, was developed based on findings from genomic region 17. This assay demonstrated superior sensitivity compared to a widely used benchmark assay, with a lower limit of detection and quantification, potentially due to reduced secondary RNA structure formation enhancing reverse transcription efficiency. The P17 assay also showed comparable or better performance in detecting PMMoV RNA in diverse wastewater samples as well as in a hot pepper sauce sample.

Beyond assay development, the study provides overlapping PCR assays spanning most of the PMMoV genome, facilitating future research efforts such as sequencing fragmented PMMoV genomes from environmental samples. The findings establish the P17 assay as a valuable tool for global WEM, offering improved sensitivity and interoperability with existing datasets, and further solidify PMMoV as a reliable normalization biomarker for WEM. This research advances the methodological framework for WEM addressing key gaps in assay sensitivity and data standardization.

8.7. Novel contributions and practical implications

This dissertation makes several novel contributions to the field of WEM, advancing its methodological, analytical, and practical applications. Key innovations include the development of a globally validated RT-qPCR assay for PMMoV, providing a standardized tool for normalization across diverse geographic and environmental contexts. Additionally, this research established PCS as a superior sample type for SARS-CoV-2 RNA detection, particularly during periods of low prevalence, and validated its use alongside PMMoV as a robust normalization biomarker. The mechanism behind this superiority likely resides in the fact that PCS has a higher concentration of wastewater and fecally-associated solids than PGS, effectively resulting in a pre-concentration of fecally-shed RNA targets of interest as part of the wastewater treatment processes themselves. The introduction of the WC ratio represents a groundbreaking metric for correlating wastewater signals with clinical data, enabling the detection of testing gaps and the emergence of variants of concern. Expanding WEM methodologies to rural and small communities addressed critical equity gaps, demonstrating the feasibility of adapting surveillance techniques to non-mechanical treatment systems like lagoons. Furthermore, this work broadened the scope of WEM by identifying novel applications for the use of tobamoviruses as potential biomarkers, enhancing data normalization capabilities. The practical implications of these contributions are significant, providing public health officials with cost-effective, scalable tools for early detection of viral outbreaks, improved monitoring of health trends in underserved areas, and the ability to anticipate and respond to epidemiological events more effectively via the use potentially novel and more relevant normalization biomarkers, and/or analytical or assay improvements. Collectively, these advancements lay the groundwork

for integrating WEM into global public health systems, enhancing community resilience and preparedness for future health challenges.

8.8. Future directions

Building on the development and advancements presented in this dissertation, I believe we have laid the groundwork for future WEM research to expand beyond acute and respiratory diseases. While the immediate applications of WEM have been focused on tracking pathogens like SARS-CoV-2, influenza and the respiratory syncytial virus, its now clear to many that there exists a largely untapped potential exists in addressing chronic diseases, cancers and their associated biomarkers. Wastewater surveillance could play a transformative role in monitoring community-level trends in conditions such as diabetes, cardiovascular disease, cancer, and even mental health disorders by detecting relevant biomarkers.

Expanding WEM to include chronic disease indicators would provide public health officials with invaluable tools to track the long-term health of populations, assess the impact of interventions, and address disparities in healthcare access and outcomes. Unfortunately, during the COVID-19 pandemic, WEM programs were disproportionately concentrated in larger, affluent urban centers in medium- and high-income countries. To fully realize the potential of WEM, it is critical to reduce costs and lower barriers to entry for resource-limited communities while ensuring the development of appropriate statistical methods, robust data analysis techniques, and seamless integration and interoperability with existing health data systems. Concrete health actioning must also be prioritized to translate insights from WEM into meaningful public health interventions, fostering widespread application that safeguards public health and enhances community resilience against a wide spectrum of current and future health challenges in an equitable and fair manner.

8.9. References

Hrudey, S.E., Bischel, H.N., Charrois, J., Chik, A.H.S., Conant, B., Delatolla, R., Dorner, S., Graber, T.E., Hubert, C., Isaac-Renton, J., Pons, W., Safford, H., Servos, M., Sikora, C., 2022. Wastewater Surveillance for SARS-CoV-2 RNA in Canada. Facets 7, 1493–1597. https://doi.org/10.1139/facets-2022-0148

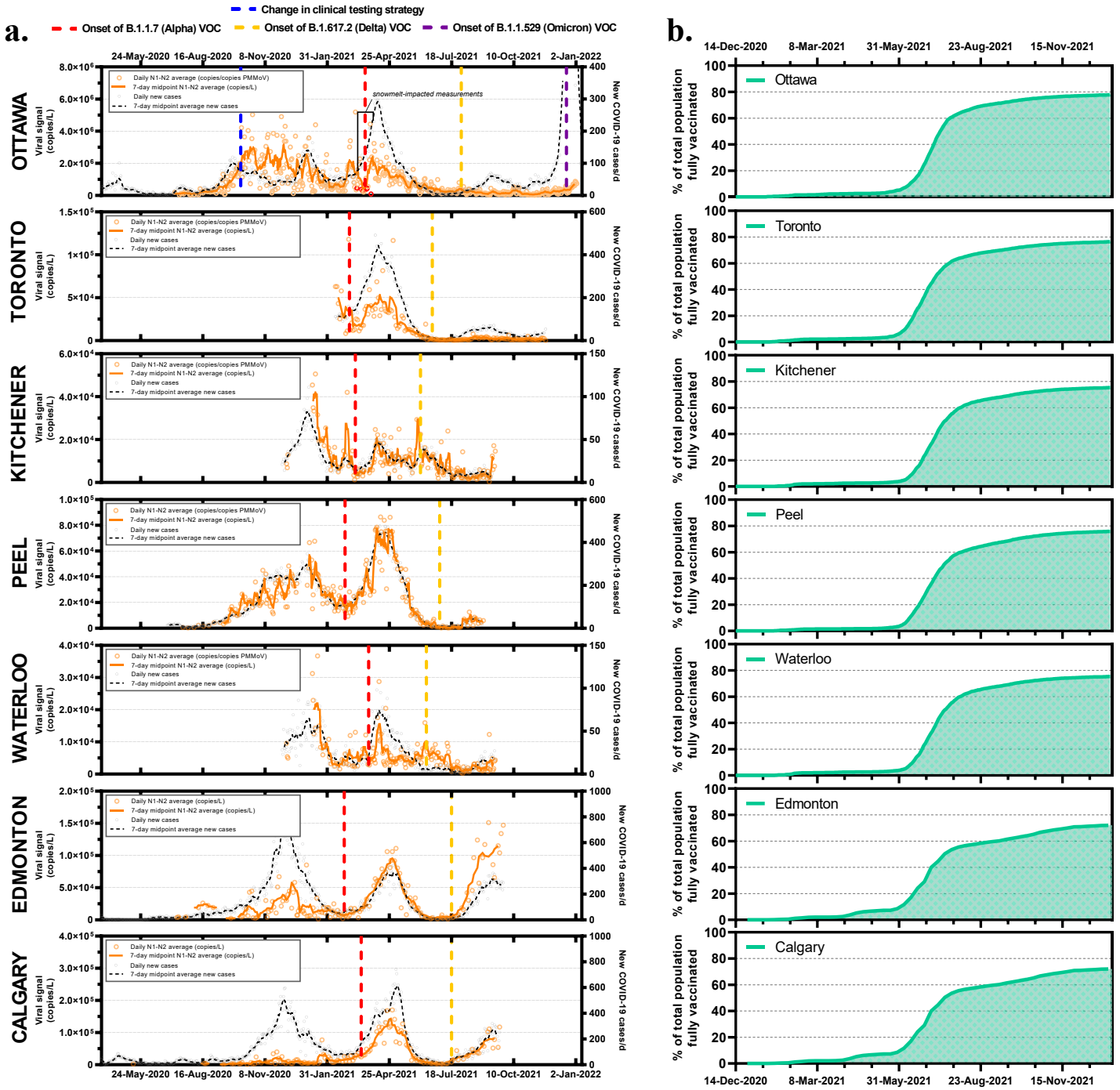


Figure S1: Comparison of a. scale-standardized SARS-CoV-2 viral signal measured in wastewater (in copies/L) to reported new daily COVID-19 cases in the communities, with the onset of events of high epidemiological importance outlined with vertical dashed lines, coupled with b. summary of the immunization status of the populations living within the studied communities.

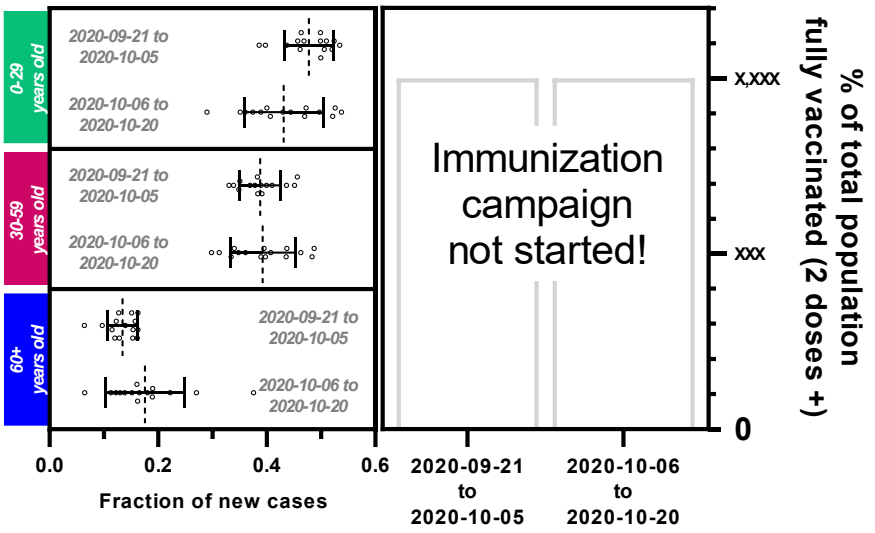


Figure S2: Comparison of the demographic distribution of new cases, per age group, and the proportion of the total population which was fully immunized (2 doses +) during the 15-day period preceding and following the change in testing rules and regulations on Oct. 6th, 2020, in Ottawa, Canada.

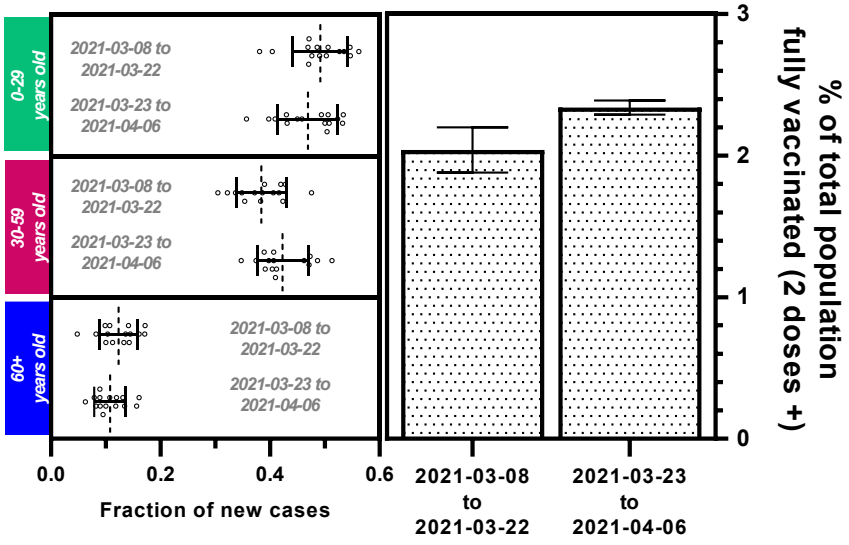


Figure S3: Comparison of the demographic distribution of new cases, per age group, and the proportion of the total population which was fully immunized (2 doses +) during the 15-day period preceding and following the onset of the Alpha (B.1.1.7) variant of concern in Ottawa, Canada.

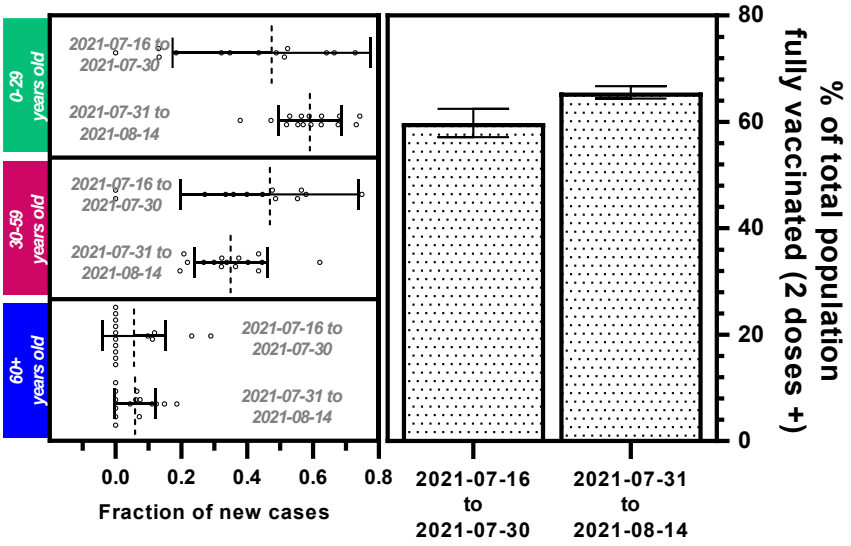


Figure S4: Comparison of the demographic distribution of new cases, per age group, and the proportion of the total population which was fully immunized (2 doses +) during the 15-day period preceding and following the onset of the Delta (B.1.617.2) variant of concern in the community.

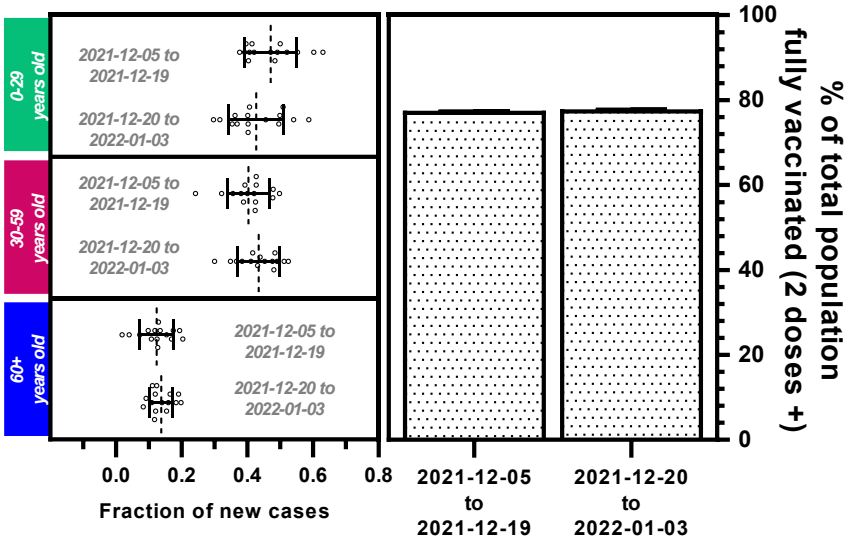


Figure S5: Comparison of the demographic distribution of new cases, per age group, and the proportion of the total population which was fully immunized (2 doses +) during the 15-day period preceding and following the onset of the Omicron (B.1.1.529) variant of concern in the community.

Table S1: Summary of studied water resource recovery facilities' treatment characteristics.

Water resource recovery facility	Average daily flow (MLD)	Treatment level (Primary, Secondary, Tertiary)	Approx. population deserved
Ottawa (Robert O. Pickard Environmental Centre)	435	Secondary	910,000
Toronto (Ashridge's Bay water resource recovery facility)	556	Secondary	1,603,700
Toronto (Highland Creek water resource recovery facility)	173	Secondary	533,000
Toronto (North Toronto water resource recovery facility)	46	Secondary	55,000
Kitchener (Kitchener water resource recovery facility)	70	Secondary	262,300
Peel (Clarkson water resource recovery facility)	446	Secondary	1,500,000
Peel (G.E. Booth water resource recovery facility)	236	Secondary	
Waterloo (Waterloo water resource recovery facility)	46	Secondary	162,000
Edmonton (EPCOR Gold Bar water resource recovery facility)	285	Tertiary	834,000
Calgary water resource recovery facility	420	Tertiary	1,000,000

Table S2: Oligonucleotide sequences used for the detection of targets in this study.

Primer/probe & supplier	Sequence	Reference
2019-nCoV_N1 forward primer (IDT)	GAC CCC AAA ATC AGC GAA AT	[1]
2019-nCoV_N1 reverse primer	TCT GGT TAC TGC CAG TTG AAT CTG	[1]
2019-nCoV_N1 probe (IDT)	**6-FAM**-ACC CCG CAT/**ZEN**/ TAC GTT TGG TGG ACC-**IBFQ**	[1]
2019-nCoV_N2 forward primer	TTA CAA ACA TTG GCC GCA AA	[1]
2019-nCoV_N2 reverse primer	GCG CGA CAT TCC GAA GAA	[1]
2019-nCoV_N2 probe (IDT)	**6-FAM**-ACA ATT TGC/**ZEN**/CCC CAG CGC TTC AG-**IBFQ**	[1]
PMMoV forward primer	GAG TGG TTT GAC CTT AAC GTT GA	[2]
PMMoV reverse primer	TTG TCG GTT GCA ATG CAA GT	[2]
PMMoV probe (ABI)	**6-FAM**-CCT ACC GAA GCA AAT G-**MGB**	[2]
VSV forward primer	ATA AGA TAC CGG GCT TGC AC	[3]
VSV reverse primer	ACA AAG ACA TGC CCG ACA C	[3]
VSV probe (ABI)	**6-FAM**-CCA TGT TGT ATT TGG ACC C-**MGB**	[3]
D3 (non-B.1.1.7) forward primer	ATC TAA ACG AAC AAA CTA AAA TGT CTG AT	[4]
D3L (B.1.1.7) forward primer	CAT CTA AAC GAA CAA ACT AAA TGT CTC TA	[4]
D63G (B.1.617.2) forward primer (ABI)	TCA CTC AAC ATG GCA AGA AAG G	*Personal communication with M. Fuzzen*
D63G (B.1.617.2) reverse primer (ABI)	GGT AGT AGC CAA TTT GGT CAT CT	*Personal communication with M. Fuzzen*
N63 (non-B.1.617.2) forward primer	CTC ACT CAA CAT GGC AAG AAA G	*Personal communication with M. Fuzzen*
D63G probe	**6-FAM**-CCT TAA ATT CCC TCG ATG ACA AGG CG-**MGB**	*Personal communication with M. Fuzzen*
N200 (B.1.617.2) forward primer	TAG TCG CAA CAG TTC AAG AAA T	[5]
N200 (B.1.617.2) reverse primer	CTG GTT CAA TCT GTC AAG CAG	[5]
N200 (B.1.617.2) universal probe	**6-FAM-**TCC TGC TAG AAT GGC-**BHQ-1**	[5]
N200 (B.1.617.2) delta probe	**CAL Fluor Orange 560**-CAG CAG TAT GGG AAC T-**BHQ-2**	[5]
C28311 (P13L) (non-B.1.1.529) forward primer	CCA AAA TCA GCG AAA TGA ACC	*This study*

C28311T (P13L) (B.1.1.529) forward primer	CCA AAA TCA GCG AAA TGA ACT	*This study*
N1 (version 2) probe (ABI)	**6-FAM**-CCG CAT TAC GTT TGG TGG ACC C-**MGB**	*This study*

Table S3: Summary of regression analyses during different resurgences of the COVID-19 pandemic in seven Canadian cities, showing good to excellent correlations between daily observed clinical COVID-19 cases and measured normalized SARS-CoV-2 viral signal in wastewater.

Location	Pearson's r, p-value, n; during 1st resurgence	Pearson's r, p-value, n; during 2nd resurgence	Pearson's r, p-value, n; during 3rd resurgence	Pearson's r, p-value, n; during 4th resurgence
Ottawa	R=0.263, p-value = 0.01, n = 91	R = 0.878, p-value < 0.01, n = 59	R = 0.760, p-value < 0.01, n = 90	R = 0.446, p-value = 0.02, n = 27
Toronto	-	-	R = 0.935, p-value < 0.01, n = 68	-
Kitchener	-	R = 0.831, p-value < 0.01, n = 32	R = 0.383, p-value < 0.01, n = 61	-
Peel	R = 0.856, p-value < 0.01, n = 124	R = 0.686, p-value < 0.01 n = 53	R = 0.910, p-value < 0.01, n = 131	-
Waterloo	-	-	R = 0.737, p-value < 0.01, n = 141	-
Edmonton	-	R = 0.012, p-value = 0.895, n = 62	R = 0.985, p-value < 0.01, n = 56	-
Calgary	-	R = 0.845, p-value < 0 .01, n = 69	R = 0.973, p-value < 0.01, n = 45	-

Table S4: Proportional changes in reported clinical cases of COVID-19, measured WEM SARS-CoV-2 viral signal and WC ratio at all seven tested locations between the preceding 15-day and following 15-day periods where 40-60% allelic proportionality of the Alpha (B.1.1.7) VOC was measured in wastewater.

Location	Date where allelic proportionality of B.1.1.7 VOC reached 40-60%	Change in reported clinical cases (%)	Change in measured SARS-CoV-2 viral signal in wastewater (%)	Change in WC ratio (%)
Ottawa	23-03-2021	+188.3	+70.8	-56.3
Toronto	02-03-2021	+45.4	+9.2%	-27.7
Kitchener	10-03-2021	-20.9	-65.7	-37.5
Peel	22-02-2021	+9.7	+2.3	-54.1
Waterloo	27-03-2021	+224.0	+119.3	-32.6
Edmonton	23-02-2021	+24.3	-10.8	-16.8
Calgary	22-03-2021	+82.7	+92.5	+6.4%

Table S5: Proportional changes in reported clinical cases of COVID-19, measured WEM SARS-CoV-2 viral signal and WC ratio at all 4 tested locations with data between the preceding 15-day and following 15-day periods where 40-60% allelic proportionality of the Delta (B.1.617.2) VOC was measured in wastewater.

Location	Date where allelic proportionality of B.1.617.2 VOC reached 40-60%	Change in reported clinical cases (%)	Change in measured SARS-CoV-2 viral signal in wastewater (%)	Change in WC ratio (%)
Ottawa	31-07-2021	+121.1	+45.8	-18.7
Toronto	22-06-2021	-53.5	-75.1	-42.2
Kitchener	06-06-2021	+51.7	+29.1	-20.2
Peel	28-05-2021	-63.3	-52.3	+9.2
Waterloo	02-07-2021	-26.8	+17.9	+42.2
Edmonton	18-07-2021	+168.0	+210.9	+10.7
Calgary	18-07-2021	+185.7	+533.8	+152.9

Table S6. This table shows the variance of the PMMoV RNA concentration (expressed as Ct values) across the PMMoV genome. It is observed that the lowest variance was observed the following locus: Region 35, 18, 17, 26 and 27. The highest variance was observed in the following locus: 32, 28, 8, 6 and 29.

Overlapping PCR assay genomic region	Overall variance (in Ct value)
Region 2	9.79
Region 3	9.65
Region 4	10.20
Region 5	8.39
Region 6	14.60
Region 7	6.63
Region 8	13.87
Region 9	8.07
Region 10	10.90
Region 11	9.93
Region 12	7.69
Region 13	6.64
Region 14	8.63
Region 15	9.83
Region 16	6.85
Region 17	6.27
Region 18	5.30
Region 19	7.19
Region 20	9.42
Region 21	10.96
Region 22	8.14
Region 23	7.25
Region 24	7.95
Region 25	7.75
Region 26	6.37
Region 27	6.41

Region 28	11.64
Region 29	15.16
Region 30	8.49
Region 31	7.95
Region 32	11.28
Region 33	8.94
Region 34	8.12
Region 35	4.60
Region 36	7.77